

**New Information Supporting the Stabilization & Restoration of the
Biloxi Marsh Complex**
A Unique and Distinct Ecosystem



Composite Map of Township Plats
Richardson & Powell Surveys – 1840s
U. S. Surveyors General Office

New Information Supporting the Stabilization & Restoration
of the Biloxi Marsh Complex
A Unique and Distinct Ecosystem

October 15, 2019

For:

Biloxi Marsh Lands Corporation, and
Lake Eugenie Land and Development, Inc.
One Galleria Blvd. #902
Metairie, LA 70001

By:

John W. Day^{1,2}
G. Paul Kemp²
Robert R. Lane¹
Elizabeth C. McDade³
Nancye H. Dawers⁴
William B. Rudolf⁵

¹Comite Resources
PO Box 66596, Baton Rouge LA 70896

²Department of Oceanography & Coastal Sciences,
Louisiana State University, Baton Rouge LA 70803

³Chinn-McDade Associates LLC
1401 Distributors Row, Suite C, Harahan, LA 70123

⁴Department of Earth & Environmental Sciences
101 Blessey Hall, Tulane University, New Orleans, LA 70118

⁵Biloxi Marsh Lands Corporation, and Lake Eugenie Land and Development, Inc.
Metairie, LA 70001

Table of Contents

| | |
|---------------------------------------------------------------------------------------------------------------------------------------------------------------------------------|-----|
| Table of Contents | 3 |
| Executive Summary | 4 |
| Introduction..... | 10 |
| Background Information..... | 14 |
| Chapter 1: Biloxi Marsh Complex: Geologic History and Tectonic Setting..... | 17 |
| Chapter 2: Field Data Collection in the Biloxi Marsh Complex | 31 |
| Chapter 3: Surface Elevation Change (SET) and Accretion at Historical Plots in the Biloxi Marshes | 49 |
| Chapter 4: Wetland Dynamics from CRMS and CPRA Polygon 11..... | 61 |
| Chapter 5: Restoration, Stabilization and Enhancement of the BMC: Project Recommendations..... | 75 |
| Conclusions and Recommendations | 80 |
| Literature Cited | 82 |
| Appendix A: Hydrology Data Tables and Field Records | 90 |
| Appendix B: Summary of Site visits | 99 |
| Appendix C: SET Project Timeline | 104 |
| Appendix D: Analyzed SET Data Tables | 105 |
| Appendix E: Raw SET Data Tables..... | 107 |
| Appendix F: CRMS Data..... | 121 |
| Appendix G: “ <i>Status of Rangia Clams in Lakes Borgne after Closure of the Mississippi River Gulf Outlet,</i> ” M. A. Poirrier 2019 | 125 |
| Appendix H: Drone video of Biloxi Marsh along the Lake Borgne Shoreline 11-23-2016..... | 125 |
| Appendix I: “ <i>Leveraging Natural Resilience to ensure Long-Term Sustainability of the Biloxi Marsh Complex Surge Barrier: An Integrated Project,</i> ” Day et al., 2019..... | 125 |
| Appendix J: “ <i>MRGO Ecosystem Restoration Fact Sheet</i> ”: USACE 2013..... | 125 |
| Appendix K: “ <i>Three Mile Pass Marsh Creation and Hydrologic Restoration,</i> ” Lake Pontchartrain Basin Foundation CMP 2023 Project Nomination..... | 125 |

Executive Summary

The Biloxi Marsh Complex (BMC) mainly suffers from peripheral and internal erosion, not subsidence. Exposure to large exterior water bodies, particularly Lake Borgne, plays a primary role in the erosion of peripheral shorelines. Meanwhile, increased hydrologic connectivity leads to tidal scouring and degradation of the interior marshes. Tidal scour is especially destructive, and when combined with other degradative processes, it results in a significant cumulative effect on inland marshes with many potential acres exposed. Areas in the Western BMC with large interior ponds/lagoons and ponded areas adjacent to Bayou La Loutre are particularly adversely affected by these cumulative degradative processes as newly formed hydrologic connections with Lake Borgne lead to greater exposure to erosive water movement. The root cause of these degradative processes can be attributed to changes in Lake Borgne's salinity caused by decades of operation of the Mississippi River Gulf Outlet (MRGO). Changes in salinity resulted in the loss of Lake Borgne's natural *Rangia* clam beach berm. As a critical first step, the widespread connectivity of interior BMC marshes with Lake Borgne must be immediately addressed and a protective beach berm restored. Successful management of land loss in the BMC will depend on projects like those presented in this report that address this root cause of marsh loss and build on the natural resiliency of the BMC.

- The Coastal Protection and Restoration Authority (CPRA) hypothesized in its 2017 Coastal Master Plan (CMP) that, with no additional action over the next 50 years, the BMC will be lost due to:
 - Subsidence and
 - Sea level rise.
- This finding was not consistent with data and information specific to the BMC or with long-term observations by landowners and other stakeholders in the BMC area. As a result, Biloxi Marsh Lands Corporation and Lake Eugenie Land and Development, Inc. commented on the draft CMP 2017 in their March 24, 2017 letter. Comments were based on review and scientific analyses of the existing data and information.
- After consideration of Biloxi Marsh Lands Corporation and Lake Eugenie Land and Development, Inc.'s comments and discussions among Biloxi Marsh Lands Corporation, Lake Eugenie Land and Development, Inc., and the CPRA, the CRPA included the following language on page 162 in the final CMP 2017:

We realize that new information may become available that alters the effectiveness of some of those projects and that there are potentially other innovative project concepts that have not yet been considered. Identifying these projects and concepts is an important next step in the master planning process. To that end, those concepts and certain elements of this plan need to be further refined to assist areas of the coast with recognized critical needs.... the Biloxi Marsh Complex for which recently evaluated specific information suggests

local factors (e.g., subsidence, accretion) may result in the area performing better and lasting longer than current estimates suggest. As such, CPRA will continue the Project Development and Implementation Program coordinated with our adaptive management program through which projects like this can be further developed using refined and improved information.

- Biloxi Marsh Lands Corporation and Lake Eugenie Land and Development, Inc. assembled a team of scientists during the fourth quarter of 2017, consisting of:
 - Dr. John W. Day, Department of Oceanography & Coastal Sciences at Louisiana State University and Comite Resources;
 - Dr. G. Paul Kemp, Department of Oceanography & Coastal Sciences at Louisiana State University;
 - Dr. Robert R. Lane, Comite Resources;
 - Dr. Nancye H. Dawers, Department of Earth & Environmental Sciences at Tulane University; and
 - Dr. Elizabeth C. McDade, Chinn-McDade Associates LLC

- During the first quarter of 2018, Biloxi Marsh Lands Corporation, and Lake Eugenie Land and Development, Inc. met again with CPRA staff and advised CPRA of their plans to collect critical data and study the unique geology of the BMC.
 - Among other goals, the purpose of the proposed data collection and study was to understand the stability of the geologic platform and subsidence and accretion rates, specifically as they pertain to the BMC.
 - CPRA provided positive feedback during this meeting and advised that localized new information would be helpful and considered.

- This report includes the conclusions and recommendations based on additional data collection and analysis. These conclusions and recommendations take into consideration:
 - The deeper subsurface geology of the BMC and surrounding areas;
 - An analysis of existing and newly collected field data, including changes in marsh surface elevation, accretion, shoreline erosion, tidal inundation, hydrology, and water level; and
 - Salinity time series before and after MRGO construction and operations, spanning more than 55 years.

Subsurface Geology

- This report considers the geology of southeastern Louisiana covering an area east of the Atchafalaya basin and south of the I-12 corridor. The report contrasts the geology beneath the BMC with the geology beneath other coastal marshes to the south and southwest. Important conclusions include:
 - The BMC has a 100-million-year history of low subsidence, and like older strata in the subsurface, the youngest sediments of Holocene-age are thin

under the coastal marshes of the BMC as compared to other coastal marshes of southeast Louisiana. The Cretaceous-age shelf edges and a lack of mobile salt-related geologic structures are strong contributors to the creation of a stable geologic platform in the BMC, and these conditions continue today.

- Other southeast Louisiana coastal marshes share similarities at the surface with the BMC, but for marshes south and southwest of the BMC, where the Holocene is thicker, the underlying geology is very different and subsidence rates are more rapid in these marshes than in the BMC. Geologic structural provinces governed by long-acting salt tectonics and growth fault trends influence Holocene thickness. Thicker Holocene in lower Plaquemines, for instance, leads to more rapid subsidence rates compared to those measured in the BMC.
- Some of these areas where the Holocene is thicker have experienced large amounts of modern land loss, but the BMC is relatively unchanged. This observation leads to a conclusion that the BMC is one of the most sustainable and resilient coastal marshes of Louisiana. With proper management, its natural resiliency will be an asset that will help the BMC to recover from the detrimental effects of MRGO.

Field Data Collection

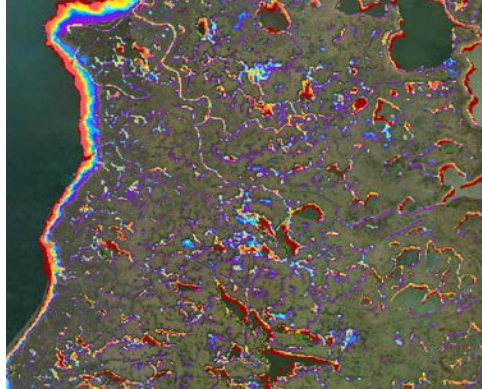
- The following data was collected for this study: Surface Elevation Table (SET) data. This data was collected for comparison to baseline data from SET stations established in 2003, spanning 15 years. (Coastwide Reference Monitoring System (CRMS) data was also used.
- Data and information collected from representative study areas, including:
 - Gauge tidal inundation,
 - Shoreline erosion,
 - Accretion,
 - Soil bulk density,
 - Vegetative species composition, and
 - Water quality parameters.
- Water quality parameters at twelve Rounsefell sites, and
- Hydrologic changes observed over time.

Conclusions Based on Field Work

The collected field data showed differences in sediment distribution between Eastern and Western portions of BMC.

- In the Eastern Portion of BMC:
 - Elevation rise was observed at SET and CRMS sites,
 - Sediment from Chandeleur Sound is nourishing marsh during hightide events,
 - Peripheral shoreline erosion adjacent to major waterbodies was observed, and

- Due to influx of sediments from Chandeleur Sound, marsh elevation is staying high within the tidal frame and is likely to keep pace with sea level rise.
- In the Western Portion of BMC:
 - Peripheral and internal erosion is mainly due to widespread hydrologic connectivity with Lake Borgne, initiated by and attributed to the construction and operation of the MRGO (see inset map, Persistent Land Loss, Couvillion et al. 2017, key to colors on p. 32).
 - Reduction of *Rangia* clam population in Lake Borgne and subsequent loss of naturally armored beach berm were caused by high salinity during operation of MRGO,
 - Loss of the beach berm has led to increased internal tidal scour, connection from Lake Borgne to internal marshes, and wave fetch in interior large lagoons/ponds, and
 - Ponds flanking natural levees along Bayou La Loutre experience localized subsidence due to compaction of peaty areas adjacent to the channel. As open water forms, interior pond shorelines are increasingly subject to wave-driven erosion.



- The following observations were made regarding the BMC's partial recovery and rebound after the MRGO ceased operations in 2009:
 - As the salinity adjusts to pre-MRGO levels, less salt-tolerant vegetation species, including Roseau Cane, Three Corner Grass, and Cattails, are recolonizing some areas of the western half of the BMC.
 - Live oak trees along Bayou La Loutre that appeared dead for years are sprouting new leaves (inset and Figure Executive Summary-1)
 - Given the return of Lake Borgne to pre-MRGO salinities, a recovery of the lake bottom clam *Rangia cuneata* can also be forecast. The loss of the *Rangia* clam beach berm along the western shore of the BMC continues to have increasingly deleterious effect on hydrology, opening pathways for Lake Borgne waters to enter the marsh through exposed bayous and newly formed tidal channels that



- present continuing and increased risk to interior marshes.
- Keeping the MRGO closed and dammed below Bayou La Loutre is critical in allowing the observed natural partial recovery to continue.

Recommendations for CPRA

Updating and refining the information concerning the BMC is necessary to better understand the causes of the BMC's deterioration and its natural resiliency and sustainability, so that appropriate projects can be designed, and funding and implementation of these projects can be accurately prioritized. This new and refined information demonstrates the BMC's natural resiliency and feasible sustainability, but CPRA models use input values that are not representative of conditions in the BMC and which result in predictions of complete loss of the BMC over 50 years. Instead of taking no action, projects that promote the natural resiliency and sustainability of the BMC should be funded and implemented. Indeed, the importance of the BMC for regional storm protection and the economy, augmented with the new information in this report, should result in the BMC being a priority for project funding and implementation. As such, we make the following recommendations:

- Project Proposals for BMC
 - Critical needs and near-term, mid-term, and long-term enhancement needs of the BMC can be addressed by:
 - Projects that focus on increasing delivery and retention of sediment and which limit erosive hydraulic connectivity (Chapter 5 and Appendices J and K) and/or
 - Projects that are designed to take advantage of marsh accretion processes and the natural stability of the BMC and thus, are expected to be self-sustaining and long-lasting due to low subsidence rates and rates of relative sea level rise.
 - One such proposed project is the BMC Integrated Project available in Appendix I, entitled "*Leveraging Natural Resiliency to Ensure Long-Term Sustainability of the Biloxi Marsh Complex: An Integrated Project.*" This project was submitted in response to CPRA's Request for Proposals (RFP) for projects to be included in CMP 2023.
 - The proposed BMC Integrated Project addresses Critical Needs to curtail the aggressive erosion of Lake Borgne shoreline and interior marshes due to loss of protective *Rangia* clam beach berm.
 - Integrity of the western BMC beach berm is needed because this berm is an essential barrier that prevents connectivity between Lake Borgne and interior marshes and thus, prevents shoreline erosion within the many bayous and small ponds that are adjacent to the shoreline.
 - The BMC Integrated Project builds on the BMC's natural resiliency by re-establishing a beach berm, providing marsh nourishment, and mitigating hydrologic connections to interior marshes.

- Modification of CMP 2017 Subsidence Polygon
 - Polygon 11 does not represent conditions in the BMC because it covers a broad area with boundaries that cross several geologic structural provinces. Incorporating geological boundaries and a better understanding of Holocene thickness variations (Kulp et al., 2002) controlled in part by Pleistocene and other relevant buried geologic structural features will lead to more representative polygon designations.
 - Based on a north-to-south CRMS profile, Polygon 11 should be divided into at least two parts, using Bayou Terre aux Boeufs as a southern boundary that separates the more stable northern portion of Polygon 11 from the less stable southern portion. The southern portion of Polygon 11 includes areas in Plaquemines Parish that are in a different geologic province with significantly thicker Holocene than the northern portion of Polygon 11.
 - Without this division, Polygon 11 is assigned a range of subsidence rates that is too broad, and with respect to the BMC, the polygon has a low-end subsidence rate which is higher than most measured rates in the BMC. Subsidence is not the major issue affecting sustainability of the BMC, as evidenced by the generally healthy nature of the marsh.
 - When considering the natural resiliency and sustainability of the BMC, CPRA should also consider the improved marsh health and other improved conditions in the BMC since closure of the MRGO.



Figure Executive Summary -1. Live Oak along Bayou La Loutre – growth regeneration

as per CPRA’s acknowledgment that factors specific to the BMC may result in the area “performing better and lasting longer than current estimates suggest” (Final CMP 2017, pg. 162). As a relatively unchanged land mass particularly in its western portion for more than 3000 years, the BMC is instantly recognizable after more than 170 years on the Richardson and Powell 1847 survey plats prepared for the U.S. General Land Office (GLO) (Cover Page).¹ The generally healthy state of much of the marsh is visual evidence that the BMC is one of the most resilient and sustainable areas of marsh in coastal Louisiana. Results presented in this report confirm our belief that the BMC is unique and distinct, and more importantly, that with regard to BMC as well as other parts of the coastal zone, local factors must be taken into consideration when coastal master plans are formulated. Simply put, one size does not fit all across the entire coastal zone of Louisiana and local factors must play an integral part of future planning.

The BMC’s natural resilience is rooted in availability of sediments from adjacent water bodies and its ability to retain sediment due to a mostly healthy marsh and low subsidence rate. Unfortunately, the natural stability of the BMC is not well-represented in CMP 2017 due to a predictive methodology driven almost exclusively by an overestimated subsidence rate that results in complete loss of the BMC by 2050. This report considers the geologic foundation under the BMC, examines the present-day condition of the marsh, and updates measurements of salinity and accretion representing decades of study. Deeper elements of the BMC subsurface structure attest to the stability of the platform and its unique geologic history compared to other coastal deltaic marshes of southeast Louisiana. Our results have direct application to project development and design in that they address the root cause of land loss and suggest solutions based on observation of successful projects and natural processes. Based on CRMS data interpreted in a context that includes the deeper geologic structure, we make recommendations for an adjustment to bounds and subsidence rates of subsidence polygons used for planning and project eligibility decision making.

Other southeast Louisiana coastal marshes east of the Atchafalaya have experienced widespread land loss due to a variety of mechanisms, many of which are not active in the BMC (Penland et al, 2008). Root causes of ongoing land loss and marsh degradation in the BMC are not associated with direct removal, subsidence, or faulting, but were instigated by hydrologic changes brought by several decades of operation of the Mississippi River Gulf Outlet (MRGO) (mid 1960s – 2009) (Shaffer et al 2009). Increased salinity in Lake Borgne led to loss of a natural *Rangia* clam beach berm along the Lake Borgne shoreline which in turn led to wave erosion and shoreline retreat, and subsequent development of hydrologic connections from Lake Borgne to interior marshes (Poirrier, 2011, 2019). Edge erosion has affected lagoons in the marsh interior associated with Bayou La Loutre and its distributaries (Treadwell 1955; Penland et al., 2001; Couvillion et al., 2017; Day et al., 2019, Ch. 2 and 3 this report). The closure of the navigation canal for the past 10 years has been beneficial to the BMC and Lake Borgne, and as salinity approaches pre-MRGO

¹ With the exception of the increased impacts following the construction and operation of the MRGO until its closure.

levels, natural floral and faunal distributions are beginning to return. Nevertheless, correcting the hydrologic connectivity now will slow the continuing degradation of interior marshes caused by increased water flow and tidal scour or perhaps even stabilize these marshes.

The report consists of five chapters that in turn discuss the geologic history and underlying geologic structure; field data collected relating to marsh health, marsh inundation, root causes of land loss, salinity and other water quality parameters, accretion, and erosion; marsh surface elevation change; the accuracy of the subsidence rates assigned to the BMC as set forth in subsidence Polygon 11 used in the 2012 and 2017 Coastal Master Plans (CMP 2012 and CMP 2017) and; a summary of potential project concepts in order of priority from critical and immediate to longer-term. We begin with an examination of energy industry interpretations of geologic structure that make clear the large contrasts in deep geology and tectonic setting between the BMC and other Louisiana coastal marshes that likely influence near-surface geology. Public and proprietary sources are used to illustrate characteristics of the unique geologic history of the BMC relative to other parts of the greater southeast Louisiana east of the Atchafalaya basin and south of the I-12 corridor. Later chapters integrate field work conducted during 2018 with archived data representing decades of measurement of salinity, accretion, and elevation change. Marsh sedimentation patterns, shoreline change, hydrologic changes, and observations of marsh health support the conclusions that marshes of the BMC are generally healthy, accreting, and gaining elevation where sediment sources are present and sediment retention is high.

Significantly, we report on targeted restoration efforts which take advantage of the natural resiliency of the BMC and can be expected to be self-sustaining and long-lasting. In fact, success has already been observed in the vicinity of recently installed structures in 2014 (CPRA Biloxi Marsh Shoreline Protection Project PO-072) that are similar in concept to plans presented in *“Leveraging Natural Resilience to Ensure Long-Term Sustainability of the Biloxi Marsh Complex Surge Barrier: An Integrated Project”* (BMC Integrated Project) submitted to the CPRA on February 28, 2019, by BMC in response to the RFP for new projects for CMP 2023. The BMC Integrated Project provides a conceptual design that focuses on the critical need for reducing hydrologic connections formed between Lake Borgne and interior marshes and ponds. Our proposed project pairs placement of a near-shore beach berm with marsh creation as well as marsh nourishment by thin-layer sediment dispersal methods. Mitigation to protect and nourish interior marshes from fast-moving channelized waters from Lake Borgne is expected to have long-lasting and sustainable effects due to generally low subsidence rates experienced in the BMC.

This report pairs the review of deeper geology with observations of near-surface geology, sedimentation patterns, and elevation change. Holocene thickness is closely correlated with subsidence rate (Kulp, 2000, Kulp et al., 2002) and also with position relative to subsurface features like Cretaceous shelf edges and the Louann salt basin in south Louisiana. This report concludes that in the dynamic and geologically young Louisiana landscape, relevant subsurface elements should be considered as boundaries for subsidence polygons. It appears that by using Polygon 11, CPRA modelers have been applying a subsidence rate to the BMC that is too high and dominates forecasting. The low and high subsidence estimates used by CPRA for Future Without Action (FWA) predictions were 4.4 and 6.5 mm/y, respectively, for both the 2012 and 2017 modeling efforts. However, these values

were applied to a vast area extending from the “Golden Triangle” (west of Lake Borgne), east to the Chandeleur Islands, and from the Mississippi state line south to Fort St. Phillip (CPRA Polygon 11; Reed and Yuill 2017). The relevant polygon extends across several geologic structural provinces with widely varying subsidence rates. As it pertains to the BMC, it appears that at a minimum, CPRA Polygon 11 should be split into 2 parts—northern and southern, roughly along the path of Bayou Terre aux Boeufs, and following Holocene thickness trends (Kulp 2012, Kulp et al., 2002). The northern portion should be assigned lower subsidence ranges representative of measured values. These lower subsidence ranges would be more in line with the structural trend that extends west including Lake Pontchartrain to Baton Rouge. This would be consistent with data from CRMS stations in the BMC area. This report’s recommendations are supported by measured subsidence rates from CRMS stations in the BMC that trend lower than the low end of the range applied to the entire subsidence polygon (Jankowski et al., 2017).

New data and information acquired and presented in this report since release of the 2017 CMP suggests that the BMC marshes should be among the best candidates for successful restoration given the high rate of naturally distributed sediment supply, relatively low subsidence, and the ongoing recovery from ecological stresses imposed by the MRGO. There is more work to be done to define the long-term path forward to manage the marsh resources of the BMC, but projects can be expected to have sustaining impact if the main causes of land loss are addressed and natural resiliency bolstered. Critical needs are addressed by the BMC Integrated Project (Appendix I) which expands on nearby projects already in place with demonstrated success. Future projects that build on the positive effects of the closure of MRGO and the BMC’s low subsidence rate and demonstrated ability to retain sediment once it is in place are outlined in Chapter 5 as well as Appendices J and K.

The BMC is critical to storm protection for the New Orleans metro area (Resio and Westerink, 2008, CPRA 2013) and has enormous value as an estuary and fishery. Polygon bounds and subsidence values used by CPRA should be updated and refined to reflect a more accurate value for the BMC. In addition, CPRA should also consider the improved marsh health and other improved conditions in the BMC since closure of the MRGO. Updating and refining this information is necessary to better understand the causes of deterioration, and the natural resiliency and sustainability of the BMC so that appropriate projects can be developed, and funding and implementation of these projects can be accurately prioritized. This new and refined information demonstrates the BMC’s natural resiliency and feasible sustainability, and coupled with the importance of the BMC for regional storm protection and the economy, should result in the BMC being a priority for project funding and implementation.

Background Information

Biloxi Marsh Complex- The Biloxi Marsh Complex (BMC) is a unique and distinct ecosystem within the Pontchartrain Basin consisting of marshes, bayous, lagoons, lakes, and bays covering a vast area over 700 square miles (~450,000 acres) about 30 miles southeast and seaward of metro New Orleans. The land portion of the BMC peninsula or “thumb” is about 45 miles by 20 miles and is an emergent area that separates Chandeleur Sound from Lake Borgne in St. Bernard Parish (Figure Background-1). The BMC was formed by the Mississippi River over 4000 years ago and was once one of the river’s primary ancient deltaic outlets. Importantly, the marshes of the BMC act as a land barrier providing regional protection and shelter from surge and waves caused by hurricanes for the rest of the Pontchartrain Basin, including the major population center of New Orleans. Additionally, the BMC is one of the largest and most important marine estuaries in the Gulf Coast region. Most of the BMC is owned by two landowners, Biloxi Marsh Lands Corporation (BLMC) and Lake Eugenie Land & Development, Inc. (LKEU) owning approximately 235 square miles (~150,000 acres). By granting a free lease to the Louisiana Department of Wildlife and Fisheries for over 60 years, BLMC has opened over 50 square miles (~35,000 acres) to the public for recreational use as a designated Wildlife Management Area (Biloxi WMA).

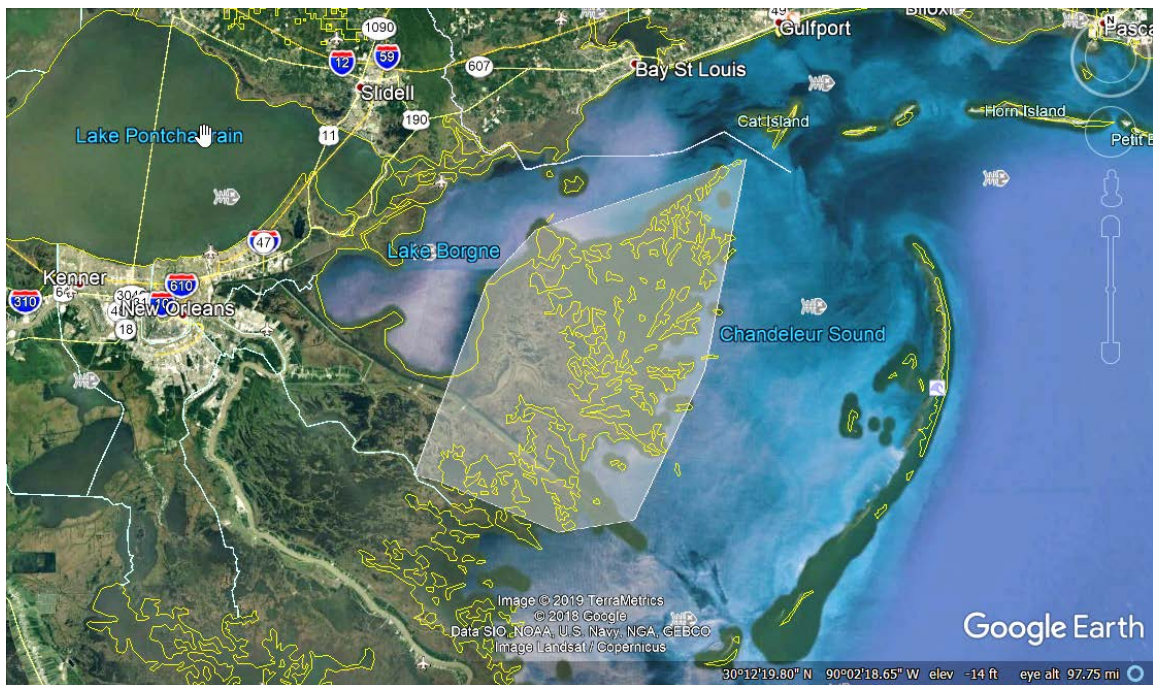


Figure Background-1. BMC AREA +/- 700 square miles (area shaded in white)

BLMC and LKEU are leading the effort in the BMC to sustain these critical coastal wetlands and have funded efforts to gather and evaluate existing data and to collect additional data, background information, and analysis. The results of these efforts are explained in this report “*New Information Supporting the Stabilization & Restoration of the Biloxi Marsh Complex.*” This new information was used to develop the conceptual

project design submitted to CPRA in February 2019, titled “*Leveraging Natural Resilience to Ensure Long-Term Sustainability of the Biloxi Marsh Complex Surge Barrier: An Integrated Project.*” (BMC Integrated Project, Appendix I). The proposed project pairs placement of a nearshore beach berm with marsh nourishment by thin-layer methods. This is an integrated technique that has natural and man-made equivalents that have been demonstrated to work in the immediate vicinity as further explained below. Additional project proposals are included in Chapter 5 and Appendices J and K of this report.

BMC Ecosystem Services. The BMC supports a vast estuarine ecosystem of intermediate, brackish, and saline marshes; shell beaches (Rangia clams on the oligohaline Lake Borgne side and oysters on mesohaline Chandeleur Sound); 3000-year-old natural levees, chenier ridges, and mounds constructed by Native Americans topped with live oaks; and oyster reefs, tidal bayous, inlets, lagoons, lakes, and bays. The BMC is only 25 to 30 miles east/southeast and seaward of the City of New Orleans, and thus it has been a preferred destination for generations of residents of southeastern Louisiana and south Mississippi who have fished, trapped and hunted there. Large bays and shell keys on the eastern side of the BMC support some of the most dependably productive commercial oyster grounds in the United States.

The 20-mile-wide BMC peninsular platform separates Chandeleur Sound from Lake Borgne. This position explains why the BMC plays such an important role in buffering the City of New Orleans and its eastern suburbs from storm surge and waves (Westerink, 2013, CPRA 2013). During passage of Hurricane Katrina in August 2005, the best “actual event” ADCIRC model hind-cast indicates BMC marshes reduced maximum surge elevation at the south end of Lake Borgne by about 8 feet relative to that at Bay St. Louis and decreased significant wave height by 6 feet. Given that the rebuilt New Orleans levees and flood walls are constructed only to a 100-year standard surge return frequency, retention of key natural buffers is crucial to the long-term survival of the City when more energetic storms strike in the future (e.g. Bhatia et al., 2019).

Mississippi River Gulf Outlet (MRGO). The MRGO navigation channel extended over 50 miles from the Gulf Intracoastal Waterway southward through the BMC into Breton Sound cutting the majority of BMC off from land to the west and southwest. After the MRGO channel was constructed in the 1960s through the wetlands south of Lake Borgne and across the Bayou La Loutre natural levee ridges, it was repeatedly dredged to more than the 40-foot project depth until the channel was permanently closed by the installation of a rock dam below the Bayou La Loutre crossing in 2009. The MRGO had devastating effects on the BMC by providing a conduit for high salinity waters from the Gulf. The operations resulted in changes to salinity and hydrology that triggered continual and widespread degradation of the BMC, including among other significant processes, the decline in Lake Borgne of the Rangia clam whose shells were important to erosion resistance of the western BMC beach berm (Poirrier, 2013, 2019).

Although numerous other degradation processes were triggered by the MRGO, the loss of the beach berm is the main cause for peripheral and internal erosion which in turn has led to widespread hydrologic connectivity with large exterior water bodies, particularly Lake Borgne. These connections play a primary role in the erosion of the internal marsh (see Figure Background-2 and drone video of the western BMC shoreline in Appendix H).

Research conducted since 2017 indicates that despite harmful effects in the past, present, and future, the post-closure BMC is partially recovering in localized areas and can become more resilient with restoration measures that build upon the natural resilience and stability of the BMC as proposed in Chapter 5, and Appendices I, J and K of this report.



Figure Background-2: Degraded shoreline along Lake Borgne (Western BMC) – Upper: 1998, Lower: 2019, Pt. Aux Marchettes Area, Google Earth image.

Chapter 1: Biloxi Marsh Complex: Geologic History and Tectonic Setting

Elizabeth Chinn McDade¹ and Nancye H. Dawers²

¹Chinn-McDade Associates LLC, Metairie, LA 70003

²Department of Earth & Environmental Sciences, Tulane University, New Orleans, LA 70118

Chapter 1: INTRODUCTION

This section addresses the geologic history and tectonic setting of the BMC and how certain attributes of its geologic setting might affect long-term stability of the complex, observed land loss patterns, and lead to improved prediction of success of certain restoration methods. We intend to provide geologic context to the results of the other sections of this report that will contribute to our present knowledge of recent sedimentation, accretion, and erosive marsh loss in the complex. The casual alignment of surface features with deeply buried geologic structural features suggests a causative relationship between geologic processes and resulting trends established long ago that set up conditions in the subsurface that have influence on geomorphology today. Coastal science in Louisiana can clearly benefit from analysis and understanding of subsurface processes using energy industry data sources. Resources are abundantly available and include 2D and 3D seismic, well log data, and regional to sub-regional interpretations based on these data in the energy industry literature.



Figure 1-1: Surficial geology and geographic regions of Louisiana coastal plain. Adapted from Heinrich et al, 2015.

The history of the BMC for the past 10,000 years is similar to other emergent south Louisiana marsh lands that share the same brackish- to salt-water setting adjacent to the

Gulf of Mexico and its bays. (Figure 1-1, Heinrich et al., 2015). Wetlands and uplands in the BMC exist as relics of the St. Bernard delta, one of the lobes of deltaic deposition responsible for building southeast Louisiana over the last 9000 years (Fisk, 1944, Frazier, 1967). Like other deltaic lobe systems, land areas in the BMC are most prominent where ancient river courses built natural levees and point bars in shallow water. Successive layers of coarser sediment laid down during flooding events build up channel systems, while areas between channels are typically dominated by swamp and marshy areas with more organic sediments (Frazier, 1967).

Below the surface, the BMC is quite different from much of the rest of southeast coastal Louisiana. Aspects of the BMC geologic history as evidenced in its subsurface geology may help explain the persistence of the BMC through time as a relatively stable rather than subsiding feature in coastal Louisiana.

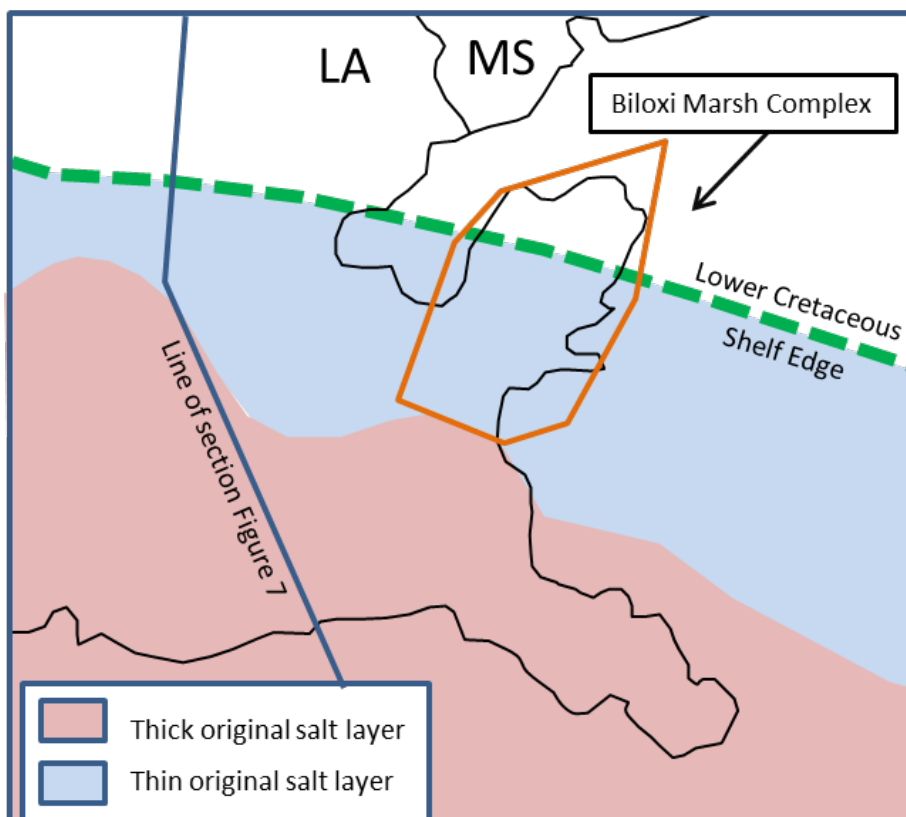


Figure 1-2: Simplified from Karlo and Shoup (2001). Regional scale interpretation of salt-tectonic structural provinces in southeast Louisiana. This work was completed at Shell, known as a leader in technical work among its peers. However, the work was completed before much of the 3D seismic which now covers much of south Louisiana was available, so this map should be considered only as a general guideline for structural provinces in south Louisiana and across the Gulf subject to updates and re-interpretation.

The position of the Cretaceous shelf edge (Figure 1-2) is a key factor in the BMC's unique geologic history. The Cretaceous shelf edge is a curvilinear trend of buried carbonate reefs that mark the northern edge of the Gulf of Mexico basin from Texas to Florida, which runs west-east across Louisiana and through the complex. Salt basins of various sizes rim the

northern Gulf. In this area, the Cretaceous shelf edge is coincident with the northern edge of the Louann Salt in south Louisiana, and thus occupies a position that separates a mostly stable tectonic setting to the north from active deformation to the south (Karlo and Shoup 1986, Schuster 1995, Peel et al. 1994).

Buried salt is an important driver of gravity-driven deformation because of its incompressibility, lack of rock strength, and buoyancy relative to typical deltaic and marine sediments. Salt is an important factor in the development of geologic faults, salt domes, and salt withdrawal basins that form in salt-tectonic dominated terrains of southeast Louisiana, and the scale and extent of these structures is related to the original thickness of salt (Karlo and Shoup 2001). Salt was originally deposited about 180 million years ago by evaporation of shallow marine basins when continental rifting first formed the Gulf of Mexico, adjacent to the evolving Atlantic Ocean basin (Hudec et al. 2013). It is unstable under an uneven load, and as sediments are deposited on top, salt tends to rise as it is pushed up and outward in a manner that has been compared to silly putty (Gagliano et al. 2003). Salt tectonics has been demonstrated to have caused broad areas of deformation in the subsurface that persist for millennia (Seglund 1974, Gagliano et al 2003, 2005). Examination of north to south well-log cross sections and interpretations from energy industry seismic lines are especially useful to compare and contrast the geologic structure below the BMC and coastal marshes to the south.

Figure 1-3 from Galloway et al. (2000) succinctly demonstrates the unique position of the BMC relative to other parts of south Louisiana and how the stability of the BMC has influenced depositional patterns for millennia. This diagram illustrates how the Gulf of Mexico basin was filled in with sediment during the last 65 million years, since the end of the Cretaceous.

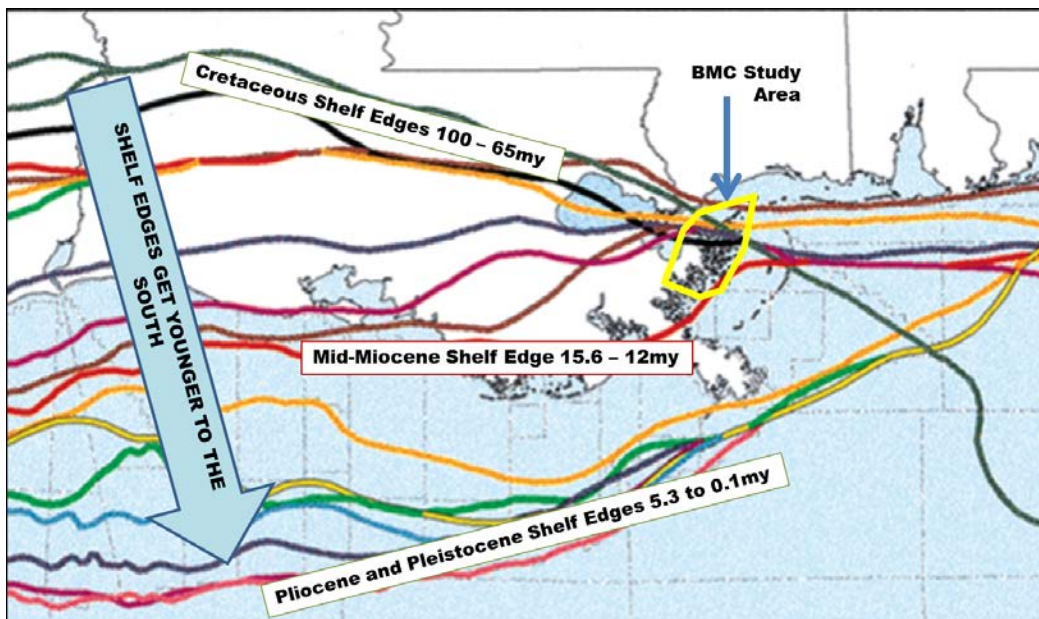


Figure 1-3: Shelf edges of the Cenozoic Period from Galloway et al., 2000.

Shelf edges of sedimentary units deposited from 65 million years ago to the present are shown as colored lines: the oldest shelf edges to the north and youngest in the south near

today's continental shelf edge offshore. Each shelf edge marks the transition from the shelf to deeper water continental slope and basinal settings. West of Lake Pontchartrain, shelf edges move southward showing progradation in a regular pattern into the Gulf of Mexico.

Notice however, how different the shelf edges are near the BMC. All the Cenozoic continental shelves before the mid-Miocene (from 65-15.6 my) are nearly coincident with one another and with the Cretaceous shelf edges, and stack on top of the BMC. This suggests that deposition there was minimal and progradation was limited. We know that this is at least in part due to the main river channel locations to the west, in central Louisiana, and partly because of a lack of subsidence and development of accommodation space for sediment to accumulate. Not until the middle Miocene (15.6-12 my ago) did river systems build out south enough to prograde into the basin past the BMC. This sedimentation pattern strongly suggests that the BMC has persisted as a relatively stable feature through much of the last 100 million years and that Cenozoic sediments in the BMC subsurface are quite thin relative to the rest of the southern part of the state.

Figure 1-4 from Kolb et al. (1975) illustrates Frazier's 1967 interpretation of deltaic deposition in south Louisiana during the Holocene. Cross-sections along MRGO show thin intervals of multiple stacked lobes deposited by Bayou La Loutre starting about 4500 years ago.

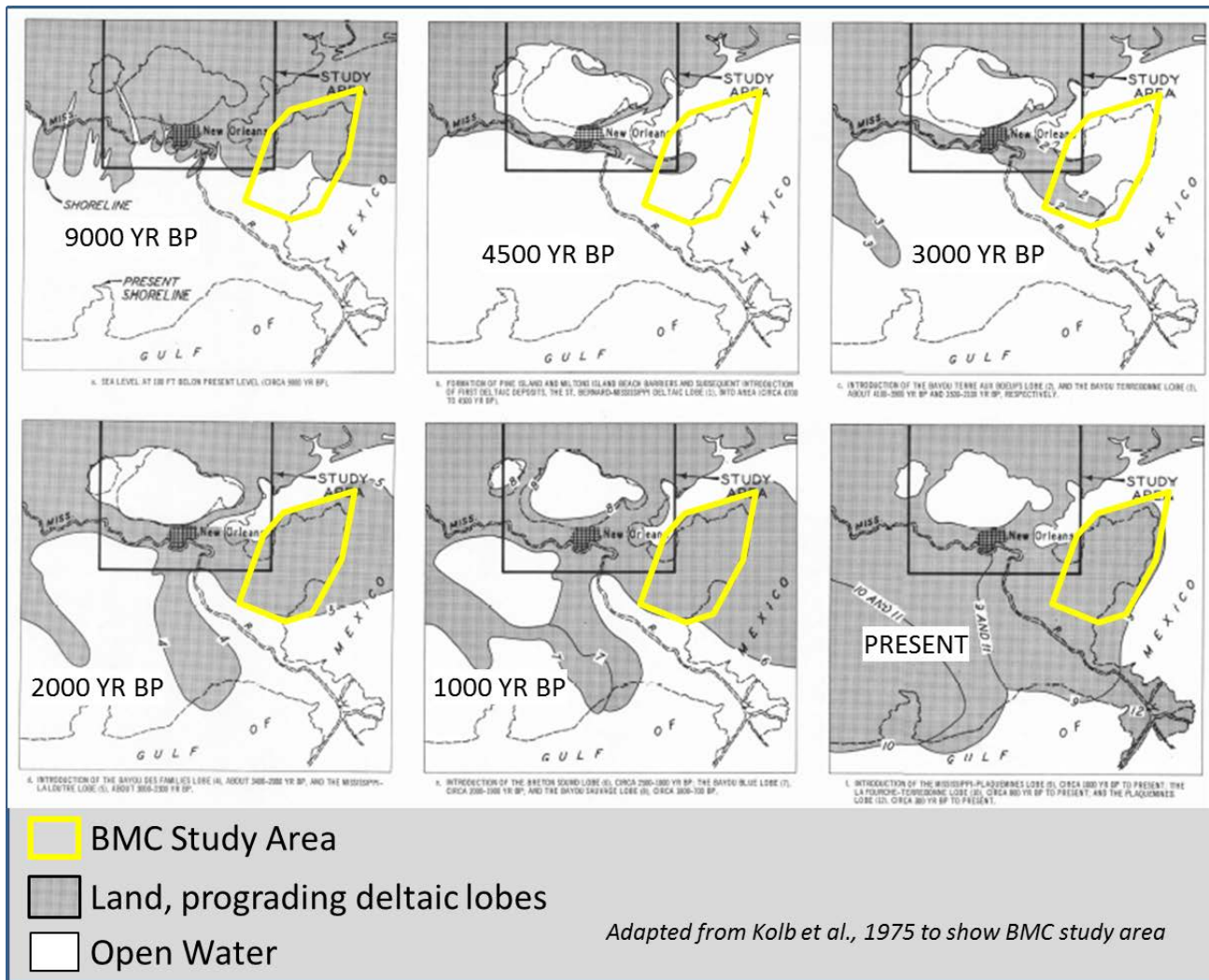


Figure 1-4: Based on Frazier's maps of deltaic deposition, this series from 9000 yrs bp to present by Kolb et al. 1975 shows how the greater Biloxi Marsh Complex, outlined in red, received sediment from the Mississippi River, particularly when the St. Bernard delta was most active (4,500-1,700 yrs ago) but even when other lobes (e.g. Lafourche, Balize) were the dominant deltaic system suggesting nearly continuous access to Mississippi River sediment through the Holocene.

Geologic faulting is well-known in the northern part of the Pontchartrain Basin (Flocks et al., 2009). Faults on the north shore of Lake Pontchartrain follow the edge of the Pleistocene terrace and form scarps visible on LIDAR. These faults are considered part of the Baton Rouge Fault trend, an extension of the Tepehate Fault zone that is roughly coincident with the Cretaceous Shelf edge west across Louisiana to Texas. A number of down-to-the south faults that trend west-east and are parallel to the Baton Rouge Fault trend were mapped on 2D and 3D seismic (Frank 2017, Lopez et al 1997, Kolb et al. 1975) within Lake Pontchartrain and Lake Borgne. Some of the faults in Lake Pontchartrain have Pleistocene and recent movement (Lopez 1997, Frank 2017) and are considered to be growth faults with active sedimentation filling in accommodation space on the downthrown side. Growth faults are characterized by thicker sedimentary section on the downthrown side of the fault as compared to the upthrown section of the same age and are well-known in the Louisiana subsurface.

It was noted early in the study of Louisiana coastal geology that deep faults may express as broad folds over the buried fault surface because of the young age and lack of compaction in the Holocene section (Fisk 1944). It is also true that by definition, a growth fault is syndepositional and some record of fault movement occurs at the surface and more sediment accumulates on the downthrown side. Depending on local conditions, multiple effects at the surface could result from fault-related causes (Heltz 2005, Yuill and Reed 2009, Gagliano 2003), but at the surface, fault zones are best considered as lines of demarcation between larger-scale provinces with different characteristics. Rates of compaction are greater in younger section (Kulp 2000), leading to the observation that near-surface processes act on faster time scales than geologic processes (Reed and Yuill 2017). Lithology can have a large influence on rate of compaction of shallow sediments as well (Meckel et al., 2008). A sandy channel and a peaty swamp will behave very differently when buried in the near-surface. The channel will remain relatively intact while compaction of peat can account for local subsidence rates several times higher than Holocene-averaged basin subsidence rates (VanAssellen 2011). Of course, in active depositional settings, fault scarps are likely to be buried and other geomorphic features may be the best indication of fault influence at the surface in the absence of examination of the near-surface with seismic or sediment borings. Clearly, an understanding of the relative subsidence characteristics on either side of a suspected fault zone will benefit from a better understanding of the possible fault pattern gained from geophysical interpretation of the subsurface as presented in the next section.

Chapter 1: SEISMIC EVALUATION OF THE BMC

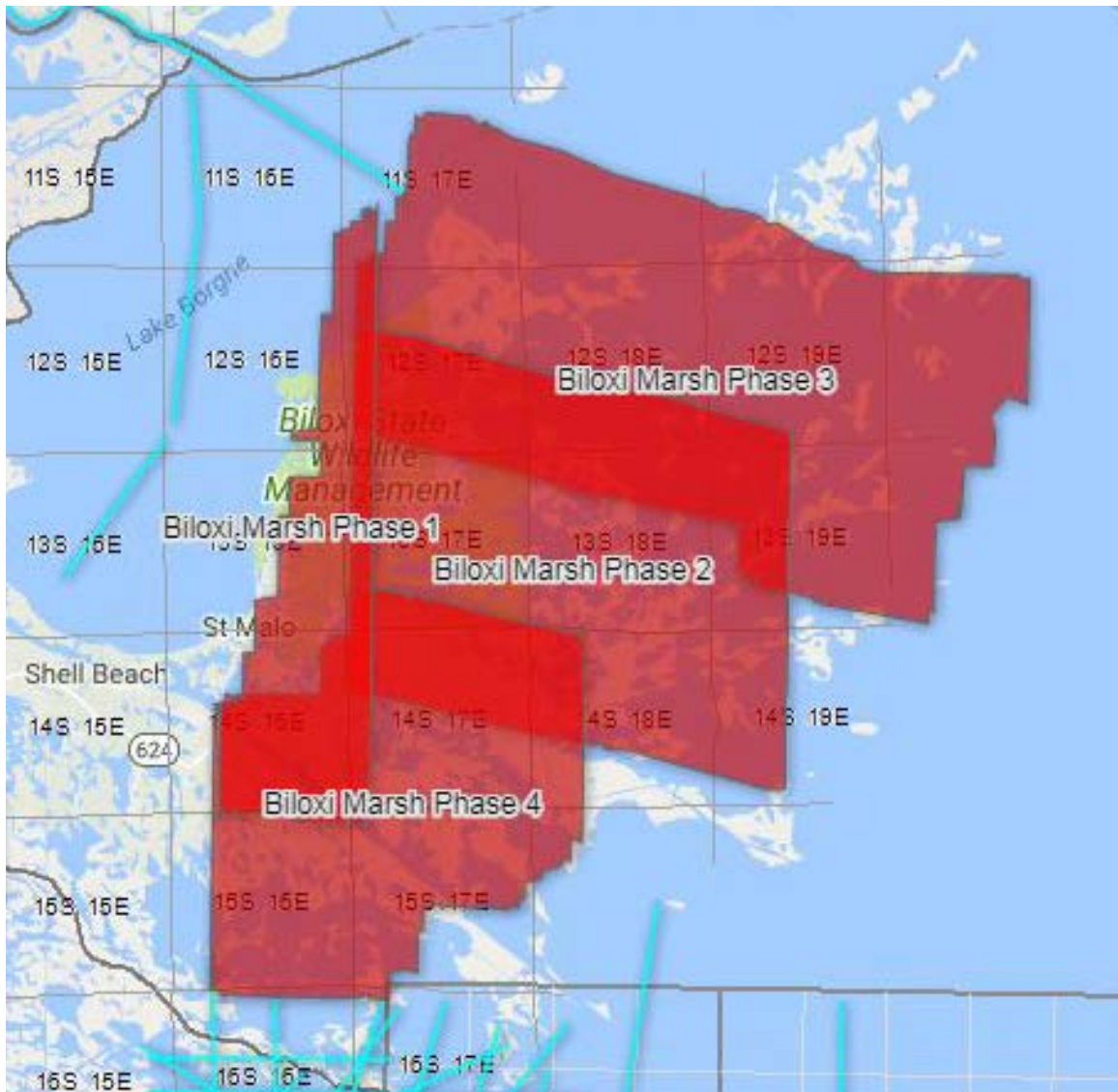


Figure 1-5: 3D Seismic data from Seitel. Data cut out areas are not shown.

Energy industry subsurface data offers important insight into age and lithology of subsurface strata. 2D lines and 3D seismic volumes are used to map structures of sedimentary horizons, faults, salt domes, and other features, while well logs are better suited to detailed lithologic analysis. As property and mineral rights owners, BLMC and LKEU have access to 3D seismic data gathered by Seitel that covers much of the BMC (Figure 1-5). This data forms an integral part of the analysis of the deep subsurface structure and confirms the general structural elements described in regional maps shown in this report.

In the course of his work, geologist Richard Provensal, PG (pers. comm. 2017) used the Seitel 3D seismic volumes and well data to prepare an interpretation of fault trends and older mapped horizons. In the deeper section, the Late Cretaceous is encountered as shallow as 16,000 feet, salt mobilization is limited, and bedding is observed to be largely

horizontal since the middle Miocene, about 13 million years ago, with a slight tilt to the south, roughly parallel to the Cretaceous shelf edges. Limited growth faulting is observed in the middle Miocene to Pliocene section and bed thickness is observed to increase slightly, progressively to the south across each fault segment.

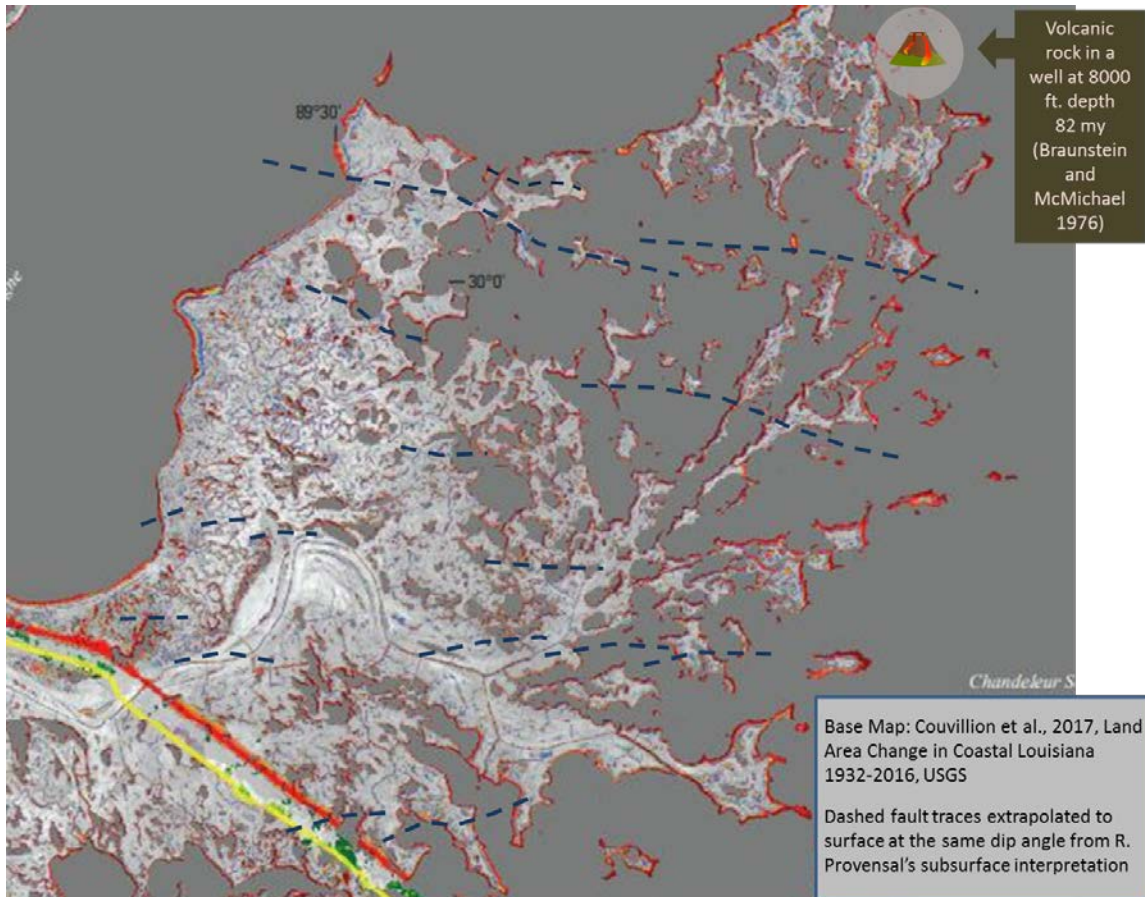


Figure 1-6: Projected traces of subsurface faults from 4000'+ and deeper on Couvillion et al., 2017 map of persistent land loss 1932 - 2016. Faults are on trend with faults of similar character observed on seismic in Lake Pontchartrain (Kindinger et al 1975, Lopez 1996) and Lake Borgne (Franks and Kulp 2016).

In the geophysical evaluation, a few of the faults appear to cut the subsurface as shallow as 0.5 sec., about 1500 feet. While clear fault planes to the surface are difficult to map, we have extrapolated the fault planes to the surface by following the trace of the fault at the same dip angle to provide a template of where surface effects of fault movement could be evaluated if warranted. This method allows aspects of the surface geomorphology to be examined with respect to the extrapolated position of the fault traces and is clearly better than examining surface features alone in the quest to evaluate tectonic subsidence.

Superimposing these projected fault traces onto the Couvillion et al. (2017) persistent land loss map allows for a direct comparison to fault trace locations (Figure 1-6). It is unknown at this time whether the subsurface faults actually extend to the surface or whether movement along them has occurred in the Holocene. All of the faults are down-to-the-

south and trend nearly parallel to one another. Fault segments in the northern part of the complex are several miles long while those in the south appear in groups of 2 or 3 and are considerably shorter – about a mile. Though there are some interesting marsh breaks that appear to line up with the fault trends, it is difficult to see any consistent land loss pattern that could be tied to Holocene fault movement on this map montage. To the northeast, the position of an 82-million-year-old volcanic feature at about 8000 feet is also shown (Braunstein and McWilliams 1974). A poorly characterized geologic body, which if laterally extensive, could add to the observed stable character of the platform. Interestingly, Fisk's (1944) speculation that the big bend in the course of Bayou La Loutre could have some fault control seems to bear out as fault groups west, north, and east of the bend are in a position to possibly control the shape and extent of the bend.

Chapter 1: REGIONAL COMPARISONS

As shown in Karlo and Shoup 2001 (Figure 1-2), the southern part of the BMC is within the most northern reaches of the Louann Salt in south Louisiana, in a province characterized by thin salt at the base of the section which largely remains buried and does not mobilize. While this salt plays a role in some tectonism, its role is limited, especially when compared to areas to the south, where salt tectonic activity in the subsurface is known to cause extensive deformation of sedimentary layers near salt features. General faulting patterns set up in the subsurface long ago are observed on seismic data to extend from great depths to near-surface, reflecting that long-term activity created fault zones (Gagliano et al, 2003). Some of the salt domes in south Louisiana are known to have affected Holocene deposition (Heinrich et al., 2013) suggesting that salt tectonic processes continue to be active today.

Energy industry interpretation of the subsurface on regional seismic lines shows the contrast between the ancient rocks underpinning the BMC and the more active tectonic setting to the south. The regional seismic-based cross-section (Fig. 7, simplified from Schuster 1995) is based on deep-imaging energy industry seismic and extends N-S from west of the BMC in Lake Pontchartrain to the Louisiana coast near Port Fourchon. Faults are indicated as green and purple lines and sedimentary units of similar age are shown as colored bands. Salt is shown in magenta and is observed at depth, where some has remained in place at the base of the sedimentary section (more than 40,000 feet), and some has mobilized into domes in association with faults and salt evacuation surfaces.

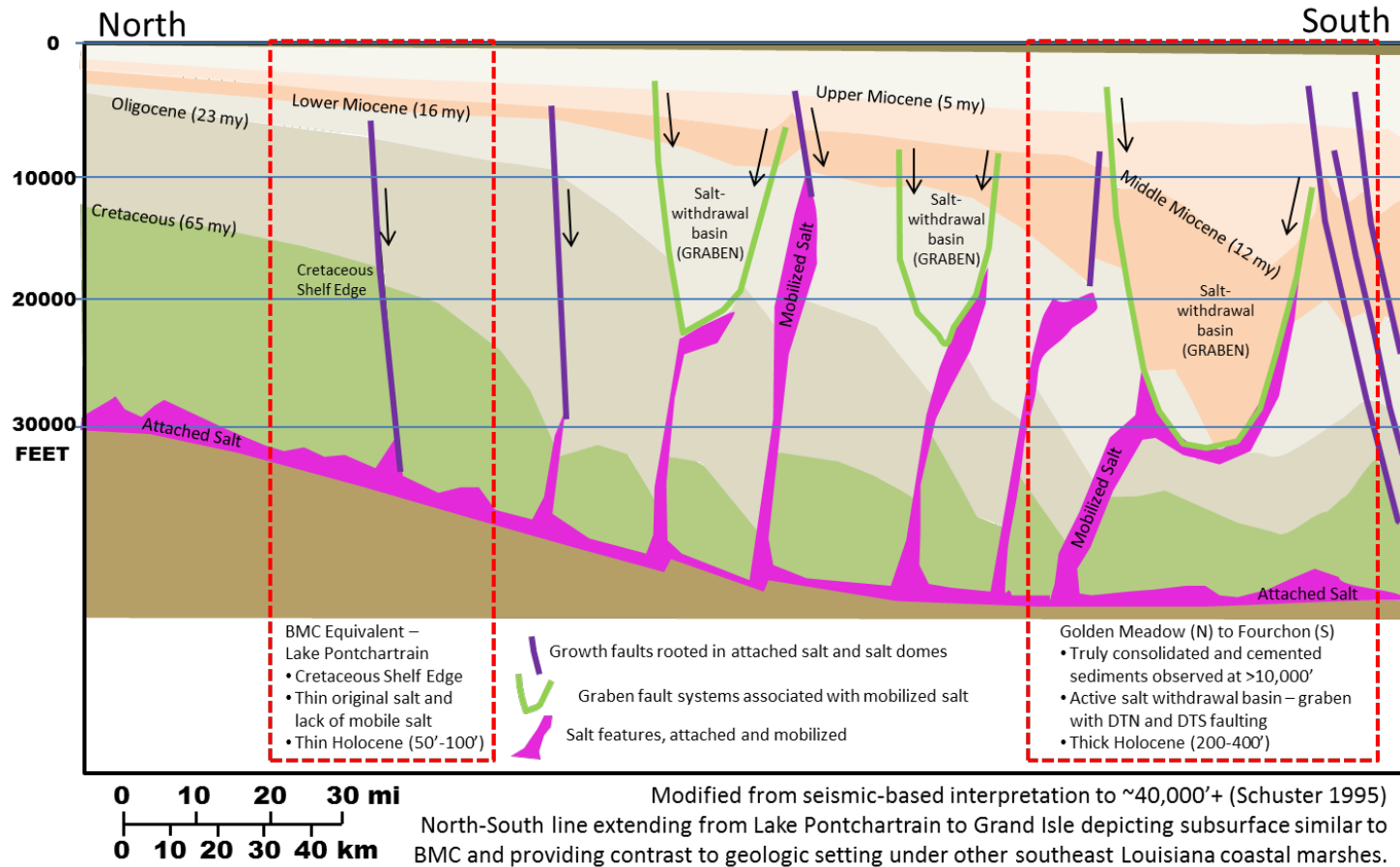


Figure 1-7 Simplified seismic interpretation of a north-south line extending from just north of Lake Pontchartrain to coastal Louisiana just east of Fourchon (see Figure 1-2 for location). Sedimentary layers are colored according to geologic age and the age at the top of the section is identified. Pliocene (5-2my) and Holocene/Pleistocene sediments (thin brown wedge at the top) fill in the uppermost part of the section above the Upper Miocene. Holocene thickness is 50-100' in the BMC and up to 400' thick in rapidly subsiding parts of the delta where salt is mobilized due to sediment loading and long-standing faults extend from depth to near surface.

Even though this discussion mostly covers processes that happened millions of years to thousands of years ago, the recent record of land loss in the BMC as recorded by 170 year-old survey maps (Cover Page) and aerial photo and topographic map-based assessments of persistent land loss (Figure 1-6, Couvillion et al., 2017) and causes of land loss (Figure 1-8, Penland et al., 2008, Day et al., 2019, Ch. 2 and 3 this report) reflects the comparatively stable base upon which the Holocene was deposited. In spite of its coastal position and exposure, the BMC is observed to remain largely intact and relatively unchanged. Wetland loss in the BMC occurs peripherally along its Lake Borgne and Chandeleur Sound shorelines and occurs as enlargement and deepening of interior marshes, ponds, and lagoons as discussed in Day et al. (2019, Ch. 2 and 3 this report), though increased hydrologic connection to Lake Borgne is accelerating this process. In contrast, land loss processes due to near-surface compaction and tectonic subsidence are far more prevalent south of the BMC, and it is not likely to be just by coincidence that these areas are also south of the Cretaceous shelf edge and the northern-most margin of salt-related structures in the subsurface (e.g. Eloi Bay and Chandeleur 25 Fields) east and south of the BMC in the “buried peripheral salt feature” province of Karlo and Shoup (1995). Land loss due to compaction and tectonic subsidence increase to the south where Holocene thickness is greater, and salt is more mobile in the subsurface.

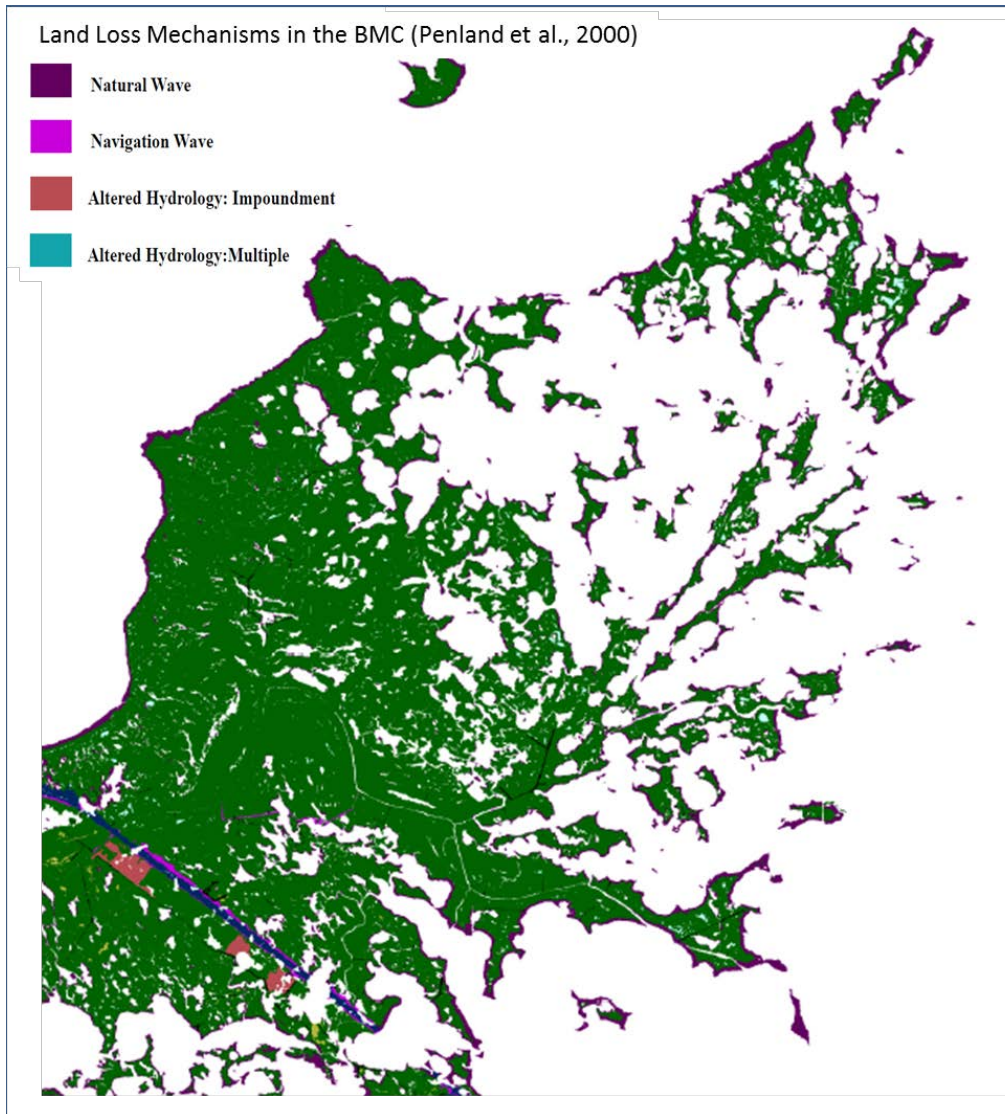


Figure 1-8 From Penland et al., 2000. Land loss in the BMC, while continuous since 1932 (Figure 1-6, Couvillion et al, 2017), is mostly related to shoreline erosion and marsh loss caused by direct removal initially, but later by hydrologic changes primarily due to MRGO and effects on salinity in Lake Borgne.

Chapter 1: CONCLUSIONS

Consideration of the subsurface, whether shallow or deep, is crucial to gain understanding of subsidence in south Louisiana. Because of its setting in an active depositional basin, large-scale processes in place for millions of years continue today, and the evidence for this is recorded in the subsurface. Three main subsurface geological factors differentiate the BMC from other coastal areas:

- 1) Thin original salt thickness,
- 2) Coincidence of the Lower Cretaceous shelf edge with the location of the BMC, and
- 3) Comparatively thinner strata of the younger sedimentary units, particularly the youngest

and least consolidated Holocene sediments.

The BMC lies atop and adjacent to an ancient carbonate platform that provides a stable base. This stable base makes it less subject to active deep subsurface processes that are more pronounced to the south and southwest in the coastal areas of lower Plaquemines, Jefferson, Lafourche, and Terrebonne Parishes. Well-known hot spots of coastal wetland loss such as Bastian Bay, Golden Meadow, and Lake Boudreaux are underlain by thicker deposits of young sediments, active faulting, and in places, continuing salt flow deep in the subsurface that have been shown to contribute to subsidence and creation of new widespread open water areas (Gagliano, 2003, Roberts et al, 2008, Kuecher et al, 2001). In the BMC, millions of years of geological stability are reflected in the lack of significant growth faulting and comparatively thinner, flat-lying strata seen on seismic. Geologic stability also influences thickness of the most recent deposition in the BMC. The Holocene here ranges from 30 feet to 130 feet compared to other coastal marsh areas south and west of the BMC where Holocene thickness ranges from 150 feet to 400 feet (Figure 1-9, Kulp et al 2002). Notably, in all areas of thicker Holocene, unlike the subsurface beneath the BMC, seismic and well log data reveal that the subsurface is characterized by salt tectonics and a long history of syndepositional, near-surface fault movement.

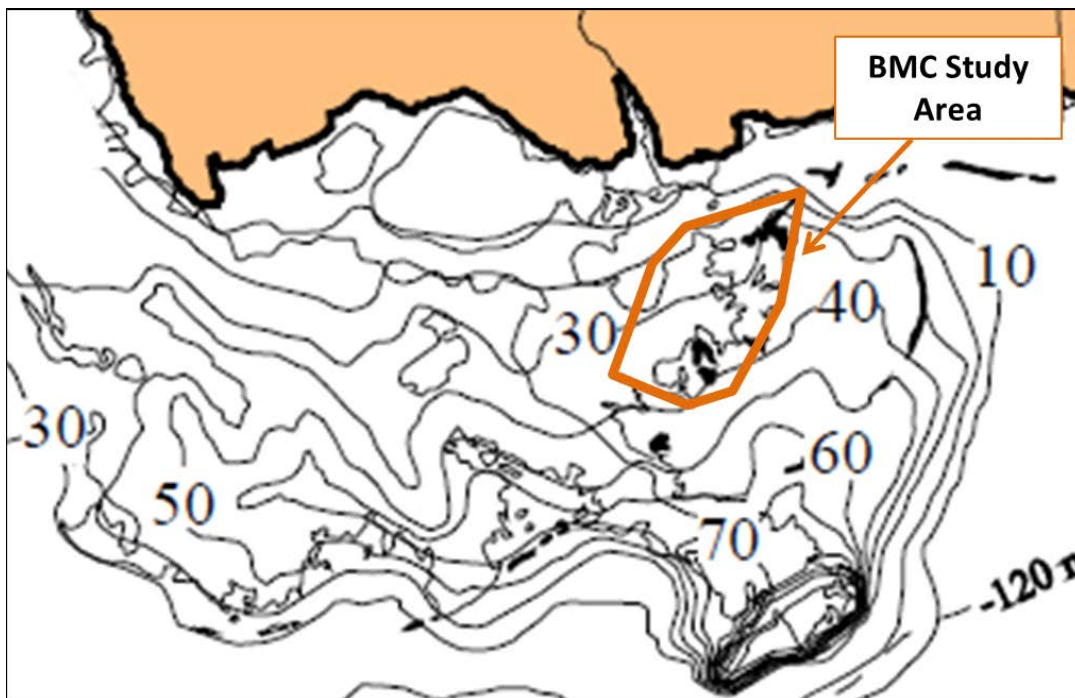


Figure 1-9 Isopachous thickness of the topstratum lithosome from Kulp et al., 2002 with generalized BMC study area indicated in red outline. The isopach represents the total thickness of Holocene and modern deltaic depocenters described by Frazier (1967) but includes some reworking during marine transgressions. Holocene thickness in the BMC is based on very few boreholes in this interpretation, most along the course of the MRGO. Holocene thickness in Jankowski et al. 2014 is similar but includes several more borehole sites, including CRMS stations around the periphery of the BMC.

There remains considerable debate on the amount of subsidence that can be attributed to fault activity versus near-surface compaction (Nienhuis et al., 2016, Olea and Coleman, 2013, Frederick et al., 2018), but in areas where salt mobility and thickness of sedimentary units are so closely linked, long-acting processes will be active during deposition of the youngest sediments as well as part of the ancient record. Thicker units of more compactible Holocene sediments in areas of fault-related subsidence will lead to more active near-surface subsidence processes when compared to areas with thin Holocene sediments like the BMC (Kulp et al., 2002). Geological stability in the BMC has had, and will continue to have, a profound effect on the ability of the marsh to maintain elevation such that inundation rates will remain low and marsh sustainability will be supported with much less effort and expense compared to areas that are more rapidly subsiding, whether related to near-surface or deep processes. Projects that take advantage of the high position and relative stability of the BMC like those outlined in Chapter 5 (and described in more detail in Appendices I, J, and K), can be expected to meet project objectives due to enhanced sediment retention, improved accretion, and less marsh inundation compared to areas subject to higher rates of shallow subsidence.

Chapter 2: Field Data Collection in the Biloxi Marsh Complex

John W. Day^{1,2}, G. Paul Kemp², and Robert R. Lane¹

¹Comite Resources, PO Box 66596, Baton Rouge LA 70896

²Dept. of Oceanography & Coastal Sciences, Louisiana State University, Baton Rouge LA 70803

Chapter 2: INTRODUCTION

In 2018, new data relevant to subsidence, marsh stability, and sea level rise throughout much of the BMC was gathered. This newly gathered data was added to existing datasets which reflect decades of data acquisition (Rounsefell, 1964). These new data were gathered to establish a present-day view of the health of the marsh in the BMC and establish baseline observations of salinity and water quality pre- and post-MRGO closure. Accretion and erosion rates were also updated at study sites in the marsh and along shorelines. Additional accretion and elevation change data using permanent observation sites (SET and CRMS data stations) are presented and discussed in Chapter 3 in the context of results of Chapter 2. Areas of active accretion accompanied by elevation gain would be expected to be more resilient to sea level rise, while erosion, bank collapse, or subsidence resulting in increased marsh inundation would be expected to lead to marsh loss and submergence. These data assisted in our efforts to find where the marsh is building land through accretion, where it is gaining elevation, and the root cause of land loss. The information was used to develop appropriate mitigation and restoration methods as outlined in Chapter 5, and to develop projects like the BMC Integrated Project (Appendix I) and other projects presented in more detail in Appendices J and K.

Chapter 2: METHODS

We carried out a yearlong study of marsh edge erosion and accretion during 2018 at locations in the marsh interior, as well as on the shorelines of Lake Borgne, Lake Robin, and Chandeleur Sound (Marsh Study Sites, Figure 2-1). This data is correlated with hydrology measurements using a combination of continuously operating fixed water level and salinity sensors, as well as water quality measurements taken periodically at historical water quality sites that were first established by Rounsefell (1964) in the early 1960s, prior to opening the MRGO. The Lake Pontchartrain Basin Foundation (LPBF) has also collected salinity data at the Rounsefell sites since 2013 on a monthly schedule as part of the Hydrocoast Program and has kindly supplied the relevant data at these sites (Lopez et al. 2015). Water quality data was collected by BLMC personnel at these and several additional locations using a multi-probe instrument as they patrolled the property.

Marsh Study Site Selection

The nine Marsh Study sites (Figure 2-2) fall into three categories that were identified based on apparent differences in the marsh degradation and land loss mechanisms operating in each (Table 2-1) including wind conditions, wave energy, and proximity to erosive channel systems. Thus, the three categories reflect the primary factors that impact marsh sustainability in the area. Location accessibility and property ownership were also a

consideration in the choice of appropriate study sites.



Figure 2-1. Marsh Study sites (black pentagons) on Biloxi Marshlands and Lake Eugenie properties shown against a backdrop of 1932 to 2016 persistent land loss mapped by Couvillion et al. 2017. Lake Borgne and Chandeleur Sound shorelines exhibit retreat over the last 90 years which shows up in bands of color, while interior loss tends to be scattered. Map from https://lacoast.gov/crms_viewer/Map/CRMSViewer

The first category of Marsh Study sites (A-Series) targets wetlands facing large bodies of open water where wave energy is expected to be high under southwest to west (A1a-c), southeast to southwest (A2), and north to northeast (A3) wind conditions, along the shorelines of Lake Borgne, Bay Eloi, and Lake Robin, respectively (Figure 2-2). The Lake Borgne shoreline (Sites A1a-c) is particularly subject to peripheral erosion during seasonal cold front passage and the accompanying strong northwest winds. B-Series stations are in interior marshes facing large ponds where wave energy is fetch and depth limited. The greatest fetch was from the northeast to southeast for B1 and from the northwest to southwest at B2. The final group (C-series) includes marshes adjacent to channels that are experiencing tidal scour and expansion. C1 is located just north of the Bayou La Loutre ridge on a pass connecting growing lakes in the vicinity of Stump Lagoon (Figure 2-2). C2 is located on the north bank of the MRGO about 6 km east of the 2009 US Army Corps of Engineers (USACE) dam, where hydrology is controlled by Chandeleur Sound. Low bottom oxygen has been reported from the de-authorized navigation channel on the Chandeleur Sound side of the barrier, indicating the presence of density stratification and lack of water circulation.

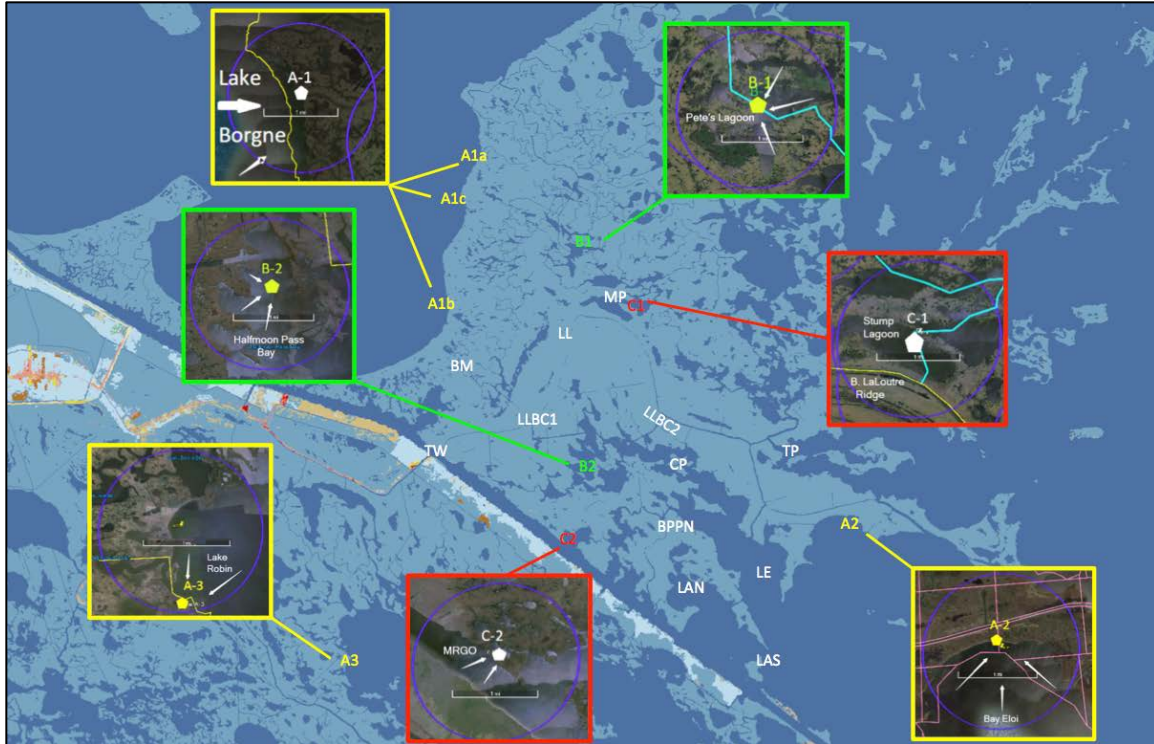


Figure 2-2. Marsh and Shoreline Study sites on Biloxi Marshlands and Lake Eugenie properties (yellow, green and red labeled sites). Arrows indicate likely directions of wave attack. White labeled sites are Rounsefell's water quality sites that were monitored for this study.

Table 2-1. Representative Marsh Study Sites

| |
|----------------------------------------------------------------------------------------------------|
| Representative Study Area A |
| A1 – (3 sites: A1a, A1b, A1c) Lake Borgne between Bayou Grande and Pointe Aux Marchettes |
| A2 - Eloi Bay Area |
| A3 - Lake Robin/Lake Coquille Bay Area |
| Representative Study Area B |
| B1 - North of Bayou La Loutre – Pete's Lagoon or Cutoff Lagoon |
| B2 - South of Bayou La Loutre – Little Halfmoon Bay (Halfmoon Pass Bay) |
| Representative Study Area C |
| C1 - North of Bayou La Loutre; waterways running between Bayou La Loutre/Stump Lagoon |
| C2 - South of Bayou La Loutre; Bayou Pisana below the dam in MRGO (dead water zone below MRGO dam) |

At each Marsh Study Site, ten PVC poles were placed as reference points for establishing the position of the top of the marsh scarp. Accretion plots were established at 5 m, 25 m, and 50 m from the marsh edge (Figure 2-2, Appendix A: Table A1). A water level staff gauge was installed at each study site, and continuous pressure sensing water level recorders were deployed at sites A1b, C2 and A3 relative to a barometric pressure reference. Conductivity and water temperature sensors were deployed at sites A1b and C2. Approximately every two months the Marsh Study sites were visited to record staff gauge levels, download water level and conductivity recorders, take water samples for total suspended sediments, and record Secchi depth and oceanographic information using a multiprobe (temperature, conductivity, dissolved oxygen). Twelve Rounsefell water quality monitoring stations were also monitored though no marsh data were collected (Figure 2-2).

Salinity and other Physical Oceanographic Measurements

Discrete water quality parameters were measured at the twelve Rounsefell sites and directly adjacent to the nine study sites on five occasions on February 20-21, April 25 and 27, June 26, September 12, and November 16, 2018. Additional measurements were made during site visits on March 2, 8, July 5 and August 13, 2018. Conductivity, salinity, temperature, and secchi depth were measured at the 9 marsh stations and the 12 locations that Rounsefell (1964) established during his 1959 to 1961 study of pre-MRGO estuarine conditions (Figure 2-2, Appendix A: Table A2). Conductivity, salinity, and temperature were also measured with a hand-held multimeter as time and routing permitted. Water clarity was measured with a secchi disk. Water samples were collected and brought back to the laboratory to determine total suspended sediments concentration after filtering 500-900 mL of sample water through pre-rinsed, dried, and weighed 47 mm 0.7 μm Whatman GF/F glass fiber filters. Filters were then dried for 1 hour at 105°C, weighed, dried for another 15 minutes, and reweighed for quality assurance (APHA 2005).

Continuous Water Level & Conductivity Probes

Water level relative to the wetland surface is a key diagnostic that controls sediment and nutrient availability to the marsh platform. ONSET HOBO[®] water level recorders were deployed at 3 sites (A1b, C2 and A3) and conductivity-temperature probes were deployed at 2 sites (A1b and C2). The probes deployed at each site were capable of recording every 15 minutes up to a year without maintenance. These probes provided key information regarding rates of inundation of marshes through comparison and analogy to nearby tidal gauges. The instruments were serviced during site visits to download data and inspect the instrument package for damage or fouling. Water level was read from staff gauges during site visits along with conductivity for salinity. Downloaded probe readings were calibrated against standards via simple linear regression using JMP statistical software produced by SAS Institute, Inc. (Sall et al. 2012). Elevation surveys were carried out in order to calibrate the gauge and water level meters to the marsh surface elevation. Surveying equipment was used to measure relative elevation at 5 m, 25 m, and 50 m into the marsh as well as at the edge of the water and staff gauge. Conductivity/salinity data from Rounsefell (1964) and from the LPBF (2013-2017) was compared with water quality data collected in 2018.

Soil Bulk Density

Soil bulk density is a measure of the density and strength of marsh soils and thus their sustainability and ability to recover after storms. High bulk density soils have been shown to speed plant recovery and boost productivity after hurricanes, droughts and other stressors (DeLaune and Pezeshki 1988). Generally, higher bulk density wetland soils are the result of sediment and clay deposition, which when incorporated into living marsh root structure forms a stable and resilient marsh platform. Bulk density samples were collected at the 25 m marker on each marsh traverse associated with Marsh Study sites. Sediment samples were taken using a 60 ml plastic syringe with the top cut off to act as piston corer with a calibrated extruder. The cores were placed into labeled plastic bags and put in a cooler for transport to the laboratory where they are refrigerated until processing. Soil samples then were weighed before and after being dried at 80°C to a constant weight. The weight difference between wet and dry samples was used for determining water content, and bulk density was based on the dry weight and the volume of the sample (Brady and Weil 2001; NRCS 2011).

Species Composition

Floral species composition based on relative dominance was assessed using the Braun-Blanquet method (Poore 1955; Kent and Coker 1998). Species composition provides information about the recent salinity history of the different sites. It also sets the context to judge the impact of MRGO closure on vegetation change. Species composition, in order of dominance, was done first for the general region to establish which species were present at the time of observation, followed by three visual plots where species composition and percent cover were recorded. Cover is the area of ground within a quadrat, or defined area, which is occupied by the aboveground parts of each species when viewed from above.

Shoreline Erosion

At each of the nine Marsh Study Sites, the edge of the waterway/wetland was marked using PVC marker poles. Each location was delineated with ten poles set directly at the wetland-water interface where there is usually a sudden drop off in elevation (scarp face). The spacing of the poles was approximately every 2 to 3 m in a line parallel to the shoreline. The rate of erosion was calculated as the mean distance between the pole and the wetland edge divided by the time since installment.

Marsh Accretion

Feldspar marker horizons were deployed at the nine wetland monitoring sites at 5 m, 25 m and 50 m along a traverse extending inland and perpendicular from the shoreline edge or bank. Powdered feldspar clay was laid on the wetland surface 1 cm thick in 0.66 m² plots (Cahoon and Turner 1989). The thickness of material deposited on top of the feldspar marker was measured using shovel and machete to reveal the marker horizon at the conclusion of the nine-month data collection period (Lane et al. 2006). The rate of vertical accretion was calculated by dividing the thickness of material above the surface of the marker horizon by the time since the feldspar was deployed.

Chapter 2: RESULTS & DISCUSSION

Salinity Monitoring Post-MRGO Closure

It is well-documented that the BMC has been and continues to be severely damaged by the construction and the more than 4 decades of operations of the MRGO navigation channel (Schaffer et al. 2009). In the BMC, most of the impacts of channel operations and maintenance were due to saltwater intrusion facilitated by the direct connection of flow between Chandeleur Sound, Lake Borgne, and Lake Pontchartrain (Poirrier 2012). The high amount of water flowing through the MRGO channel, in conjunction with internal changes to the tidal channel network, led to changes in the hydrology and salinity of the BMC and internal marsh erosion.

In Lake Borgne and throughout the BMC, the salinity has lowered by about 5 ppt and rapid salinity swings of more than 10 ppt over a few days have become less frequent since the MRGO closure dam at Bayou La Loutre was completed in 2009 (Swarzenski and Mize 2014). Spikes of 15 to 20 ppt were common in Lake Borgne prior to closure, and salinity now rarely exceeds 10 ppt. Salinities in the MRGO below the dam have increased, however, and are now as high as those in Chandeleur Sound (Swarzenski and Mize 2014).

Rounsefell's (1964) original data (Pre-MRGO, 1959-1961) were compared with data collected by LPBF Hydrocoast (2013-2017) and data collected as part of this study (February to November 2018) (Figure 2-3). Post-MRGO closure salinity means are still 1 to 2 ppt higher than those reported by Rounsefell (1964), but differences between the pre-MRGO and the two post-closure datasets fall within natural variability.

The linear salinity gradient is slightly steeper west to east for the pre-MRGO study (0.63 ppt/km, $r^2 = 0.95$) while the two post closure datasets yield identical 0.5 ppt/km gradients (LPBF, $r^2 = 0.92$; Comite, $r^2 = 0.88$). So, mean salinity today increases 0.5 ppt per kilometer with distance from Lake Borgne, the source of low salinity water to the BMC. Since closure of the navigation channel has removed a significant source of salt to Lake Borgne, salinity there is once more controlled by freshwater discharges of the Pearl River and smaller streams emptying into Lakes Maurepas and Pontchartrain. Neither of the two post-closure datasets includes a year when the Bonnet Carré Spillway was opened, but USGS data from 2011 shows that Lake Borgne salinity dropped almost to zero ppt during that high river opening (Swarzenski and Mize 2014). The mean salinity for Lake Borgne ranges from 4 to 6 ppt in all three datasets, suggesting that with respect to salinity, the Lake has nearly returned to a pre-MRGO condition (Figure 2-3). The Chandeleur Sound salinity end member continues to be governed by Mississippi River discharge and shows more variability, with mean salinity for the three datasets ranging from 15 to 18 ppt.

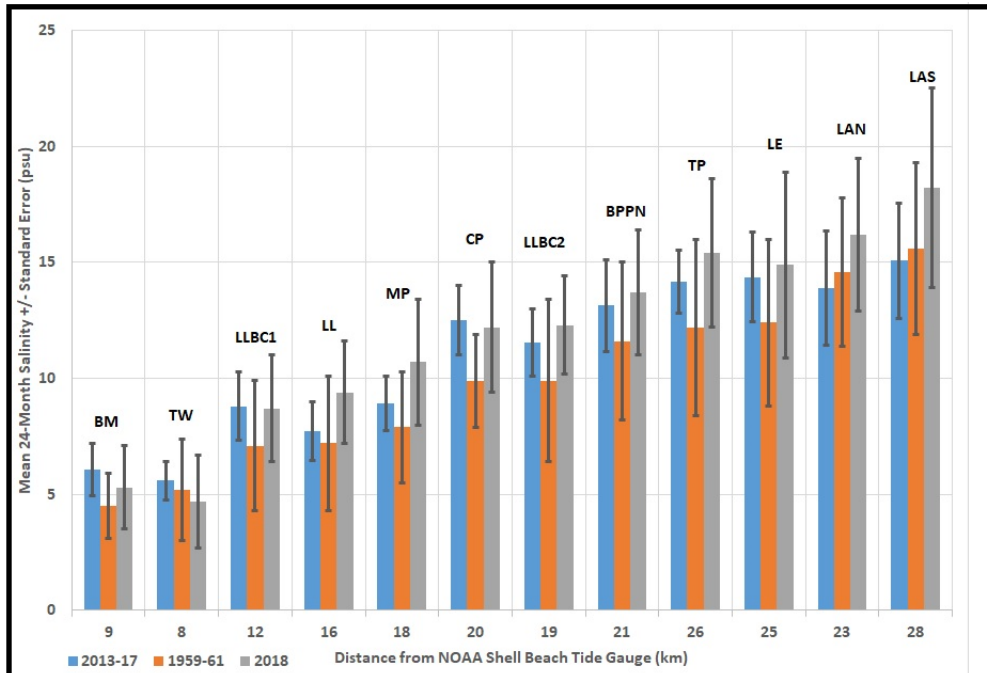


Figure 2-3. Comparing salinity at sites established by Rounsefell (1964) from 1959-61, Lake Pontchartrain Basin Foundation (LPBF) from 2013-17, and from this 2018 sampling. Stations are ranked by distance from the NOAA Shell Beach Gauge at the south end of Lake Borgne. No significant differences between the three datasets were detected.

Salinity change and flora and faunal species response

As the salinity adjusts to pre-MRGO levels, less salt-tolerant vegetation species, including Roseau Cane and Cattails, were observed recolonizing some areas of the western half of the BMC (Kemp and Day 2017). These plants were quite widespread in the BMC before construction of the MRGO (Wright et al. 1960). Also, live oak trees along Bayou La Loutre that appeared dead for years are sprouting new leaves. Given the return of Lake Borgne to pre-MRGO salinities, a recovery of the lake bottom clam *Rangia cuneata* can also be forecast (Poirrier 2013). The loss of the *Rangia* clam beach berm along the western shore of the BMC continues to have an increasingly deleterious effect on hydrology, opening pathways for Lake Borgne waters to enter the marsh through exposed bayous and newly formed tidal channels that in themselves pose a risk to interior marshes. The western BMC, particularly along the shoreline of Lake Borgne, has experienced a significant amount of land loss directly as a result of MRGO and the loss of the natural shell berm. As the *Rangia* population recovers, a process that can be accelerated with management (Poirrier, 2019), new shell for future beaches should be available, which can slow down shoreline retreat.

Near-surface compaction and local subsidence

The BMC provides excellent examples of how local rather than regional or global factors tend to dominate both marsh submergence and shoreline retreat. The direct effect of the loss of shell material in Lake Borgne available to be redeposited on beaches and shoreline protection has already been noted. But effects of underlying shallow geology on marsh submergence have received less attention, though they were well documented by Russell

et al. (1936) and his doctoral student R.G. Treadwell (1955), who spent much time in the BMC long before the construction of the MRGO.

The presence of elongate ponds, often called “lagoons,” in the back swamp position on either side of the Bayou La Loutre ridge is evidence of a localized component of subsidence that occurs parallel to the partially buried natural levee flanks of abandoned distributary channels (Figure 2-4) and leads to a phenomenon called levee flank depression (Treadwell, 1955). Locally distributed lithologic differences between the 50 feet to 100 feet thick sandy channel system of Bayou La Loutre and the clay- and organic-rich bays and swamps adjacent to either side of distributary channels are responsible for their development. (Figure 2-4). Clays and peat deposited in interfluvial areas are highly compactible while sandy channels are relatively non-compactible (Meckel et al. 2007). Organic materials like peat are especially compactible due to high water content and susceptibility to degradation, thereby setting the stage for channel-parallel land submergence. Ponds formed in this way often lack hydrologic connections to other water bodies (Treadwell 1955), a feature that further emphasizes the typical isolation of these interior ponds and local influence of levee flank subsidence patterns. The levee flank lagoons associated with Bayou La Loutre have irregular outlines that have changed surprisingly little since the late 1930s (Figure 2-4), though erosion of the low marsh banks by fetch- and depth-limited waves and by boat wakes has gradually led to enlargement, typically on the side away from the Bayou and closer to Lake Borgne or other open water areas.

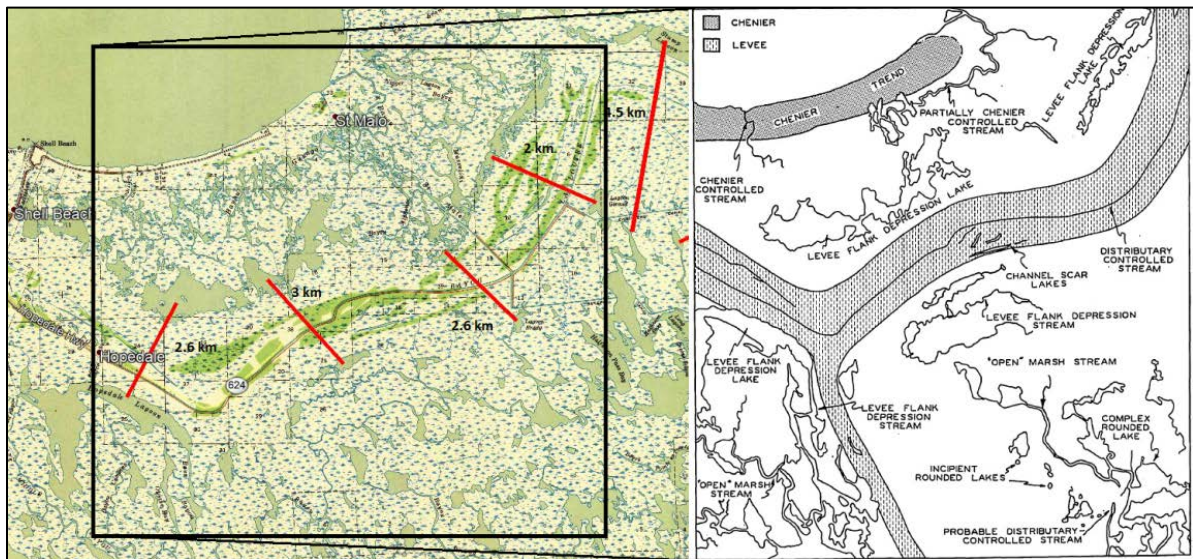


Figure 2-4. Diagram from Treadwell (1955) on right labelling “levee flank depressions” and other water features adjacent to Bayou La Loutre from a section of the 1941 USGS Shell Beach 15-minute quadrangle. Red traverses are labeled with the distance between depressions on opposite sides of the former distributary channel ranging from 2.0 to 4.5 km.

On the 1848 GLO survey map (Cover Page), many of the lagoons that later showed up as waterbodies were described as prairie, palmetto swamp, and marsh, suggesting

development of these ponds happened rapidly and with little effect on marshes outside their immediate vicinity. Gagliano et al. (2010) determined the Great Hurricane of 1915 accelerated pond formation, and Couvillion et al. (2017) revealed that the ponds were well established by 1932. Organic-rich, low-density marsh susceptible to detachment and displacement by wind and wave-driven shear forces during storm events can account for the rapid development of certain ponds in the BMC interior. Stump Lagoon in particular is an area described as prairie in 1847 but which became a well-established open water lagoon by 1932. The Great Hurricane of 1915 is a very plausible cause, but muskrat eat-outs or natural peat burns are also considered as possible triggers for the rapid conversion of prairie to open water in the Stump Lagoon area (Gagliano et al., 2010). The lack of systematic land loss along the edges of Stump Lagoon (Couvillion et al. 2017) suggests that whatever caused the conversion happened quickly in one event since for the most part, the record indicates little change in the shape or shoreline position within Stump Lagoon over the past 90 years.

Bulk Density/Soil Stability

Bulk density is an important diagnostic integrator of wetland soil accretion, strength, mineral content, and organic matter accumulation, as well as carbon sequestration. All these parameters play a role in wetland sustainability. Mean soil bulk density is generally greatest in salt-tolerant marshes ($0.24 \pm 0.11 \text{ g/cm}^3$) with progressively lower values from brackish ($0.16 \pm 0.07 \text{ g/cm}^3$) to fresh ($0.08 \pm 0.05 \text{ g cm}^{-3}$; Nyman et al. 1990). This is related to a considerable degree to the mineral sediments deposited on the marshes during storms.

Spartina alterniflora marsh requires a bulk density of approximately $0.20\text{-}0.30 \text{ g/cm}^3$ for vegetation to become established and remain stable (DeLaune et al. 1990; Delaune & Pezeshki 2003). If such marshes are not supplied with sufficient inorganic sediment (sand, silt, clay), those with bulk densities lower than 0.2 g/cm^3 will likely decrease in surface elevation relative to the tidal frame, and eventually convert to open water (Day et al. 2011). Also, lower bulk density soils are more buoyant and prone to rip-up by storm surge and waves (Boesch 2006b), or conversion into floating marsh where sufficiently sheltered from waves. This is because a large portion of the volume of these low-density marsh soils is actually void space occupied by water and entrapped gases (Day et al. 2011; Delaune and Pezeshki 2003; Sasser et al. 1995).

Considering that the Marsh Study sites were selected in order to observe a variety of potential marsh degradation and land loss mechanisms, large variation in soil bulk density corresponding to setting were expected. Using the 0.20 g/cm^3 criteria outlined above, bulk densities at sites B1 (0.12 g/cm^3), B2 (0.11 g/cm^3) and C1 (0.07 g/cm^3) indicate that degradation or lowering of elevation is already affecting the sustainability of these salt marshes (Appendix A: Table A3). The endangered sites are in interior wetlands near ponds and lagoons parallel to Bayou La Loutre (Figure 2-4) that are connected by tidal channels to other waterways. Sites A1a and A1b on the Lake Borgne shore, in contrast, had intermediate bulk densities of 0.21 and 0.24 g/cm^3 , respectively, while stations A2, A3, and C2 on the shores of large saltier bays on the eastern side of the BMC had bulk densities ranging from 0.33 to 0.36 g/cm^3 . The highest soil bulk density came from site A1c (0.45 g/cm^3) behind a rock berm placed in 2014 as part of PO-72, where a significant amount of shell was incorporated into the soil profile. So, there appear to be steps in the bulk densities,

and therefore, the strength of these soils that are derived from the positions of each relative to wave energy and availability of coarse shell material. Parts of the BMC that do not have access to high density mineral material from either peripheral lakes or Chandeleur Sound are the most susceptible to shallow compaction, marsh loss and require critical attention.

Species Composition

The study sites along the shore of Lake Borgne (A1a, A1b & A1c) were dominated by *Spartina alterniflora* at the marsh edge and then *Spartina patens* with distance from the edge of the water (Appendix A: Table A4). This pattern was also observed at study sites B1 and C1. A different association was found at sites A2, B2 and C2 where *Juncus roemerianus* was dominant with some *Spartina alterniflora* and *patens* present (Appendix A: Table A4). All sites are considered saline to brackish marshes.

Shoreline Erosion

Shoreline erosion was observed to be highest along unprotected shorelines such as Lake Borgne, and lowest at interior marsh settings without large fetch. Interestingly, there was shoreline advancement behind a recently installed rock revetment along the western shoreline of the BMC with Lake Borgne. The highest March to November marsh edge erosion (283.3 cm) was found at A1a, the northernmost Lake Borgne shoreline site (Table 2-2), twice the transgression at A1c, the other unprotected Lake Borgne site (121.7 cm). These convert to annual retreat rates of 4.0 and 1.7 m/y. Sites A2 (1.8 m/y), A3 (1.4 m/y) and C2 (1.8 m/y), are adjacent to large water bodies, though on the east and south sides of the BMC. But the most interesting result occurred at A1b, which is a Lake Borgne shore site similar to A1c that is, however, protected by detached rock breakwaters. There, the shoreline advanced into the lake (Figure 2-5), which is indicated by a negative retreat rate -1.2 m/y (Table 2-2). Interior marsh sites B1, B2 and C1 had much lower shoreline translation rates, reflecting the much lower wave energy. B1 was the lowest, at 0.13 m/y, while B2 and C1 both retreated at 0.37 m/y.



Figure 2-5. Shoreline advance at Site A1b where the marsh edge is protected from waves by detached shore parallel rock revetment.

Marsh Accretion

Overall, the BMC marsh sites are accreting at a very high rate, with results from the 5 m

plots ranging from 4.0 to 1.7 cm/y, and averaging 2.5 cm/y of accretion, excluding A1c which was buried under an anomalous 29.7 cm shell deposit (Table 2-2). Elsewhere, the highest accretion occurred at sites adjacent to large water bodies like Lake Borgne, Chandeleur Sound, and Lake Robin where storm waves coupled with wind-induced water level rise regularly suspends bottom sediments and conveys them onto the marsh surface. Sediment delivered in this way drops out of suspension as it moves inland from the marsh edge, so that the accretion rate is generally lower at 25 m and 50 m than at the 5 m plot. The accretion rate drop-off from 5 m to 50 m ranged from 37 to 83 percent with an average of 58 percent, except at A2 and A3 where accretion for the interior marsh plots was the same as at the 5 m mark.

Other than the shell deposit at A1c, Site A1a experienced the most rapid accretion with an annualized rate of 4 cm/y at the 5 m marker. This is believed to have been caused by the rapid shoreline retreat at that site which brought the marsh edge closer to the 5 m plot over time (Table 2). Lowest annualized accretion was found at the interior marsh sites B1, B2 and C1 where an average of only 0.8 cm/y was retained at the 50 m location, compared to 2.4 cm/y at the 5 m position (Table 2-2). So, while streamside accretion was similar for the interior and exterior sites, sedimentation dropped off more rapidly along the 50 m traverse for the interior sites (B1, B2, C1) than for those bordering large water bodies. Also, accretion rates and sedimentation pattern at the A1b station, where the marsh edge advanced into Lake Borgne behind a revetment, was essentially the same as for the other exterior sites.

Table 2-2. Bulk density, shoreline erosion and accretion at the nine study sites.

| | A1a | A1b | A1c | A2 | A3 | B1 | B2 | C1 | C2 |
|-----------------------------------|-----------------|-----------------|-----------------|-----------------|-----------------|-----------------|-----------------|-----------------|-----------------|
| Bulk Density (g/cm ³) | 0.211± 0.012 | 0.241± 0.014 | 0.459± 0.016 | 0.359± 0.021 | 0.357± 0.027 | 0.119± 0.016 | 0.109± 0.007 | 0.067± 0.004 | 0.334± 0.026 |
| Edge Erosion (cm±se) | 283.3± 32.8 | -85.5± 10.4 | 121.7± 28.7 | 123.8± 10.6 | 96.0± 28.6 | 9.1± 6.9 | 26.3± 7.4 | 25.9± 8.2 | 99.0± 11.1 |
| Edge Erosion Rate (cm/yr) | 401.1 | -121.0 | 172.2 | 175.2 | 135.9 | 12.9 | 37.2 | 36.6 | 140.2 |
| Accretion - 5m (mm±se) | 27.8± 1.2 | 16.0± 0.7 | 210.0* | 12.6± 1.1 | 16.8± 1.9 | 15.6± 1.0 | 13.3± 0.8 | 22.0± 1.3 | 14.8± 1.0 |
| Accretion Rate - 5m (mm/yr) | 39.4 | 22.7 | 297.3 | 17.8 | 23.8 | 22.1 | 18.8 | 31.1 | 21.0 |
| Accretion - 25m (mm±se) | 13.0± 1.2 | 14.8± 1.0 | 13.8± 3.0 | 21.7± 3.4 | 20.0± 2.9 | 7.4± 1.3 | 10.2± 1.2 | 5.6± 0.7 | 11.0± 1.7 |
| Accretion Rate - 25m (mm/yr) | 18.4 | 21.0 | 19.5 | 30.7 | 28.3 | 10.5 | 14.4 | 7.9 | 15.6 |
| Accretion - 50m (mm±se) | 5.2± 0.4 | 9.2± 0.4 | 21.0± 1.1 | 17.4± 1.4 | 20.7± 0.7 | 2.6± 0.2 | 8.4± 1.2 | 6.2± 1.1 | 6.2± 0.6 |
| Accretion Rate - 50m (mm/yr) | 7.4 | 13.0 | 29.7 | 24.6 | 29.3 | 3.7 | 11.9 | 8.8 | 8.8 |

* Only one measurement taken. This was a shell deposit on top of the feldspar.

Physical Hydrographic Measurements

On February 20-21, 2018, temperature ranged from 21.8°C to 24.6°C with a mean±se of 23.5±0.18°C (Appendix A: Table A9). Dissolved oxygen ranged from 6.7 mg/L to 8.3

mg/L with a mean±se of 7.2±0.09 mg/L. Specific conductance ranged from 1342 mS to 34512 mS with a mean±se of 16762± 2360 mS. Salinity ranged from 4.2 ppt to 23.0 ppt with a mean±se of 11.2±1.4 ppt. Secchi depth ranged from 29 cm to 151 cm with a mean±se of 62.6±6.2 cm. Total suspended sediments ranged from 6.7 mg/L to 8.3 mg/L with a mean±se of 7.2±0.1 mg/L. It should be noted that no sampling occurred during storm events when TSS levels would be much higher (e.g., Perez et al. 2000). Water level gauges ranged from 38 to 44 cm with a mean of 41.8 cm (Appendix A: Table A9).

Additional water level gauge and salinity measurements were made during site visits on March 2 and March 8, 2018 (Appendix A: Table A10). Salinity measurements were also taken on March 8, which ranged from 4.6 to 22.1 ppt.

Water probe measurements were taken on April 25 at all sites except TW and A3, which were taken on April 27 (Appendix A: Table A11). Temperature ranged from 21.8°C to 24.3°C with a mean±se of 23.2±0.13°C. Dissolved oxygen ranged from 7.0 mg/L to 9.5 mg/L with a mean±se of 7.9±0.14 mg/L. Specific conductance ranged from 2558 mS to 19983 mS with a mean±se of 11605± 1324 mS. Salinity ranged from 1.4 ppt to 12.3 ppt with a mean±se of 7.1±0.8 ppt. Secchi depth ranged from 30 cm to 80 cm with a mean±se of 55.2±2.8 cm. Total suspended sediments ranged from 12.5 mg/L to 54.6 mg/L with a mean±se of 26.6±2.4 mg/L. Water level gauges ranged from 6 to 38 cm with a mean of 41.8 cm (Appendix A: Table A11).

A third full set of water quality measurements were taken on June 26, 2018 (Appendix A: Table A12). Temperature ranged from 30.7°C to 32.6°C with a mean±se of 31.7±0.13°C. Dissolved oxygen ranged from 5.2 mg/L to 11.1 mg/L with a mean±se of 6.8±0.33 mg/L. Specific conductance ranged from 3658 mS to 27509 mS with a mean±se of 18741± 1892 mS. Salinity ranged from 1.7 ppt to 15.0 ppt with a mean±se of 9.9±1.0 ppt. Secchi depth ranged from 40 cm to 79 cm with a mean±se of 56.3±2.7 cm. Total suspended sediments ranged from 10.5 mg/L to 44.4 mg/L with a mean±se of 24.1±2.0 mg/L. Water level gauges ranged from 21 to 52 cm with a mean of 40.0 cm (Appendix A: Table A12).

On July 5 and August 13, 2018, probe and secchi disk data from the twelve Rounsefell water quality monitoring stations and 3 marsh sites were collected (Appendix A: Table A13, Appendix A: Table A14). Temperature ranged from 28.8°C to 30.6°C with a mean±se of 29.9±0.10°C. Dissolved oxygen ranged from 0.1 mg/L to 7.7 mg/L with a mean±se of 3.7±0.84 mg/L. Specific conductance ranged from 3448 mS to 31428 mS with a mean±se of 22935± 2157 mS. Salinity ranged from 1.8 ppt to 19.5 ppt with a mean±se of 13.6±1.0 ppt. Secchi depth ranged from 40 cm to 70 cm with a mean±se of 52.9±2.8 cm.

The fourth full set of water quality measurements were taken on September 13, 2018 (Appendix A: Table A15). Temperature ranged from 28.4°C to 30.1°C with a mean±se of 29.2±0.19°C. Dissolved oxygen ranged from 3.1 mg/L to 6.9 mg/L with a mean±se of 4.7±0.23 mg/L. Specific conductance ranged from 13386 mS to 38580 mS with a mean±se of 23966± 1675 mS. Salinity ranged from 7.1 ppt to 22.9 ppt with a mean±se of 13.6±1.0 ppt. Secchi depth ranged from 33 cm to 103 cm with a mean±se of 57.2±3.5 cm. Total suspended sediments ranged from 9.3 mg/L to 63.8 mg/L with a mean±se of 28.2±3.2 mg/L. Water level gauges ranged from 40 to 68 cm with a mean of 50.1 cm (Appendix A: Table A15).

The final set of water quality measurements were taken on November 16, 2018 (Appendix A: Table A16). Temperature ranged from 9.1°C to 12.4°C with a mean±se of 10.4±0.22°C. Dissolved oxygen ranged from 8.6 mg/L to 10.2 mg/L with a mean±se of 9.7±0.07 mg/L. Specific conductance ranged from 8232 mS to 19473 mS with a mean±se of 12575± 627 mS. Salinity ranged from 6.3 ppt to 15.7 ppt with a mean±se of 10.2±0.6 ppt. Secchi depth ranged from 30 cm to 135 cm with a mean±se of 70.8±5.7 cm. Total suspended sediments ranged from 9.5 mg/L to 35.8 mg/L with a mean±se of 17.4±1.7 mg/L. Water level gauges ranged from 7 to 28 cm with a mean of 17.4 cm (Appendix A: Table A16).

Water Level & Salinity Time-Series

Continuous monitoring of water level at 3 sites was an important part of this study following the observations of Day et al. (2011) at sites in the Atchafalaya basin where marsh health and resilience during flooding events were found to be related to the amount of time the marsh remained submerged. We compared highs and lows of local tidal gauge records with the water level data to estimate percent inundation at each site. Astronomical tides at the Shell Beach NOAA Gauge on the south shore of Lake Borgne have a long-term average range of 0.4 m, though local winds often exert at least as much influence on water level in Lake Borgne (NOAA Tides & Currents, Shell Beach, LA). Water level at Shell Beach ranged over 1.79 m from -0.55 to +1.24 relative to Mean Sea Level (MSL) during the March to November 2018 recording period, with an obvious high-water spike on October 9 as Hurricane Michael made landfall on the Florida Panhandle (Figure 2-6). Mean water level was +0.15 m (15 cm, MSL).

Water level relative to local marsh elevation at site A1b on the east bank of Lake Borgne (Figure 2-6) ranged from -0.57 to 0.56 m for a span of 1.13 m, 37 percent less than the range at Shell Beach, with a mean water level of -0.18±0.01 m. To estimate the elevation of the A1b marsh surface, we subtracted the difference on the staff gauge between the marsh surface and local mean water level from the mean relative to MSL at the Shell Beach Gauge (+0.15 – (-0.18) = +0.33 m MSL). This yields an estimate of 33 cm MSL for the elevation of the adjacent marsh surface, only 11 cm below Mean High Water (MHW) on the Shell Beach gauge. From this, we infer that Lake Borgne got high enough at Site A1b to flood the marsh surface only 20 percent of the period monitored.

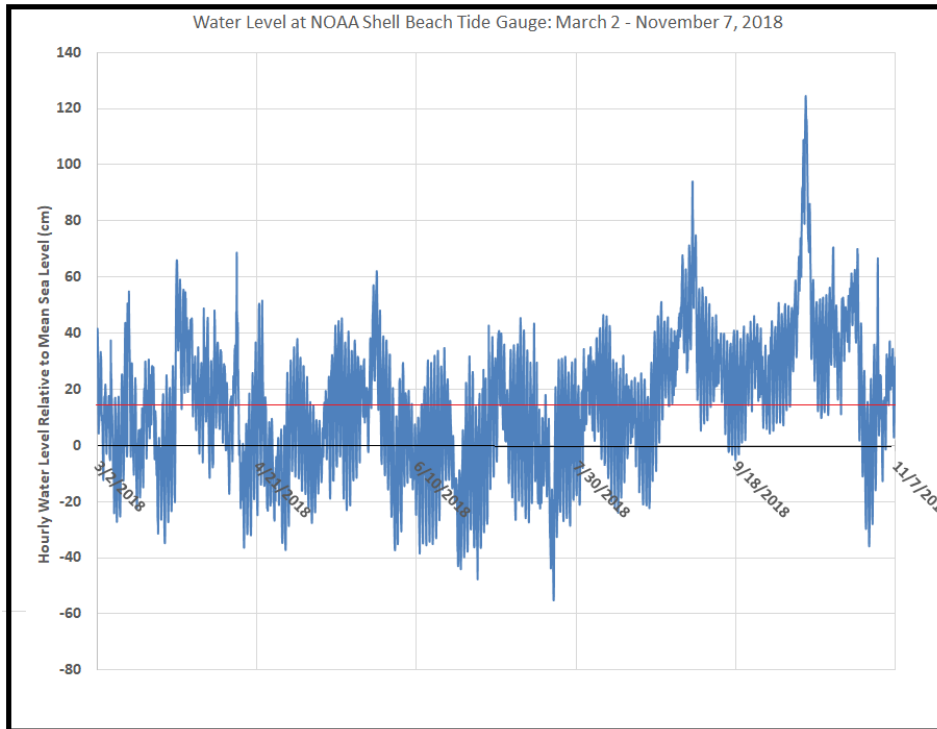
Site C2 had the same mean water level as site A1b, -0.18±0.01 m (Figure 2-7), and ranged from -0.57 m to 0.55 m (1.07 m). Thus, we infer that the marsh elevation at C2 is also approximately 0.33 m (MSL). The data at site A3 is incomplete due to instrument failure in late June, but water level during the 4-month period recorded ranged from -0.47 m to +0.07 m with a mean±se of -0.31±0.01 m. Based on cross-correlation with the record from the NOAA tide gauge at the south end of Lake Borgne, the adjacent marsh elevation at all three stations is close to 33 cm MSL.

The data from the Biloxi sites are very similar to that reported by Day et al. (2011) for marshes in the Atchafalaya basin that, like BMC, are strongly impacted by flooding and frontal passages. Day et al. (2011) found that wetlands that flooded only 15% of the time remained stable for over half a century. In contrast, marshes that were flooded for 85% of the time rapidly deteriorate and experience marsh collapse. These results suggest that much of the BMC is very healthy with regard to flooding.

The three marshes that were instrumented face large water bodies and are clearly supplied with enough sediment to maintain a high position in the tidal frame. However, these healthy marshes remain susceptible to loss from lateral erosion, shoreline retreat, and tidal scour.

Fouling by barnacles and oyster spat was an issue with the probes, especially the specific conductivity probe at site C2, which consistently fouled within 3-weeks of initial deployment or cleaning and redeployment (Figure 2-8). Neither of the conductivity probes would download at the end of the study and were sent back to the manufacturer to be downloaded. ONSET was able to download both sensors. The probe at A1b yielded a complete record, but that at C2 returned little data that could be used.

Geographic and seasonal differences in salinity between the 3 sites were expected. Comparing the two salinity time-series and results of discrete sampling, Chandeleur Sound water on the east shore of the BMC peninsula (3 – 24 ppt) usually has a salinity 3 times that in Lake Borgne (1 – 9 ppt). During the 2018 sampling period, salinity was highest in the fall (September – October) and lowest in the late spring and summer (April – July), a condition that is now conducive to growth of the Rangia clam in Lake Borgne.



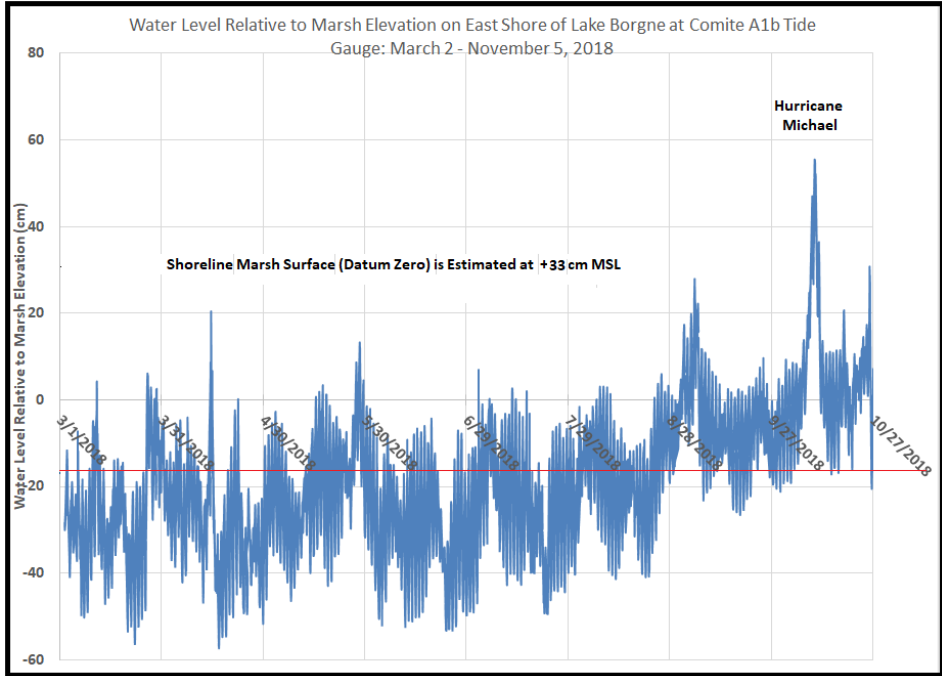


Figure 2-6. Top Panel: Water level (MSL) at Shell Beach NOAA Gauge for the March to November 2018 Study Period. Red line at 15 cm shows the mean of this record. Bottom Panel: Water Level Relative to Marsh Surface with Red Line showing the mean of this record. Information from the two time-series is combined to obtain an estimate of Marsh Elevation relative to MSL.

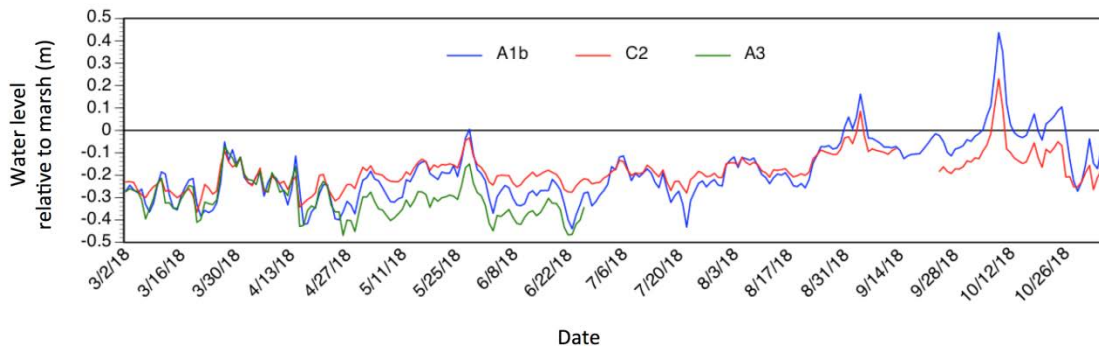


Figure 2-7. Water level relative to marsh elevation at sites A1b (blue), C2 (red), and A3 (green).

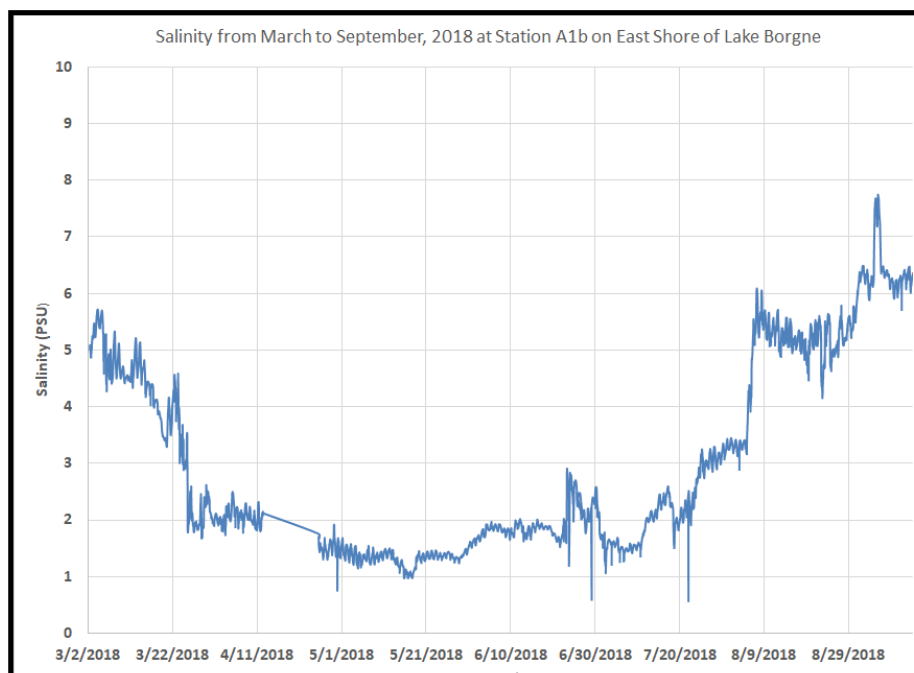
Chapter 2: CONCLUSIONS

Marshes in the BMC, like other coastal Louisiana wetlands, are transformed into open water by two basic mechanisms, one related to submergence and inundation and the other as a result of wave action and erosion. Sustained submergence and inundation results in plant death and subsequent marsh collapse. Marsh edges exposed to wave erosion and tidal scour lose land by undercutting of shorelines followed by scarp failure. These mechanisms produce different patterns of loss. When the marsh surface is flooded more than 50 percent

of the time, the marsh soil is continuously saturated and does not drain or dry. Even if such marshes receive significant sediment flux, little accretion is measured because the drying and consolidation cycle necessary to permanently attach sediment to the soil surface does not occur (Day et al. 2011). Collapse can occur in place without erosion when the elevation of the marsh surface drops below a critical point in the tidal frame (Day et al. 2011; Chambers et al. 2019).

One purpose of this study was to determine the relative importance of these two mechanisms on the BMC. Clearly the submergence process is enhanced by land subsidence and a lack of new sediment and organic matter to fill the accommodation space created. This mechanism is affected by both global and local factors. Sea level rise, for example, has a global eustatic component but local and seasonal wind and tide factors also have significant influence on submergence and inundation as well as wave action and erosion. Subsidence also has a large-scale component in that it generally increases in the Mississippi River delta in a seaward direction as discussed in Chapter 1.

In this study and in Day and Kemp (2017), marshes located on the shorelines of large water bodies appear to be well supplied with suspended sediment and tend to be able to sustain elevations near mean high tide with flooding frequency below 20 percent. Due to MRGO and the loss of the natural beach berm, these perimeter marshes are however, quite susceptible to loss through lateral wave erosion, and also to development of tidal channels that create passage into interior marsh areas. Local subsidence of organic and clay-rich sediments laid down adjacent to distributary channels and natural levees creates ponds isolated from sediment input (Treadwell 1955, Gagliano 2010). However, with the loss of the natural beach berm, these interior marshes are increasingly impacted by widespread hydrologic connections to Lake Borgne, tidal scour and accelerated erosion.



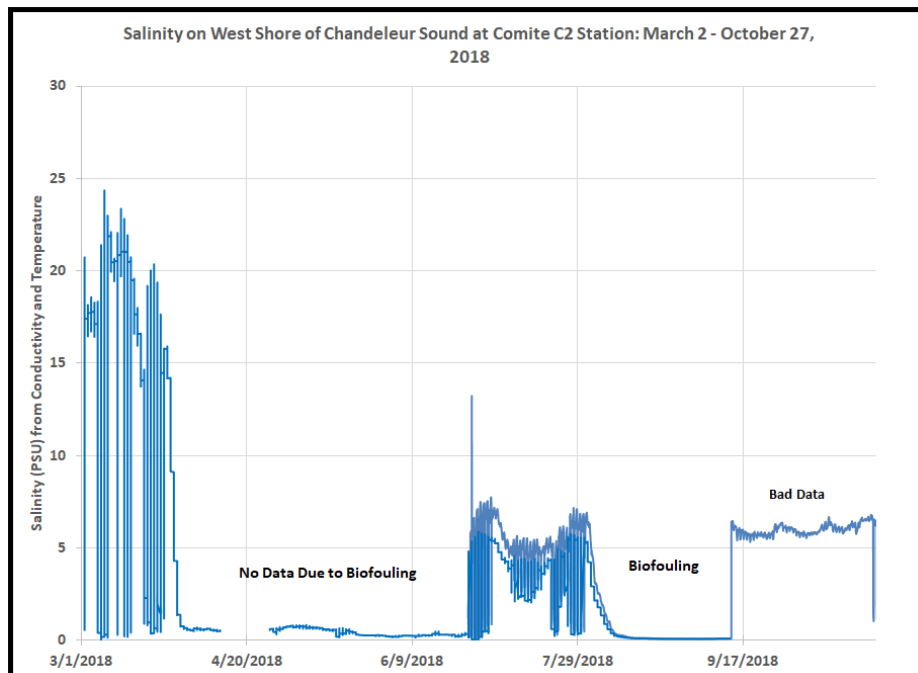


Figure 2-8. Top Panel: Salinity in Lake Borgne at A1b for the March to November, 2018 Study Period. Bottom Panel: Partial Record of Salinity adjacent to the MRGO at C2.

During our year of data collection, we have gained a great deal of understanding about what has made the BMC so much more durable than other deltaic marshes. From a restoration standpoint, it will be advisable to create projects that will take advantage of the new salinity regime, and to prioritize both the problem of healthy marshes on the lake shores that are experiencing rapid rates of lateral and tidal erosion that may require protection, and submerging marshes affected by hotspots of subsidence in interior marshes that would benefit from marsh nourishment.

Projects proposed in Chapter 5 and Appendices I, J, and K build on natural, observed processes currently in action in the BMC. For the wave threat, we find that detached shore-parallel wave berms like those installed in PO-72, 10 m offshore and no higher than the marsh surface, seem to work very well, and they do not appear to obstruct vital sediment transport onshore. Similar berms are proposed in the BMC Integrated Project (Appendix I). Blocking newly formed hydrologic passages through former marsh into the marsh interior will help prevent continued development of tidal channels by fast moving erosive waters and entry of more saline water into interior lagoons. Berms will initially act as wave barriers and reduce hydrologic connectivity, but in time, we expect they will also promote natural outbuilding of the shoreline as they limit seaward loss of marshland and stabilize shoreline retreat as observed in our marsh site located landward of the berm installed in 2014. It is our strong contention that restoring the beach berm along the western edge of Lake Borgne represents the single most critical need required to maintain the integrity of the BMC before ongoing marsh loss reaches a more dire stage.

It appears that at least some of the interior marsh loss is related to localized shallow subsidence and peripheral erosion and not due to compaction of strata except at very shallow depths less than 10 ft. Mid- to long-term project needs in the BMC outlined in

Chapter 5 recognize that where such sinking continues, as in some of the lagoons that have formed on the flanks of the Bayou LaLoutre distributary, repeated input of sediment pumped from Lake Borgne or other water bodies and sprayed onto the existing marshes and lagoon bottoms will be necessary. A small dredge was recently used with successful results in a similar project at Rainey Sanctuary in Vermilion Parish. This approach of nourishment of existing marshes is much cheaper than rebuilding marshes in open water. In the longer term, sediment capture from the Mississippi or Pearl River would help to prolong the life of the western BMC for decades.

Results from this study and decades of observation and measurement of marsh sustaining processes resulted in the BMC Integrated Project proposed to CPRA in *Leveraging Natural Resiliency to ensure Long-Term Sustainability of the Biloxi Marsh Complex Surge Barrier: An Integrated Project*, Day et al., 2019 (Appendix I). BMC Integrated Project was conceptualized based on analysis of new data presented here which identified the root causes of the degradation of the BMC and determined the BMC's critical restoration needs. Immediate implementation is required to achieve the primary goal: to prevent further degradation of the western side of the BMC caused primarily by MRGO operations. The proposed BMC Integrated Project is designed to create and nourish almost 700 acres of marsh and can be expanded. Restoration of the natural beach berm and closure of key hydrologic passages will re-establish natural barriers to flow, thus allowing natural processes to reestablish thousands of acres near shore and in the interior marshes by protection from wave and tidal action. The BMC Integrated Project's implementation will ensure that this valuable resource is given a chance to take advantage of natural processes and to act as a storm surge barrier and critical marine estuary for the region. Immediate action is necessary to secure the BMC in its present condition, limiting further degradation from widespread hydrologic continuity, and buy time so that additional projects outlined in Chapter 5 can be implemented.

Chapter 3: Surface Elevation Change (SET) and Accretion at Historical Plots in the Biloxi Marshes

John W. Day^{1,2}, G. Paul Kemp², and Robert R. Lane¹

¹Comite Resources, PO Box 66596, Baton Rouge LA 70896

²Dept. of Oceanography & Coastal Sciences, Louisiana State University, Baton Rouge LA 70803

Chapter 3: INTRODUCTION

This chapter presents new elevation and accretion data obtained at Surface Elevation Table (SET) sites established in 2003. Accretion markers, where found, were used in conjunction with elevation measurements to calculate subsidence. These data were analyzed along with similar data from CPRA-established CRMS measurement sites in the BMC. These data present a complex landscape that is maintaining elevation at its periphery and eastern half, but which is losing elevation in part of the interior wetlands.

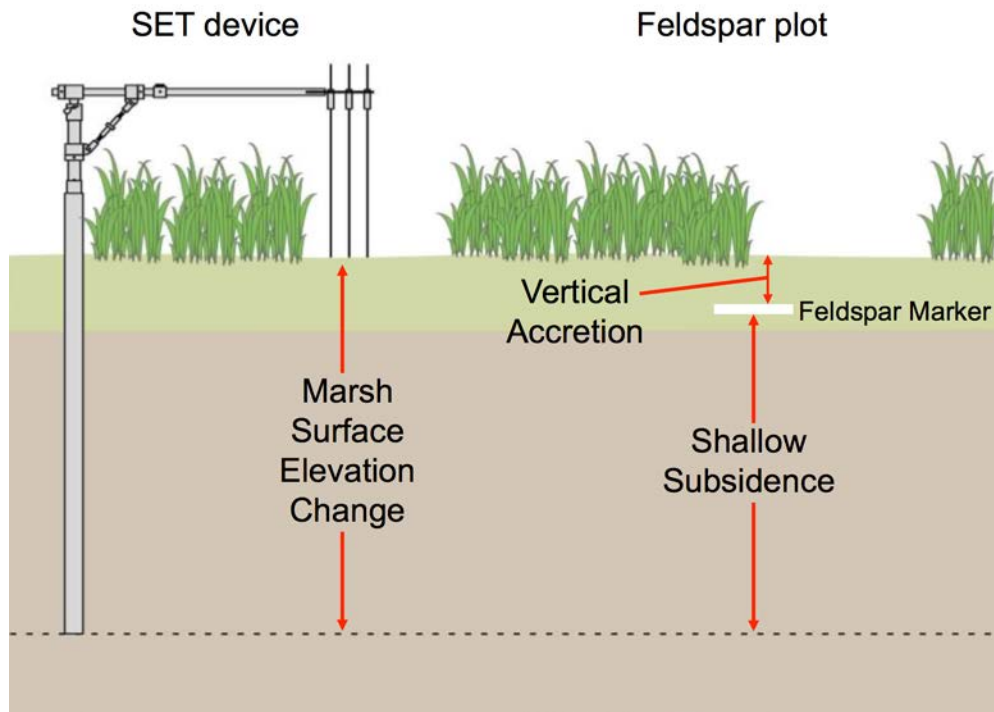


Figure 3-1. Schematic of SET device and feldspar marker horizon and associated measurements of marsh surface elevation change and shallow subsidence.

Wetland soil elevation is directly influenced by a complex relationship between subsidence and accretion. Accretion is defined as the vertical accumulation of material on the wetland surface, as measured using a marker (i.e., feldspar, ¹³⁷Cs, ²¹⁰Pb; Callaway et al. 1996; Figure 3-1). Subsidence is defined as all local factors that contribute to the lowering of the

elevation an intact wetland surface (Reed and Yuill 2017) but does not include elevation loss due to erosion. Compaction and consolidation of sediments (both shallow and deep) are likely to be the main processes that lead to subsidence in the BMC.

The relationship between vertical accretion and soil elevation change in the coastal marshes of Louisiana is complicated. The frequency, duration, and depth of flooding (i.e., hydroperiod) directly control sediment delivery to the wetland surface (Cahoon et al. 1999; Day et al. 2011). Accumulation of both organic and mineral matter is often significantly related to duration of flooding, implying that allochthonous organic matter as well as mineral matter is delivered to the marsh surface during flooding (Cahoon and Reed 1994). Although the increased flooding duration enhances sediment deposition, the total amount of flooding may also contribute to marsh deterioration through submergence stress on plant vigor (Pezeshki and DeLaune 1990, 1993, 1996). Hydroperiod controls the oxidative state of the wetland soil, and thereby influences growth of plant shoots and roots, as well as soil organic matter decomposition (Bandyopadhyay et al. 1993). There is a feedback between elevation and hydroperiod since elevation directly controls hydroperiod (Cahoon et al. 1999).

Climatological forcing is often a more important regulator of water levels in the microtidal estuaries of Louisiana than astronomical tidal variability (Perez et al. 2000; Lane et al. 2015). As a result, sedimentation in microtidal marshes is strongly event related. Accretion is often greater during periods of long and deep flooding events, implying the importance of storms in increasing the supply of suspended sediment to Louisiana coastal marshes (Cahoon and Reed 1994; Perez et al. 2000; Day et al. 2011). Both upland runoff or erosion during storms (Cahoon 2006) and release of sediment-laden Mississippi River water, such as during the 2019 opening of the Bonnet Carré Spillway, can deliver sediment to coastal wetlands. Mechanisms by which storms affect coastal wetland soil elevation include the erosive effects of substrate disruption and subsequent sediment redistribution and accretion by storm surge. Storms elevate water levels and resuspend sediments, which are then deposited on the marsh surface (Perez et al. 2000). Storms can also generate high-velocity flows over the marsh surface, causing the redistribution of previously deposited sediments (Baumann et al. 1984; Howes et al. 2010). These energy intensive events also result in wave-induced shoreline erosion (Karimpour et al. 2016; Trosclair 2013).

Chapter 3: METHODS

A series of surface elevation monitoring sites in the BMC were established on behalf of BLMC in 2003. The sites were positioned in two marsh areas near Stump Lagoon to the west and Blind Lagoon to the east (Figure 3-2), referred to as the Western and Eastern sites. Each site was originally comprised of 15 SET stations distributed across interior marsh widely interspersed with small ponds and larger lagoons north of Bayou La Loutre. Measurements of elevation and accretion were taken at these sites in 2003, 2004, and 2005, as well as 2008 at the eastern sites, in an effort to measure changes in elevation due to frontal passages and major storms, including Hurricane Katrina. Accretion markers were also deployed at all the sites in February 2003. Wetland elevation was measured using a surface elevation table (SET; Figure 3-1; Boumans and Day 1993; Cahoon et al. 2000; Day et al. 1998, 1999; Lane et al. 2006; Osland et al. 2017) and vertical accretion was measured using feldspar marker horizons (Cahoon and Turner 1989; Lane et al. 2006, 2017).

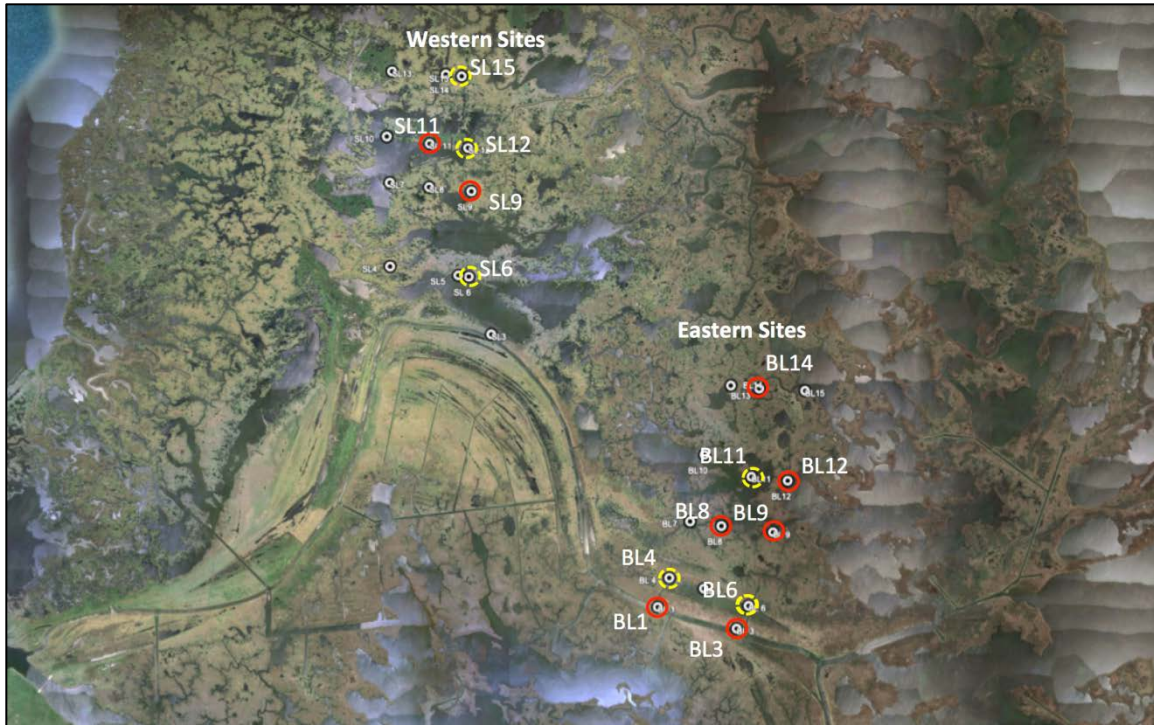


Figure 3-2. Yellow circles indicate where elevations were measured, and red circles indicate where accretion and elevation were measured. Additional historical SET sites established in the BMC by UNO are indicated by white circles.

Wetland Surface Elevation

Each SET site consists of a supporting base support pipe of a 7.5-cm diameter thin walled aluminum driven vertically into the soil 4-6 m (13-20 ft) until refusal with a vibracorer (Boumans and Day 1993; Cahoon et al. 2000, 2002a). The upper end of the base support pipe was fitted with another machined notched pipe designed to receive the upper portable part of the SET (Figure 3-3). The portable part of the SET is a precisely machined device that can be leveled in two planes and positioned in four directions around the base support pipe. Once leveled, the plate at the end of the SET is in the exact same position during every measurement, providing a constant reference plane in space from which the distance to the sediment surface will be measured repetitively through time (Cahoon and Reed 1994; Cahoon et al. 1999). Nine 3-mm diameter 91-cm-long metal rods (i.e. pins) were used to measure the distance to the wetland surface in the four quadrants, providing 36 measurements per sampling effort. The accuracy of this technique is ± 1.5 mm (Boumans and Day 1993; Cahoon et al. 2002a). The rate of elevation change was calculated as the mean difference between individual pin measurements divided by the amount of time since the first measurement. Two 1"x 8"x 8' boards were brought to each surface elevation table (SET) station and walked on during measurements to minimize disturbance of the surrounding surface (Lane et al. 2006).



Figure 3-3. Dr. Lane taking measurements using the SET device.

Wetland Vertical Accretion

Vertical accretion was measured as the rate of accumulation above feldspar marker horizons laid upon the soil surface at the same time as the first SET measurements by University of New Orleans. Powdered feldspar clay was laid on the wetland surface 1 cm thick at plots next to each SET platform. The thickness of material deposited on top of the feldspar marker was measured by taking a ~20 cm x 20 cm plug using a shovel, cleanly slicing the core into several sections to reveal the horizon, then measuring the thickness of material above the surface of the horizon at 5-10 different locations (Lane et al. 2006, 2017). The rate of vertical accretion was calculated by dividing the thickness of material above the surface of the horizon by the amount of time the horizon had been in the sediment. The rate of shallow subsidence was calculated by subtracting the rate of vertical accretion from that of surface elevation change (Cahoon and Turner 1989; Cahoon and Reed 1994; Cahoon et al. 1999).

Chapter 3: SET MEASUREMENT RESULTS

Five SET sites were measured at the Western area: SL6, SL9, SL11, SL12 and SL15 (Figure 3-2). All Western area sites except site SL9 decreased in elevation ~-4 to -9 cm by 2018 compared to initial measurements taken in 2003 (Table 3-1; Figure 3-4). SL9 maintained elevation with 2018 measurements 1.24 cm higher than initial measurements taken in 2004, indicating an elevation rate increase of 0.08 cm/y. Site SL9 was the only site without 2003 initial data. The other Western area sites had decreasing rates of elevation change ranging from -0.27 to -0.62 cm/y (Table 3-1). We note that several of the Western SET marsh sites were located in close proximity to the edge of lagoons and ponds and could be subject to bank erosion, suggesting that estimates of subsidence rate based on SET measurements in these locations could be skewed by the effects of erosion as well as

subsidence. Accretion markers were found at two Western sites: SL9 (5.13 cm) and SL11 (9.75 cm), which equates to 0.35 and 0.63 cm/y, respectively.

Nine SET sites were measured at in the Eastern area: BL1, BL3, BL4, BL6, BL8, BL9, BL11, BL12 and BL14 (Figure 3-2). All these sites had positive 2018 elevations ranging from ~4 to 9 cm, and elevation rates ranging from 0.27 to 0.57 cm/y (Table 3-1, Figure 3-5). Accretion was found at six of the nine sites, ranging from 8.50 to 14.74 cm, equivalent to 0.50 to 0.94 cm/y (Table 3-1).

At all sites, vertical accretion was always greater than surface elevation gain, with the difference due to shallow subsidence caused by compaction and consolidation of the substrate between the wetland surface and the end of the SET pipe (Cahoon et al. 1995). Subsidence, calculated as the difference between mean elevation and mean accretion, ranged from 2.00 cm at SL9 to 19.27 cm at SL11, with rates of 0.14 and 1.25 cm/y respectively. Thus, both the highest and lowest subsidence measurements were found at the Western sites. At the Eastern sites, subsidence ranged from 2.07 to 7.71 cm, corresponding to rates of 0.13 to 0.49 cm/y, respectively.

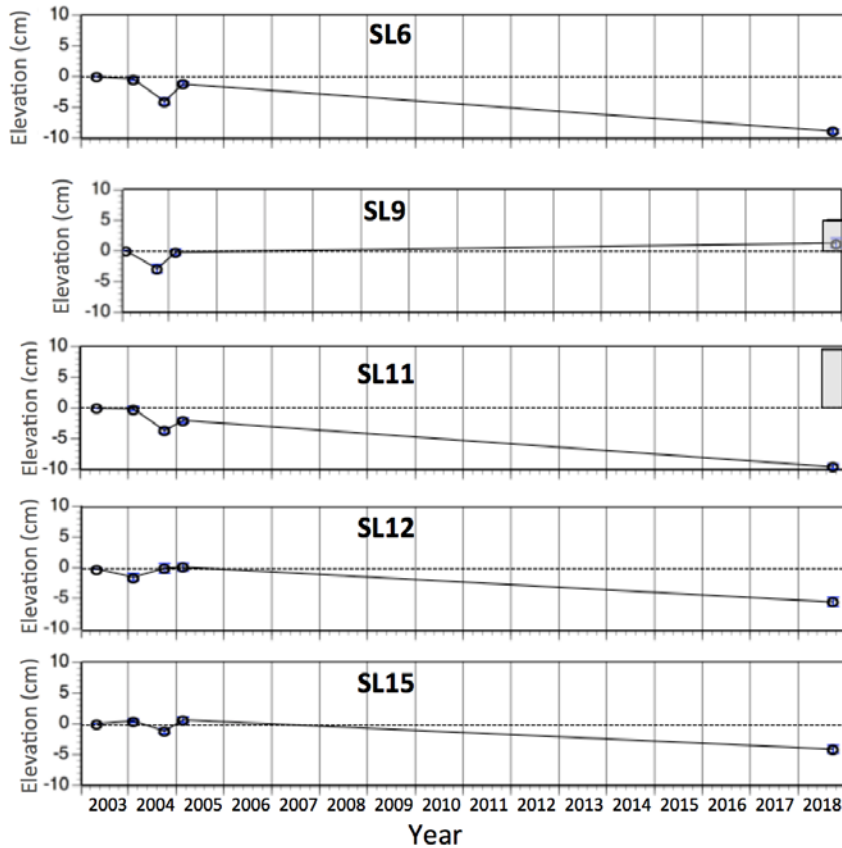


Figure 3-4. Elevation (dots connected by lines) and accretion (shaded bars) at the Western SET sites. Note that 2003 data were not available for site SL9.

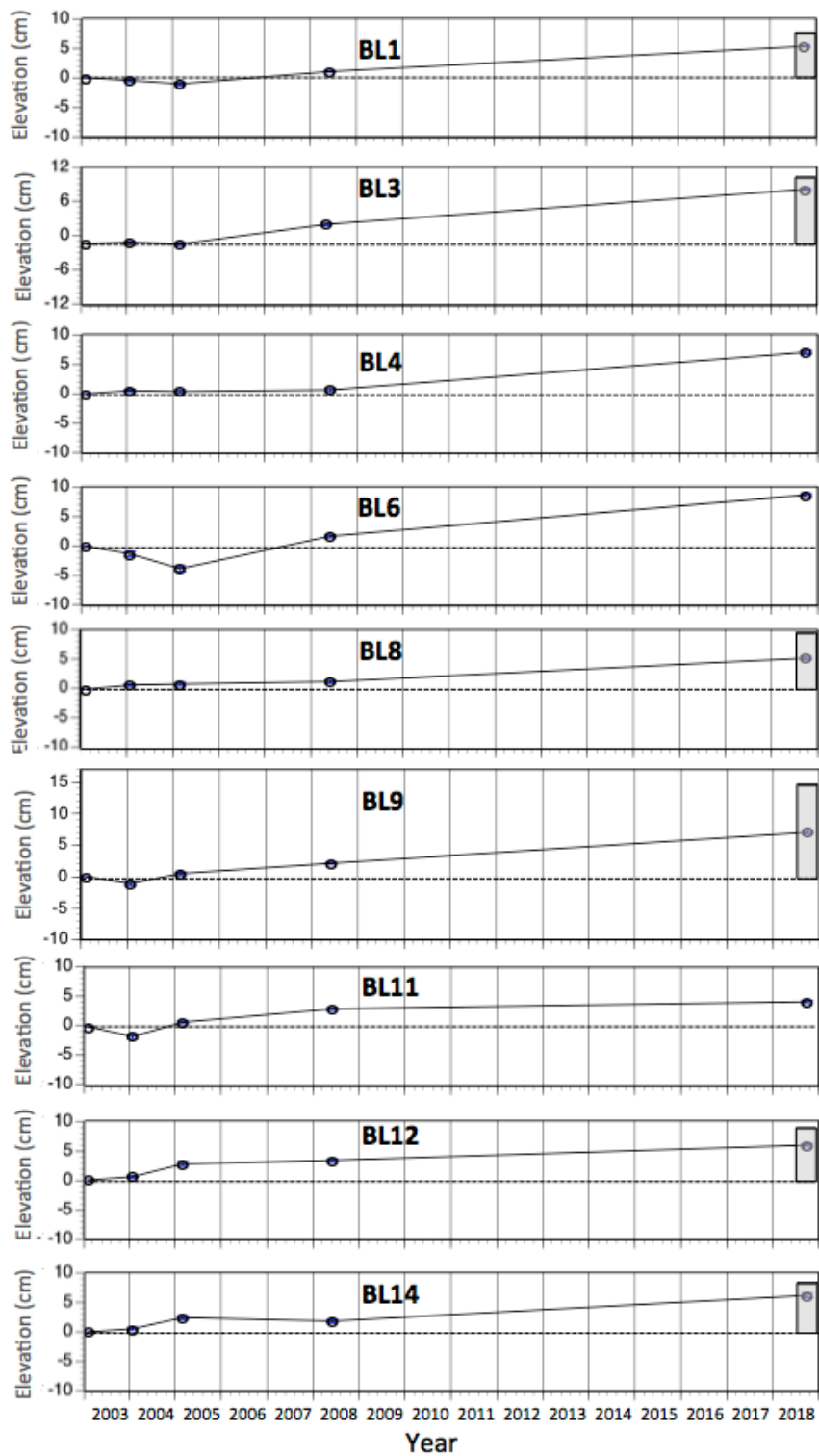


Figure 3-5. Elevation (dots connected by lines) and accretion (shaded bars) at the Eastern (Eastern) SET sites.

Table 3-1. Elevation and accretion data using 2018 data compared to initial data (2003 for all sites except SL9, which is 2004).

| Site | Elevation (cm) | Elevation Change Rate (cm/y) | Accretion (cm) | Accretion Rate (cm/y) | Subsidence (cm) | Subsidence Rate (cm/y) |
|------|----------------|------------------------------|----------------|-----------------------|-----------------|------------------------|
| SL6 | -8.85 | -0.58 | . | . | . | . |
| SL9 | 1.24 | 0.08 | 5.13 | 0.35 | 2.00 | 0.14 |
| SL11 | -9.52 | -0.62 | 9.75 | 0.63 | 19.27 | 1.25 |
| SL12 | -5.34 | -0.35 | . | . | . | . |
| SL15 | -4.12 | -0.27 | . | . | . | . |
| BL1 | 5.30 | 0.34 | 7.76 | 0.50 | 2.46 | 0.16 |
| BL3 | 8.90 | 0.57 | 10.97 | 0.70 | 2.07 | 0.13 |
| BL4 | 6.99 | 0.45 | . | . | . | . |
| BL6 | 7.42 | 0.47 | . | . | . | . |
| BL8 | 5.22 | 0.33 | 9.48 | 0.60 | 4.26 | 0.27 |
| BL9 | 7.03 | 0.45 | 14.74 | 0.94 | 7.71 | 0.49 |
| BL11 | 4.22 | 0.27 | . | . | . | . |
| BL12 | 5.90 | 0.37 | 8.96 | 0.57 | 3.06 | 0.19 |
| BL14 | 6.16 | 0.39 | 8.50 | 0.54 | 2.34 | 0.15 |

Chapter 3: CRMS RSET & ACCRETION RESULTS

In 2003, the Louisiana Office of Coastal Protection and Restoration (CPRA) and the U.S. Geological Survey (USGS) began implementing the Coastwide Reference Monitoring System (CRMS) as a mechanism to monitor and evaluate the effectiveness of coastal restoration projects (<https://cims.coastal.louisiana.gov>; Jankowski et al. 2017). There are a total of six CRMS sites located within the contiguous BMC (Figure 3-6). On either side of western Bayou La Loutre near MRGO CRMS4551 is to the north and CRMS4557 to the south. On the northern reaches of the contiguous BMC are CRMS4572 and CRMS4596, and to the east are sites CRMS0108 and CRMS1024 (Figure 3-5).

The CPRA uses the Rod Surface Elevation Table (RSET) method to estimate surface elevation change rates (Cahoon et al. 2002b). This method is very similar to the SET methodology described above. Accretion was measured as the thickness of material deposited above a feldspar marker horizon, as described in the methods above. Original marker horizons were established concurrently with baseline RSET measurements, and new feldspar marker horizons were regularly established every two years, providing multiple accretion data sets.



Figure 3-6. CRMS sites in the BMC (red dots). Orange rectangles indicate where SET stations are located in the Western (SL) and Eastern (BL) areas.

The CRMS sites had relatively high mean accretion rates, ranging from 0.99 cm/y at the northernmost site CRMS4572, to 1.70 cm/y at site CRMS4557 located south of the MRGO rock berm (Figure 3-5; Table 3-2). Marsh surface elevations changes were all positive, ranging from 0.41 to 1.03 cm/y. The highest rate of elevation change was at the same site as the highest accretion, CRMS4557. The lowest rates of elevation change were at the three northeastern sites; CRMS4596, CRMS4572 and CRMS0108. Subsidence ranged from 0.29 cm/y at CRMS1024 to 1.07 cm/y at CRMS4596 (Table 3-2). Full descriptions of each CRMS site are available in Appendix D.

Table 3-2. Summary table of CRMS data from sites in the BMC.

| site | Accretion | Accretion | Accretion | Accretion | Accretion | Mean | Elevation | Subsidence |
|----------|-----------|-----------|-----------|-----------|-----------|-----------|-----------|------------|
| | Est.2008 | Est.2010 | Est.2012 | Est.2014 | Est.2016 | Accretion | | |
| | (cm/y) |
| CRMS4551 | 1.44 | 1.25 | 0.78 | 1.32 | 2.03 | 1.36 | 0.82 | 0.54 |
| CRMS4557 | 1.61 | 1.55 | 1.17 | 2.38 | 1.79 | 1.70 | 1.03 | 0.67 |
| CRMS4572 | 0.86 | 0.69 | 0.54 | 0.79 | 2.05 | 0.99 | 0.56 | 0.43 |
| CRMS4596 | 1.08 | 0.90 | 1.66 | 1.70 | 2.06 | 1.48 | 0.41 | 1.07 |
| CRMS0108 | 0.61 | 0.92 | 1.37 | 0.88 | 1.94 | 1.14 | 0.68 | 0.53 |
| CRMS1024 | 1.66 | 0.96 | 0.57 | 1.20 | 1.24 | 1.13 | 0.84 | 0.29 |

Chapter 3: DISCUSSION OF SET AND CRMS DATA

There was a general pattern of elevation loss at the Western SET sites and elevation gain at the Eastern SET sites (Table 3-1). The rate of elevation loss at the Western sites ranged from -0.62 to 0.08 cm/y, while at the Eastern sites rates of elevation gain ranged from 0.27 to 0.57 cm/y. The CRMS sites, which essentially encircle the periphery of the contiguous BMC (Figure 3-5), all had positive elevation gain, ranging from 0.41 to 1.03 cm/y (Table 3-2, Jankowski et al. 2017).

Accretion was lower at the Western sites, with an average of 0.49 cm/y compared to 0.64 cm/y at the Eastern sites, though they were not statistically different using a standard t-Test (Sall et al. 2012). However, because only two accretion sites were found in the Western area, such statistical conclusions are tenuous at best. Furthermore, it appears that erosion caused at least some of the elevation loss in the Western sites, particularly those for which accretion could not be measured because the feldspar layer was no longer present. Accretion at the CRMS sites was much higher, ranging from 0.99 to 1.70 cm/y, presumably due to proximity to open bay waters where re-suspended mineral sediments are present. Accretion measured at CRMS stations is in line with accretion reported at the Violet Canal of 0.34 to 0.44 cm/y, and at the Breton Sound estuary of 0.75 to 1.57 cm/y (Lane et al. 2006).

Subsidence rate at the two Western sites with accretion markers was 0.14 and 1.25 cm/y. The near order of magnitude difference between the two rates was driven by an unexpected elevation gain at site SL9 compared to the other Western sites. Whereas all of the other Western sites had losses of elevation, SL9 maintained elevation relative to initial measurements. If the average accretion rate for the Western area (0.49 cm/y) were applied to the sites with missing accretion data, average subsidence at the Western sites would range from 0.76 to 1.06 cm/y. This is much higher than that measured at the Eastern sites, which range from 0.13 to 0.49 cm/y (Table 3-1) but is within the range measured at the CRMS sites, which spanned from 0.29 to 1.07 cm/y (Table 3-2).

In general, these results are similar but tend to run low relative to other reports of shallow subsidence rate in southeast Louisiana east of the Atchafalaya basin and south of the I-12 corridor. Shinkle and Dokka (2004) inferred that subsidence rates in some areas of the Mississippi delta are in excess of 2.5 cm/y, while Jankowski et al., 2017 reported peak subsidence of ~1.5 cm/y using data from the 185 CRMS site array in the delta. Lane et al. (2006) reported rates of subsidence in the Breton Sound estuary to range from 0.59 to 1.21 cm/y and from 1.52 to 2.78 cm/y along the Violet Canal. Cahoon et al. (1995, 1999) reported shallow subsidence of 0.5 and 1.5 cm/y for Old Oyster Bayou and Bayou Chitigue, respectively, located in coastal Louisiana. The Western sites are located relatively near the old Bayou La Loutre distributary channel where local subsidence could be due to near-surface compaction of buried peats sediments, but based on a study of Stump Lagoon (Gagliano et al., 2010), storms or other rapid acting events are likely to have accelerated the creation of some lagoons.

Current eustatic sea-level rise (ESLR) is between 2-3 mm/y (Miller and Douglas 2004; FitzGerald et al. 2008; Rahmstorf 2007; Williams 2013), and there is a strong scientific consensus that the rate of ESLR may accelerate dramatically in the future (Meehl et al. 2007; McCarthy et al. 2009). The USGS estimates the current rate of eustatic sea level rise

to be 3 mm/y (0.3 cm/y) at the CRMS sites in the BMC. Wetland surface elevation gain was greater than ESLR for all of the CRMS sites and the Eastern sites with exception of perhaps BL11, which had an elevation change rate of 0.27 cm/y (Table 3-1), and which is on the cusp of survival as an extant marsh setting.

At the five SET sites in the Western study area found in usable condition, mean elevation change over the 15 years monitored for these stations was -0.35 cm/y, indicating that accretion was not enough to offset subsidence +/- erosion. Applying additional data from traverses B1, B2, and C1 presented in Chapter 2, we can estimate a mean accretion value for Western study area of 0.12 cm/y, from which a subsidence rate of -0.47 cm/y can be deduced. Because all the sites measured in Western SET area had decreased elevation (with exception of SL9) in 2018 compared to 2003, we conclude marsh near these locations will not keep pace with sea level rise without intervention.

In contrast, 9 SET sites were recovered in the Eastern study area (Figure 3-1). Elevation at these stations increased at an average rate of +0.40 cm/y, with a mean accretion of 0.64 cm/y, indicating a mean rate of subsidence of only -0.24 cm/y. This means that wetland surface elevation gain from 2003-2018 was greater than sea level rise at the Eastern SET sites (with exception of BL11), suggesting that the eastern interior wetlands of the BMC are more likely to keep pace with sea level rise, as will wetlands on the periphery of the BMC, as indicated by data from the CRMS stations. These trends are consistent with the observation that mineral sediment is brought in from Chandeleur Sound to the east or Lake Borgne to the west and is attenuated as deposition occurs across the landscape from east to west.

Chapter 3: CONCLUSIONS

One of the more important aspects of this study was our ability to locate historical SET and marker horizon study sites to aid longer-term understanding of sedimentation and erosion processes in the BMC. The original Surface Elevation Table (SET) used at SET sites in the BMC prior to 2009 was available to make a new set of measurements in 2018, thus extending the record to 15 years. The stations monitored overlie the subsurface portion of the Bayou La Loutre natural levee north of the modern dredged channel: at Western sites (SL) and Eastern sites (BL; Figure 3-7).

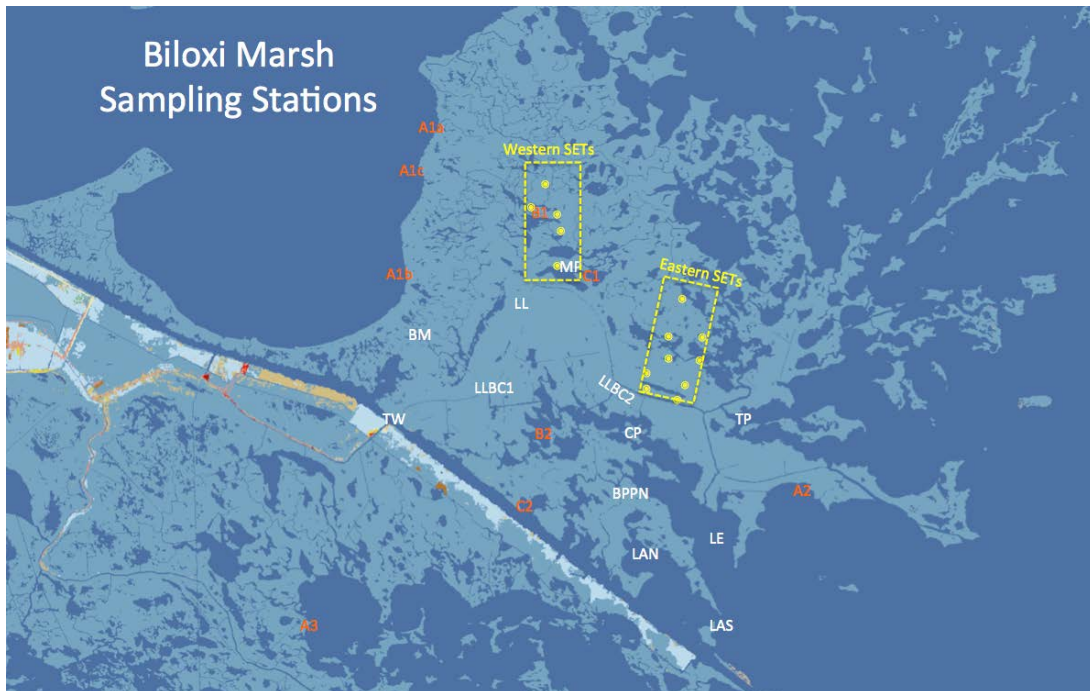


Figure 3-7: Sampling sites for SET data (yellow), as well as shoreline erosion and accretion (orange), and water quality (white; Rounsefell, 1964) study sites presented in Chapter 2 of this report for the BMC area.

Generally, there was elevation gain at the Eastern SET sites and elevation loss at the Western SET sites. The Western sites certainly appear to be in danger of submergence without intervention, and marsh nourishment as discussed in Chapter 5 could be implemented in an effort to offset net elevation loss. In contrast, the increase in elevation at Eastern sites suggests that accretion kept up with subsidence and that the eastern sites are within an effective sediment transport and retention system.

These results suggest that both accretion and subsidence are site specific and can vary significantly across a marsh landscape that all looks homogenous. Subsidence also may vary over time, perhaps starting, increasing, decreasing and ending at different times, as may be the case with the levee flank depressions in both the Western and Eastern study areas.

Flooding history and its effect on salt marshes was studied by Day et al. (2011) at two contrasting sites that are similar in some ways to locations in the BMC. One of the Day et al. (2011) sites is adjacent to the Atchafalaya River mouth with access seasonally to suspended river sediments, is well drained and flooded only about 15% of the time, like most of the exterior BMC. Unlike the lake and bay shore marshes of the BMC, however, there was little indication at the Atchafalaya site of significant lateral erosion. The other Day et al. (2011) location is located much farther away in the Terrebonne marshes and lacks a source of fluvial sediment input, similar to interior marshes of the BMC. However, due to low elevation and position in the tidal frame, the Terrebonne marsh became subject to marsh collapse and the salt marsh plants eventually died in place from the metabolic impacts of prolonged inundation (Mendelssohn and Morris 2000). This condition is not often experienced in the BMC due to higher elevation and position in the tidal frame.

Day et al. (2011) concluded that sediment capture and retention, consolidation and soil strength, and organic matter content were dependent on position in the upper part of the tidal frame while the mineral content is related to the proximity of a fluvial source. Because the Terrebonne marsh elevation was low at the initiation of the study, the Terrebonne marsh sits lower in the tidal frame and was thus subject to inundation more than 85 percent of the time, more than any BMC site in this report.

In contrast, sediment input to the marshes near the Atchafalaya River was lower but had a higher mineral content than the Terrebonne site, reflecting higher elevation and proximity of the sites to the sediment delivered by the Atchafalaya River. Drainage of the higher elevation marsh near the Atchafalaya River allowed the soil surface to dry so that sediment recently deposited during storms was retained. These processes are likely very similar in the BMC, especially along the shoreline with Lake Borgne and Chandeleur Sound.

The collapse observed at the Terrebonne site is not the same as soil removal by erosive waves and tidal currents. Once collapse occurs, low elevation and fluidized soils prevent revegetation. At the Terrebonne site, the rate of subsidence is greater than that of accretion, and the marsh is said to be in an “accretion deficit.” This condition is representative of many interior deltaic marshes now isolated from a fluvial sediment source that sit low in the tidal frame (Baumann et al. 1984; Hatton et al. 1983; DeLaune et al. 1995; Nyman et al. 1995). Although much of the BMC is covered with marsh like that at the Atchafalaya site that sits high in the tidal frame and is inundated less than 40 percent of the time (thus not yet subject to marsh collapse), much of the interior BMC marsh is suffering from accretion deficit like the Terrebonne marsh, in that subsidence is happening faster than accretion.

All of the Western SET study sites decreased in elevation since 2003 (with exception of SL9). In the marsh interior, study of historical conditions (Gagliano et al. 2010) suggests that at least some areas that are now open water in the immediate vicinity of the SET sites were quickly converted from marsh, palmetto swamp, or prairie between 1847 and 1932. Marsh nourishment with introduction of mineral sediment to these locations to offset the lack of new mineral sediment in the interior marsh and lagoons is considered a Mid-Term priority as discussed in Chapter 5. In contrast, wetland surface elevation gain was greater than sea level rise at the Eastern SET sites (with exception of BL11), suggesting that the northeastern interior wetlands of the BMC can keep pace with current rates of sea level rise, as will the wetlands on the periphery of the BMC, as indicated by data from the CRMS stations. These trends are consistent with the observation that sediment is brought in from Chandeleur Sound to the east and deposition occurs across the landscape from east to west.

Chapter 4: Wetland Dynamics from CRMS and CPRA Polygon 11

John W. Day^{1,2}, G. Paul Kemp², Robert R. Lane¹, and Elizabeth C. McDade³

¹Comite Resources, PO Box 66596, Baton Rouge LA 70896

²Dept. of Oceanography & Coastal Sciences, Louisiana State University, Baton Rouge LA 70803

³Chinn-McDade Associates LLC, Harahan, LA 70123

Chapter 4: INTRODUCTION

Land loss between 1932 and 2016 in the BMC was dominated regionally by hydrologic changes caused by construction of the Mississippi River Gulf Outlet (MRGO) in the early 1960s, by wave erosion at the margins of large water bodies that have breached beach berms and increased hydrologic connectivity between Lake Borgne and interior marsh drainage systems. Edge erosion of levee flank depressions associated with the sinking of the ponds adjacent to the natural levees of Bayou La Loutre and its distributaries also has had local effects (Treadwell 1955; Penland et al., 2001; Couvillion et al., 2017, Day et al, 2019, Ch. 2 and 3 this report). Marsh degradation in the BMC was hastened by increased salinity variation and other hydrologic changes brought by the opening of the Mississippi River Gulf Outlet (MRGO; Shaffer et al. 2009). Signs of recovery are increasingly evident throughout the greater BMC area since the canal was closed by a rock barrier just south of the Bayou La Loutre crossing in 2009. We have measurements that confirm BMC marshes are currently accreting and gaining elevation on both west and east shorelines, especially on the eastern side nearest to Chandeleur Sound (Day et al, 2019, Ch. 2 this report).

One of the more significant effects of the MRGO during the 50 years of operation was a doubling of mean salinity in Lake Borgne (Day et al. 2019b, Ch. 3 of this report). This caused a reduction in population of the lake bottom Rangia clam, which is outcompeted by other species in a higher salinity setting (Porrier 2019). After canal closure, lake salinity returned to 1950s levels and the Rangia are expected to regain status as a dominant benthic keystone species, though this may take some time (Poirrier 2019). Interruption of the supply of Rangia clam shells to the beach berms has enhanced shoreline retreat and development of new hydrologic connections to the interior marshes (Day et al, 2019, this report). But accretion and advancement of the shoreline into Lake Borgne has been documented where the CPRA has installed low, nearshore, detached wave-breaking rock berms such as those proposed in BMC Integrated Project. Projects like these that efficiently address the root causes of marsh degradation in the BMC, even if on a temporary basis, can slow the rate of detrimental changes in hydrologic connectivity and allow for rebuilding of the marsh berm.

The inherent stability of the BMC as a depositional platform is evidenced by its persistence for more than 3000 years, making the BMC among the oldest still extant in the Mississippi deltaic plain (Day et al. 2019, 1840s Map on Cover, and Ch. 1 this report). Deeper elements

of the BMC subsurface structure contribute to the stability of the Pleistocene and Holocene platforms that support BMC marshes. The coincidence of the Cretaceous shelf edge trend with the southern part of the BMC forms a line of demarcation between a mostly stable subsurface platform and the northern extent of the Louann salt in south Louisiana. Importantly, the relative stability of the BMC Pleistocene platform led to deposition of thin Holocene layers (50-100' thick) compared to areas just south that are off the platform (150' to 400' thick) (Jankowski et al., 2017, Day et al. 2019, Ch. 1 this report). This observation supports a recommendation that relevant subsurface geologic elements should be considered in future when drawing boundaries for subsidence polygons.

The CMP 2017 wetland change model predicts complete loss of BMC marshlands on the peninsula by between 2030 and 2050, despite their relative durability when compared to the rest of the deltaic plain (Day et al. 2017). The relevant subsidence polygon extends across several deltaic and geologic provinces, as shown in Day et al, 2019 (Ch. 1 this report). Measured subsidence from CRMS stations (Jankowski et al., 2017) in the BMC trend lower than the low end of the range applied to the entire subsidence polygon. The subsidence rate applied in the model acts to boost the Relative Sea Level Rise (RSLR) applied within the greater BMC, and the rate may be higher than is warranted. Here, this report compares a decade of archived data on surface elevation and accretion changes reported from 15 Coastal Reference Monitoring Stations (CRMS) along a 50-mile transect that transects both the BMC and Breton Marshes (Figure 4-1). As it pertains to the BMC, CPRA Polygon 11 should at a minimum be split into northern and southern parts, roughly along the path of Bayou Terre aux Boeufs where it divides St. Bernard and Plaquemines Parishes (Figure 4-1). We recommend that a separate polygon for the northern portion, which includes the BMC, be created and assigned lower subsidence ranges consistent with measured values from relevant CRMS. This is consistent with the recognition that geologically the area is on trend with Baton Rouge and Lake Pontchartrain and is unique among Louisiana coastal marshes.



Figure 4-1. Northeast to southwest transect showing CRMS sites from Biloxi Marsh through the Breton Marsh across Bayou Terre aux Boeufs to the Mississippi River

Chapter 4: METHODS

We draw on Karegar et al. (2015) and Jankowski et al. (2017) to contrast sustainability of the part of the BMC peninsula north of Bayou Terre aux Boeufs with the Breton Marsh between Bayou Terre aux Boeufs and the Mississippi River (Figure 4-1). Karegar et al. (2015) provide estimates of Deep Subsidence (DS) based on 10 years of vertical elevation data from 36 Continuously Operating (GPS) Recording Stations (CORS) deployed on buildings along roads and waterways. They found a simple linear relationship between DS (mm/y) and Latitude ($^{\circ}$ N) that explains about 87 percent of the variability observed coastwide.

$$DS = - 3.7147 (LAT) - 114.26 \quad (\text{Eq. 4-1})$$

Using this equation, it is possible to estimate DS for the 15 CRMS sites downloaded (Table 4-1). Both Karegar et al. (2015) and Jankowski et al. (2017) apply a decadal estimate of Local Sea Level Rise (LSLR) of 2 mm/y. This base rate is modified at any marsh station by the net upward or downward shift of the marsh soil surface to yield a Relative Sea Level Rise (RSLR), which is the stressor to which marsh plants respond.

Jankowski et al. (2017) provides insight into how other marsh sustainability parameters are measured or inferred (Figure 4-2). Relevant measurements are made at Coastal Reference Monitoring Stations (CRMS) that have been regularly reoccupied and maintained by personnel of the CPRA and its contractors (Figure 4-1). Data have been gathered at these sites for over 10 years following a rigorous and consistent monitoring protocol (Folse et al. 2014). More than 390 of these sites have been deployed throughout Louisiana's coastal wetlands to support the coastal restoration initiative. This study discusses data downloaded from 15 sites, including 9 stations from the BMC peninsula north of the MRGO, and 6 stations between the MRGO and the Mississippi River channel (Figure 4-1) south of Bayou Terre aux Boeufs.

One purpose of the CRMS program is to provide guidance on how long the marsh surface will be naturally maintained at a healthy position within the 0.5 m tidal frame, as the land builds upward and sea level rises. Comparison of these two velocities (mm/y) is key to assessing if and when a specific marsh will be submerged and converted to open water. Marsh health can be inferred from parameters measured repeatedly at CRMS locations, including marsh elevation (H_m), mean water level (H_w), and tide range (TR), all relative to the NAVD88 Geoid12A datum, as well as from soil properties like bulk density (BD, g/cm^3), salinity (SAL, ppt) and organic matter percentage (%OM). Soil properties used here are from the upper 4 cm of the marsh (Table 4-1).

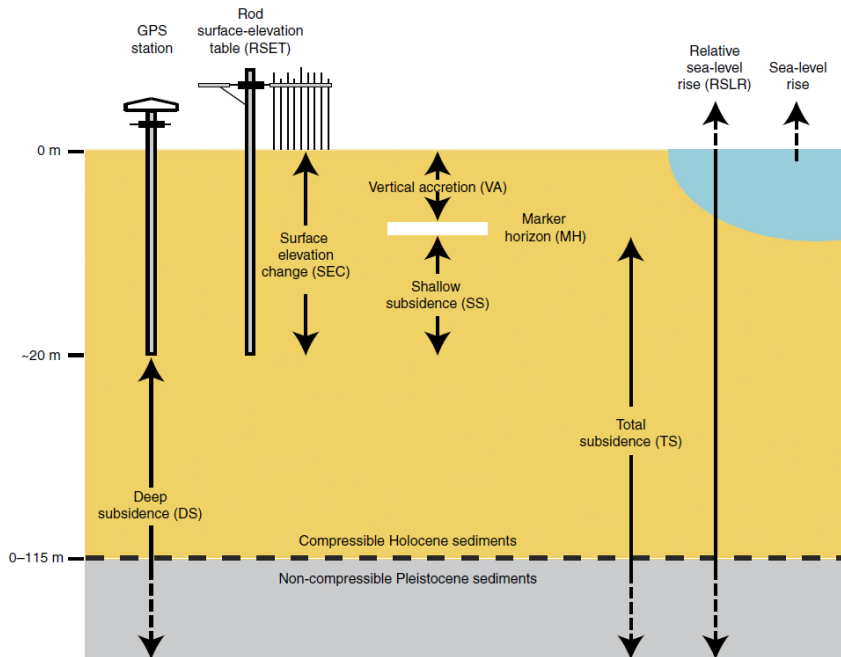


Figure 4-2. Direct (SEC, VA) measurements were made at CRMS sites from Jankowski et al. (2017), in addition to Deep Subsidence (DS) inferred from the CORS station network (Karegar et al. 2015).

All other measures made at CRMS sites are in units of elevation change (\pm -mm/y) of the marsh surface. During each occupation a removable Surface Elevation Table (SET) is fitted to a collar permanently attached to a survey rod driven about 20 m, or until refusal, into the marsh surface (Boumanns and Day 1993, Cahoon et al. 2002, Day et al. 2019, Ch. 3 this report). The table is leveled and a number of thin brass rods, or pins, are lowered through it to the marsh surface (Figure 4-2). The extension of each of the pins required to reach the irregular marsh surface is measured relative to the surveyed elevation of the SET collar. This process is repeated in four quadrants at regular intervals (usually annually) to provide a statistically robust record of Surface Elevation Change (SEC).

The final direct soil measurement made at CRMS sites is of Vertical Accretion (VA). VA is the rate at which sediment, both inorganic and organic, accumulates on the marsh surface. It is operationally determined by repeatedly measuring the thickness in sample cores through the layer of new sediment deposited above a white feldspar clay layer or marker horizon previously spread on the soil surface. Shallow Subsidence (SS), sinking

caused by compaction and consolidation of the soil column to the depth of rod penetration is not directly measured but is indirectly calculated by Jankowski et al. (2017) as:

$$SS = VA - SEC \quad \text{so that} \quad (\text{Eq. 4-2})$$

$$SEC = VA - SS \quad (\text{Eq. 4-3})$$

Along with DS, SEC is all that is needed to solve for marsh surface elevation dynamics, as it is by definition the net of VA and SS.

To survive, tidal marshes must grow upward or aggrade at a rate comparable to Relative Sea Level Rise (RSLR), which Jankowski et al. (2017) calculate as:

$$RSLR = LSLR + DS + SS \quad (\text{Eq. 4-4})$$

For these calculations, Jankowski et al. (2017) treat DS, SS and VA as measures of different processes that would each take place at the same rate independently of the others. In fact, as Jankowski et al. (2017) note, there is an unknown and probably variable overlap between DS and SS, so the sum of these two subsidence components, which Jankowski et al. (2017) report as Total Subsidence (TS) must be considered an upper bound (Figure 4-2). On the other hand, VA can drive SS, which is known to occur primarily in the upper meter of the soil column (Cahoon et al. 2002), as newly deposited sediments apply a load to the marsh surface and are themselves consolidated during wetting and drying to create accommodation space (Day et al. 2011). Accordingly, we calculate RSLR without a separate SS component but including SEC as:

$$RSLR = LSLR - SEC + DS \quad (\text{Eq. 4-5})$$

Chapter 4: RESULTS AND DISCUSSION

Data posted from 15 CRMS stations were acquired along a 50-mile transect (Figure 4-1) from the northern tip of the BMC peninsula south across the MRGO and Bayou Terre aux Boeufs to the Mississippi River near Bohemia (Table 4-1). Following Karegar et al. (2015), DS is imposed as a linear function of latitude ranging from 2.5 to 3.5 mm/y across the BMC and from 3.5 to 4.25 mm/y south of Bayou Terre aux Boeufs in the Breton Marshes (Figure 4-3).

Mean water level (H_w) and mean tide range (TR) also have linear relationships with latitude (Figure 4-4). TR increases by 10 cm from south to north, while H_w decreases slightly by about 4 cm over the same distance. %OM also decreases from around 30 percent near the Mississippi River to about 5 percent at the northern tip of the BMC in a linear trend that explains 53 percent of the variability at CRMS sites (Figure 4-5).

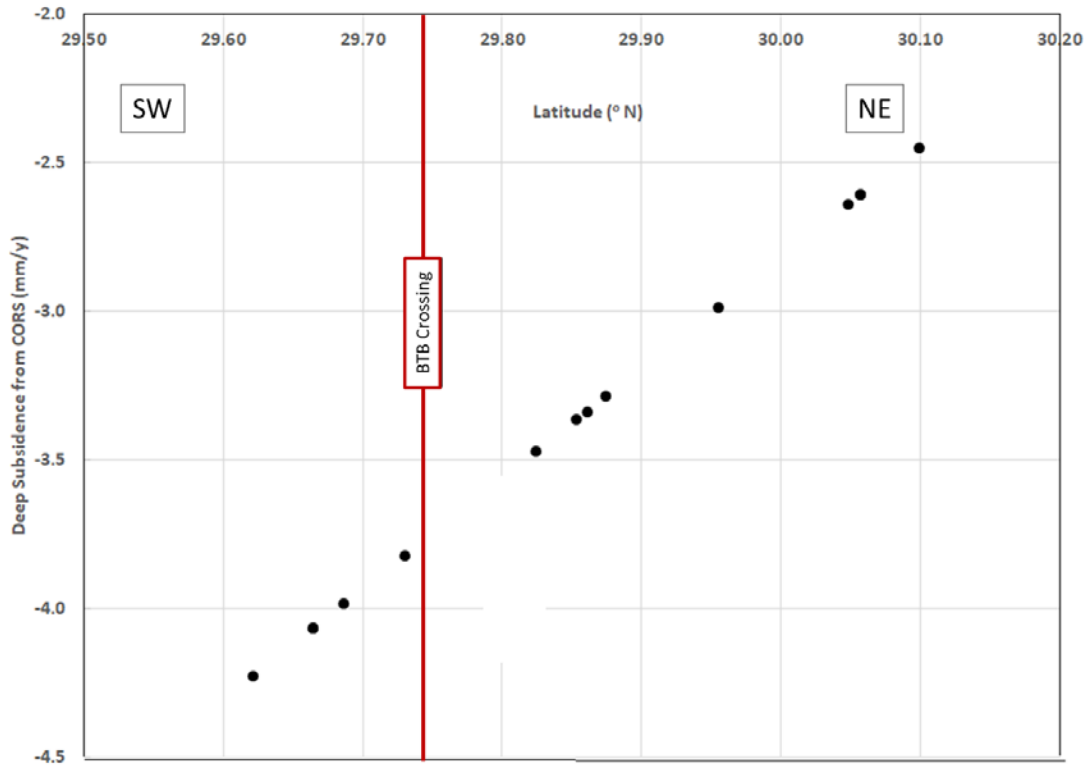


Figure 4-3. Deep Subsidence and Latitude at CORS from Eq. 4-1. Bayou Terre aux Boeufs (BTB)

BD from the upper 4 cm follows a quadratic relationship ($r^2 = 0.47$), increasing from 0.2 g/cm^3 in the Breton marshes to nearly 1.0 g/cm^3 in the northernmost BMC (Figure 4-6). %OM can be predicted from BD at CRMS sites with a high level of confidence ($r^2 = 0.85$), again following a binomial regression (Figure 4-7). BMC CRMS marsh sites experience more inorganic sediment input and increased drying and consolidation, while the Breton marshes to the south relies more on vegetation mediated processes to build soil.

Other differences between BMC marshes north of Bayou Terre aux Boeufs and Breton Sound marshes to the south are not linear and become apparent only when parameters are plotted against latitude. SEC, the vertical shifting of the marsh soil surface, averages 6 mm/y of aggradation in the BMC but is negative at most CRMS locations in the Breton Marsh, averaging 0.5 mm/y in aggregate (Table 4-1). SEC peaks just north of the Bayou Terre aux Boeufs divider with 8 to 10 mm/y aggradation, but trends downward to below 2 mm/y on both ends of the Transect (Figure 4-8). The correlation with latitude explains 67 percent of the observed variation in SEC among CRMS sites on Transect 1.

Marsh surface elevation (H_m), vertical accretion (VA) and shallow subsidence (SS) show no correlation with latitude or with each other. But there is enough information to estimate Relative Sea Level Rise (RSLR), the uncompensated stressor that affects marsh sustainability in the absence of lateral wave erosion.

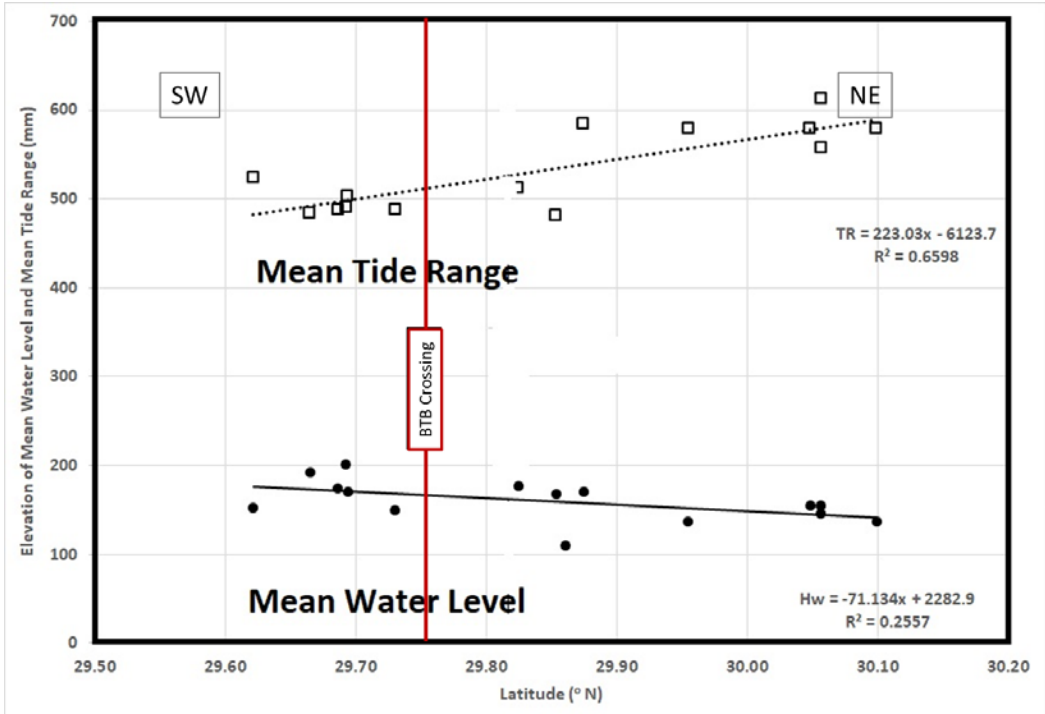


Figure 4-4. Mean water level and tide range with latitude along Transect 1.

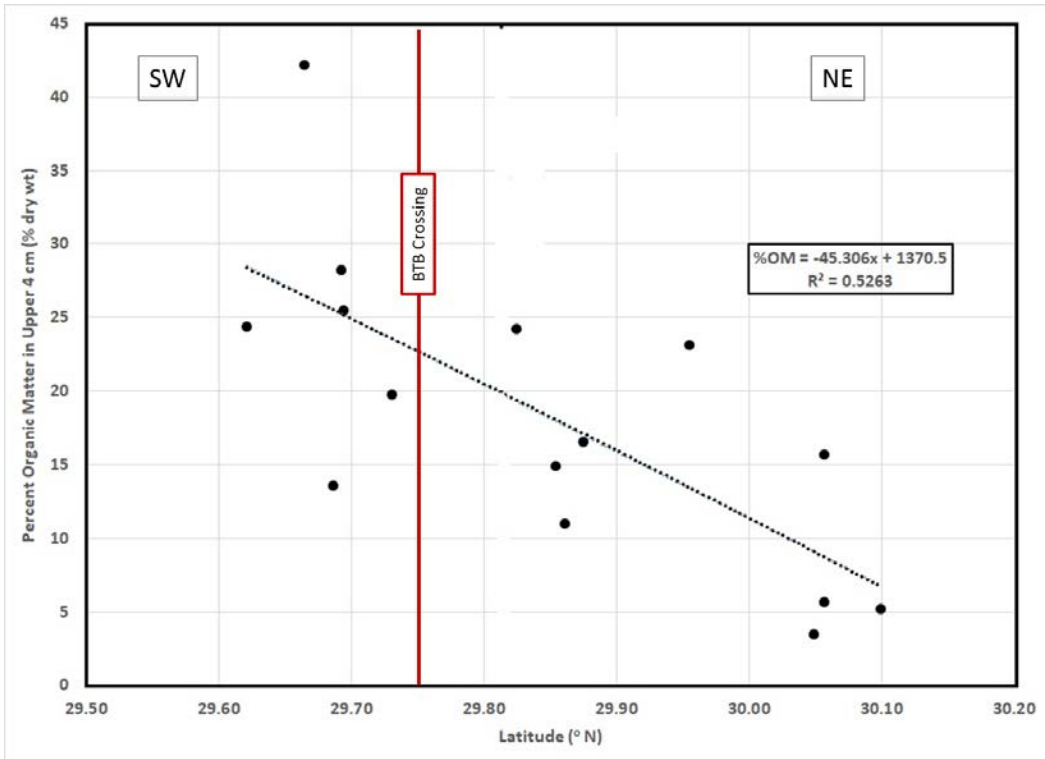


Figure 4-5. Percent organic matter in upper 4 cm of marsh soil along Transect 1.

Table 4-1. Characteristics (2008-2018) of the Biloxi and Breton Marshes at 15 CRMS Locations

| CRMS Number | Latitude ° North | H _{marsh} mm > NAVD88 | SEC mm/y | VA mm/y | DS mm/y | % ORG Upper 4 cm | BD Upper 4 cm g/cc | Mean Tide Range mm | SS = VA - SEC mm/y | RSLR = LSLR - SEC + DS mm/y |
|---------------------------------|------------------|--------------------------------|-------------|--------------|-------------|------------------|--------------------|--------------------|--------------------|-----------------------------|
| 0003 | 30.10 | 268.80 | 2.00 | 17.50 | 2.45 | 5.23 | 0.71 | 579.12 | 15.50 | 2.45 |
| 4572 | 30.06 | 231.20 | 5.50 | 8.60 | 2.61 | 15.68 | 0.46 | 557.78 | 3.10 | -0.89 |
| 4596 | 30.06 | 168.70 | 3.90 | 10.80 | 2.61 | 5.68 | 0.77 | 612.65 | 6.90 | 0.71 |
| 1069 | 30.05 | 284.00 | 1.30 | 11.60 | 2.64 | 3.46 | 0.98 | 579.12 | 10.30 | 3.34 |
| 0108 | 29.96 | 245.90 | 7.10 | 7.20 | 2.99 | 23.14 | 0.23 | 579.12 | 0.10 | -2.11 |
| 1024 | 29.87 | 263.80 | 8.90 | 12.80 | 3.28 | 16.53 | 0.41 | 585.22 | 3.90 | -3.62 |
| 4548 | 29.86 | 158.50 | 6.90 | 10.00 | 3.34 | 10.98 | 0.61 | | 3.10 | -1.56 |
| 4551 | 29.85 | 106.40 | 8.80 | 14.40 | 3.36 | 14.96 | 0.45 | 481.58 | 5.60 | -3.44 |
| 4557 | 29.82 | 161.40 | 10.30 | 12.70 | 3.47 | 24.28 | 0.26 | 512.06 | 2.40 | -4.83 |
| Bayou Terre aux Boeufs Crossing | | | | | | | | | | |
| 0146 | 29.73 | 165.50 | 6.10 | 14.30 | 3.82 | 19.76 | 0.31 | 487.68 | 8.20 | -0.28 |
| 0121 | 29.69 | 70.10 | -1.27 | 7.90 | 3.96 | 25.47 | 0.18 | 502.92 | 9.17 | 7.23 |
| 0131 | 29.69 | 314.40 | -2.20 | 5.40 | 3.96 | 28.24 | 0.29 | 490.73 | 7.60 | 8.16 |
| 0135 | 29.69 | 247.90 | -0.20 | 6.20 | 3.98 | 13.58 | 0.46 | 487.68 | 6.40 | 6.18 |
| 0132 | 29.66 | 228.40 | -0.60 | 10.30 | 4.06 | 42.21 | 0.17 | 484.63 | 10.90 | 6.66 |
| 0136 | 29.62 | 304.34 | 1.13 | 11.30 | 4.23 | 24.41 | 0.37 | 524.26 | 10.17 | 5.10 |
| Biloxi Mean (Stdv) | 29.96 (0.11) | 209.86 (62.27) | 6.08 (3.15) | 11.73 (3.10) | 2.97 (0.40) | 13.33 (7.60) | 0.54 (0.25) | 560.83 (43.01) | 5.66 (4.71) | 1.54 (2.78) |
| Breton Mean (Stdv) | 29.68 (0.04) | 221.77 (91.97) | 0.49 (2.96) | 9.23 (3.37) | 4.00 (0.13) | 25.61 (9.62) | 0.30 (0.11) | 496.32 (15.11) | 8.74 (1.67) | 3.59 (3.11) |

Given that SEC and DS, two of the three terms in Eq. 4-5, are correlated with latitude, and that LSLR is the same everywhere, it is not surprising that RSLR is also correlated with latitude (Figure 4-9). What is unexpected is the strength of the correlation in the binomial regression ($r^2 = 0.71$). Six of the 9 CRMS sites in the BMC have a negative RSLR, indicating that the marsh surface is actually aggrading more rapidly than LSLR, but much of this rapid increase in elevation is associated with unconsolidated organic matter input (Table 4-1). It is also possible that the relative stability of these sites may be related to the partial MRGO recovery or to the presence of the Bayou La Loutre natural levees (Figure 4-1). CRMS sites at the northern end of the transect are experiencing an RSLR of 2 to 4 mm/y as the new inorganic sediment being introduced rapidly dries and consolidates, leading to the high BDs there. Highest RSLR is experienced by Breton Sound marshes which range to more than 8 mm/y. Had SS been factored in, as in Jankowski et al. (2017), RSLR would have been twice the values posted in Table 4-1.

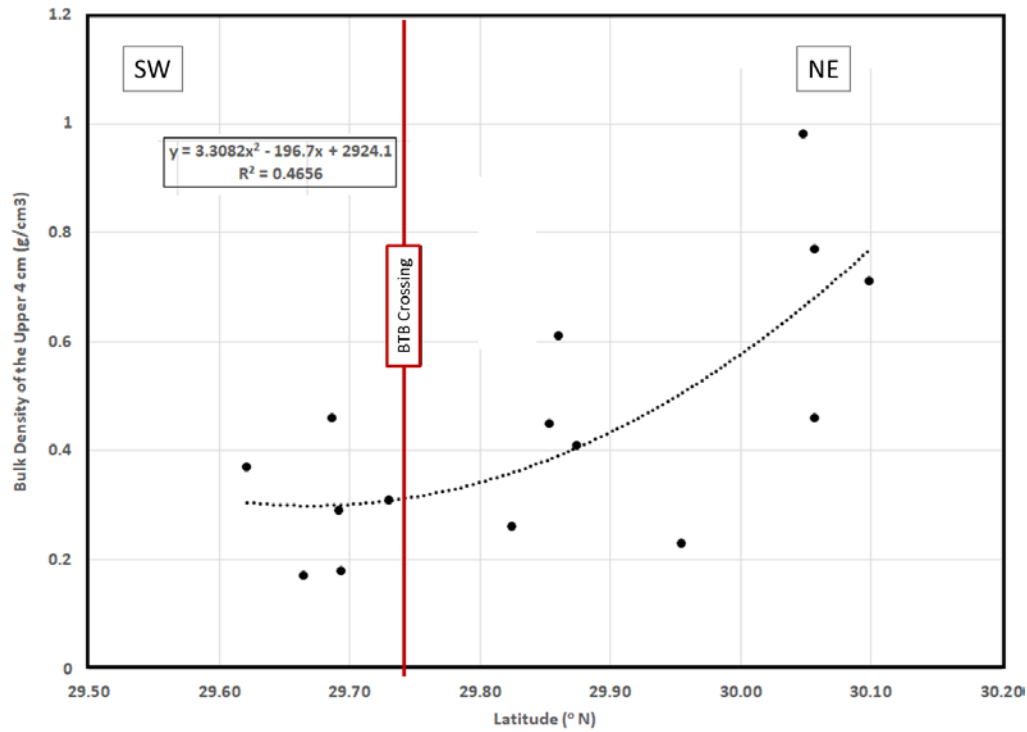


Figure 4-6. Bulk density in upper 4 cm of marsh soil at CRMS locations along Transect 1.

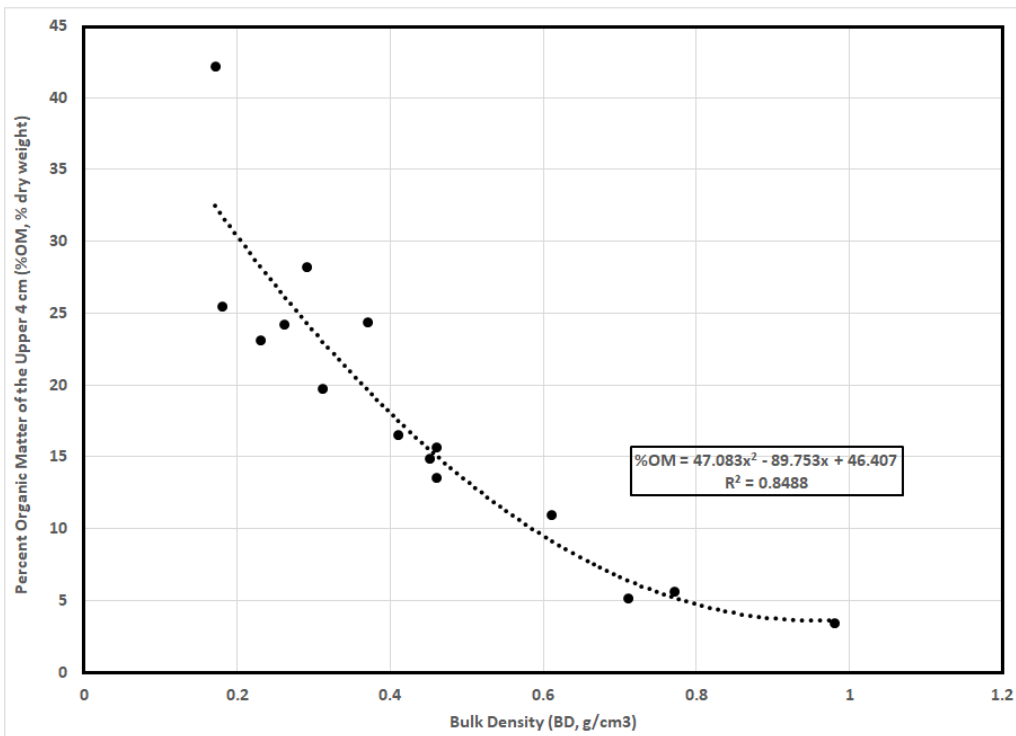


Figure 4-7. Bulk density and Percent Organic Matter in upper 4 cm of marsh soil at CRMS sites.

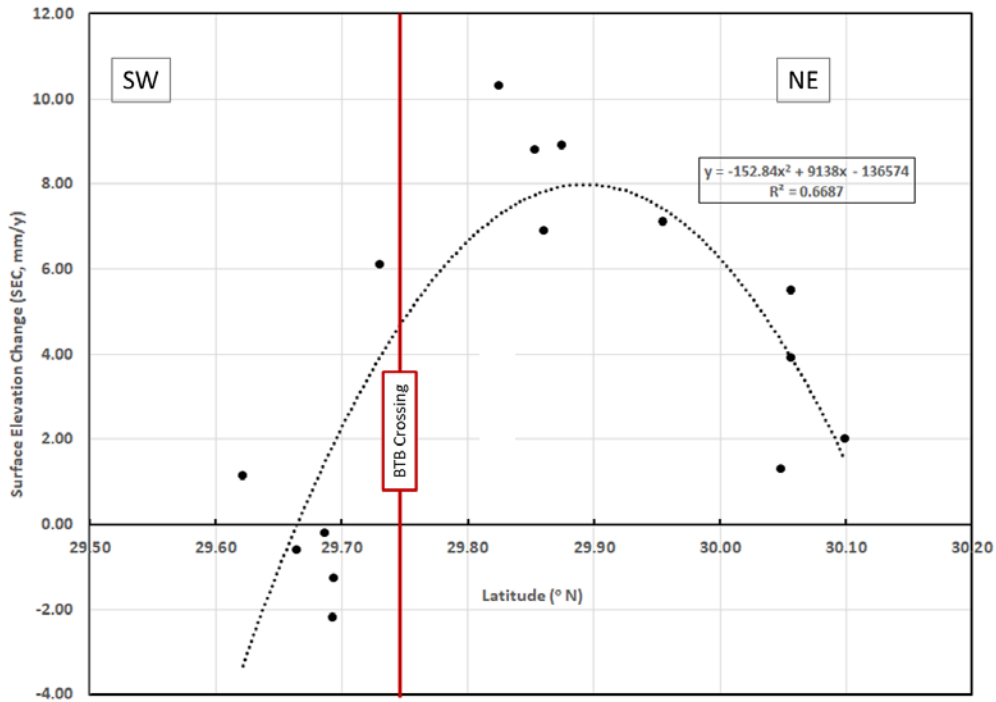


Figure 4-8. SEC Relationship with Latitude at CRMS locations in the Biloxi and Breton Marshes.

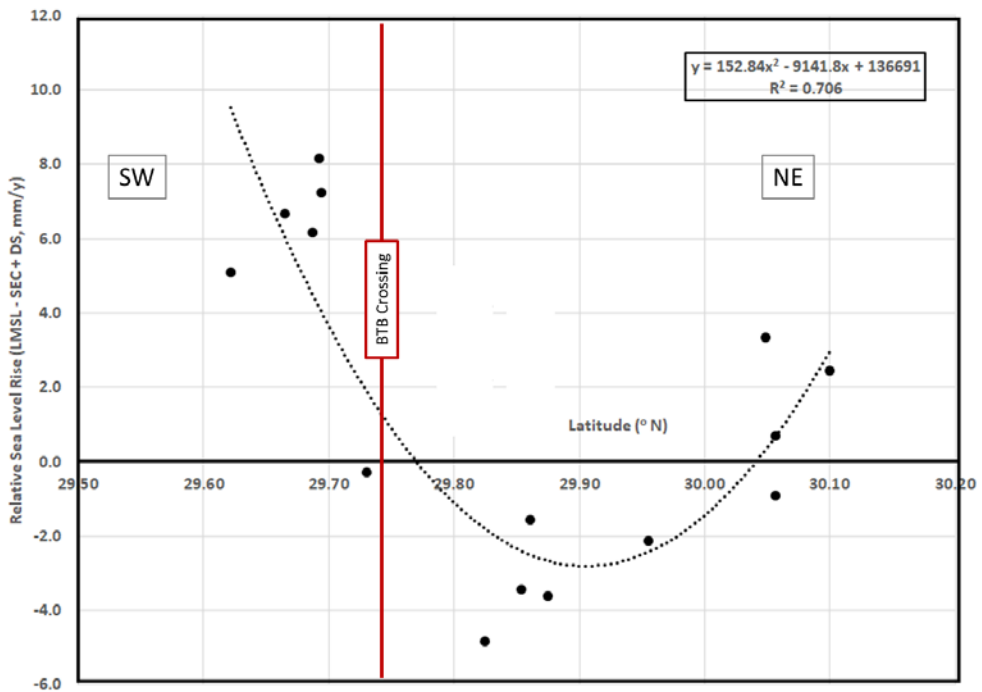


Figure 4-9. RSLR and Latitude at CRMS sites along Transect 1.

Chapter 4: CONCLUSIONS – CRMS DATA AND POLYGON 11

In preparation for CMP 2012, CPRA convened a Subsidence Advisory Panel consisting of geologists and geotechnical engineers familiar with the Southeast Louisiana landscape and its subsidence and land loss areas (Figure 4-10). The panel outlined 15 subsidence polygons for coastal Louisiana and assigned a range of subsidence estimates for each polygon (Figure 4-11). A subsequent publication prepared for CMP 2017 by Reed and Yuill (2017) outlines a plan for acquiring and verifying pertinent subsidence values from present and future studies, but the publication offers little detail as to how the subsidence ranges and polygon outlines were determined.

| Subsidence Advisory Panel Members | |
|---------------------------------------------------------------|--|
| Louis Britsch, PhD, PG, United States Army Corps of Engineers | |
| Roy Dokka*, PhD, Louisiana State University | |
| Joseph Dunbar, PG, United States Army Corps of Engineers-ERDC | |
| Mark Kulp, PhD, University of New Orleans | |
| Michael Stephen, PhD, PG, Coastal Engineering Consultants | |
| Kyle Straub, PhD, Tulane University | |
| Torbjörn Törnqvist, PhD, Tulane University | |

Figure 4-10: Participants on the 1st Subsidence Advisory Panel for CMP 2012.



Figure 4-11: Subsidence polygons and estimated ranges of subsidence rates estimated for each polygon in southeast Louisiana as designated for CMP 2012 and left unchanged in CMP 2017 (Reed and Yuill 2017) which governs project development to 2023.

CMP 2017 did not update the subsidence polygons due to a lack of new published reports on large-scale subsidence patterns in south Louisiana prior to 2015 (Reed and Yuill, 2017). In the published final CMP 2012 and CMP 2017, the BMC is included in Polygon 11, one of the largest polygons in southeast Louisiana. It includes abandoned distributary channels, marsh, and bay environments east of the Mississippi River in Plaquemines Parish, north to Mississippi Sound, and east-west from Caernarvon and the Golden Triangle to Breton and Chandeleur Sounds. Polygon 11 has a low-high range of subsidence rates of 7 mm, estimated as 3-10 mm/yr across the entire polygon. The concern with regard to the BMC is that the broad range in subsidence values strongly influences models for land loss that use the highest subsidence values as though the values apply across the Polygon. Thus, CPRA modeling tends to place the BMC into a subsidence regime which does not reflect the majority of values documented in Chapter 3 which trend below or on the low end of the assigned range (Tables 1 and 2, Chapter 3). However, BMC subsidence values (Day et al. 2019, Ch. 3 this report) compare quite favorably to those assigned to Polygons 2 and 3 which share a number of characteristics with the northern part of Polygon 11 (and the BMC), and not the southern part of Polygon 11.

New polygon designations were presented at the March 20, 2019 CPRA board meeting (Jankowski 2019, Figure 4-12). The outlines do not appear to have changed, and it appears that what was called Polygon 11 in CMP 2012 and CMP 2017 is called Polygon 5 in a map labeled for CMP 2023. Because the new CMP 2023 polygons have not been officially issued, nor new subsidence rates presented with the input of advisory groups, this study uses the CMP 2017 nomenclature and refers to Polygon 11 when discussing the polygon in which the BMC is located.

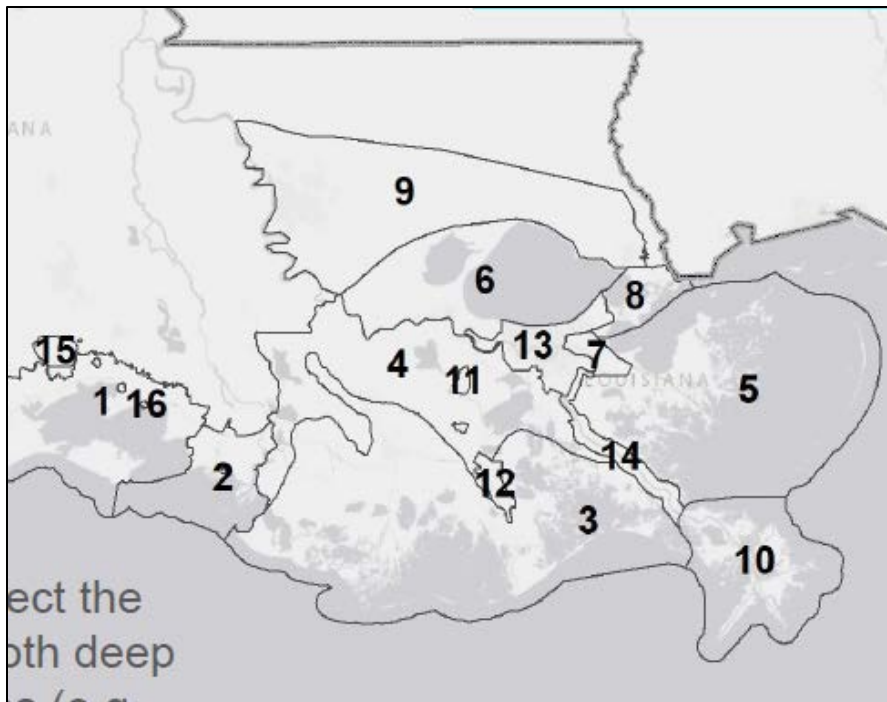


Figure 4-12: Polygon designations as presented at the March 20, 2019 CPRA board meeting (Jankowski 2019). No change in outline is apparent, but the numbers designating

different polygons have changed and Polygon 11 is Polygon 5 in this map labeled for CMP 2023.

Chapter 1 of this report links Holocene thickness to geologic province and notes that faulting and active salt tectonics have contributed to create distinct areas of more rapid subsidence and accumulation of highly compatible young sediment (Gagliano, 2003, 2005) in parts of coastal Louisiana, and that these effects have been in place for millennia. Polygon 11 is observed to extend across at least three structural geologic provinces (c.f. Figure 4-2, Chapter 1, and Karlo and Shoup, 2001) with mobile salt much more active in the south than in the north under the BMC. Correspondingly, Holocene thickness is several times greater in the southern part of Polygon 11 (c.f. Figure 4-9, Chapter 1) than in the north. On Figure 4-13, it is apparent that the northern boundary of Polygon 13 was guided by the 40m contour for Holocene thickness of Kulp et al, 2002 so that the coastal areas within it are entirely in a polygon with 40 m or greater Holocene section (Reed and Yuill 2017), but the 40 m contour was not followed for Polygon 11.

Based on our analysis and the guidelines established by CPRA, Polygon 11 should be separated into two parts: northern and southern, along a line of demarcation defined by Bayou Terre aux Boeufs and the 40 m Holocene thickness contour. BMC would then be part of a Pontchartrain Basin polygon with subsidence rates more representative of its geologic affinity with other parts of the more stable and less tectonically active Pontchartrain Basin that also have thin Holocene section. Accordingly, the southern part of Polygon 11 which is underlain by salt and a salt-tectonics dominated system and characterized by thicker Holocene section would be in a Breton Basin polygon with subsidence rates that are sometimes several orders of magnitude greater than those measured in the northern portion. Corresponding adjustments to subsidence rates used for model development and project eligibility for the BMC region will correct the problem of unreasonably high estimated rates of RSLR and subsidence. Then, projects that focus on the BMC can be implemented in future CPRA plans. In contrast to the dire predictions of extreme land loss in CMP 2012 and 2017, this report demonstrates that multiple lines of evidence point to a positive outlook for the BMC given that the marsh is generally healthy and has not changed in historical times, that the root cause of land loss is not subsidence-related, and that projects similar to those proposed here for the BMC are demonstrated to be effective and sustainable because of the BMC's unique qualities including underlying geology and thickness of Holocene sediments.

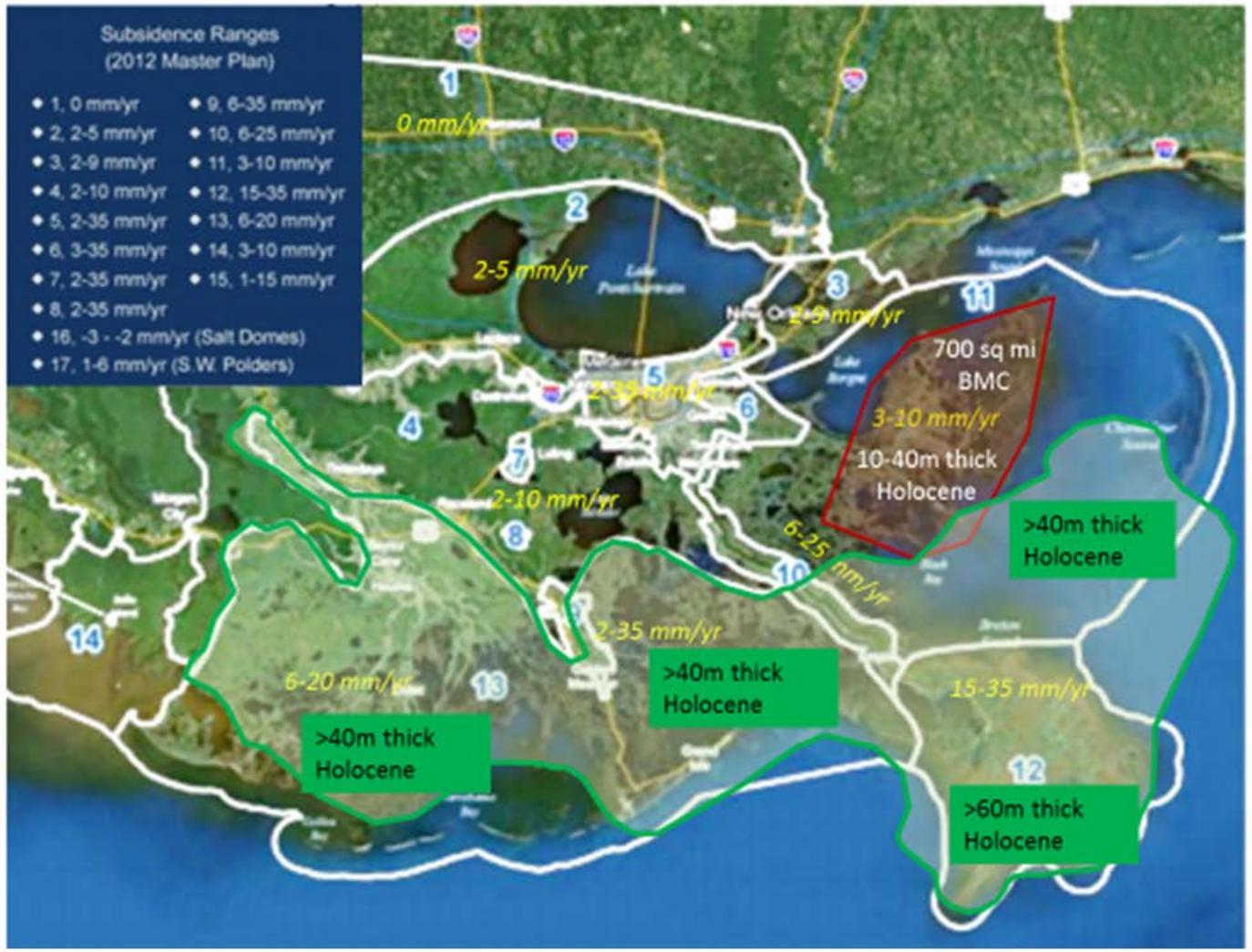


Figure 4-13 CPRA subsidence polygons for southeast LA from Final CMP 2017 (Reed and Yuill 2017) with Holocene thickness >40m from Kulp et al. (2002) outlined in green. Holocene thickness >40m was considered in placement of the northern boundary of Polygon 13, but areas of significantly thinner Holocene were included in the northern part of Polygon 11. The 700 sq. mi. BMC lies entirely within an area with <40m thick Holocene.

Chapter 5: Restoration, Stabilization and Enhancement of the BMC: Project Recommendations

William B. Rudolf¹, John W. Day^{2,3}, G. Paul Kemp³, Robert R. Lane², Elizabeth C. McDade⁴

¹Biloxi Marsh Lands Corporation, and Lake Eugenie Land and Development Inc.,
Metairie, LA 70001

²Comite Resources, PO Box 66596, Baton Rouge LA 70896

³Dept. of Oceanography & Coastal Sciences, Louisiana State University, Baton Rouge LA
70803

⁴Chinn-McDade Associates LLC, Harahan, LA 70123

Chapter 5: INTRODUCTION: ECOLOGICAL SUCCESS AND LONG-TERM SUSTAINABILITY

The stability of the BMC's geologic platform established in this report justifies expenditures on projects that build on the BMC's natural resilience to assure its ecological success and long-term sustainability. CMP 2023 should include projects that are designed to restore, stabilize, and enhance the BMC. They should be prioritized by importance, as a Critical Need or a Near-Term, Mid-Term, or Long-Term Requirement. Timely implementation of projects to address Critical Needs will support the BMC's natural resilience and processes which will buy time to fund and implement additional future projects to further stabilize and enhance the BMC. Adaptive management will need to be employed while moving through the project design and implementation process.

Critical Needs – 1-to-3-year implementation

- *Leveraging Natural Resilience to Ensure Long-Term Sustainability of the Biloxi Marsh Complex: An Integrated Project* (BMC Integrated Project, Appendix I) which the Biloxi Marsh Land Corporation and Lake Eugenie Land & Development, Inc. submitted in response to CPRA's September 19, 2018 RFP addresses the immediate, **Critical Needs** of the BMC. The prompt implementation of this integrated project is essential to protect the Western BMC from near-term peripheral and internal erosion caused by widespread hydrologic connectivity with Lake Borgne's southeastern shoreline. This shoreline is particularly subject to peripheral erosion during seasonal cold front passage and the accompanying strong Northwest winds. Thin-layer marsh nourishment of nearshore marsh is a secondary component of this proposed project (Figure 5-1).



Figure 5-1. High-pressure spray disposal of dredged material (photograph courtesy of Bob Blama, USACE). As effectively demonstrated in Rainey Sanctuary in Vermilion Parish, the primary method of thin-layer placement is to deposit thin layers of sediment by spraying sediment slurry under high pressure over the marsh surface. The technique is essentially a modification of existing hydraulic dredging methods in which sediments are hydraulically dredged, liquefied, and then pumped through a high-pressure spray nozzle.

Near-Term Needs – 3-to-5-year implementation

- The components of the USACE – *MRGO Ecosystem Restoration Plan* (Appendix J) which pertain directly to the BMC should be implemented during this timeframe. Many components of the MRGO Ecosystem Restoration Plan are included in the foregoing Critical Needs section,
- *Three Mile Pass Marsh Creation and Hydrologic Restoration* as proposed by John Lopez, Ph. D. with the Lake Pontchartrain Basin Foundation (Appendix K). This project addresses near-term needs of the Northeastern BMC and possibly could be coordinated with the State of Mississippi.

Mid-Term Needs – 5-to-7-year implementation

- Additional Thin-Layer Marsh Nourishment should be applied throughout the BMC (time accelerated, if funding available). There are numerous locations throughout the BMC that this technique can be successfully applied without any interdependency.

Long-Term – Enhancement – 7-to-10-year implementation

- Identification of means of moving available sediment from the Mississippi River into Lake Borgne (Figure 5-2) will provide a sediment source to enhance the Western BMC. Similarly, harnessing sediment from the Pearl River will enhance the northeastern BMC,
- The natural resiliency of Chandeleur Island lends support for future restoration investment. The Island is reestablishing itself after Hurricane Katrina (Figures 5-3 & 5-4).



Figure 5-4. Mississippi River Plume with Bonnet Carré Spillway open –June 13, 2019

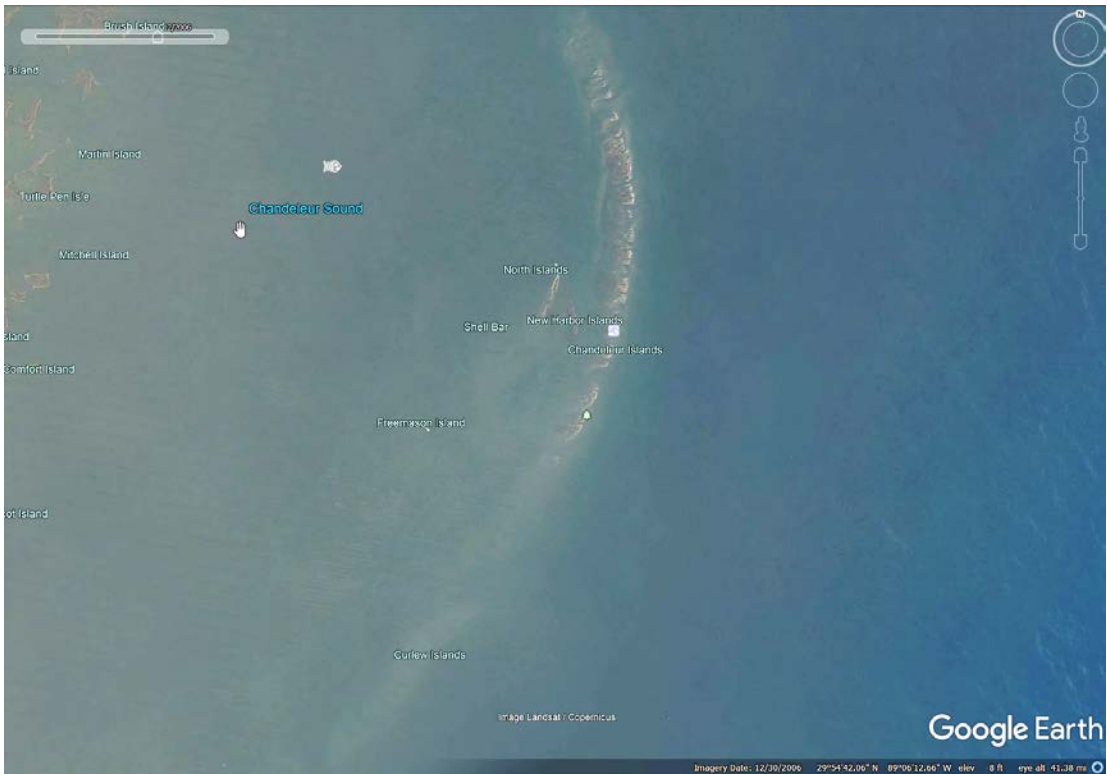


Figure 5-3. Chandeleur Island December – 2006

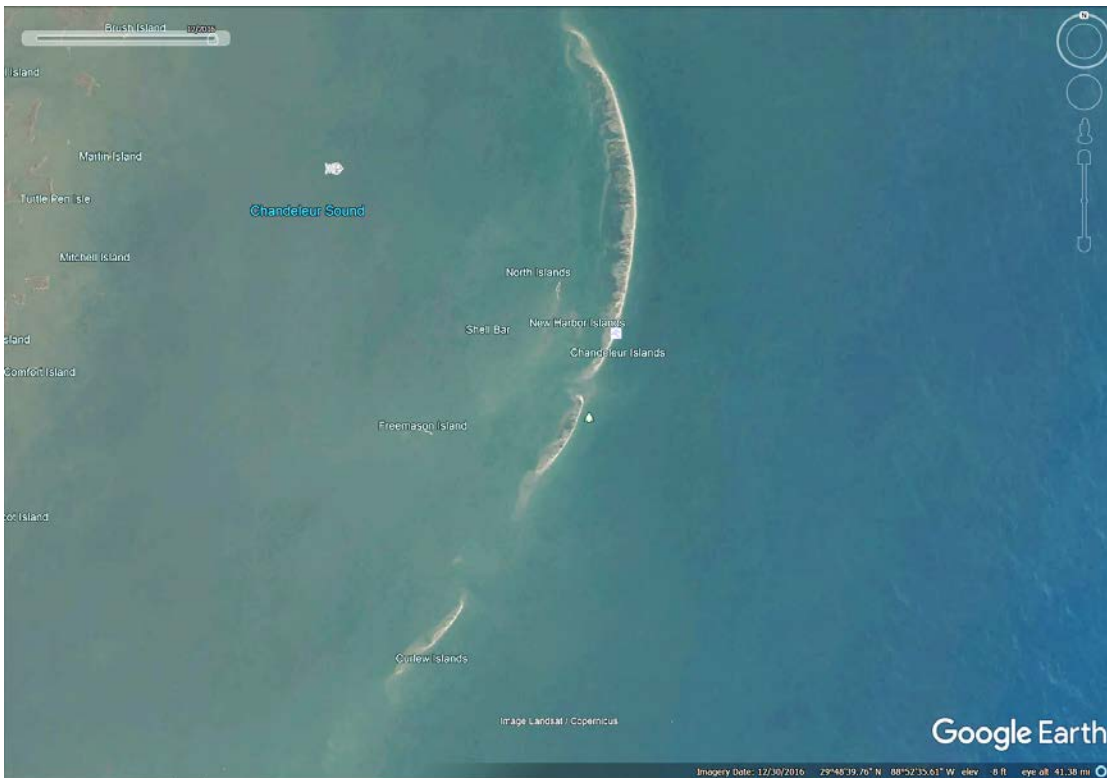


Figure 5-4. Chandeleur Island – December – 2016

Adaptive Management

As conditions within the BMC change, new information and effects of projects that are implemented will become apparent, and prudent adaptive management may dictate changes in priorities, changes in projects, changes in project design, changes in operation parameters of projects, and whether additional projects should be implemented.

Chapter 5: CONCLUSIONS

This report establishes that the BMC is geologically stable and warrants future investment in restoration projects. The BMC's geographic location makes it a critical natural buffer from storm surge for the Greater New Orleans Area (Resio and Westerink, 2008, CPRA 2013) as emergent marsh offers frictional resistance to advancing storm surge and specifics of basin configuration can direct surge. Based on knowledge of the BMC and extensive field study, this chapter identifies the BMC's Critical Needs and Near-Term, Mid-Term, and Long-Term (Enhancement) needs. This chapter sets forth projects to address these needs and suggests a timetable for implementing projects based on need category. Adaptive management must be employed to adapt to real world conditions. Thus, to move forward to stabilize, restore and enhance the BMC, Biloxi Marsh Lands Corporation and Lake Eugenie Land and Development, Inc. stand ready to work with all stakeholders must work together to preserve this critical natural and resilient feature.

Conclusions and Recommendations

1) The parts of the western BMC where marsh elevation is decreasing and shoreline erosion is taking place require marsh nourishment and beach berm reconstruction due to the loss of the natural *Rangia* shell beach berm that armored the shoreline and prevented hydrologic connectivity to Lake Borgne prior to the construction of the MRGO. The BMC Integrated Project concept outlined in Appendix I and submitted to CPRA for inclusion in CMP 2023 is a critical, immediate need to ensure the long-term sustainability of the BMC. As discussed in Chapter 5, preferably the project would be implemented before the CMP 2023, i.e. within 1 to 3 years. Re-establishing the integrity of the western BMC beach berm is essential to provide a hydrological barrier that prevents further connectivity and arrests the spread of erosion into the interior along the many bayous and small ponds that are adjacent to the shoreline. The project will build on the BMC's natural resiliency by re-establishing a beach berm, providing marsh nourishment, and blocking hydrologic connections to interior marshes;

2) There is clear evidence of partial recovery and rebound post MRGO-Closure which can be attributed to the dam in the MRGO below Bayou La Loutre. As the salinity adjusts to pre-MRGO levels, less salt-tolerant vegetation species, including Roseau Cane and Cattails, are recolonizing some areas of the western half of the BMC. Live oak trees along Bayou La Loutre that appeared dead for years are sprouting new leaves. The loss of the *Rangia* clam beach berm along the western shore of the BMC continues to have an increasingly deleterious effect on hydrology, opening pathways for Lake Borgne waters to enter the marsh through exposed bayous and newly formed tidal channels that, in themselves, pose a risk to interior marshes. Given the return of Lake Borgne to pre-MRGO salinities, a recovery of the lake bottom clam *Rangia cuneata* can also be forecast. Maintaining the closure and damming of the MRGO below Bayou La Loutre is critical in allowing the natural partial recovery to continue.

3) Accretion rates and marsh surface elevation gain are positive for almost all areas tested over a 15-year period based on measurements of SET-accretion stations established in 2003 and accretion sites established in 2018. The positive accretion rates and marsh surface elevation gain are due to sediment sources from both Chandeleur Sound and Lake Borgne;

4) Greater elevation gain occurred near Lake Borgne and Chandeleur Sound, and elevation gain was lower in interior marshes further away from sediment sources. Accretion was sufficient to offset relative sea level rise in most areas;

5) Wave action causes erosion along shorelines with effects dependent on wave fetch along the periphery and in internal marsh areas. Interior marshes are also susceptible to tidal scour in areas of hydrologic connection;

6) Where wave action is reduced by nearshore breakwaters, the marsh is observed to quickly extend the vegetated shoreline seaward, reversing the previous trend. Given that these marshes are otherwise healthy and tracking a relatively low RSLR, projects that re-establish a beach berm offer a proven, and very effective, way to sustain BMC wetlands;

7) Poirrier (2019) reviewed the status of Rangia clams in Lake Borgne. He concluded that the high salinities related to the opening of MRGO likely led to a reduction in Rangia clam populations. This interrupted shell supply would have contributed to the deterioration of the shoreline berm on the eastern shore of Lake Borgne. Rangia clam populations and associated shell production can be increased by managing salinity and distributing clams to optimized areas. Rangia clams require salinity shifts of plus or minus five to stimulate spawning and a salinity above two for embryo development and larval survival;

8) The underlying geologic structure of the BMC contrasts with other areas of coastal southeast Louisiana. The BMC is built on a tectonically stable platform. CPRA should use subsidence rates for the BMC representative of its geologic affinity with more stable and less tectonically active areas of the Pontchartrain Basin. Subsidence is not the major issue affecting sustainability of the BMC as evidenced by the generally healthy nature of the marsh.

9) CRMS data analysis confirms the marshes are self-sustaining if lateral shoreline erosion along the margin of Lake Borgne is controlled. Projects proposed in Chapter 5 and in Appendices I, J, and K build upon these key aspects of the BMC;

10) Importantly, the generally healthy nature of the marsh and measured mean water level suggest the BMC is of sufficient elevation to keep the marsh inundation at less than 50% of the time for almost all marshes and less than 20% of the time for some marshes, avoiding water levels that lead to marsh collapse;

11) The excellent CRMS data acquired by CPRA shows that the greatest rates of positive surface elevation change (aggradation) in the BMC are at CRMS sites close to the MRGO footprint;

12) CPRA subsidence Polygon 11 is assigned a range of subsidence rate that is too broad, and with respect to the BMC, Polygon 11 has a low-end rate which is higher than most measured rates in the BMC. As defined in CMP 2017, Polygon 11 covers a large area with boundaries that could be improved.

13) Based on measurements of marsh sustainability made along north-south CRMS profile, the discontinuity at Bayou Terre aux Boeuf provides a good rationale for dividing CPRA subsidence Polygon 11. This will improve wetland sustainability forecasting. Further refinement of a new subsidence polygon for the BMC and Lake Borgne should also incorporate the boundary defined by Holocene thickness, using a Holocene thickness greater than 40 m to define boundaries east and south of the BMC as was used for Polygon 13 in the Terrebonne and Barataria Bay areas.

Literature Cited

- APHA, AWWA, and WCF. 2005. Standard methods for the examination of water and wastewater, 17th ed. American Public Health Association, Washington, DC.
- Bandyopadhyay, B.K., S.R. Pezeshki, R.D. DeLaune, and C.W. Lindau. 1993. Influence of soil oxidation-reduction potential and salinity on nutrition, N-15 uptake, and growth of *Spartina patens*. *Wetlands* 13: 10-15.
- Baumann, R.H., J.W. Day and C.A. Miller. 1984. Mississippi deltaic wetland survival: sedimentation versus coastal submergence. *Science* 224: 1093-1095.
- Boumans, R.M.J. and J.W. Day. 1993. High precision measurements of sediment elevation in shallow coastal areas using a sedimentation-erosion table. *Estuaries* 16(2): 375-380.
- Boesch D.F., L. Shabman, L.G. Antle, et al. 2006. A new framework for planning the future of coastal Louisiana after the hurricanes of 2005. Cambridge, MD: University of Maryland Center for Environmental Science.
- Brady, N.C., R.R. Weil. 2001. *The Nature and Properties of Soils* (13th Edition). Prentice Hall, Upper Saddle River, NJ.
- Braunstein, J., and C. McMichael, 1976, Door Point: A Volcano in Southeastern Louisiana, *GCAGS Transactions*, v. 27, pp. 79-80.
- Cahoon, D.R. 2006. A review of major storm impacts on coastal wetland elevations. *Estuaries & Coasts* 29: 889-898.
- Cahoon, D.R. and D.J. Reed. 1994. Relationships among marsh surface topography, hydroperiod, and soil accretion in a deteriorating Louisiana salt marsh. *Journal of Coastal Research* 11(2): 357-369.
- Cahoon, D.R., and R.E. Turner. 1989. Accretion and canal impacts in a rapidly subsiding wetland II. Feldspar marker horizon technique. *Estuaries* 12: 260-268.
- Cahoon, D.R., B.C. Perez, B.D. Segura, J.C. Lynch. 2011. Elevation trends and shrink swell response of wetland soils to flooding and drying. *Estuarine, Coastal & Shelf Science* 91: 463-474.
- Cahoon, D.R., D.J. Reed, and J.W. Day. 1995. Estimating shallow subsidence in microtidal salt marshes of the southeastern United States: Kaye and Barghoorn revisited. *Marine Geology* 128: 1-9.
- Cahoon, D.R., J.C. Lynch, B.C. Perez, B. Segura, R.D. Holland, C. Stelly, G. Stephenson, and P. Hensel. 2002b. High-precision measurements of wetland sediment elevation: II. The rod surface elevation table. *Journal of sediment research* 72: 734-739.
- Cahoon, D.R., J.C. Lynch, P. Hensel, R. Boumans, B.C. Perez, B. Segura, and J.W. Day. 2002a. High-precision measurements of wetland sediment elevation: I. Recent improvements to the sedimentation-erosion table. *Journal of sediment research* 72:

730-733.

- Cahoon, D.R., J.W. Day, and D.J. Reed. 1999. The influence of surface and shallow subsurface soil processes on wetland elevation: a synthesis. *Current Topics in Wetland Biogeochemistry* 3: 72-88.
- Cahoon, D.R., P.E. Marin, B.K. Black, and J.C. Lynch. 2000. A method for measuring vertical accretion, elevation, and compaction of soft, shallow-water sediments. *Journal of Sedimentary Research* 70: 1250-1253.
- Couvillion, B.R., Beck, H., Schoolmaster, D., and M. Fischer. 2017. Land Area Change in Coastal Louisiana (1932 to 2016). U.S. Geological Survey Scientific Investigations Map 3381, 16 p. pamphlet. <https://doi.org/10.3381/sim3381>.
- Callaway, J.C., J.A. Nyman, and R.D. DeLaune. 1996. Sediment accretion in coastal wetlands: a review and a simulation model of processes. *Current Topics in Wetland Biogeochemistry* 2: 2-23.
- Day, J.W., F. Scarton, A. Rismondo, and D. Arc. 1998. Rapid deterioration of a salt marsh in Venice Lagoon, Italy. *Journal of Coastal Research* 14: 583-590.
- Day, J.W., J. Rybczyk, F. Scarton, A. Rismondo, D. Are, and G. Cecconi. 1999. Soil accretionary dynamics, sea-level rise and the survival of wetlands in Venice Lagoon: a field and modelling approach. *Estuarine, Coastal & Shelf Science* 49: 607-628.
- Day, J.W., Kemp, G.P., Reed, D.J., Cahoon, D.R., Boumans, R.M., Suhayda, J.M., and R. Gambrell. 2011. Vegetation death and rapid loss of surface elevation in two contrasting Mississippi delta salt marshes: the role of sedimentation, autocompaction and sea-level rise. *Ecological Engineering* 37: 229-240.
- DeLaune, R. D., and S. R. Pezeshki. 1988. Relationship of mineral nutrients to growth of *Spartina alterniflora* in Louisiana salt marshes. *Northeast Gulf Science* 10: 195-204.
- Delaune, R. D., and S. R. Pezeshki. 2003. The role of soil organic carbon in maintaining surface elevation in rapidly subsiding U.S. Gulf of Mexico coastal marshes. *Water, Air, & Soil Pollution* 3: 167-179.
- DeLaune, R. D., W. H. Patrick, and N. V. Breemen. 1990. Processes governing marsh formation in a rapidly subsiding coastal environment. *Catena* 17: 277-288.
- Fisk, H. N., 1944, Geological Investigation of the Lower Alluvial Valley of the Lower Mississippi River, USACE, Vicksburg, MS,.
- FitzGerald, D.M., M.S. Fenster, B.A. Argow, and I.V. Buynevich. 2008. Coastal impacts due to sea-level rise. *Annual Revue Earth & Planetary Sciences* 36: 601-647.
- Flocks, J., M. Kulp, J. Smith, and S. J. Williams, 2009, Review of the Geologic History of the Pontchartrain Basin, Northern Gulf of Mexico: *Journal of Coastal Research*, v. 54, no. Special Issue, p. 12–22.
- Ford, M.A. and J.B. Grace. 1998b. The interactive effects of fire and herbivory on a coastal marsh in Louisiana. *Wetlands* 18: 1-8.

- Frank, J., 2017, Evidence of fault movement during the Holocene in Southern Louisiana: integrating 3-D seismic data with shallow high-resolution seismic data: MS Thesis, University of New Orleans, 91 pp.
- Frank, J., and M. Kulp, 2016, Integrating 3-D Industry seismic with shallow high resolution seismic: Have deep seated faults affected Pleistocene through Holocene environments of south Louisiana, Geological Society of America Annual Meeting DOI 10.1130/abs/2016AM-287106.
- Frazier, D. E., 1967, Recent Deltaic Deposits of the Mississippi River: Their Development and Chronology: Transactions Gulf Coast Association of Geological Societies, v. 17, p. 287–315.
- Frederick, B. C., M. Blum, R. Fillon, and H. H. Roberts, 2019, Resolving the contributing factors to Mississippi Delta subsidence: Past and Present: Basin Research, v. 31, no. 1, p. 171–190.
- Gagliano, S. M., 2005, Effects of Earthquakes, Fault Movements and subsidence on the South Louisiana Landscape: The Louisiana Civil Engineer, Journal of the Louisiana Section, American Society of Civil Engineers, v. 13, no. 2, p. 23.
- Gagliano, S. M., E. B. Kemp, K. M. Wicker, K. S. Wiltenmuth, and R. W. Sabate, 2003, Neotectonic framework of southeast Louisiana and applications to coastal restoration: Gulf Coast Association of Geological Societies, v. 53, p. 262–276.
- Gagliano, S. M., K. M. Wicker, J. Battle, G. Wang, J. T. Arnold, and G. Castille, 2010, Navigability Assessment of Stump Lagoon in St. Bernard Parish, Louisiana, Coastal Environments, Inc., Report no. 28095, 268 pp.
- Galloway, W., Patricia E. Ganey-Curry, Xiang Li, and Richard T. Buffler 2000, Cenozoic depositional history of the Gulf of Mexico basin, AAPG Bulletin, v. 85, no. 11, pp. 1743-1774.
- Hackney, C.T. and A.A. de la Cruz. 1983. Effects of winter fire on the productivity and species composition of two brackish marsh communities in Mississippi. International Journal of Ecology and Environmental Science 9: 185-208.
- Hatton, R.S., R.D. Delaune, and J.W.H. Patrick. 1983. Sedimentation, accretion, and subsidence in marshes of Barataria Basin, Louisiana. Limnology & Oceanography 28: 494-502.
- Heinrich, Paul, Robert Paulsell, Riley Milner, John Snead and Hampton Peele, 2015, Investigation and GIS development of the buried Holocene-Pleistocene surface in the Louisiana coastal plain: Baton Rouge, LA, Louisiana Geological Survey-Louisiana State University for Coastal Protection and Restoration Authority of Louisiana, 140 p., 3 pls.
- Heltz, 2005, Evidence of Neotectonic Activity in Southwestern Louisiana: Louisiana State University, 89 pp.
- Hensel, P.F., J.W. Day, and D. Pont. 1999. Wetland vertical accretion and soil elevation change in the Rhone River delta, France: the importance of riverine flooding. Journal

of Coastal Research 15: 668-681.

- Howes, N.C., D.M. FitzGerald, Z.J. Hughes, I.Y. Georgiou, M.A. Kulp, M.D. Miner, J.M. Smith, and J.A. Barras. 2010. Hurricane-induced failure of low salinity wetlands. *Proceedings of the National Academy of Sciences* 107: 14014-14019.
- Hudec, M., Ian O. Norton, Martin P. Jackson, and Frank J. Peel, 2013, Jurassic Evolution of the Gulf of Mexico Basin, *AAPG Bulletin*, v. 97, no. 10, p. 1683-1710.
- Ibáñez, C., A. Canicio, J.W. Day and A. Curco. 1997. Morphologic development, relative sea level rise and sustainable management of water and sediment in the Ebre Delta, Spain. *Journal of Coastal Conservation*. 3: 191-202.
- Jankowski, K. L., 2019, MASTER PLAN ENVIRONMENTAL SCENARIOS UPDATE SUBSIDENCE, Slide Presentation: Baton Rouge, CPRA Board Meeting, March 2019.
- Jankowski, K. L., T. E. Törnqvist, and A. M. Fernandes, 2017, Vulnerability of Louisiana's coastal wetlands to present-day rates of relative sea-level rise: *Nature Communications*, v. 8, p. 14792.
- Karimpour, A., Q. Chen, and R.R. Twilley. 2016. A field study of how wind waves and currents may contribute to the deterioration of saltmarsh fringe. *Estuaries & Coasts* 39: 935-950.
- Karlo, J., and Shoup, 2001, Classifications of Syndepositional Systems of the Northern Gulf of Mexico, **Search and Discovery Article #30004 (2000)** <http://www.searchanddiscovery.com/documents/karlo/index.htm>
- Kent, M., and P. Coker. 1992. *Vegetation description and analysis: a practical approach*. John Wiley & Sons Ltd.
- Kindinger, J., S. J. Williams, S. Penland, J. Flocks, and P. Connor, 1997, Holocene Geologic Framework of Lake Pontchartrain Basin and Lakes of Southeastern Louisiana: *Gulf Coast Association of Geological Societies Transactions*, v. 47, p. 635–638.
- Kolb, C. R., F. L. Smith, and R. C. Silva, 1975, Pleistocene sediments of the New Orleans-Lake Pontchartrain area, Technical Report S-75-6: Vicksburg, MS, U. S. Army Corps of Engineers, 9 p.
- Kuecher, G. J., H. H. Roberts, M. D. Thompson, and L. Matthews, 2001, Evidence of Active Growth Faulting in the Terrebonne Delta Plain, South Louisiana: Implications for Wetland Loss and the Vertical Migration of Petroleum; *Environmental Geosciences*, v. 8, no. 2, p. 77–94.
- Kulp, M. A., 2000, Holocene Stratigraphy, History, and Subsidence: Mississippi River Delta region, North-Central Gulf of Mexico, Ph.D. Dissertation: University of Kentucky, 359 p.
- Kulp, M., P. Howell, S. Adiau, S. Penland, J. Kindinger, and S. J. Williams, 2002, Latest Quaternary Stratigraphic Framework of the Mississippi River Delta Region: *Gulf*

Coast Association of Geological Societies Transactions, v. 52, p. 573–582.

- Lane, R.R., J.W. Day Jr., and J.N. Day. 2006. Wetland surface elevation, vertical accretion, and subsidence at three Louisiana estuaries receiving diverted Mississippi River water. *Wetlands* 26: 1130-1142.
- Lane, R.R., J.W. Day, G.P. Shaffer, R.G. Hunter, J.N. Day, W.B. Wood, and P. Settoon. 2015b. Hydrology and water budget analysis of the East Joyce wetlands: Past history and prospects for the future. *Ecological Engineering* 87: 34-44.
- Lane, R.R., S.K. Mack, J.W. Day, R. Kempka, L.J. Brady. 2017. Carbon sequestration at a forested wetland receiving treated municipal effluent. *Wetlands* 37(5): 861-873.
- Lane, R.R., Day, J.W., Jr., and G.P. Kemp 2019. SET and Accretion Data at Historical Plots in the Biloxi Marshes. Comite Resources Report to Biloxi Marshlands Corporation, New Orleans, LA 16pp, Apps.
- Lopez, J., Henkel, T., and P. Connor. 2015. Methodology for Hydrocoast Mapping of the Pontchartrain Basin: 2012 to 2015. Technical Report, Lake Pontchartrain Basin Foundation, New Orleans, LA. 38pp.
- Lopez, J., S. Penland, and S. J. Williams, 1997, Confirmation of Active Geologic Faults in Lake Pontchartrain in southeast Louisiana: *Gulf Coast Association of Geological Societies Transactions*, v. 47, p. 299–303.
- Lynch, J. J. 1941. The place of burning in wildlife management of the Gulf coast wildlife refuges. *Journal of Wildlife Management* 5: 454-457.
- McCarthy, and J. James. 2009. Reflections on: our planet and its life, origins, and futures." *Science* 326: 1646-1655.
- McFalls, T.B., P.A. Keddy, D. Campbell, and G. Shaffer. 2010. Hurricanes, floods, levees, and nutria: vegetation responses to interacting disturbance and fertility regimes with implications for coastal wetland restoration. *Journal of Coastal Research* 26: 901-911.
- Meehl, G.A., C. Tebaldi, G. Walton, D. Easterling, and L. McDaniel. 2009. Relative increase of record high maximum temperatures compared to record low minimum temperatures in the US. *Geophysical Research Letters* 36, no. 23: L23701.
- Mendelssohn, I.A. and J.T. Morris. 2000. Eco-physiological controls on the productivity of *Spartina alterniflora* loisel. In: *Concepts and controversies in tidal marsh ecology*, M.P. Weinstein and D.A. Kreeger eds. p. 59-80. Kuwer Academic Publishers, Boston, Mass
- Miller, L., and B.C. Douglas. 2004. Mass and volume contributions to twentieth-century global sea level rise. *Nature* 428: 406-409.
- Morton, R.A., N.A. Buster, and D.M. Krohn. 2002. Subsurface Controls on historical subsidence rates and associated wetland loss in southcentral Louisiana. *Gulf Coast Association of Geological Societies Transactions* 52: 767-778.

- Nienhuis, J. H., T. E. Tornqvist, K. L. Jankowski, A. M. Fernandes, and M. E. Keogh, 2017, A New Subsidence Map for Coastal Louisiana: *GSA Today*, v. 27, doi:[doi:10.1130/GSATG337GW.1](https://doi.org/10.1130/GSATG337GW.1).
- NRCS. 2011. Soil survey laboratory information manual. Soil Survey Investigations Report No. 45, Version 2.0. R. Burt (ed.). U.S. Department of Agriculture, Natural Resources Conservation Service. <http://soils.usda.gov/survey/nscd/lim/>
- Nyman, J.A., R.D. Delaune, & W.H. Patrick. 1990. Wetland soil formation in the rapidly subsiding Mississippi River deltaic plain: mineral and organic matter relationships. *Estuarine, Coastal & Shelf Science* 31: 57-69.
- Nyman, J.A., and R.H. Chabreck. 1995. Fire in coastal marshes: history and recent concerns. In: *Fire in wetlands: a management perspective*. Proceedings of the Tall Timbers Fire Ecology Conference. No. 19.
- Olea, R. A., and J. L. Coleman Jr., 2014, A Synoptic Examination of the causes of land loss in southern Louisiana: *Journal of Coastal Research*, v. 30, no. 5, p. 1025–1044.
- Osland, M.J., K.T. Griffith, J.C. Larriviere, L.C. Feher, D.R. Cahoon, N.M. Enwright, D.A. Oster, J.M. Tirpak, M.S. Woodrey, R.C. Collini, J.J. Baustian, J.L. Breithaupt, J.A. Cherry, J.R. Conrad, N. Cormier, C.A. Coronado-Molina, J.F. Donoghue, S.A. Graham, J.W. Harper, M.W. Hester, R.J. Howard, K. W. Krauss, D.E. Kroes, R.R. Lane, K.L. McKee, I.A. Mendelsohn, B.A. Middleton, J.A. Moon, S.C. Piazza, N.M. Rankin, F.H. Sklar, G.D. Steyer, K.M. Swanson, C.M. Swarzenski, W.C. Vervaeke, J.M. Willis, K. VanWilson. 2017. Assessing coastal wetland vulnerability to sea-level rise along the northern Gulf of Mexico coast: Gaps and opportunities for developing a coordinated regional sampling network. *PLoS one* 12: e0183431.
- Pahl, J., 2017, Eustatic Sea Level Rise. Version Final. (p. 23).: Baton Rouge, Louisiana, Coastal Protection and Restoration Authority, 2017 Coastal Master Plan: Attachment C2-1.
- Peel, F., C. Travis, and J. R. Hossack, 1995, *Genetic Structural Provinces of the*: AAPG Memoir 65, p. 153–175.
- Penland, S., L. Wayne, L. D. Britsch, S. J. Williams, A. D. Beall, and V. C. Butterworth, 2000, Process classification of coastal land loss between 1932 and 1990 in the Mississippi River Delta Plain, southeastern Louisiana, USGS Numbered Series: Open-File Report, 1 map 50-90 cm on sheet p.
- Perez, B.C., J.W. Day, L.J. Rouse, R.F. Shaw, and M. Wang. 2000. Influence of Atchafalaya River discharge and winter frontal passage and flux in Fourleague Bay, Louisiana. *Estuarine, Coastal & Shelf Science* 50: 271-290.
- Pezeshki, S.R., and R.D. DeLaune. 1990. Influence of sediment oxidation-reduction potential on root elongation in *Spartina patens*. *Acta Oecologica* 11: 377-383.
- Pezeshki, S.R., and R.D. DeLaune. 1993. Effects of soil hypoxia and salinity on gas exchange and growth of *Spartina patens*. *Marine Ecology Progress Series* 96: 75-81.

- Pezeshki, S.R., and R.D. DeLaune. 1996. Responses of *Spartina alterniflora* and *Spartina patens* to rhizosphere oxygen deficiency. *Acta Oecologica* 17: 365-378.
- Poirrier, M.A. 2013. Effects of closure of the Mississippi River Gulf Outlet on saltwater intrusion and bottom water hypoxia in Lake Pontchartrain. *Gulf and Caribbean Research* 25: 105-109.
- Poore, M.E.D. 1955. The use of phytosociological methods in ecological investigations. The Braun-Blanquet System. *Journal of Ecology* 43: 226.
- Rahmstorf, S. 2007. A semi-empirical approach to projecting future sea-level rise. *Science* 315: 368-370.
- Reed, D., and B. Yuill, 2017, Coastal Master Plan 2017 Attachment C2-2: Subsidence.
- Roberts, H., R. Morton, and A. Freeman, 2008, A High-Resolution Seismic Assessment of Faulting in the Louisiana Coastal Plain: Gulf Coast Association of Geological Societies, v. 58, p. 733–745.
- Rounsefell., G. A. 1964. Preconstruction study of the fisheries of the estuarine areas traversed by the Mississippi River-Gulf Outlet project. *Fish. Bull.* 63: 373-393.
- Russell, R.J. et al. 1936. Lower Mississippi River Delta. Louisiana Geological Survey Bulletin 8. 454 pp.
- Sall, J., A. Lehman, M. Stephens, and L. Creighton. 2012. *JMP Start Statistics: A Guide to Statistical and Data Analysis using JMP*, Fifth Edition. Cary, NC: SAS Institute Inc. 625p.
- Sasser, C.E., J.G. Gosselink, E.M. Swenson, and D.E. Evers. 1995. Hydrologic, vegetation, and substrate characteristics of floating marshes in sediment-rich wetlands of the Mississippi river delta plain, Louisiana, USA. *Wetlands Ecology* 3: 171-187.
- Schuster, D. C., 1995, Deformation of Allochthonous Salt and Evolution of Related Salt-Structural Systems: AAPG Memoir, v. 66.
- Seglund, J. A., 1974, Collapse Fault Systems of the Louisiana Gulf Coast: Gulf Coast Association of Geological Societies Transactions, v. 24, p. 1–3.
- Shaffer, Gary P., John W. Day, Jr., Sarah Mack, G. Paul Kemp, Ivor van Heerden, Michael A. Poirrier, Karen A. Westphal, Duncan FitzGerald, Andrew Milanes, Chad A. Morris, Robert Bea, and P. Shea Penland, 2009, The MRGO Navigation Project: A Massive Human-Induced Environmental, Economic, and Storm Disaster, *Journal of Coastal Research*, S1, v. 54, pp. 206-224.
- Shinkle, K.D. and Dokka, R.K., 2004. Rates of vertical displacement at benchmarks in the lower Mississippi valley and the northern Gulf coast. National Oceanic and Atmospheric Administration (NOAA) Technical Report NOS/NGS 50, 135p.
- Swarzenski, C.M., and S.V. Mize. 2014. Effects of Hydrologic Modifications on Salinity and Formation of Hypoxia in the Mississippi River-Gulf Outlet and Adjacent Waterways, Southeastern Louisiana, 2008 to 2012. U.S. Geological Survey Scientific

- Investigations Report 2014-5077. 21pp.
- Treadwell, R.C. 1955. Sedimentology and Ecology of Southeast Coastal Louisiana. Technical Report No. 6. Louisiana State University, Baton Rouge, LA. 42 pp.
- Trosclair, K.J. 2013. Wave transformation at a saltmarsh edge and resulting marsh edge erosion: observations and modeling. University of New Orleans Theses & Dissertations. Paper 1777.
- Viosca, P. 1931. Spontaneous combustion in the Marshes of Southern Louisiana. *Ecology* 12: 439-442.
- Whipple, S.A. and D. White. 1977. The effects of fire on two Louisiana marshes. *Association of Southeastern Biologists Bulletin* 24: 95.
- Williams, S.J. 2013. Sea-level rise implications for coastal regions. *Journal of Coastal Research* 63: 184-196.
- Wright, R.L., Sperry, J.J., and D.L. Huss. 1960. Vegetation Type Mapping Studies of the Marshes of Southeastern Louisiana. Texas A&M Research Foundation Project 191 report submitted to the Bureau of Sports Fisheries and Wildlife, Fish and Wildlife Service, U.S. Department of Interior. College Station, TX 41 pp. and maps.
- Yuill, B., D. Lavoie, and D. Reed, 2009, Understanding subsidence processes in coastal Louisiana: *Journal of Coastal Research (JCR)*, v. SI(54), p. 23–36.
- van Asseelen, S., 2011, The contribution of peat compaction to total basin subsidence: implication for the provision of accommodation space in organic-rich deltas: *Basin Research*, v. 23, no. 2, p. 239–255.

Appendix A: Hydrology Data Tables and Field Records

Table A1. Coordinates of marsh study sites.

| Site | Latitude | Longitude |
|------------|--------------|--------------|
| A1a | 29° 57.877'N | 89° 34.066'W |
| A1b | 29° 54.108'N | 89° 35.447'W |
| A1c | 29° 56.777'N | 89° 34.842'W |
| A2 | 29° 47.556'N | 89° 22.720'W |
| A3 | 29° 43.818'N | 89° 39.041'W |
| B1 | 29° 55.183'N | 89° 30.824'W |
| B2 | 29° 49.311'N | 89° 31.610'W |
| C1 | 29° 53.416'N | 89° 29.844'W |
| C2 | 29° 47.180'N | 89° 32.037'W |

Table A2. Coordinates and location names of Rounsefell (1964) stations visited in this study. The Rounsefell station abbreviations are shown in Figure 3.

| Station | Latitude | Longitude | Station | Latitude | Longitude |
|-----------------|--------------|--------------|--------------------------|--------------|--------------|
| BM | 29° 51.910'N | 89° 35.093'W | LE | 29° 46.343'N | 89° 26.113'W |
| B. St. Malo | | | Lake Eloi | | |
| BPPN | 29° 47.523'N | 89° 28.874'W | TP | 29° 49.380'N | 89° 24.987'W |
| B. Pointe N | | | Treasure Pass | | |
| CP | 29° 49.067'N | 89° 28.679'W | LL | 29° 53.107'N | 89° 31.404'W |
| China Pass | | | B.La Loutre | | |
| BPPS | 29° 47.523'N | 89° 28.874'W | LLBC1 | 29° 50.313'N | 89° 32.852'W |
| B. Pointe S | | | La Loutre & Bakers Can W | | |
| LAN | 29° 45.824'N | 89° 28.224'W | LLBC2 | 29° 50.445'N | 89° 28.729'W |
| L. Athanasio N | | | La Loutre & Bakers Can E | | |
| LAS | 29° 43.790'N | 89° 25.907'W | MP | 29° 53.570'N | 89° 29.992'W |
| L. Athanasio S | | | Mike's Pass | | |
| TW | 29° 49.574'N | 89° 36.078'W | | | |
| La Loutre Tower | | | | | |

Table A3. Mean bulk density at the study sites.

| Site | Bulk Density (g/cm ³) | Site | Bulk Density (g/cm ³) | Site | Bulk Density (g/cm ³) |
|------------|-----------------------------------|-----------|-----------------------------------|-----------|-----------------------------------|
| A1a | 0.211±0.012 | A2 | 0.359±0.021 | B2 | 0.109±0.007 |
| A1b | 0.241±0.014 | A3 | 0.357±0.027 | C1 | 0.067±0.004 |
| A1c | 0.459±0.016 | B1 | 0.119±0.016 | C2 | 0.334±0.026 |

Table A4. Species composition at the study sites.

| Site | Dist. (m) | Species | % cover | Site | Dist. (m) | Species | % cover |
|------|-----------|------------------------------|---------|------|-----------|------------------------------|---------|
| A1a | 5 | <i>Spartina alterniflora</i> | 75 | B1 | 5 | <i>Spartina alterniflora</i> | 99 |
| A1a | 5 | <i>Spartina patens</i> | 25 | B1 | 5 | <i>Spartina patens</i> | 1 |
| A1a | 25 | <i>Spartina patens</i> | 70 | B1 | 25 | <i>Spartina patens</i> | 50 |
| A1a | 25 | open | 25 | B1 | 25 | open | 40 |
| A1a | 25 | <i>Spartina alterniflora</i> | 5 | B1 | 25 | <i>Spartina alterniflora</i> | 10 |
| A1a | 50 | <i>Spartina patens</i> | 80 | B1 | 50 | <i>Spartina alterniflora</i> | 95 |
| A1a | 50 | open | 15 | B1 | 50 | <i>Spartina patens</i> | 5 |
| A1a | 50 | <i>Spartina alterniflora</i> | 5 | B2 | 5 | <i>Juncus roemerianus</i> | 75 |
| A1b | 5 | <i>Spartina alterniflora</i> | 50 | B2 | 5 | open | 25 |
| A1b | 5 | <i>Spartina patens</i> | 40 | B2 | 25 | <i>Juncus roemerianus</i> | 50 |
| A1b | 5 | open | 10 | B2 | 25 | <i>Spartina patens</i> | 25 |
| A1b | 25 | <i>Spartina patens</i> | 80 | B2 | 25 | <i>Spartina alterniflora</i> | 20 |
| A1b | 25 | open | 10 | B2 | 25 | open | 5 |
| A1b | 25 | <i>Spartina alterniflora</i> | 10 | B2 | 50 | <i>Juncus roemerianus</i> | 50 |
| A1b | 50 | <i>Spartina alterniflora</i> | 80 | B2 | 50 | <i>Spartina alterniflora</i> | 40 |

| | | | | | | | |
|-----|----|------------------------------|----|----|----|------------------------------|----|
| A1b | 50 | open | 10 | B2 | 50 | <i>Spartina patens</i> | 5 |
| A1b | 50 | <i>Spartina patens</i> | 5 | B2 | 50 | open | 5 |
| A1b | 50 | <i>Juncus roemerianus</i> | 5 | C1 | 5 | <i>Spartina alterniflora</i> | 50 |
| A1c | 5 | <i>Spartina alterniflora</i> | 50 | C1 | 5 | open | 40 |
| A1c | 5 | open | 25 | C1 | 5 | <i>Spartina patens</i> | 10 |
| A1c | 5 | <i>Juncus roemerianus</i> | 15 | C1 | 25 | <i>Spartina patens</i> | 75 |
| A1c | 5 | <i>Spartina patens</i> | 5 | C1 | 25 | <i>Spartina alterniflora</i> | 20 |
| A1c | 25 | <i>Spartina alterniflora</i> | 40 | C1 | 25 | <i>Juncus roemerianus</i> | 10 |
| A1c | 25 | open | 40 | C1 | 50 | <i>Spartina alterniflora</i> | 80 |
| A1c | 25 | <i>Spartina patens</i> | 15 | C1 | 50 | <i>Spartina patens</i> | 15 |
| A1c | 25 | <i>Juncus roemerianus</i> | 5 | C1 | 50 | <i>Distichlis spicata</i> | 5 |
| A1c | 50 | open | 50 | C2 | 5 | <i>Spartina patens</i> | 50 |
| A1c | 50 | <i>Spartina alterniflora</i> | 45 | C2 | 5 | <i>Spartina alterniflora</i> | 25 |
| A1c | 50 | <i>Spartina patens</i> | 5 | C2 | 5 | <i>Juncus roemerianus</i> | 25 |
| A2 | 5 | open | 35 | C2 | 25 | <i>Spartina alterniflora</i> | 80 |
| A2 | 5 | <i>Juncus roemerianus</i> | 25 | C2 | 25 | <i>Juncus roemerianus</i> | 15 |
| A2 | 5 | <i>Distichlis spicata</i> | 25 | C2 | 25 | open | 5 |
| A2 | 5 | <i>Batis m</i> | 10 | C2 | 50 | <i>Spartina alterniflora</i> | 50 |
| A2 | 5 | <i>Spartina alterniflora</i> | 5 | C2 | 50 | <i>Juncus roemerianus</i> | 45 |
| A2 | 25 | <i>Juncus roemerianus</i> | 50 | C2 | 50 | open | 5 |
| A2 | 25 | <i>Distichlis spicata</i> | 50 | | | | |
| A2 | 50 | <i>Juncus roemerianus</i> | 60 | | | | |
| A2 | 50 | <i>Spartina patens</i> | 30 | | | | |
| A2 | 50 | <i>Spartina alterniflora</i> | 10 | | | | |
| A3 | 5 | <i>Juncus roemerianus</i> | 90 | | | | |
| A3 | 5 | <i>Spartina alterniflora</i> | 5 | | | | |
| A3 | 5 | open | 5 | | | | |
| A3 | 25 | <i>Juncus roemerianus</i> | 75 | | | | |
| A3 | 25 | <i>Distichlis spicata</i> | 20 | | | | |
| A3 | 25 | <i>Spartina alterniflora</i> | 5 | | | | |
| A3 | 50 | <i>Juncus roemerianus</i> | 75 | | | | |
| A3 | 50 | <i>Distichlis spicata</i> | 20 | | | | |
| A3 | 50 | <i>Spartina alterniflora</i> | 5 | | | | |

Table A5. Percent water and bulk density (BD) raw data.

| Site | Depth (cm) | Water (%) | BD g/cm ³ | Site | Depth (cm) | Water (%) | BD g/cm ³ | Site | Depth (cm) | Water (%) | BD g/cm ³ |
|---------------|------------|-----------|----------------------|---------------|------------|-----------|----------------------|---------------|------------|-----------|----------------------|
| A1a | 0-2 | 75% | 0.25 | A2 | 0-2 | 63% | 0.20 | B2 | 0-2 | 85% | 0.08 |
| A1a | 2-4 | 74% | 0.27 | A2 | 2-4 | 62% | 0.25 | B2 | 2-4 | 80% | 0.11 |
| A1a | 4-6 | 77% | 0.16 | A2 | 4-6 | 63% | 0.37 | B2 | 4-6 | 74% | 0.11 |
| A1a | 6-8 | 76% | 0.21 | A2 | 6-8 | 64% | 0.42 | B2 | 6-8 | 66% | 0.14 |
| A1a | 8-10 | 76% | 0.20 | A2 | 8-10 | 62% | 0.30 | B2 | 8-10 | 79% | 0.10 |
| A1a | 10-12 | 75% | 0.18 | A2 | 10-12 | 66% | 0.35 | B2 | 10-12 | 81% | 0.08 |
| A1a | 12-14 | 69% | 0.22 | A2 | 12-14 | 66% | 0.32 | B2 | 12-14 | 83% | 0.08 |
| A1a | 14-16 | 67% | 0.27 | A2 | 14-16 | 56% | 0.42 | B2 | 14-16 | 84% | 0.10 |
| A1a | 16-18 | 66% | 0.25 | A2 | 16-18 | 53% | 0.51 | B2 | 16-18 | 84% | 0.09 |
| A1a | 18-20 | 68% | 0.27 | A2 | 18-20 | 56% | 0.45 | B2 | 18-20 | 85% | 0.10 |
| A1a | 20-22 | 72% | 0.17 | A2 | 20-22 | 63% | 0.43 | B2 | 20-22 | 86% | 0.10 |
| A1a | 22-24 | 76% | 0.13 | A2 | 22-24 | 67% | 0.29 | B2 | 22-24 | 85% | 0.09 |
| A1a | 24-26 | 79% | 0.15 | A2 | 24-26 | 68% | 0.34 | B2 | 24-26 | 84% | 0.13 |
| A1a | 26-28 | 68% | 0.21 | A2 | 26-28 | 70% | 0.34 | B2 | 26-28 | 83% | 0.15 |
| A1a | 28-30 | 72% | 0.23 | A2 | 28-30 | 67% | 0.39 | B2 | 28-30 | 80% | 0.17 |
| Total: | | | 0.21 | Total: | | | 0.36 | Total: | | | 0.11 |
| A1b | 0-2 | 73% | 0.27 | A3 | 0-2 | 63% | 0.24 | C1 | 0-2 | 85% | 0.09 |
| A1b | 2-4 | 74% | 0.17 | A3 | 2-4 | 70% | 0.22 | C1 | 2-4 | 84% | 0.05 |
| A1b | 4-6 | 75% | 0.23 | A3 | 4-6 | 69% | 0.29 | C1 | 4-6 | 83% | 0.09 |
| A1b | 6-8 | 73% | 0.19 | A3 | 6-8 | 66% | 0.26 | C1 | 6-8 | 83% | 0.06 |
| A1b | 8-10 | 70% | 0.23 | A3 | 8-10 | 64% | 0.30 | C1 | 8-10 | 82% | 0.06 |
| A1b | 10-12 | 64% | 0.26 | A3 | 10-12 | 64% | 0.42 | C1 | 10-12 | 83% | 0.07 |

| | | | | | | | | | | | |
|--------------------|-------|-----|------|--------------------|-------|-----|------|--------------------|-------|-----|------|
| A1b | 12-14 | 69% | 0.22 | A3 | 12-14 | 62% | 0.38 | C1 | 12-14 | 82% | 0.09 |
| A1b | 14-16 | 71% | 0.16 | A3 | 14-16 | 65% | 0.35 | C1 | 14-16 | 81% | 0.06 |
| A1b | 16-18 | 58% | 0.34 | A3 | 16-18 | 65% | 0.43 | C1 | 16-18 | 85% | 0.05 |
| A1b | 18-20 | 63% | 0.24 | A3 | 18-20 | 64% | 0.63 | C1 | 18-20 | 87% | 0.05 |
| A1b | 20-22 | 69% | 0.27 | A3 | 20-22 | 68% | 0.44 | C1 | 20-22 | 87% | 0.05 |
| A1b | 22-24 | 71% | 0.29 | A3 | 22-24 | 68% | 0.42 | C1 | 22-24 | 88% | 0.05 |
| A1b | 24-26 | 66% | 0.33 | A3 | 24-26 | 69% | 0.36 | C1 | 24-26 | 84% | 0.06 |
| A1b | 26-28 | 70% | 0.25 | A3 | 26-28 | 72% | 0.29 | C1 | 26-28 | 85% | 0.09 |
| A1b | 28-30 | 74% | 0.17 | A3 | 28-30 | 74% | 0.32 | C1 | 28-30 | 86% | 0.08 |
| Total: 0.24 | | | | Total: 0.36 | | | | Total: 0.07 | | | |
| A1c | 0-2 | 47% | 0.54 | B1 | 0-2 | 82% | 0.23 | C2 | 0-2 | 73% | 0.26 |
| A1c | 2-4 | 54% | 0.51 | B1 | 2-4 | 79% | 0.17 | C2 | 2-4 | 72% | 0.35 |
| A1c | 4-6 | 56% | 0.51 | B1 | 4-6 | 81% | 0.16 | C2 | 4-6 | 67% | 0.25 |
| A1c | 6-8 | 58% | 0.43 | B1 | 6-8 | 79% | 0.18 | C2 | 6-8 | 62% | 0.41 |
| A1c | 8-10 | 63% | 0.51 | B1 | 8-10 | 80% | 0.17 | C2 | 8-10 | 58% | 0.38 |
| A1c | 10-12 | 57% | 0.46 | B1 | 10-12 | 77% | 0.19 | C2 | 10-12 | 59% | 0.41 |
| A1c | 12-14 | 58% | 0.50 | B1 | 12-14 | 80% | 0.15 | C2 | 12-14 | 50% | 0.53 |
| A1c | 14-16 | 64% | 0.38 | B1 | 14-16 | 84% | 0.11 | C2 | 14-16 | 54% | 0.53 |
| A1c | 16-18 | 63% | 0.45 | B1 | 16-18 | 88% | 0.06 | C2 | 16-18 | 66% | 0.27 |
| A1c | 18-20 | 57% | 0.53 | B1 | 18-20 | 83% | 0.10 | C2 | 18-20 | 67% | 0.34 |
| A1c | 20-22 | 64% | 0.36 | B1 | 20-22 | 86% | 0.05 | C2 | 20-22 | 70% | 0.28 |
| A1c | 22-24 | 66% | 0.43 | B1 | 22-24 | 88% | 0.05 | C2 | 22-24 | 72% | 0.28 |
| A1c | 24-26 | 62% | 0.48 | B1 | 24-26 | 87% | 0.05 | C2 | 24-26 | 71% | 0.26 |
| A1c | 26-28 | 67% | 0.34 | B1 | 26-28 | 86% | 0.07 | C2 | 26-28 | 73% | 0.26 |
| A1c | 28-30 | 62% | 0.45 | B1 | 28-30 | 86% | 0.05 | C2 | 28-30 | 76% | 0.20 |
| Total: 0.46 | | | | Total: 0.12 | | | | Total: 0.33 | | | |

Table A6. Total suspended sediment raw data.

| Date | Site | PreWgt (g) | Volume (ml) | PstWgt (g) | TSS (mg/L) | Date | Site | PreWgt (g) | Volume (ml) | PstWgt (g) | TSS (mg/L) |
|----------|------|------------|-------------|------------|------------|----------|-------|------------|-------------|------------|------------|
| 2/20/18 | A1a | 0.0931 | 835 | 0.1064 | 15.9 | 2/21/18 | CP | 0.0922 | 840 | 0.1048 | 15.0 |
| 4/25/18 | A1a | 0.0929 | 530 | 0.1059 | 24.5 | 4/25/18 | CP | 0.0948 | 500 | 0.1084 | 27.2 |
| 6/26/18 | A1a | 0.0928 | 885 | 0.1028 | 11.3 | 6/26/18 | CP | 0.0927 | 753 | 0.1153 | 30.0 |
| 9/12/18 | A1a | 0.0932 | 820 | 0.1035 | 12.6 | 9/12/18 | CP | 0.0928 | 500 | 0.1095 | 33.4 |
| 11/16/18 | A1a | 0.0937 | 600 | 0.1138 | 33.5 | 11/16/18 | CP | 0.0927 | 868 | 0.1058 | 15.1 |
| 2/20/18 | A1b | 0.0929 | 850 | 0.0984 | 6.5 | 2/21/18 | LAN | 0.0936 | 770 | 0.1203 | 34.7 |
| 4/25/18 | A1b | 0.0921 | 490 | 0.1052 | 26.7 | 4/25/18 | LAN | 0.0932 | 725 | 0.1099 | 23.0 |
| 6/26/18 | A1b | 0.093 | 760 | 0.1027 | 12.8 | 6/26/18 | LAN | 0.0921 | 700 | 0.1047 | 18.0 |
| 9/12/18 | A1b | 0.0928 | 933 | 0.1015 | 9.3 | 9/12/18 | LAN | 0.0933 | 625 | 0.1191 | 41.3 |
| 11/16/18 | A1b | 0.0936 | 625 | 0.1096 | 25.6 | 11/16/18 | LAN | 0.0922 | 915 | 0.1011 | 9.7 |
| 4/25/18 | A1c | 0.092 | 500 | 0.1062 | 28.4 | 2/21/18 | LAS | 0.0931 | 840 | 0.1157 | 26.9 |
| 6/26/18 | A1c | 0.0928 | 820 | 0.1079 | 18.4 | 4/25/18 | LAS | 0.0919 | 755 | 0.1048 | 17.1 |
| 9/12/18 | A1c | 0.0921 | 870 | 0.1053 | 15.2 | 6/26/18 | LAS | 0.0927 | 345 | 0.1027 | 29.0 |
| 11/16/18 | A1c | 0.0937 | 610 | 0.1117 | 29.5 | 9/12/18 | LAS | 0.0918 | 500 | 0.1154 | 47.2 |
| 2/21/18 | A2 | 0.0932 | 673 | 0.1321 | 57.8 | 11/16/18 | LAS | 0.0937 | 850 | 0.1061 | 14.6 |
| 4/25/18 | A2 | 0.0928 | 780 | 0.1057 | 16.5 | 2/21/18 | LE | 0.0941 | 610 | 0.121 | 44.1 |
| 6/26/18 | A2 | 0.0913 | 500 | 0.1135 | 44.4 | 4/25/18 | LE | 0.0932 | 535 | 0.1075 | 26.7 |
| 9/12/18 | A2 | 0.0925 | 425 | 0.1018 | 21.9 | 6/26/18 | LE | 0.0915 | 700 | 0.1053 | 19.7 |
| 11/16/18 | A2 | 0.0919 | 950 | 0.1066 | 15.5 | 9/12/18 | LE | 0.0926 | 580 | 0.1119 | 33.3 |
| 2/20/18 | A3 | 0.0925 | 500 | 0.1091 | 33.2 | 11/16/18 | LE | 0.0931 | 865 | 0.1101 | 19.7 |
| 4/27/18 | A3 | 0.0928 | 500 | 0.106 | 26.4 | 2/20/18 | LL | 0.0929 | 600 | 0.1095 | 27.7 |
| 6/26/18 | A3 | 0.0929 | 553 | 0.1048 | 21.5 | 4/25/18 | LL | 0.0941 | 500 | 0.1108 | 33.4 |
| 9/12/18 | A3 | 0.0925 | 337 | 0.1119 | 57.6 | 6/26/18 | LL | 0.0917 | 600 | 0.1056 | 23.2 |
| 11/16/18 | A3 | 0.0937 | 905 | 0.1045 | 11.9 | 9/12/18 | LL | 0.093 | 690 | 0.11 | 24.6 |
| 2/20/18 | B1 | 0.0931 | 840 | 0.1108 | 21.1 | 11/16/18 | LL | 0.0935 | 500 | 0.1114 | 35.8 |
| 4/25/18 | B1 | 0.0936 | 683 | 0.1098 | 23.7 | 2/20/18 | LLBC1 | 0.0926 | 830 | 0.1135 | 25.2 |
| 6/26/18 | B1 | 0.0916 | 620 | 0.1087 | 27.6 | 4/25/18 | LLBC1 | 0.0931 | 385 | 0.1112 | 47.0 |
| 9/12/18 | B1 | 0.0924 | 655 | 0.1108 | 28.1 | 6/26/18 | LLBC1 | 0.0926 | 500 | 0.1116 | 38.0 |
| 11/16/18 | B1 | 0.0929 | 825 | 0.1007 | 9.5 | 9/12/18 | LLBC1 | 0.0915 | 655 | 0.1041 | 19.2 |
| 2/21/18 | B2 | 0.0929 | 730 | 0.114 | 28.9 | 11/16/18 | LLBC1 | 0.0943 | 850 | 0.1037 | 11.1 |
| 4/25/18 | B2 | 0.0931 | 635 | 0.1046 | 18.1 | 2/21/18 | LLBC2 | 0.0911 | 770 | 0.1089 | 23.1 |
| 6/26/18 | B2 | 0.0914 | 500 | 0.1043 | 25.8 | 4/25/18 | LLBC2 | 0.0908 | 355 | 0.1102 | 54.6 |

| | | | | | | | | | | | |
|----------|------|--------|-----|--------|------|----------|-------|--------|-----|--------|------|
| 9/12/18 | B2 | 0.091 | 348 | 0.1132 | 63.8 | 6/26/18 | LLBC2 | 0.0927 | 700 | 0.1138 | 30.1 |
| 11/16/18 | B2 | 0.094 | 900 | 0.1066 | 14.0 | 9/12/18 | LLBC2 | 0.0925 | 500 | 0.1072 | 29.4 |
| 2/20/18 | BM | 0.0927 | 830 | 0.1106 | 21.6 | 11/16/18 | LLBC2 | 0.093 | 857 | 0.1064 | 15.6 |
| 4/25/18 | BM | 0.0916 | 770 | 0.1027 | 14.4 | 2/20/18 | MP | 0.0922 | 750 | 0.1112 | 25.3 |
| 6/26/18 | BM | 0.0936 | 800 | 0.102 | 10.5 | 4/25/18 | MP | 0.0946 | 415 | 0.1064 | 28.4 |
| 9/12/18 | BM | 0.0908 | 800 | 0.1048 | 17.5 | 6/26/18 | MP | 0.0941 | 500 | 0.108 | 27.8 |
| 11/16/18 | BM | 0.0923 | 825 | 0.1094 | 20.7 | 9/12/18 | MP | 0.0933 | 725 | 0.1094 | 22.2 |
| 2/21/18 | BPPN | 0.095 | 500 | 0.1122 | 34.4 | 11/16/18 | MP | 0.0933 | 845 | 0.107 | 16.2 |
| 4/25/18 | BPPN | 0.0933 | 500 | 0.1069 | 27.2 | 2/21/18 | TP | 0.0923 | 840 | 0.1211 | 34.3 |
| 6/26/18 | BPPN | 0.0906 | 700 | 0.1104 | 28.3 | 4/25/18 | TP | 0.0922 | 500 | 0.1072 | 30.0 |
| 9/12/18 | BPPN | 0.0918 | 745 | 0.1147 | 30.7 | 6/26/18 | TP | 0.0952 | 500 | 0.1107 | 31.0 |
| 11/16/18 | BPPN | 0.0929 | 825 | 0.1062 | 16.1 | 9/12/18 | TP | 0.093 | 583 | 0.1058 | 22.0 |
| 2/20/18 | C1 | 0.0916 | 785 | 0.1149 | 29.7 | 11/16/18 | TP | 0.0946 | 810 | 0.1072 | 15.6 |
| 4/25/18 | C1 | 0.0943 | 330 | 0.1035 | 27.9 | 2/20/18 | TW | 0.0918 | 820 | 0.1077 | 19.4 |
| 6/26/18 | C1 | 0.092 | 500 | 0.1089 | 33.8 | 4/27/18 | TW | 0.0924 | 680 | 0.1009 | 12.5 |
| 9/12/18 | C1 | 0.0933 | 750 | 0.1045 | 14.9 | 6/26/18 | TW | 0.0926 | 600 | 0.1018 | 15.3 |
| 11/16/18 | C1 | 0.0929 | 935 | 0.1068 | 14.9 | 9/12/18 | TW | 0.0938 | 948 | 0.1042 | 11.0 |
| 2/21/18 | C2 | 0.0926 | 850 | 0.1142 | 25.4 | 11/16/18 | TW | 0.0935 | 805 | 0.1019 | 10.4 |
| 4/25/18 | C2 | 0.0935 | 500 | 0.1076 | 28.2 | | | | | | |
| 6/26/18 | C2 | 0.0917 | 700 | 0.1034 | 16.7 | | | | | | |
| 9/12/18 | C2 | 0.0924 | 628 | 0.1157 | 37.1 | | | | | | |
| 11/16/18 | C2 | 0.0934 | 910 | 0.1023 | 9.8 | | | | | | |

Table A7: Physical oceanographic raw data.

| Date | Site | Temp. (°C) | DO (mg/l) | Cond. (mS) | Salinity (ppt) | Secchi (cm) | Date | Site | Temp. (°C) | DO (mg/l) | Cond. (mS) | Salinity (ppt) | Secchi (cm) |
|----------|------|------------|-----------|------------|----------------|-------------|----------|-------|------------|-----------|------------|----------------|-------------|
| 2/20/18 | A1a | 22.2 | 7.7 | 7914 | 4.2 | 76 | 2/21/18 | CP | 24.0 | 7.3 | 19944 | 12.3 | 108 |
| 4/25/18 | A1a | 21.8 | 8.2 | 3010 | 1.7 | 39 | 4/25/18 | CP | 23.3 | 7.5 | 13533 | 8.2 | 55 |
| 6/26/18 | A1a | 30.7 | 7.0 | 3658 | 1.7 | 74 | 6/26/18 | CP | 32.4 | 7.1 | 24429 | 13.0 | 49 |
| 9/12/18 | A1a | 29.0 | 4.0 | 17593 | 9.7 | 78 | 8/13/18 | CP | 30.2 | 6.3 | 25030 | 15.7 | 60 |
| 11/16/18 | A1a | 12.4 | 9.9 | 10589 | 8.1 | 30 | 9/12/18 | CP | 29.3 | 4.4 | 25204 | 14.3 | 59 |
| 2/20/18 | A1b | 22.6 | 7.3 | 7406 | 4.4 | 151 | 11/16/18 | CP | 9.3 | 9.8 | 11796 | 9.8 | 75 |
| 4/25/18 | A1b | 23.3 | 9.5 | 2569 | 1.4 | 42 | 2/21/18 | LAN | 23.0 | 6.8 | 28202 | 18.3 | 60 |
| 6/26/18 | A1b | 31.7 | 7.3 | 4669 | 2.2 | 79 | 4/25/18 | LAN | 24.0 | 7.9 | 19983 | 12.3 | 57 |
| 9/12/18 | A1b | 29.4 | 5.9 | 18351 | 10.1 | 103 | 6/26/18 | LAN | 32.4 | 6.7 | 25516 | 13.7 | 54 |
| 11/16/18 | A1b | 11.3 | 10.2 | 9041 | 7.0 | 38 | 8/13/18 | LAN | 29.5 | 1.8 | 30000 | 18.5 | 60 |
| 4/25/18 | A1c | 23.2 | 8.5 | 3147 | 1.7 | 35 | 9/12/18 | LAN | 30.0 | 4.7 | 35229 | 20.4 | 46 |
| 6/26/18 | A1c | 31.4 | 6.9 | 3918 | 1.9 | 63 | 11/16/18 | LAN | 9.4 | 9.9 | 16314 | 13.8 | 135 |
| 9/12/18 | A1c | 29.5 | 5.2 | 18266 | 10.0 | 71 | 2/21/18 | LAS | 22.4 | 6.8 | 34405 | 23.0 | 69 |
| 11/16/18 | A1c | 11.7 | 10.1 | 9815 | 7.5 | 33 | 4/25/18 | LAS | 23.2 | 8.7 | 19067 | 11.9 | 80 |
| 2/21/18 | A2 | 23.2 | 7.0 | 34512 | 22.8 | 55 | 6/26/18 | LAS | 32.0 | 8.5 | 26452 | 14.3 | 66 |
| 4/25/18 | A2 | 23.5 | 8.2 | 19847 | 12.3 | 70 | 8/13/18 | LAS | 29.6 | 4.6 | 31428 | 19.5 | 70 |
| 6/26/18 | A2 | 32.2 | 7.1 | 26793 | 14.5 | 47 | 9/12/18 | LAS | 29.7 | 5.3 | 36281 | 21.2 | 56 |
| 9/12/18 | A2 | 29.5 | 5.3 | 38580 | 22.9 | 41 | 11/16/18 | LAS | 12.2 | 8.6 | 19473 | 15.7 | 81 |
| 11/16/18 | A2 | 10.5 | 9.7 | 15407 | 12.7 | 71 | 2/21/18 | LE | 23.0 | 7.0 | 27883 | 18.1 | 45 |
| 2/20/18 | A3 | 24.1 | 7.6 | 12291 | 7.3 | 39 | 4/25/18 | LE | 22.9 | 7.5 | 18454 | 11.6 | 70 |
| 4/27/18 | A3 | 23.4 | 7.8 | 6222 | 4.6 | 30 | 6/26/18 | LE | 31.7 | 8.1 | 25640 | 10.6 | 71 |
| 6/26/18 | A3 | 32.4 | 11.1 | 8996 | 4.4 | 41 | 8/13/18 | LE | 29.7 | 6.6 | 30260 | 18.7 | 60 |
| 9/12/18 | A3 | 30.1 | 6.9 | 15541 | 8.4 | 33 | 9/12/18 | LE | 29.7 | 4.6 | 32484 | 18.8 | 47 |
| 11/16/18 | A3 | 11.5 | 9.2 | 11165 | 6.8 | 105 | 11/16/18 | LE | 10.4 | 9.5 | 14414 | 11.8 | 74 |
| 2/20/18 | B1 | 24.2 | 7.1 | 13208 | 7.9 | 75 | 2/20/18 | LL | 24.5 | 7.5 | 10113 | 5.8 | 41 |
| 4/25/18 | B1 | 22.3 | 7.0 | 7906 | 4.7 | 60 | 4/25/18 | LL | 23.2 | 7.4 | 11458 | 6.8 | 55 |
| 6/26/18 | B1 | 31.7 | 5.2 | 18155 | 9.5 | 56 | 6/26/18 | LL | 30.8 | 5.3 | 20062 | 10.8 | 51 |
| 9/12/18 | B1 | 28.5 | 3.2 | 21742 | 12.4 | 53 | 8/13/18 | LL | 29.6 | 0.1 | 16660 | 11.2 | 55 |
| 11/16/18 | B1 | 9.8 | 9.9 | 11665 | 9.6 | 91 | 9/12/18 | LL | 28.9 | 3.8 | 19999 | 11.2 | 46 |
| 2/21/18 | B2 | 23.7 | 6.7 | 11079 | 6.5 | 43 | 11/16/18 | LL | 9.5 | 9.7 | 12276 | 10.2 | 38 |
| 4/25/18 | B2 | 23.8 | 8.0 | 11953 | 7.1 | 57 | 2/20/18 | LLBC1 | 23.9 | 7.6 | 12593 | 7.5 | 52 |
| 6/26/18 | B2 | 30.8 | 5.6 | 20299 | 11.0 | 40 | 4/25/18 | LLBC1 | 23.2 | 7.1 | 10207 | 6.0 | 45 |
| 9/12/18 | B2 | 29.6 | 6.4 | 19701 | 10.9 | 35 | 6/26/18 | LLBC1 | 31.1 | 5.5 | 21863 | 11.9 | 60 |
| 11/16/18 | B2 | 9.1 | 9.9 | 10309 | 8.5 | 50 | 8/13/18 | LLBC1 | 29.5 | 5.8 | 20166 | 11.9 | 40 |
| 2/20/18 | BM | 22.7 | 7.0 | 7428 | 4.3 | 57 | 9/12/18 | LLBC1 | 28.5 | 3.1 | 15130 | 8.3 | 61 |
| 4/25/18 | BM | 23.4 | 7.5 | 6061 | 3.4 | 68 | 11/16/18 | LLBC1 | 10.0 | 9.5 | 9797 | 7.9 | 66 |
| 6/26/18 | BM | 31.7 | 6.9 | 7283 | 3.7 | 73 | 2/21/18 | LLBC2 | 24.3 | 7.2 | 18102 | 11.0 | 72 |

| | | | | | | | | | | | | | |
|----------|------|------|-----|-------|------|----|----------|-------|------|-----|-------|------|----|
| 8/13/18 | BM | 30.2 | 0.3 | 10820 | 6.1 | 40 | 4/25/18 | LLBC2 | 23.6 | 7.5 | 14195 | 8.6 | 46 |
| 9/12/18 | BM | 29.5 | 5.7 | 13386 | 7.1 | 52 | 6/26/18 | LLBC2 | 31.4 | 5.7 | 24182 | 13.1 | 40 |
| 11/16/18 | BM | 10.9 | 9.9 | 9432 | 7.4 | 43 | 8/13/18 | LLBC2 | 29.6 | 6.0 | 24704 | 14.9 | 40 |
| 2/21/18 | BPPN | 23.5 | 6.9 | 24188 | 15.4 | 44 | 9/12/18 | LLBC2 | 28.5 | 3.2 | 24096 | 13.8 | 51 |
| 4/25/18 | BPPN | 23.9 | 7.9 | 15783 | 9.6 | 61 | 11/16/18 | LLBC2 | 9.7 | 9.7 | 13757 | 11.5 | 86 |
| 6/26/18 | BPPN | 32.5 | 7.0 | 25722 | 13.9 | 44 | 2/20/18 | MP | 23.9 | 7.4 | 1444 | 8.4 | 53 |
| 8/13/18 | BPPN | 30.5 | 0.1 | 26730 | 16.3 | 60 | 4/25/18 | MP | 22.8 | 7.3 | 10959 | 6.6 | 54 |
| 9/12/18 | BPPN | 29.5 | 5.6 | 27575 | 15.7 | 62 | 6/26/18 | MP | 31.1 | 5.2 | 21782 | 11.8 | 45 |
| 11/16/18 | BPPN | 9.4 | 9.6 | 13282 | 11.1 | 76 | 8/13/18 | MP | 30.1 | 0.2 | 21516 | 12.8 | 50 |
| 2/20/18 | C1 | 24.6 | 7.5 | 1342 | 8.2 | 58 | 9/12/18 | MP | 28.5 | 4.1 | 24068 | 13.8 | 56 |
| 4/25/18 | C1 | 22.3 | 7.4 | 10953 | 6.7 | 54 | 11/16/18 | MP | 9.7 | 9.6 | 12809 | 10.6 | 99 |
| 6/26/18 | C1 | 30.9 | 5.2 | 21697 | 11.8 | 46 | 2/21/18 | TP | 24.3 | 7.2 | 29221 | 18.6 | 29 |
| 9/12/18 | C1 | 28.5 | 3.8 | 23841 | 13.7 | 69 | 4/25/18 | TP | 23.5 | 7.8 | 16760 | 10.3 | 51 |
| 11/16/18 | C1 | 9.8 | 9.6 | 12984 | 10.7 | 82 | 6/26/18 | TP | 31.3 | 5.2 | 27254 | 15.0 | 53 |
| 2/21/18 | C2 | 23.1 | 6.9 | 25974 | 16.0 | 42 | 8/13/18 | TP | 30.3 | 6.8 | 28680 | 17.7 | 50 |
| 4/25/18 | C2 | 24.3 | 8.9 | 19090 | 11.6 | 61 | 9/12/18 | TP | 29.3 | 4.7 | 32355 | 18.8 | 53 |
| 6/26/18 | C2 | 32.6 | 8.9 | 27509 | 14.8 | 61 | 11/16/18 | TP | 9.9 | 9.7 | 15238 | 12.7 | 66 |
| 9/12/18 | C2 | 29.6 | 4.8 | 29524 | 16.9 | 50 | 2/20/18 | TW | 21.8 | 8.3 | 7981 | 4.8 | 81 |
| 11/16/18 | C2 | 10.7 | 9.5 | 16271 | 13.5 | 79 | 4/27/18 | TW | 23.1 | 7.8 | 2558 | 1.6 | 70 |
| | | | | | | | 6/26/18 | TW | 31.9 | 7.8 | 7679 | 3.8 | 69 |
| | | | | | | | 8/13/18 | TW | 30.1 | 5.9 | 9231 | 5.1 | 50 |
| | | | | | | | 9/12/18 | TW | 28.4 | 4.4 | 14343 | 7.9 | 80 |
| | | | | | | | 11/16/18 | TW | 11.5 | 9.6 | 8232 | 6.3 | 69 |

Table A8. Raw elevation data.

| | | | | | |
|------------|--------------|-------|----------|-------|-------|
| A1b | Water Level: | 1.745 | WLgauge: | 28 | |
| 5m | 1.470 | 1.465 | 1.460 | 1.480 | 1.480 |
| 25m | 1.470 | 1.490 | 1.500 | 1.490 | 1.500 |
| 50m | 1.540 | 1.530 | 1.530 | 1.540 | 1.550 |
| C2 | Water Level: | 1.605 | WLgauge: | 36 | |
| 5m | 1.400 | 1.390 | 1.380 | 1.365 | 1.390 |
| 25m | 1.390 | 1.390 | 1.360 | 1.360 | 1.360 |
| 50m | 1.430 | 1.410 | 1.420 | 1.430 | 1.420 |
| A3 | Water Level: | 1.700 | WLgauge: | 31 | |
| 5m | 1.510 | 1.520 | 1.525 | 1.495 | 1.450 |
| 25m | 1.475 | 1.445 | 1.404 | 1.440 | 1.440 |
| 50m | 1.420 | 1.425 | 1.420 | 1.430 | 1.420 |
| C2 | Water Level: | 1.645 | WLgauge: | 22 | |
| 5m | 1.380 | 1.375 | 1.370 | 1.360 | 1.380 |
| 25m | 1.375 | 1.385 | 1.390 | 1.410 | 1.420 |
| 50m | 1.360 | 1.365 | 1.370 | 1.385 | 1.385 |
| B1 | Water Level: | 1.600 | WLgauge: | 16 | |
| 5m | 1.240 | 1.320 | 1.300 | 1.325 | 1.345 |
| 25m | 1.325 | 1.270 | 1.315 | 1.350 | 1.355 |
| 50m | 1.285 | 1.290 | 1.270 | 1.265 | 1.275 |
| A1a | Water Level: | 1.635 | WLgauge: | 24 | |
| 5m | 1.400 | 1.400 | 1.415 | 1.410 | 1.400 |
| 25m | 10.465 | 1.480 | 1.480 | 1.470 | 1.470 |
| 50m | 1.450 | 1.425 | 1.425 | 1.440 | 1.430 |
| A1c | Water Level: | 1.795 | WLgauge: | 17 | |
| 5m | 1.500 | 1.460 | 1.470 | 1.485 | 1.495 |
| 25m | 1.490 | 1.480 | 1.490 | 1.500 | 1.480 |
| 50m | 1.650 | 1.655 | 1.600 | 1.570 | 1.550 |
| B2 | Water Level: | 1.650 | WLgauge: | 40 | |
| 5m | 1.550 | 1.565 | 1.545 | 1.540 | 1.550 |

| | | | | | |
|-----------|-------|--------------|-------|----------|-------|
| 25m | 1.530 | 1.530 | 1.520 | 1.525 | 1.520 |
| 50m | 1.600 | 1.590 | 1.600 | 1.610 | 1.620 |
| A2 | | Water Level: | 1.750 | WLgauge: | 45 |
| 5m | 1.385 | 1.380 | 1.395 | 1.390 | 1.400 |
| 25m | 1.420 | 1.410 | 1.400 | 1.410 | 1.410 |
| 50m | 1.450 | 1.450 | 1.460 | 1.550 | 1.500 |

Table A9. Water quality probe, secchi disk, and total suspended sediment (TSS) data from February 20-21, 2018.

| Date | Time | Site | Temp. (°C) | DO (mg/l) | Cond. (mS) | Salinity (ppt) | Secchi (cm) | TSS (mg/L) | WL staff (cm) |
|---------|-------|-------|------------|-----------|------------|----------------|-------------|------------|---------------|
| 2/20/18 | 11:00 | A1a | 22.2 | 7.7 | 7914 | 4.2 | 76 | 15.9 | 44 |
| 2/20/18 | 10:00 | A1b | 22.6 | 7.3 | 7406 | 4.4 | 151 | 6.5 | 40 |
| 2/21/18 | 11:32 | A2 | 23.2 | 7.0 | 34512 | 22.8 | 55 | 57.8 | 42 |
| 2/20/18 | 16:10 | A3 | 24.1 | 7.6 | 12291 | 7.3 | 39 | 33.2 | 42 |
| 2/20/18 | 11:45 | B1 | 24.2 | 7.1 | 13208 | 7.9 | 75 | 21.1 | 38 |
| 2/21/18 | 8:47 | B2 | 23.7 | 6.7 | 11079 | 6.5 | 43 | 28.9 | 43 |
| 2/20/18 | 8:50 | BM | 22.7 | 7.0 | 7428 | 4.3 | 57 | 21.6 | |
| 2/21/18 | 10:36 | BPPN | 23.5 | 6.9 | 24188 | 15.4 | 44 | 34.4 | |
| 2/20/18 | 13:13 | C1 | 24.6 | 7.5 | 1342 | 8.2 | 58 | 29.7 | 43 |
| 2/21/18 | 9:43 | C2 | 23.1 | 6.9 | 25974 | 16.0 | 42 | 25.4 | 42 |
| 2/21/18 | 12:47 | CP | 24.0 | 7.3 | 19944 | 12.3 | 108 | 15.0 | |
| 2/21/18 | 10:24 | LAN | 23.0 | 6.8 | 28202 | 18.3 | 60 | 34.7 | |
| 2/21/18 | 10:13 | LAS | 22.4 | 6.8 | 34405 | 23.0 | 69 | 26.9 | |
| 2/21/18 | 10:47 | LE | 23.0 | 7.0 | 27883 | 18.1 | 45 | 44.1 | |
| 2/20/18 | 13:35 | LL | 24.5 | 7.5 | 10113 | 5.8 | 41 | 27.7 | |
| 2/20/18 | 13:40 | LLBC1 | 23.9 | 7.6 | 12593 | 7.5 | 52 | 25.2 | |
| 2/21/18 | 12:32 | LLBC2 | 24.3 | 7.2 | 18102 | 11.0 | 72 | 23.1 | |
| 2/20/18 | 12:30 | MP | 23.9 | 7.4 | 1444 | 8.4 | 53 | 25.3 | |
| 2/21/18 | 12:19 | TP | 24.3 | 7.2 | 29221 | 18.6 | 29 | 34.3 | |
| 2/20/18 | 13:49 | TW | 21.8 | 8.3 | 7981 | 4.8 | 81 | 19.4 | |

* Resting on bottom.

Table A10. Water quality probe, secchi disk, and total suspended sediment (TSS) data from March 2, 2018.

| Time | Time | Site | WL gauge (cm) | Salinity (ppt) |
|--------|-------|------|---------------|----------------|
| 3/2/18 | 12:05 | A1b | 28 | . |
| 3/2/18 | 13:00 | C2 | 36 | . |
| 3/2/18 | 14:00 | A3 | 31 | . |
| 3/8/18 | 10:45 | C2 | 22 | . |
| 3/8/18 | 12:00 | A1a | 24 | 4.6 |
| 3/8/18 | 12:45 | A1c | 17 | 4.6 |
| 3/8/18 | 13:20 | A1b | 24 | 4.7 |
| 3/8/18 | 13:40 | B2 | 40 | 14.0 |
| 3/8/18 | 14:30 | A2 | 45 | 22.1 |

Table A11. Water quality probe, secchi disk, and total suspended sediment (TSS) data from April 25 & 27, 2018.

| Date | Time | Site | Temp. (°C) | DO (mg/l) | Cond. (mS) | Salinity (ppt) | Secchi (cm) | TSS (mg/L) | WL staff (cm) |
|---------|-------|------|------------|-----------|------------|----------------|-------------|------------|---------------|
| 4/25/18 | 12:17 | A1a | 21.8 | 8.2 | 3010 | 1.7 | 39 | 24.5 | 17 |
| 4/25/18 | 13:09 | A1b | 23.3 | 9.5 | 2569 | 1.4 | 42 | 26.7 | 17 |
| 4/25/18 | 12:25 | A1c | 23.2 | 8.5 | 3147 | 1.7 | 35 | 28.4 | 8 |
| 4/25/18 | 14:54 | A2 | 23.5 | 8.2 | 19847 | 12.3 | 70 | 16.5 | 38 |

| | | | | | | | | | |
|---------|-------|-------|------|-----|-------|------|----|------|----|
| 4/27/18 | 11:22 | A3 | 23.4 | 7.8 | 6222 | 4.6 | 30 | 26.4 | 17 |
| 4/25/18 | 11:52 | B1 | 22.3 | 7.0 | 7906 | 4.7 | 60 | 23.7 | 6 |
| 4/25/18 | 13:42 | B2 | 23.8 | 8.0 | 11953 | 7.1 | 57 | 18.1 | 37 |
| 4/25/18 | 13:22 | BM | 23.4 | 7.5 | 6061 | 3.4 | 68 | 14.4 | |
| 4/25/18 | 15:42 | BPPN | 23.9 | 7.9 | 15783 | 9.6 | 61 | 27.2 | |
| 4/25/18 | 11:35 | C1 | 22.3 | 7.4 | 10953 | 6.7 | 54 | 27.9 | 12 |
| 4/25/18 | 15:56 | C2 | 24.3 | 8.9 | 19090 | 11.6 | 61 | 28.2 | 35 |
| 4/25/18 | 14:00 | CP | 23.3 | 7.5 | 13533 | 8.2 | 55 | 27.2 | |
| 4/25/18 | 15:34 | LAN | 24.0 | 7.9 | 19983 | 12.3 | 57 | 23.0 | |
| 4/25/18 | 15:14 | LAS | 23.2 | 8.7 | 19067 | 11.9 | 80 | 17.1 | |
| 4/25/18 | 14:27 | LE | 22.9 | 7.5 | 18454 | 11.6 | 70 | 26.7 | |
| 4/25/18 | 11:25 | LL | 23.2 | 7.4 | 11458 | 6.8 | 55 | 33.4 | |
| 4/25/18 | 13:30 | LLBC1 | 23.2 | 7.1 | 10207 | 6.0 | 45 | 47.0 | |
| 4/25/18 | 13:52 | LLBC2 | 23.6 | 7.5 | 14195 | 8.6 | 46 | 54.6 | |
| 4/25/18 | 11:37 | MP | 22.8 | 7.3 | 10959 | 6.6 | 54 | 28.4 | |
| 4/25/18 | 16:25 | TP | 23.5 | 7.8 | 16760 | 10.3 | 51 | 30.0 | |
| 4/27/18 | 11:53 | TW | 23.1 | 7.8 | 2558 | 1.6 | 70 | 12.5 | |

Table A12. Water quality probe, secchi disk, and total suspended sediment (TSS) data from June 26, 2018.

| Date | Time | Site | Temp. (°C) | DO (mg/l) | Cond. (mS) | Salinity (ppt) | Secchi (cm) | TSS (mg/L) | WL gauge (cm) |
|---------|-------|-------|------------|-----------|------------|----------------|-------------|------------|---------------|
| 6/26/18 | 11:55 | A1a | 30.7 | 7.0 | 3658 | 1.7 | 74 | 11.3 | 52 |
| 6/26/18 | 12:15 | A1b | 31.7 | 7.3 | 4669 | 2.2 | 79 | 12.8 | 47* |
| 6/26/18 | 12:05 | A1c | 31.4 | 6.9 | 3918 | 1.9 | 63 | 12.0 | |
| 6/26/18 | 15:10 | A2 | 32.2 | 7.1 | 26793 | 14.5 | 47 | 44.4 | 31 |
| 6/26/18 | 18:11 | A3 | 32.4 | 11.1 | 8996 | 4.4 | 41 | 21.5 | 21 |
| 6/26/18 | 11:35 | B1 | 31.7 | 5.2 | 18155 | 9.5 | 56 | 27.6 | 31 |
| 6/26/18 | 13:07 | B2 | 30.8 | 5.6 | 20299 | 11.0 | 40 | 25.8 | 52 |
| 6/26/18 | 12:50 | BM | 31.7 | 6.9 | 7283 | 3.7 | 73 | 10.5 | |
| 6/26/18 | 13:58 | BPPN | 32.5 | 7.0 | 25722 | 13.9 | 44 | 28.3 | |
| 6/26/18 | 11:22 | C1 | 30.9 | 5.2 | 21697 | 11.8 | 46 | 33.8 | 40 |
| 6/26/18 | 13:45 | C2 | 32.6 | 8.9 | 27509 | 14.8 | 61 | 16.7 | 46 |
| 6/26/18 | 15:56 | CP | 32.4 | 7.1 | 24429 | 13.0 | 49 | 30.0 | |
| 6/26/18 | 14:06 | LAN | 32.4 | 6.7 | 25516 | 13.7 | 54 | 18.0 | |
| 6/26/18 | 14:25 | LAS | 32.0 | 8.5 | 26452 | 14.3 | 66 | 29.0 | |
| 6/26/18 | 14:18 | LE | 31.7 | 8.1 | 25640 | 10.6 | 71 | 19.7 | |
| 6/26/18 | 11:15 | LL | 30.8 | 5.3 | 20062 | 10.8 | 51 | 23.2 | |
| 6/26/18 | 11:20 | LLBC1 | 31.1 | 5.5 | 21863 | 11.9 | 60 | 38.0 | |
| 6/26/18 | 15:49 | LLBC2 | 31.4 | 5.7 | 24182 | 13.1 | 40 | 30.1 | |
| 6/26/18 | 11:30 | MP | 31.1 | 5.2 | 21782 | 11.8 | 45 | 27.8 | |
| 6/26/18 | 15:38 | TP | 31.3 | 5.2 | 27254 | 15.0 | 53 | 31.0 | |
| 6/26/18 | 10:58 | TW | 31.9 | 7.8 | 7679 | 3.8 | 69 | 15.3 | |

Table A13. Water quality probe and secchi disk data from July 5, 2018

| Date | Time | Site | Temp. (°C) | DO (mg/l) | Cond. (mS) | Salinity (ppt) | Secchi (cm) |
|--------|-------|-------|------------|-----------|------------|----------------|-------------|
| 7/5/18 | 09:25 | A1a | 28.8 | 7.0 | 3448 | 1.8 | 50 |
| 7/5/18 | 13:00 | B1 | 30.0 | 6.1 | 13673 | 7.8 | 55 |
| 7/5/18 | 13:18 | C1 | 30.3 | 6.8 | 17720 | 10.4 | 80 |
| 7/5/18 | 14:40 | TW | 29.9 | 6.8 | 6778 | 3.7 | 60 |
| 7/5/18 | 13:20 | LAS | 29.6 | 4.6 | 31428 | 19.5 | 70 |
| 7/5/18 | 14:15 | LL | 30.6 | 7.4 | 16600 | 9.7 | 50 |
| 7/5/18 | 14:25 | LLBC1 | 30.5 | 6.7 | 13292 | 7.6 | 40 |
| 7/5/18 | 14:05 | LLBC2 | 30.5 | 6.7 | 21876 | 13.1 | 40 |
| 7/5/18 | 13:49 | TP | 30.3 | 7.7 | 24819 | 15.0 | 50 |

Table A14. Water quality probe and secchi disk data from August 13, 2018.

| Date | Time | Site | Temp. | DO | Cond. | Salinity | Secchi |
|------|------|------|-------|----|-------|----------|--------|
|------|------|------|-------|----|-------|----------|--------|

| | | | (°C) | (mg/l) | (mS) | (ppt) | (cm) |
|---------|-------|-------|------|--------|-------|-------|------|
| 8/13/18 | 10:52 | BM | 30.2 | 0.3 | 10820 | 6.1 | 40 |
| 8/13/18 | 13:55 | BPPN | 30.5 | 0.1 | 26730 | 16.3 | 60 |
| 8/13/18 | 12:40 | CP | 30.2 | 6.3 | 25030 | 15.7 | 60 |
| 8/13/18 | 13:45 | LAN | 29.5 | 1.8 | 30000 | 18.5 | 60 |
| 8/13/18 | 13:20 | LAS | 29.6 | 4.6 | 31428 | 19.5 | 70 |
| 8/13/18 | 12:55 | LE | 29.7 | 6.6 | 30260 | 18.7 | 60 |
| 8/13/18 | 11:18 | LL | 29.6 | 0.1 | 16660 | 11.2 | 55 |
| 8/13/18 | 10:36 | LLBC1 | 29.5 | 5.8 | 20166 | 11.9 | 40 |
| 8/13/18 | 12:05 | LLBC2 | 29.6 | 6.0 | 24704 | 14.9 | 40 |
| 8/13/18 | 11:35 | MP | 30.1 | 0.2 | 21516 | 12.8 | 50 |
| 8/13/18 | 12:20 | TP | 30.3 | 6.8 | 28680 | 17.7 | 50 |
| 8/13/18 | 10:21 | TW | 30.1 | 5.9 | 9231 | 5.1 | 50 |

Table A15. Water quality probe, secchi disk, and total suspended sediment (TSS) data from September 12, 2018.

| Date | Time | Site | Temp. (°C) | DO (mg/l) | Cond. (mS) | Salinity (ppt) | Secchi (cm) | TSS (mg/L) | WL gauge (cm) |
|---------|-------|-------|------------|-----------|------------|----------------|-------------|------------|---------------|
| 9/12/18 | 13:34 | A1a | 29.0 | 4.0 | 17593 | 9.7 | 78 | 12.6 | 48 |
| 9/12/18 | 13:09 | A1b | 29.4 | 5.9 | 18351 | 10.1 | 103 | 9.3 | 40 |
| 9/12/18 | 13:26 | A1c | 29.5 | 5.2 | 18266 | 10.0 | 71 | 15.2 | . |
| 9/12/18 | 10:08 | A2 | 29.5 | 5.3 | 38580 | 22.9 | 41 | 21.9 | 44 |
| 9/12/18 | 18:00 | A3 | 30.1 | 6.9 | 15541 | 8.4 | 33 | 57.6 | 68 |
| 9/12/18 | 8:59 | B1 | 28.5 | 3.2 | 21742 | 12.4 | 53 | 28.1 | 48 |
| 9/12/18 | 12:33 | B2 | 29.6 | 6.4 | 19701 | 10.9 | 35 | 63.8 | 55 |
| 9/12/18 | 12:55 | BM | 29.5 | 5.7 | 13386 | 7.1 | 52 | 17.5 | |
| 9/12/18 | 10:51 | BPPN | 29.5 | 5.6 | 27575 | 15.7 | 62 | 30.7 | |
| 9/12/18 | 8:39 | C1 | 28.5 | 3.8 | 23841 | 13.7 | 69 | 14.9 | 48 |
| 9/12/18 | 11:24 | C2 | 29.6 | 4.8 | 29524 | 16.9 | 50 | 37.1 | 50 |
| 9/12/18 | 9:24 | CP | 29.3 | 4.4 | 25204 | 14.3 | 59 | 33.4 | |
| 9/12/18 | 10:40 | LAN | 30.0 | 4.7 | 35229 | 20.4 | 46 | 41.3 | |
| 9/12/18 | 10:28 | LAS | 29.7 | 5.3 | 36281 | 21.2 | 56 | 47.2 | |
| 9/12/18 | 9:46 | LE | 29.7 | 4.6 | 32484 | 18.8 | 47 | 33.3 | |
| 9/12/18 | 8:31 | LL | 28.9 | 3.8 | 19999 | 11.2 | 46 | 24.6 | |
| 9/12/18 | 8:22 | LLBC1 | 28.5 | 3.1 | 15130 | 8.3 | 61 | 19.2 | |
| 9/12/18 | 9:12 | LLBC2 | 28.5 | 3.2 | 24096 | 13.8 | 51 | 29.4 | |
| 9/12/18 | 8:34 | MP | 28.5 | 4.1 | 24068 | 13.8 | 56 | 22.2 | |
| 9/12/18 | 9:35 | TP | 29.3 | 4.7 | 32355 | 18.8 | 53 | 22.0 | |
| 9/12/18 | 8:13 | TW | 28.4 | 4.4 | 14343 | 7.9 | 80 | 11.0 | |

Table A16. Water quality probe, secchi disk, and total suspended sediment (TSS) data from November 16, 2018.

| Date | Time | Site | Temp. (°C) | DO (mg/l) | Cond. (mS) | Salinity (ppt) | Secchi (cm) | TSS (mg/L) | WL gauge (cm) |
|----------|-------|-------|---------------|--------------|---------------|-------------------|----------------|---------------|------------------|
| 11/16/18 | 12:11 | A1a | 12.4 | 9.9 | 10589 | 8.1 | 30 | 33.5 | 13 |
| 11/16/18 | 12:33 | A1b | 11.3 | 10.2 | 9041 | 7.0 | 38 | 25.6 | 7 |
| 11/16/18 | 12:20 | A1c | 11.7 | 10.1 | 9815 | 7.5 | 33 | 29.5 | |
| 11/16/18 | 9:34 | A2 | 10.5 | 9.7 | 15407 | 12.7 | 71 | 15.5 | 20 |
| 11/16/18 | 14:33 | A3 | 11.5 | 9.2 | 11165 | 6.8 | 105 | 11.9 | 14 |
| 11/16/18 | 11:44 | B1 | 9.8 | 9.9 | 11665 | 9.6 | 91 | 9.5 | 11 |
| 11/16/18 | 8:26 | B2 | 9.1 | 9.9 | 10309 | 8.5 | 50 | 14.0 | 28 |
| 11/16/18 | 12:44 | BM | 10.9 | 9.9 | 9432 | 7.4 | 43 | 20.7 | |
| 11/16/18 | 8:56 | BPPN | 9.4 | 9.6 | 13282 | 11.1 | 76 | 16.1 | |
| 11/16/18 | 11:24 | C1 | 9.8 | 9.6 | 12984 | 10.7 | 82 | 14.9 | 24 |
| 11/16/18 | 8:45 | C2 | 10.7 | 9.5 | 16271 | 13.5 | 79 | 9.8 | 26 |
| 11/16/18 | 10:40 | CP | 9.3 | 9.8 | 11796 | 9.8 | 75 | 15.1 | |
| 11/16/18 | 9:05 | LAN | 9.4 | 9.9 | 16314 | 13.8 | 135 | 9.7 | |
| 11/16/18 | 9:15 | LAS | 12.2 | 8.6 | 19473 | 15.7 | 81 | 14.6 | |
| 11/16/18 | 9:24 | LE | 10.4 | 9.5 | 14414 | 11.8 | 74 | 19.7 | |
| 11/16/18 | 11:19 | LL | 9.5 | 9.7 | 12276 | 10.2 | 38 | 35.8 | |
| 11/16/18 | 8:16 | LLBC1 | 10.0 | 9.5 | 9797 | 7.9 | 66 | 11.1 | |
| 11/16/18 | 10:11 | LLBC2 | 9.7 | 9.7 | 13757 | 11.5 | 86 | 15.6 | |
| 11/16/18 | 11:27 | MP | 9.7 | 9.6 | 12809 | 10.6 | 99 | 16.2 | |
| 11/16/18 | 9:53 | TP | 9.9 | 9.7 | 15238 | 12.7 | 66 | 15.6 | |
| 11/16/18 | 8:04 | TW | 11.5 | 9.6 | 8232 | 6.3 | 69 | 10.4 | |

Appendix B: Summary of Site visits

February 7, 2018: Comite Resources staff Drs. John Day and Robert Lane, as well as Dr. Paul Kemp met at the Biloxi landholding corporate headquarters in Metairie. There they determined the exact locations of eight wetland monitoring sites. In addition, twelve Rounsefell water quality monitoring stations were also identified.

February 20, 2018: Comite Resources staff Dr. Robert Lane and Jason Day met Monty Montelongo and Manuel Montelongo at the Hopedale boat launch at 8am. Since ELOS was not meeting until 9:30, the Comite team left in their boat and set up station **A1b** and then traveled to **A1a** where they met Monty and Brian Fortson from ELOS. After setting up the site, Comite followed the Biloxi corporation boat to **B1** and **C1** to track the path for future trips. The Biloxi corporation boat left and Comite staff continued to station **A3**. Installed at each wetland site were accretion markers at 5 m, 25 m, and 50 m from the shoreline, ten shoreline erosion markers, a staff gauge and receptacle for water level and salinity probes. In addition, species composition was also recorded at 5 m, 25 m, and 50 m from the shoreline, and a 30 cm soil core was collected at 25 m for bulk density analysis. Secchi disk and probe measurements and water samples were taken at Rounsefell stations **BM, MP, LL, LLBC1, and TW** as well from water directly in front of the wetland stations.



Shoreline erosion markers at site A1b.



Feldspar plots at site A1a.



Water level gauge and shoreline markers at site A3.

February 21, 2018: Comite Resources staff Dr. Robert Lane and Jason Day met Manuel Montelongo senior at the Hopedale boat launch at 8am. Manuel offered to drive Biloxi corporation boat to the sites for the day, which we accepted. We traveled to marsh sites **B2** and **C2**, and then collected secchi disk and probe measurements at Rounsefell stations **LAS**, **LAN**, **BPPN**, and **LE** before reaching wetland site **A2**. After setting up the wetland site, Rounsefell stations **TP**, **LLBC2**, and **CP** were visited.



Jason Day deploying feldspar marker horizons (left) and a core for bulk density (right).



Dr. Lane installing a water level gauge at station C2.

March 2, 2018: Comite Resources staff Dr. Robert Lane and Jason Day installed water level and conductivity probes at the following sites:

A1b: water level, conductivity & barometric

C2: water level, conductivity

A3: water level

In addition, at each of the three sites elevation surveys were carried out. Relative measures of elevation were made five times spaced approximately one meter apart at 5, 25, and 50

m as well as at the water level (i.e., end of pole at water level). Water level at the fixed gauges was also recorded. Below are the raw data.

March 8, 2018: Drs. Robert Lane and Paul Kemp as well as Jason Day carried out elevation surveys at the remaining sites. Salinity measurements were also taken at each location. An additional site was set up at coordinates 29° 56.777'N 89° 34.842'W and designated as **A1c**. The site was located on a historical Indian mound. Shoreline erosion poles and accretion plots were deployed, a core for bulk density collected, and a water level gauge was installed. Species composition was recorded.



Surveying equipment at site A1c.

April 25, 2018: Comite Resources staff Dr. Robert Lane and Jason Day traveled to Hopedale and carried out the second water quality transect. All stations and samples obtained except **A3** and **TW**. Water level recorders were downloaded at sites **A1b** and **C2**, and conductivity was downloaded at **C2**. The staff gauge at site **A1c** was leaning from what appeared to be a boat strike. It was fixed so it was upright and the water level measurement taken.

April 27, 2018: Comite Resources staff Dr. Robert Lane and Jason Day traveled to the Biloxi sites and collected samples at sites **A3** and **TW**. Water level and conductivity recorders were downloaded at site **A3**.

June 26, 2018: Comite Resources staff Dr. Robert Lane and Jason Day traveled to Hopedale and carried out the third water quality transect. All stations and samples were successfully obtained. Water level recorders and conductivity probes were downloaded at sites **A1b** and **C2**. The water level recorder was downloaded at site **A3**, however, the entire recorder housing had to be reset in order to retrieve the recorder, so the height of the recorder was altered. As was found during the last monitoring trip, the staff gauge at site **A1c** was leaning from what appeared to be a boat strike. Since the PVC housing was damaged, it was not possible to upright the gauge. The raw data collected are provided below.

September 12, 2018: Comite Resources staff Dr. Robert Lane and Jason Day traveled to Hopedale and carried out the fourth water quality transect. All stations and samples were successfully obtained.

November 5, 2018: Comite Resources staff Dr. Robert Lane and Jason Day measured shoreline erosion and accretion at all of the sites. All probes were pulled and brought back to Comite Resource's lab.



Shoreline erosion at site A3 on November 5, 2018.

November 16, 2018: Comite Resources staff Dr. Robert Lane and Jason Day traveled to Hopedale and carried out the final water quality transect. All stations and samples were successfully obtained.



Accretion at site A3, 5 m plot on November 5, 2018.

Appendix C: SET Project Timeline

In May 2018, Drs. Day, Kemp and Lane met with a representative of UNO and discussed plans to re-measure the sites established in the Biloxi marshes. This entailed taking measurements of the UNO SET device so that we could cross-calibrate with our SET device. While carefully going through the UNO field books coordinates were found that are different from those initially provided which instead, coincide with the sites found thus far (Table C1; Figure C1). We were able to match up the correct data sets to the sites, leaving no doubt to accuracy.

Table C1. Coordinates found in the field books.

| Site | Latitude | Longitude | Site | Latitude | Longitude |
|------|------------|------------|------|------------|------------|
| SL1 | . | . | BL1 | 29° 50.137 | 89° 27.991 |
| SL2 | . | . | BL2 | 29° 49.999 | 89° 27.479 |
| SL3 | 29° 53.108 | 89° 30.053 | BL3 | 29° 49.892 | 89° 26.986 |
| SL4 | 29° 53.846 | 89° 31.322 | BL4 | 29° 50.335 | 89° 27.397 |
| SL5 | 29° 53.750 | 89° 30.466 | BL5 | 29° 50.404 | 89° 27.656 |
| SL6 | 29° 53.732 | 89° 30.336 | BL6 | 29 50.116 | 89° 26.846 |
| SL7 | 29° 54.756 | 89° 31.326 | BL7 | 29 51.076 | 89° 27.560 |
| SL8 | 29° 54.708 | 89° 30.833 | BL8 | 29 51.026 | 89° 27.168 |
| SL9 | 29° 54.662 | 89° 30.303 | BL9 | 29 50.975 | 89° 26.515 |
| SL10 | 29° 55.258 | 89° 31.365 | BL10 | 29 51.800 | 89° 27.380 |
| SL11 | 29° 55.175 | 89° 30.828 | BL11 | 29 51.562 | 89° 26.792 |
| SL12 | 29° 55.129 | 89° 30.346 | BL12 | 29 51.518 | 89° 26.337 |
| SL13 | 29° 55.965 | 89° 31.298 | BL13 | 29 52.552 | 89° 27.049 |
| SL14 | 29° 55.932 | 89° 30.625 | BL14 | 29 52.520 | 89° 26.693 |
| SL15 | 29° 55.913 | 89° 30.425 | BL15 | 29 52.495 | 89° 26.119 |

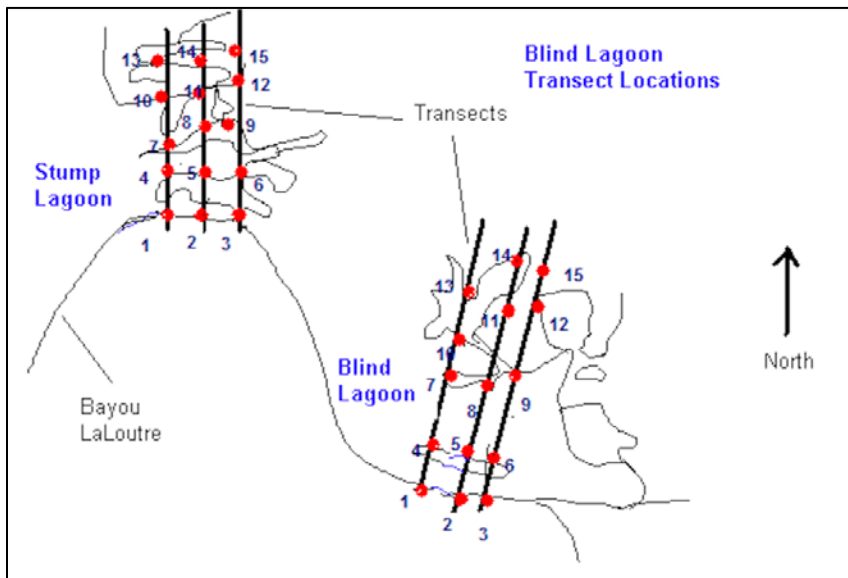


Figure C1. Locations of the historical SET & accretion sites in the Biloxi marshes.

Appendix D: Analyzed SET Data Tables

Table D1. Elevation, accretion and subsidence data for the Western SET sites.

| | | | | | | |
|----------------|----------------|---------------------|----------------|---------------------|--------------------|----------------------|
| 5/8/03 SL6 | Elevation (cm) | Elevation (cm/y) | | | | |
| 2/10/04 | -0.38 | -0.50 | | | | |
| 10/5/04 | -4.01 | -2.84 | | | | |
| 2/24/05 | -1.17 | -0.65 | | | | |
| 9/25/18 | -8.85 | -0.58 | | | | |
| 2/12/04 SL9 | Elevation (cm) | Elevation (cm/y) | Accretion (cm) | Accretion (cm/y) | Subsidence (cm) | Subsidence (cm/y) |
| 10/5/04 | -2.95 | -4.56 | | | | |
| 2/24/05 | -0.25 | -0.24 | | | | |
| 11/19/18 | 1.24 | 0.08 | 5.13 | 0.35 | 2.00 | 0.14 |
| 5/8/03 SL11 | Elevation (cm) | Elevation (cm/y) | Accretion (cm) | Accretion (cm/y) | Subsidence (cm) | Subsidence (cm/y) |
| 2/12/04 | -0.10 | -0.13 | | | | |
| 10/5/04 | -3.66 | -2.59 | | | | |
| 2/24/05 | -2.00 | -1.11 | | | | |
| 10/2/18 | -9.52 | -0.62 | 9.75 | 0.63 | 19.27 | 1.25 |
| 5/8/03 SL12 | Elevation (cm) | Elevation (cm/y) | | 5/8/03 SL15 | Elevation (cm) | Elevation (cm/y) |
| 2/12/04 | -1.34 | -1.74 | | 2/12/04 | 0.46 | 0.60 |
| 10/5/04 | 0.12 | 0.08 | | 10/5/04 | -1.18 | -0.84 |
| 2/24/05 | 0.31 | 0.17 | | 2/24/05 | 0.63 | 0.35 |
| 10/2/18 | -5.34 | -0.35 | | 10/2/18 | -4.12 | -0.27 |

Table D2. Elevation, accretion and subsidence data for the Eastern SET sites.

| | | | | | | |
|-----------------|----------------|---------------------|----------------|---------------------|--------------------|----------------------|
| 2/14/03 BL1 | Elevation (cm) | Elevation (cm/y) | Accretion (cm) | Accretion (cm/y) | Subsidence (cm) | Subsidence (cm/y) |
| 1/28/04 | -0.44 | -0.46 | | | | |
| 3/2/05 | -1.03 | -0.51 | | | | |
| 6/4/08 | 1.04 | 0.20 | | | | |
| 10/2/18 | 5.30 | 0.34 | 7.76 | 0.50 | 2.46 | 0.16 |
| 2/14/03 BL3 | Elevation (cm) | Elevation (cm/y) | Accretion (cm) | Accretion (cm/y) | Subsidence (cm) | Subsidence (cm/y) |
| 1/28/04 | 0.25 | 0.26 | | | | |
| 3/2/05 | -0.04 | -0.02 | | | | |
| 5/4/08 | 3.20 | 0.61 | | | | |
| 10/2/18 | 8.90 | 0.57 | 10.97 | 0.70 | 2.07 | 0.13 |
| 2/14/03 BL4 | Elevation (cm) | Elevation (cm/y) | | 2/14/03 BL6 | Elevation (cm) | Elevation (cm/y) |
| 1/28/04 | 0.54 | 0.56 | | 4/20/04 | -1.30 | -1.10 |
| 3/2/05 | 0.38 | 0.19 | | 3/2/05 | -3.80 | -1.86 |
| 6/4/08 | 0.65 | 0.12 | | 6/3/08 | 1.69 | 0.32 |
| 10/2/18 | 6.99 | 0.45 | | 10/2/18 | 7.42 | 0.47 |
| 2/12/03 BL8 | Elevation (cm) | Elevation (cm/y) | Accretion (cm) | Accretion (cm/y) | Subsidence (cm) | Subsidence (cm/y) |
| 4/20/04 | 0.71 | 0.60 | | | | |
| 3/2/05 | 0.88 | 0.43 | | | | |
| 6/4/08 | 1.27 | 0.24 | | | | |
| 11/19/18 | 5.22 | 0.33 | 9.48 | 0.60 | 4.26 | 0.27 |
| 2/14/03 BL9 | Elevation (cm) | Elevation (cm/y) | Accretion (cm) | Accretion (cm/y) | Subsidence (cm) | Subsidence (cm/y) |
| 4/20/04 | -1.11 | -0.94 | | | | |
| 3/1/05 | 0.51 | 0.25 | | | | |
| 6/3/08 | 2.12 | 0.40 | | | | |
| 10/2/18 | 7.03 | 0.45 | 14.74 | 0.94 | 7.71 | 0.49 |
| 2/12/03 BL11 | Elevation (cm) | Elevation (cm/y) | | | | |
| 4/20/04 | -1.67 | -1.41 | | | | |
| 3/2/05 | 0.75 | 0.37 | | | | |
| 6/4/08 | 2.99 | 0.56 | | | | |
| 11/19/18 | 4.22 | 0.27 | | | | |
| 2/12/03 BL12 | Elevation (cm) | Elevation (cm/y) | Accretion (cm) | Accretion (cm/y) | Subsidence (cm) | Subsidence (cm/y) |
| 4/20/04 | 0.57 | 0.48 | | | | |
| 3/1/05 | 2.73 | 1.33 | | | | |
| 6/3/08 | 3.34 | 0.63 | | | | |
| 11/19/18 | 5.90 | 0.37 | 8.96 | 0.57 | 3.06 | 0.19 |
| 2/12/03 BL14 | Elevation (cm) | Elevation (cm/y) | Accretion (cm) | Accretion (cm/y) | Subsidence (cm) | Subsidence (cm/y) |
| 4/20/04 | 0.53 | 0.45 | | | | |
| 3/1/05 | 2.43 | 1.19 | | | | |
| 6/4/08 | 1.84 | 0.35 | | | | |
| 11/19/18 | 6.16 | 0.39 | 8.50 | 0.54 | 2.34 | 0.15 |

Appendix E: Raw SET Data Tables

Table E1. Site SL6 raw data.

| SL6 | 5/8/03 | 2/10/04 | 10/5/04 | 2/24/05 | 9/25/18 | 10/2/18corr | Accretion |
|-------------------------|--------|---------|---------|---------|---------|-------------|-----------|
| 1 site 6 position 1-s | 341 | 341 | 311 | 340 | 287 | 275 | none |
| 2 | 343 | 342 | 311 | 342 | 285 | 273 | |
| 3 | 348 | 346 | 320 | 348 | 266 | 254 | |
| 4 | 350 | 345 | 307 | 339 | 266 | 254 | |
| 5 | 344 | 347 | 339 | 338 | 265 | 253 | |
| 6 | 348 | 358 | 349 | 359 | 273 | 261 | |
| 7 | 346 | 356 | 304 | 347 | 260 | 248 | |
| 8 | 342 | 367 | 311 | 327 | 255 | 243 | |
| 9 | 378 | 366 | 330 | 354 | 271 | 259 | |
| 1 site 6 position 2 -w | 369 | 341 | 268 | 345 | 263 | 251 | |
| 2 | 364 | 333 | 293 | 345 | 255 | 243 | |
| 3 | 348 | 313 | 293 | 343 | 260 | 248 | |
| 4 | 366 | 342 | 280 | 347 | 264 | 252 | |
| 5 | 364 | 334 | 274 | 346 | 258 | 246 | |
| 6 | 360 | 348 | 283 | 347 | 250 | 238 | |
| 7 | 357 | 342 | 275 | 342 | 270 | 258 | |
| 8 | 351 | 329 | 274 | 340 | 290 | 278 | |
| 9 | 358 | 338 | 278 | 344 | 264 | 252 | |
| 1 site 6 position 3 - n | 349 | 346 | 356 | 344 | 260 | 248 | |
| 2 | 344 | 333 | 350 | 343 | 298 | 286 | |
| 3 | 348 | 339 | 343 | 342 | 279 | 267 | |
| 4 | 344 | 366 | 354 | 346 | 272 | 260 | |
| 5 | 353 | 355 | 351 | 345 | 293 | 281 | |
| 6 | 348 | 344 | 341 | 346 | 271 | 259 | |
| 7 | 346 | 347 | 359 | 376 | 298 | 286 | |
| 8 | 354 | 312 | 373 | 363 | 277 | 265 | |
| 9 | 362 | 346 | 344 | 345 | 270 | 258 | |
| 1 site 6 position 4 -e | 330 | 346 | 280 | 282 | 261 | 249 | |
| 2 | 337 | 348 | 283 | 277 | 266 | 254 | |
| 3 | 346 | 355 | 286 | 326 | 281 | 269 | |
| 4 | 341 | 351 | 279 | 309 | 280 | 268 | |
| 5 | 336 | 351 | 289 | 306 | 302 | 290 | |
| 6 | 339 | 349 | 285 | 334 | 271 | 259 | |
| 7 | 336 | 355 | 287 | 301 | 285 | 273 | |
| 8 | 340 | 351 | 284 | 343 | 291 | 279 | |
| 9 | 341 | 352 | 283 | 330 | 262 | 250 | |

Table E2. Site SL9 raw data.

| | 5/8/03 | 2/12/04 | 10/5/04 | 2/24/05 | 11/19/18 | 11/19/18corr | 2004 diff 04 | 2004 diff 10 | 2005diff | 2018dif | Accretion |
|---------------------|--------|---------|---------|---------|----------|--------------|--------------|--------------|----------|---------|-----------|
| 1 site 9 position 1 | | 284 | 199 | 275 | 331 | 319 | | -85 | -9 | 35 | 62 |
| 2 | | 280 | 256 | 289 | 399 | 387 | | -24 | 9 | 107 | 55 |
| 3 | | 278 | 253 | 276 | 325 | 313 | | -25 | -2 | 35 | 45 |
| 4 | | 254 | 220 | 273 | 328 | 316 | | -34 | 19 | 62 | 43 |
| 5 | | 280 | 238 | 278 | 338 | 326 | | -42 | -2 | 46 | |
| 6 | | 273 | 256 | 277 | 324 | 312 | | -17 | 4 | 39 | |
| 7 | | 258 | 259 | 297 | 305 | 293 | | 1 | 39 | 35 | |
| 8 | | 318 | 200 | 262 | 297 | 285 | | -118 | -56 | -33 | |
| 9 | | 283 | 198 | 261 | 284 | 272 | | -85 | -22 | -11 | |
| 1 site 9 position 2 | | 328 | 270 | 283 | 362 | 350 | | -58 | -45 | 22 | |
| 2 | | 286 | 326 | 311 | 376 | 364 | | 40 | 25 | 78 | |
| 3 | | 270 | 265 | 296 | 351 | 339 | | -5 | 26 | 69 | |
| 4 | | 302 | 303 | 268 | 368 | 356 | | 1 | -34 | 54 | |
| 5 | | 275 | 297 | 284 | 359 | 347 | | 22 | 9 | 72 | |
| 6 | | 273 | 215 | 312 | 348 | 336 | | -58 | 39 | 63 | |
| 7 | | 282 | 303 | 262 | 350 | 338 | | 21 | -20 | 56 | |
| 8 | | 270 | 199 | 257 | 367 | 355 | | -71 | -13 | 85 | |
| 9 | | 272 | 271 | 296 | 340 | 328 | | -1 | 24 | 56 | |
| 1 site 9 position 3 | | 296 | 267 | 267 | 284 | 272 | | -29 | -29 | -24 | |
| 2 | | 304 | 197 | 277 | 282 | 270 | | -107 | -27 | -34 | |
| 3 | | 306 | 244 | 295 | 279 | 267 | | -62 | -11 | -39 | |
| 4 | | 286 | 226 | 274 | 278 | 266 | | -60 | -12 | -20 | |
| 5 | | 285 | 215 | 273 | 272 | 260 | | -70 | -12 | -25 | |
| 6 | | 307 | 224 | 278 | 284 | 272 | | -83 | -29 | -35 | |
| 7 | | 293 | 371 | 289 | 290 | 278 | | 78 | -4 | -15 | |
| 8 | | 282 | 261 | 292 | 285 | 273 | | -21 | 10 | -9 | |
| 9 | | 277 | 248 | 279 | 288 | 276 | | -29 | 2 | -1 | |
| 1 site 9 position 4 | | 288 | 261 | 308 | 259 | 247 | | -27 | 20 | -41 | |
| 2 | | 289 | 299 | 291 | 271 | 259 | | 10 | 2 | -30 | |
| 3 | | 309 | 306 | 288 | 276 | 264 | | -3 | -21 | -45 | |
| 4 | | 287 | 271 | 310 | 272 | 260 | | -16 | 23 | -27 | |
| 5 | | 291 | 282 | 387 | 283 | 271 | | -9 | 96 | -20 | |
| 6 | | 298 | 296 | 267 | 275 | 263 | | -2 | -31 | -35 | |
| 7 | | 306 | 282 | 290 | 308 | 296 | | -24 | -16 | -10 | |
| 8 | | 324 | 285 | 286 | 311 | 299 | | -39 | -38 | -25 | |
| 9 | | 309 | 248 | 280 | 280 | 268 | | -61 | -29 | -41 | |

Table E3. Site SL11 raw data.

| SL11 | 5/8/03 | 2/12/04 | 10/5/04 | 2/24/05 | 10/2/18 | 10/2/18corr | 2004 diff 04 | 2004 diff 10 | 2005diff | 2018dif | 10/2018 Accretion | 11/2018 Accretion |
|----------------------|--------|---------|---------|---------|---------|-------------|--------------|--------------|----------|---------|-------------------|-------------------|
| 1 site 11 position 1 | 313 | 301 | 306 | 314 | 240 | 228 | -12 | -7 | 1 | -85 | 102 | 95 |
| 2 | 319 | 317 | 274 | 315 | 240 | 228 | -2 | -45 | -4 | -91 | 105 | 100 |
| 3 | 331 | 300 | 283 | 334 | 233 | 221 | -31 | -48 | 3 | -110 | 120 | |
| 4 | 316 | 314 | 280 | 303 | 235 | 223 | -2 | -36 | -13 | -93 | 103 | |
| 5 | 316 | 290 | 316 | 295 | 232 | 220 | -26 | 0 | -21 | -96 | 106 | |
| 6 | 317 | 320 | 281 | 295 | 235 | 223 | 3 | -36 | -22 | -94 | | |
| 7 | 319 | 314 | 315 | 312 | 230 | 218 | -5 | -4 | -7 | -101 | | |
| 8 | 323 | 318 | 245 | 316 | 240 | 228 | -5 | -78 | -7 | -95 | | |
| 9 | 317 | 295 | 232 | 314 | 233 | 221 | -22 | -85 | -3 | -96 | | |
| 1 site 11 position 2 | 333 | 324 | 271 | 332 | 235 | 223 | -9 | -62 | -1 | -110 | | |
| 2 | 318 | 333 | 263 | 326 | 233 | 221 | 15 | -55 | 8 | -97 | | |
| 3 | 320 | 340 | 284 | 326 | 294 | 282 | 20 | -36 | 6 | -38 | | |
| 4 | 327 | 321 | 240 | 309 | 233 | 221 | -6 | -87 | -18 | -106 | | |
| 5 | 326 | 329 | 281 | 311 | 216 | 204 | 3 | -45 | -15 | -122 | | |
| 6 | 325 | 332 | 285 | 304 | 245 | 233 | 7 | -40 | -21 | -92 | | |
| 7 | 328 | 328 | 279 | 341 | 240 | 228 | 0 | -49 | 13 | -100 | | |
| 8 | 320 | 328 | 278 | 300 | 240 | 228 | 8 | -42 | -20 | -92 | | |
| 9 | 326 | 332 | 342 | 307 | 255 | 243 | 6 | 16 | -19 | -83 | | |
| 1 site 11 position 3 | 324 | 329 | 318 | 279 | 244 | 232 | 5 | -6 | -45 | -92 | | |
| 2 | 311 | 324 | 260 | 266 | 239 | 227 | 13 | -51 | -45 | -84 | | |
| 3 | 307 | 327 | 250 | 289 | 253 | 241 | 20 | -57 | -18 | -66 | | |
| 4 | 315 | 332 | 270 | 319 | 250 | 238 | 17 | -45 | 4 | -77 | | |
| 5 | 322 | 335 | 272 | 295 | 289 | 277 | 13 | -50 | -27 | -45 | | |
| 6 | 308 | 336 | 285 | 289 | 255 | 243 | 28 | -23 | -19 | -65 | | |
| 7 | 322 | 330 | 280 | 298 | 300 | 288 | 8 | -42 | -24 | -34 | | |
| 8 | 328 | 341 | 289 | 309 | 279 | 267 | 13 | -39 | -19 | -61 | | |
| 9 | 307 | 343 | 285 | 308 | 230 | 218 | 36 | -22 | 1 | -89 | | |
| 1 site 11 position 4 | 338 | 357 | 348 | 308 | 238 | 226 | 19 | 10 | -30 | -112 | | |
| 2 | 353 | 330 | 346 | 304 | 256 | 244 | -23 | -7 | -49 | -109 | | |
| 3 | 339 | 324 | 282 | 339 | 238 | 226 | -15 | -57 | 0 | -113 | | |
| 4 | 343 | 360 | 331 | 264 | 247 | 235 | 17 | -12 | -79 | -108 | | |
| 5 | 348 | 327 | 353 | 306 | 251 | 239 | -21 | 5 | -42 | -109 | | |
| 6 | 354 | 328 | 286 | 326 | 225 | 213 | -26 | -68 | -28 | -141 | | |
| 7 | 348 | 349 | 318 | 259 | 237 | 225 | 1 | -30 | -89 | -123 | | |
| 8 | 372 | 348 | 345 | 334 | 225 | 213 | -24 | -27 | -38 | -159 | | |
| 9 | 358 | 298 | 301 | 325 | 234 | 222 | -60 | -57 | -33 | -136 | | |

Table E4. Site SL12 raw data.

| SL12 | 5/8/03 | 2/12/04 | 10/5/04 | 2/24/05 | 10/2/18 | 10/2/18corr | 2004diff04 | 2004diff10 | 2005diff | 2018diff | Accretion |
|----------------------|--------|---------|---------|---------|---------|-------------|------------|------------|----------|----------|-----------|
| 1 site 12 position 1 | 230 | 208 | 184 | 263 | 235 | 223 | -22 | -46 | 55 | -7 | none |
| 2 | 216 | 215 | 250 | 228 | 232 | 220 | -1 | 34 | 12 | 4 | |
| 3 | 224 | 226 | 267 | 205 | 181 | 169 | 2 | 43 | -19 | -55 | |
| 4 | 218 | 200 | 263 | 254 | 159 | 147 | -18 | 45 | 36 | -71 | |
| 5 | 231 | 254 | 167 | 219 | 152 | 140 | 23 | -64 | -12 | -91 | |
| 6 | 252 | 185 | 233 | 221 | 164 | 152 | -67 | -19 | -31 | -100 | |
| 7 | 187 | 198 | 292 | 254 | 183 | 171 | 11 | 105 | 67 | -16 | |
| 8 | 173 | 140 | 294 | 296 | 203 | 191 | -33 | 121 | 123 | 18 | |
| 9 | 273 | 176 | 201 | 237 | 142 | 130 | -97 | -72 | -36 | -143 | |
| 1 site 12 position 2 | 213 | 204 | 168 | 216 | 162 | 150 | -9 | -45 | 3 | -63 | |
| 2 | 219 | 208 | 200 | 200 | 188 | 176 | -11 | -19 | -19 | -43 | |
| 3 | 203 | 205 | 205 | 201 | 167 | 155 | 2 | 2 | -2 | -48 | |
| 4 | 203 | 204 | 223 | 212 | 191 | 179 | 1 | 20 | 9 | -24 | |
| 5 | 216 | 207 | 228 | 222 | 183 | 171 | -9 | 12 | 6 | -45 | |
| 6 | 207 | 205 | 208 | 204 | 173 | 161 | -2 | 1 | -3 | -46 | |
| 7 | 209 | 203 | 183 | 216 | 180 | 168 | -6 | -26 | 7 | -41 | |
| 8 | 176 | 206 | 173 | 210 | 180 | 168 | 30 | -3 | 34 | -8 | |
| 9 | 204 | 206 | 211 | 179 | 186 | 174 | 2 | 7 | -25 | -30 | |
| 1 site 12 position 3 | 230 | 185 | 201 | 259 | 164 | 152 | -45 | -29 | 29 | -78 | |
| 2 | 180 | 189 | 196 | 193 | 174 | 162 | 9 | 16 | 13 | -18 | |
| 3 | 194 | 189 | 197 | 194 | 189 | 177 | -5 | 3 | 0 | -17 | |
| 4 | 263 | 199 | 215 | 234 | 167 | 155 | -64 | -48 | -29 | -108 | |
| 5 | 190 | 209 | 185 | 196 | 177 | 165 | 19 | -5 | 6 | -25 | |
| 6 | 186 | 208 | 211 | 206 | 196 | 184 | 22 | 25 | 20 | -2 | |
| 7 | 239 | 191 | 227 | 184 | 180 | 168 | -48 | -12 | -55 | -71 | |
| 8 | 213 | 190 | 212 | 221 | 172 | 160 | -23 | -1 | 8 | -53 | |
| 9 | 205 | 209 | 232 | 229 | 186 | 174 | 4 | 27 | 24 | -31 | |
| 1 site 12 position 4 | 207 | 200 | 216 | 199 | 189 | 177 | -7 | 9 | -8 | -30 | |
| 2 | 198 | 195 | 209 | 213 | 150 | 138 | -3 | 11 | 15 | -60 | |
| 3 | 190 | 204 | 209 | 200 | 161 | 149 | 14 | 19 | 10 | -41 | |
| 4 | 258 | 195 | 170 | 239 | 201 | 189 | -63 | -88 | -19 | -69 | |
| 5 | 260 | 198 | 224 | 205 | 148 | 136 | -62 | -36 | -55 | -124 | |
| 6 | 181 | 260 | 274 | 200 | 164 | 152 | 79 | 93 | 19 | -29 | |
| 7 | 200 | 192 | 216 | 239 | 167 | 155 | -8 | 16 | 39 | -45 | |
| 8 | 241 | 239 | 279 | 234 | 136 | 124 | -2 | 38 | -7 | -117 | |
| 9 | 294 | 200 | 202 | 189 | 112 | 100 | -94 | -92 | -105 | -194 | |

Table E5. Site SL15 raw data.

| | 5/8/03 | 2/12/04 | 10/5/04 | 2/24/05 | 11/19/18 | 11/19/18corr | 2004 diff 04 | 2004 diff 10 | 2005diff | 2018dif | Accretion |
|----------------------|--------|---------|---------|---------|----------|--------------|--------------|--------------|----------|---------|-----------|
| 1 site 15 position 1 | 263 | 253 | 266 | 263 | 219 | 207 | -10 | 3 | 0 | -56 | None |
| 2 | 264 | 260 | 270 | 268 | 280 | 268 | -4 | 6 | 4 | 4 | |
| 3 | 265 | 267 | 283 | 273 | 280 | 268 | 2 | 18 | 8 | 3 | |
| 4 | 255 | 257 | 234 | 265 | 261 | 249 | 2 | -21 | 10 | -6 | |
| 5 | 258 | 266 | 253 | 263 | 285 | 273 | 8 | -5 | 5 | 15 | |
| 6 | 248 | 274 | 234 | 246 | 210 | 198 | 26 | -14 | -2 | -50 | |
| 7 | 275 | 277 | 228 | 284 | 212 | 200 | 2 | -47 | 9 | -75 | |
| 8 | 279 | 278 | 260 | 263 | 207 | 195 | -1 | -19 | -16 | -84 | |
| 9 | 250 | 303 | 245 | 249 | 212 | 200 | 53 | -5 | -1 | -50 | |
| 1 site 15 position 2 | 292 | 308 | 256 | 312 | 261 | 249 | 16 | -36 | 20 | -43 | |
| 2 | 312 | 306 | 304 | 313 | 224 | 212 | -6 | -8 | 1 | -100 | |
| 3 | 317 | 321 | 273 | 264 | 244 | 232 | 4 | -44 | -53 | -85 | |
| 4 | 289 | 299 | 307 | 339 | 223 | 211 | 10 | 18 | 50 | -78 | |
| 5 | 324 | 329 | 284 | 319 | 219 | 207 | 5 | -40 | -5 | -117 | |
| 6 | 313 | 308 | 275 | 295 | 232 | 220 | -5 | -38 | -18 | -93 | |
| 7 | 288 | 265 | 327 | 398 | 217 | 205 | -23 | 39 | 110 | -83 | |
| 8 | 318 | 328 | 308 | 298 | 222 | 210 | 10 | -10 | -20 | -108 | |
| 9 | 302 | 305 | 270 | 270 | 268 | 256 | 3 | -32 | -32 | -46 | |
| 1 site 15 position 3 | 260 | 241 | 249 | 257 | 264 | 252 | -19 | -11 | -3 | -8 | |
| 2 | 262 | 263 | 257 | 262 | 266 | 254 | 1 | -5 | 0 | -8 | |
| 3 | 254 | 259 | 265 | 302 | 227 | 215 | 5 | 11 | 48 | -39 | |
| 4 | 250 | 239 | 233 | 261 | 240 | 228 | -11 | -17 | 11 | -22 | |
| 5 | 241 | 241 | 206 | 255 | 249 | 237 | 0 | -35 | 14 | -4 | |
| 6 | 229 | 257 | 236 | 274 | 232 | 220 | 28 | 7 | 45 | -9 | |
| 7 | 251 | 255 | 175 | 262 | 271 | 259 | 4 | -76 | 11 | 8 | |
| 8 | 247 | 253 | 234 | 283 | 272 | 260 | 6 | -13 | 36 | 13 | |
| 9 | 256 | 265 | 244 | 277 | 285 | 273 | 9 | -12 | 21 | 17 | |
| 1 site 15 position 4 | 251 | 288 | 296 | 258 | 234 | 222 | 37 | 45 | 7 | -29 | |
| 2 | 254 | 253 | 240 | 275 | 225 | 213 | -1 | -14 | 21 | -41 | |
| 3 | 296 | 258 | 245 | 256 | 226 | 214 | -38 | -51 | -40 | -82 | |
| 4 | 244 | 265 | 251 | 251 | 218 | 206 | 21 | 7 | 7 | -38 | |
| 5 | 241 | 260 | 253 | 252 | 232 | 220 | 19 | 12 | 11 | -21 | |
| 6 | 266 | 261 | 257 | 237 | 234 | 222 | -5 | -9 | -29 | -44 | |
| 7 | 261 | 258 | 241 | 258 | 220 | 208 | -3 | -20 | -3 | -53 | |
| 8 | 249 | 266 | 251 | 241 | 233 | 221 | 17 | 2 | -8 | -28 | |
| 9 | 262 | 273 | 270 | 258 | 230 | 218 | 11 | 8 | -4 | -44 | |

Table E6. Site BL1 raw data.

| | 2/14/03 | 1/28/04 | 3/2/05 | 3/2/2005corr | 6/4/08 | 6/4/2008corr | 10/2/18 | 10/2/18corr | 2004diff | 2005diff | 2008diff | 2018diff | Accretion |
|---------------------|---------|---------|--------|--------------|--------|--------------|---------|-------------|----------|----------|----------|----------|-----------|
| 1 site 1 position s | 309 | 307 | 458 | 300.8 | 482 | 324.8 | 372 | 360 | -2 | -8.2 | 15.8 | 51 | 64 |
| 2 | 305 | 300 | 463 | 305.8 | 487 | 329.8 | 373 | 361 | -5 | 0.8 | 24.8 | 56 | 78 |
| 3 | 302 | 297 | 463 | 305.8 | 479 | 321.8 | 373 | 361 | -5 | 3.8 | 19.8 | 59 | 74 |
| 4 | 310 | 275 | 435 | 277.8 | 476 | 318.8 | 371 | 359 | -35 | -32.2 | 8.8 | 49 | 85 |
| 5 | 301 | 298 | 458 | 300.8 | 472 | 314.8 | 364 | 352 | -3 | -0.2 | 13.8 | 51 | 87 |
| 6 | 301 | 289 | 467 | 309.8 | 468 | 310.8 | 374 | 362 | -12 | 8.8 | 9.8 | 61 | |
| 7 | 303 | 301 | 460 | 302.8 | 477 | 319.8 | 364 | 352 | -2 | -0.2 | 16.8 | 49 | |
| 8 | 299 | 309 | 464 | 306.8 | 470 | 312.8 | 366 | 354 | 10 | 7.8 | 13.8 | 55 | |
| 9 | 299 | 306 | 470 | 312.8 | 478 | 320.8 | 360 | 348 | 7 | 13.8 | 21.8 | 49 | |
| 1 site 1 position w | 304 | 299 | 443 | 285.8 | 462 | 304.8 | 363 | 351 | -5 | -18.2 | 0.8 | 47 | |
| 2 | 301 | 291 | 449 | 291.8 | 461 | 303.8 | 373 | 361 | -10 | -9.2 | 2.8 | 60 | |
| 3 | 300 | 290 | 442 | 284.8 | 468 | 310.8 | 370 | 358 | -10 | -15.2 | 10.8 | 58 | |
| 4 | 307 | 298 | 443 | 285.8 | 468 | 310.8 | 364 | 352 | -9 | -21.2 | 3.8 | 45 | |
| 5 | 302 | 306 | 451 | 293.8 | 469 | 311.8 | 364 | 352 | 4 | -8.2 | 9.8 | 50 | |
| 6 | 304 | 297 | 452 | 294.8 | 469 | 311.8 | 363 | 351 | -7 | -9.2 | 7.8 | 47 | |
| 7 | 301 | 302 | 456 | 298.8 | 462 | 304.8 | 366 | 354 | 1 | -2.2 | 3.8 | 53 | |
| 8 | 294 | 290 | 457 | 299.8 | 469 | 311.8 | 369 | 357 | -4 | 5.8 | 17.8 | 63 | |
| 9 | 300 | 293 | 451 | 293.8 | 462 | 304.8 | 367 | 355 | -7 | -6.2 | 4.8 | 55 | |
| 1 site 1 position n | 296 | 297 | 422 | 264.8 | 457 | 299.8 | 380 | 368 | 1 | -31.2 | 3.8 | 72 | |
| 2 | 303 | 297 | 439 | 281.8 | 456 | 298.8 | 362 | 350 | -6 | -21.2 | -4.2 | 47 | |
| 3 | 294 | 294 | 431 | 273.8 | 462 | 304.8 | 360 | 348 | 0 | -20.2 | 10.8 | 54 | |
| 4 | 305 | 302 | 427 | 269.8 | 461 | 303.8 | 363 | 351 | -3 | -35.2 | -1.2 | 46 | |
| 5 | 304 | 293 | 436 | 278.8 | 463 | 305.8 | 367 | 355 | -11 | -25.2 | 1.8 | 51 | |
| 6 | 292 | 283 | 439 | 281.8 | 463 | 305.8 | 364 | 352 | -9 | -10.2 | 13.8 | 60 | |
| 7 | 300 | 298 | 437 | 279.8 | 466 | 308.8 | 362 | 350 | -2 | -20.2 | 8.8 | 50 | |
| 8 | 298 | 304 | 438 | 280.8 | 468 | 310.8 | 360 | 348 | 6 | -17.2 | 12.8 | 50 | |
| 9 | 288 | 285 | 438 | 280.8 | 461 | 303.8 | 357 | 345 | -3 | -7.2 | 15.8 | 57 | |
| 1 site 1 position e | 306 | 307 | 450 | 292.8 | 486 | 328.8 | 359 | 347 | 1 | -13.2 | 22.8 | 41 | |
| 2 | 300 | 310 | 406 | 248.8 | 478 | 320.8 | 360 | 348 | 10 | -51.2 | 20.8 | 48 | |
| 3 | 305 | 318 | 455 | 297.8 | 472 | 314.8 | 365 | 353 | 13 | -7.2 | 9.8 | 48 | |
| 4 | 303 | 314 | 438 | 280.8 | 473 | 315.8 | 362 | 350 | 11 | -22.2 | 12.8 | 47 | |
| 5 | 304 | 305 | 453 | 295.8 | 474 | 316.8 | 385 | 373 | 1 | -8.2 | 12.8 | 69 | |
| 6 | 298 | 263 | 461 | 303.8 | 457 | 299.8 | 359 | 347 | -35 | 5.8 | 1.8 | 49 | |
| 7 | 306 | 272 | 461 | 303.8 | 468 | 310.8 | 373 | 361 | -34 | -2.2 | 4.8 | 55 | |
| 8 | 296 | 304 | 460 | 302.8 | 463 | 305.8 | 365 | 353 | 8 | 6.8 | 9.8 | 57 | |
| 9 | 309 | 296 | 463 | 305.8 | 475 | 317.8 | 373 | 361 | -13 | -3.2 | 8.8 | 52 | |

Table E7. Site BL3 raw data.

| BL3 | 2/14/03 | 1/28/04 | 3/2/05 | 3/2/2005corr | 5/4/08 | 5/4/2008corr | 10/2/18 | 10/2/18corr | 2004diff | 2005diff | 2008diff | 2018diff | Accretion |
|---------------------|---------|---------|--------|--------------|--------|--------------|---------|-------------|----------|----------|----------|----------|-----------|
| 1 site 1 position s | 296 | 300 | 440 | 283 | 468 | 311 | 385 | 373 | 4 | -13 | 15 | 77 | 111 |
| 2 | 284 | 291 | 459 | 302 | 471 | 314 | 386 | 374 | 7 | 18 | 30 | 90 | 122 |
| 3 | 293 | 304 | 466 | 309 | 469 | 312 | 388 | 376 | 11 | 16 | 19 | 83 | 112 |
| 4 | 286 | 296 | 459 | 302 | 466 | 309 | 380 | 368 | 10 | 16 | 23 | 82 | 114 |
| 5 | 290 | 295 | 455 | 298 | 474 | 317 | 402 | 390 | 5 | 8 | 27 | 100 | 101 |
| 6 | 286 | 294 | 436 | 279 | 475 | 318 | 388 | 376 | 8 | -7 | 32 | 90 | 98 |
| 7 | 287 | 286 | 454 | 297 | 466 | 309 | 385 | 373 | -1 | 10 | 22 | 86 | |
| 8 | 293 | 289 | 441 | 284 | 478 | 321 | 402 | 390 | -4 | -9 | 28 | 97 | |
| 9 | 296 | 290 | 442 | 285 | 480 | 323 | 406 | 394 | -6 | -11 | 27 | 98 | |
| 1 site 1 position w | 298 | 306 | 449 | 292 | 484 | 327 | 389 | 377 | 8 | -6 | 29 | 79 | |
| 2 | 296 | 309 | 452 | 295 | 482 | 325 | 405 | 393 | 13 | -1 | 29 | 97 | |
| 3 | 295 | 297 | 433 | 276 | 485 | 328 | 405 | 393 | 2 | -19 | 33 | 98 | |
| 4 | 299 | 310 | 452 | 295 | 481 | 324 | 391 | 379 | 11 | -4 | 25 | 80 | |
| 5 | 301 | 311 | 452 | 295 | 476 | 319 | 396 | 384 | 10 | -6 | 18 | 83 | |
| 6 | 292 | 302 | 451 | 294 | 473 | 316 | 394 | 382 | 10 | 2 | 24 | 90 | |
| 7 | 296 | 307 | 445 | 288 | 473 | 316 | 389 | 377 | 11 | -8 | 20 | 81 | |
| 8 | 293 | 302 | 456 | 299 | 484 | 327 | 380 | 368 | 9 | 6 | 34 | 75 | |
| 9 | 289 | 294 | 452 | 295 | 482 | 325 | 394 | 382 | 5 | 6 | 36 | 93 | |
| 1 site 1 position n | 287 | 293 | 431 | 274 | 473 | 316 | 372 | 360 | 6 | -13 | 29 | 73 | |
| 2 | 290 | 292 | 426 | 269 | 470 | 313 | 391 | 379 | 2 | -21 | 23 | 89 | |
| 3 | 295 | 297 | 439 | 282 | 481 | 324 | 390 | 378 | 2 | -13 | 29 | 83 | |
| 4 | 282 | 292 | 439 | 282 | 470 | 313 | 379 | 367 | 10 | 0 | 31 | 85 | |
| 5 | 286 | 283 | 437 | 280 | 472 | 315 | 398 | 386 | -3 | -6 | 29 | 100 | |
| 6 | 291 | 287 | 424 | 267 | 466 | 309 | 387 | 375 | -4 | -24 | 18 | 84 | |
| 7 | 285 | 295 | 450 | 293 | 476 | 319 | 389 | 377 | 10 | 8 | 34 | 92 | |
| 8 | 285 | 293 | 445 | 288 | 473 | 316 | 390 | 378 | 8 | 3 | 31 | 93 | |
| 9 | 279 | 293 | 430 | 273 | 479 | 322 | 401 | 389 | 14 | -6 | 43 | 110 | |
| 1 site 1 position e | 290 | 286 | 451 | 294 | 499 | 342 | 380 | 368 | -4 | 4 | 52 | 78 | |
| 2 | 288 | 260 | 442 | 285 | 485 | 328 | 370 | 358 | -28 | -3 | 40 | 70 | |
| 3 | 288 | 282 | 443 | 286 | 490 | 333 | 391 | 379 | -6 | -2 | 45 | 91 | |
| 4 | 275 | 273 | 449 | 292 | 491 | 334 | 387 | 375 | -2 | 17 | 59 | 100 | |
| 5 | 272 | 259 | 443 | 286 | 483 | 326 | 394 | 382 | -13 | 14 | 54 | 110 | |
| 6 | 290 | 284 | 443 | 286 | 485 | 328 | 395 | 383 | -6 | -4 | 38 | 93 | |
| 7 | 280 | 275 | 453 | 296 | 489 | 332 | 393 | 381 | -5 | 16 | 52 | 101 | |
| 8 | 291 | 280 | 460 | 303 | 491 | 334 | 390 | 378 | -11 | 12 | 43 | 87 | |
| 9 | 290 | 296 | 460 | 303 | 486 | 329 | 389 | 377 | 6 | 13 | 39 | 87 | |

Table E8. Site BL4 raw data.

| | 2/14/03 | 1/28/04 | 3/2/05 | 3/2/2005corr | 6/4/08 | 6/4/2008corr | 10/2/18 | 10/2/18corr | 2004diff | 2005diff | 2008diff | 2018diff | Accretion |
|---------------------|---------|---------|--------|--------------|--------|--------------|---------|-------------|----------|----------|----------|----------|-----------|
| 1 site 4 position s | 355 | 313 | 498 | 341 | 515 | 358 | 438 | 426 | -42 | -14 | 3 | 71 | none |
| 2 | 358 | 365 | 511 | 354 | 507 | 350 | 438 | 426 | 7 | -4 | -8 | 68 | |
| 3 | 356 | 360 | 511 | 354 | 529 | 372 | 444 | 432 | 4 | -2 | 16 | 76 | |
| 4 | 354 | 361 | 505 | 348 | 513 | 356 | 463 | 451 | 7 | -6 | 2 | 97 | |
| 5 | 353 | 362 | 505 | 348 | 520 | 363 | 448 | 436 | 9 | -5 | 10 | 83 | |
| 6 | 351 | 359 | 507 | 350 | 515 | 358 | 422 | 410 | 8 | -1 | 7 | 59 | |
| 7 | 353 | 357 | 514 | 357 | 519 | 362 | 446 | 434 | 4 | 4 | 9 | 81 | |
| 8 | 350 | 374 | 536 | 379 | 516 | 359 | 445 | 433 | 24 | 29 | 9 | 83 | |
| 9 | 354 | 352 | 523 | 366 | 507 | 350 | 426 | 414 | -2 | 12 | -4 | 60 | |
| 1 site 4 position w | 338 | 348 | 523 | 366 | 501 | 344 | 422 | 410 | 10 | 28 | 6 | 72 | |
| 2 | 342 | 360 | 493 | 336 | 504 | 347 | 410 | 398 | 18 | -6 | 5 | 56 | |
| 3 | 332 | 342 | 495 | 338 | 498 | 341 | 420 | 408 | 10 | 6 | 9 | 76 | |
| 4 | 337 | 348 | 527 | 370 | 488 | 331 | 407 | 395 | 11 | 33 | -6 | 58 | |
| 5 | 336 | 354 | 507 | 350 | 500 | 343 | 416 | 404 | 18 | 14 | 7 | 68 | |
| 6 | 340 | 345 | 516 | 359 | 504 | 347 | 392 | 380 | 5 | 19 | 7 | 40 | |
| 7 | 343 | 349 | 486 | 329 | 500 | 343 | 428 | 416 | 6 | -14 | 0 | 73 | |
| 8 | 335 | 342 | 494 | 337 | 499 | 342 | 410 | 398 | 7 | 2 | 7 | 63 | |
| 9 | 325 | 351 | 525 | 368 | 504 | 347 | 417 | 405 | 26 | 43 | 22 | 80 | |
| 1 site 4 position n | 317 | 321 | 485 | 328 | 476 | 319 | 391 | 379 | 4 | 11 | 2 | 62 | |
| 2 | 322 | 324 | 490 | 333 | 482 | 325 | 390 | 378 | 2 | 11 | 3 | 56 | |
| 3 | 318 | 325 | 485 | 328 | 483 | 326 | 397 | 385 | 7 | 10 | 8 | 67 | |
| 4 | 325 | 330 | 446 | 289 | 485 | 328 | 404 | 392 | 5 | -36 | 3 | 67 | |
| 5 | 321 | 331 | 474 | 317 | 490 | 333 | 383 | 371 | 10 | -4 | 12 | 50 | |
| 6 | 321 | 329 | 470 | 313 | 494 | 337 | 419 | 407 | 8 | -8 | 16 | 86 | |
| 7 | 323 | 331 | 464 | 307 | 486 | 329 | 433 | 421 | 8 | -16 | 6 | 98 | |
| 8 | 325 | 322 | 470 | 313 | 484 | 327 | 435 | 423 | -3 | -12 | 2 | 98 | |
| 9 | 322 | 319 | 479 | 322 | 485 | 328 | 430 | 418 | -3 | 0 | 6 | 96 | |
| 1 site 4 position e | 330 | 335 | 499 | 342 | 510 | 353 | 385 | 373 | 5 | 12 | 23 | 43 | |
| 2 | 333 | 348 | 504 | 347 | 579 | 422 | 403 | 391 | 15 | 14 | 89 | 58 | |
| 3 | 336 | 343 | 503 | 346 | 503 | 346 | 410 | 398 | 7 | 10 | 10 | 62 | |
| 4 | 345 | 344 | 511 | 354 | 457 | 300 | 417 | 405 | -1 | 9 | -45 | 60 | |
| 5 | 334 | 353 | 516 | 359 | 492 | 335 | 422 | 410 | 19 | 25 | 1 | 76 | |
| 6 | 341 | 334 | 485 | 328 | 492 | 335 | 412 | 400 | -7 | -13 | -6 | 59 | |
| 7 | 337 | 341 | 487 | 330 | 505 | 348 | 420 | 408 | 4 | -7 | 11 | 71 | |
| 8 | 335 | 350 | 492 | 335 | 494 | 337 | 440 | 428 | 15 | 0 | 2 | 93 | |
| 9 | 346 | 314 | 503 | 346 | 501 | 344 | 412 | 400 | -32 | 0 | -2 | 54 | |

Table E9. Site BL6 raw data.

| | 2/14/03 | 4/20/04 | 3/2/05 | 3/2/2005corr | 6/3/08 | 6/3/2008corr | 10/2/18 | 10/2/18corr | 2004diff | 2005diff | 2008diff | 2018diff | Accretion |
|---------------------|---------|---------|--------|--------------|--------|--------------|---------|-------------|----------|----------|----------|----------|-----------|
| 1 site 6 position s | 319 | 319 | 460 | 302.8 | 499 | 341.8 | 426 | 414 | 0 | -16.2 | 22.8 | 107 | none |
| 2 | 322 | 330 | 435 | 277.8 | 495 | 337.8 | 419 | 407 | 8 | -44.2 | 15.8 | 97 | |
| 3 | 331 | 328 | 440 | 282.8 | 492 | 334.8 | 419 | 407 | -3 | -48.2 | 3.8 | 88 | |
| 4 | 314 | 330 | 424 | 266.8 | 511 | 353.8 | 412 | 400 | 16 | -47.2 | 39.8 | 98 | |
| 5 | 322 | 268 | 446 | 288.8 | 512 | 354.8 | 401 | 389 | -54 | -33.2 | 32.8 | 79 | |
| 6 | 324 | 318 | 450 | 292.8 | 510 | 352.8 | 410 | 398 | -6 | -31.2 | 28.8 | 86 | |
| 7 | 318 | 329 | 445 | 287.8 | 497 | 339.8 | 411 | 399 | 11 | -30.2 | 21.8 | 93 | |
| 8 | 324 | 324 | 416 | 258.8 | 504 | 346.8 | 438 | 426 | 0 | -65.2 | 22.8 | 114 | |
| 9 | 312 | 298 | 414 | 256.8 | 510 | 352.8 | 416 | 404 | -14 | -55.2 | 40.8 | 104 | |
| 1 site 6 position w | 320 | 328 | 453 | 295.8 | 500 | 342.8 | 425 | 413 | 8 | -24.2 | 22.8 | 105 | |
| 2 | 317 | 325 | 421 | 263.8 | 496 | 338.8 | 423 | 411 | 8 | -53.2 | 21.8 | 106 | |
| 3 | 351 | 326 | 393 | 235.8 | 505 | 347.8 | 417 | 405 | -25 | -115.2 | -3.2 | 66 | |
| 4 | 328 | 335 | 442 | 284.8 | 492 | 334.8 | 430 | 418 | 7 | -43.2 | 6.8 | 102 | |
| 5 | 337 | 300 | 423 | 265.8 | 493 | 335.8 | 416 | 404 | -37 | -71.2 | -1.2 | 79 | |
| 6 | 326 | 330 | 452 | 294.8 | 505 | 347.8 | 428 | 416 | 4 | -31.2 | 21.8 | 102 | |
| 7 | 324 | 341 | 445 | 287.8 | 502 | 344.8 | 417 | 405 | 17 | -36.2 | 20.8 | 93 | |
| 8 | 320 | 273 | 463 | 305.8 | 496 | 338.8 | 416 | 404 | -47 | -14.2 | 18.8 | 96 | |
| 9 | 320 | 330 | 423 | 265.8 | 503 | 345.8 | 405 | 393 | 10 | -54.2 | 25.8 | 85 | |
| 1 site 6 position n | 323 | 322 | 423 | 265.8 | 501 | 343.8 | 403 | 391 | -1 | -57.2 | 20.8 | 80 | |
| 2 | 324 | 328 | 435 | 277.8 | 511 | 353.8 | 410 | 398 | 4 | -46.2 | 29.8 | 86 | |
| 3 | 326 | 330 | 419 | 261.8 | 507 | 349.8 | 398 | 386 | 4 | -64.2 | 23.8 | 72 | |
| 4 | 323 | 289 | 464 | 306.8 | 510 | 352.8 | 408 | 396 | -34 | -16.2 | 29.8 | 85 | |
| 5 | 327 | 314 | 457 | 299.8 | 500 | 342.8 | 411 | 399 | -13 | -27.2 | 15.8 | 84 | |
| 6 | 326 | 324 | 404 | 246.8 | 508 | 350.8 | 415 | 403 | -2 | -79.2 | 24.8 | 89 | |
| 7 | 330 | 314 | 462 | 304.8 | 485 | 327.8 | 409 | 397 | -16 | -25.2 | -2.2 | 79 | |
| 8 | 333 | 301 | 441 | 283.8 | 505 | 347.8 | 409 | 397 | -32 | -49.2 | 14.8 | 76 | |
| 9 | 328 | 325 | 455 | 297.8 | 504 | 346.8 | 409 | 397 | -3 | -30.2 | 18.8 | 81 | |
| 1 site 6 position e | 333 | 328 | 469 | 311.8 | 503 | 345.8 | 420 | 408 | -5 | -21.2 | 12.8 | 87 | |
| 2 | 338 | 225 | 459 | 301.8 | 496 | 338.8 | 415 | 403 | -113 | -36.2 | 0.8 | 77 | |
| 3 | 348 | 319 | 434 | 276.8 | 494 | 336.8 | 411 | 399 | -29 | -71.2 | -11.2 | 63 | |
| 4 | 324 | 331 | 448 | 290.8 | 498 | 340.8 | 426 | 414 | 7 | -33.2 | 16.8 | 102 | |
| 5 | 331 | 265 | 480 | 322.8 | 496 | 338.8 | 409 | 397 | -66 | -8.2 | 7.8 | 78 | |
| 6 | 323 | 306 | 473 | 315.8 | 505 | 347.8 | 405 | 393 | -17 | -7.2 | 24.8 | 82 | |
| 7 | 343 | 314 | 485 | 327.8 | 495 | 337.8 | 414 | 402 | -29 | -15.2 | -5.2 | 71 | |
| 8 | 324 | 305 | 557 | 399.8 | 497 | 339.8 | 356 | 344 | -19 | 75.8 | 15.8 | 32 | |
| 9 | 338 | 331 | 452 | 294.8 | 502 | 344.8 | 419 | 407 | -7 | -43.2 | 6.8 | 81 | |

Table E10. Site BL8 raw data.

| | 2/12/03 | 4/20/04 | 3/2/05 | 3/2/2005corr | 6/4/08 | 6/4/2008corr | 11/19/18 | 11/19/18corr | 2004 diff | 2005 diff | 2008diff | 2018dif | Accretion |
|---------------------|---------|---------|--------|--------------|--------|--------------|----------|--------------|-----------|-----------|----------|---------|-----------|
| 1 site 8 position 1 | 320 | 325 | 498 | 340.8 | 497 | 339.8 | 400 | 388 | 5 | 20.8 | 19.8 | 68 | 87 |
| 2 | 322 | 331 | 481 | 323.8 | 503 | 345.8 | 381 | 369 | 9 | 1.8 | 23.8 | 47 | 105 |
| 3 | 349 | 338 | 490 | 332.8 | 502 | 344.8 | 386 | 374 | -11 | -16.2 | -4.2 | 25 | 92 |
| 4 | 322 | 328 | 500 | 342.8 | 498 | 340.8 | 391 | 379 | 6 | 20.8 | 18.8 | 57 | 95 |
| 5 | 323 | 329 | 501 | 343.8 | 496 | 338.8 | 380 | 368 | 6 | 20.8 | 15.8 | 45 | |
| 6 | 335 | 334 | 497 | 339.8 | 490 | 332.8 | 386 | 374 | -1 | 4.8 | -2.2 | 39 | |
| 7 | 324 | 326 | 505 | 347.8 | 499 | 341.8 | 390 | 378 | 2 | 23.8 | 17.8 | 54 | |
| 8 | 324 | 326 | 498 | 340.8 | 495 | 337.8 | 386 | 374 | 2 | 16.8 | 13.8 | 50 | |
| 9 | 326 | 334 | 497 | 339.8 | 485 | 327.8 | 386 | 374 | 8 | 13.8 | 1.8 | 48 | |
| 1 site 8 position 2 | 307 | 308 | 478 | 320.8 | 484 | 326.8 | 398 | 386 | 1 | 13.8 | 19.8 | 79 | |
| 2 | 309 | 313 | 482 | 324.8 | 482 | 324.8 | 389 | 377 | 4 | 15.8 | 15.8 | 68 | |
| 3 | 323 | 328 | 474 | 316.8 | 474 | 316.8 | 388 | 376 | 5 | -6.2 | -6.2 | 53 | |
| 4 | 318 | 321 | 483 | 325.8 | 470 | 312.8 | 387 | 375 | 3 | 7.8 | -5.2 | 57 | |
| 5 | 322 | 327 | 466 | 308.8 | 482 | 324.8 | 388 | 376 | 5 | -13.2 | 2.8 | 54 | |
| 6 | 325 | 329 | 475 | 317.8 | 463 | 305.8 | 390 | 378 | 4 | -7.2 | -19.2 | 53 | |
| 7 | 311 | 324 | 485 | 327.8 | 477 | 319.8 | 394 | 382 | 13 | 16.8 | 8.8 | 71 | |
| 8 | 333 | 336 | 474 | 316.8 | 476 | 318.8 | 389 | 377 | 3 | -16.2 | -14.2 | 44 | |
| 9 | 325 | 332 | 467 | 309.8 | 471 | 313.8 | 392 | 380 | 7 | -15.2 | -11.2 | 55 | |
| 1 site 8 position 3 | 300 | 327 | 517 | 359.8 | 510 | 352.8 | 395 | 383 | 27 | 59.8 | 52.8 | 83 | |
| 2 | 330 | 338 | 519 | 361.8 | 506 | 348.8 | 398 | 386 | 8 | 31.8 | 18.8 | 56 | |
| 3 | 328 | 329 | 514 | 356.8 | 505 | 347.8 | 396 | 384 | 1 | 28.8 | 19.8 | 56 | |
| 4 | 320 | 351 | 508 | 350.8 | 500 | 342.8 | 400 | 388 | 31 | 30.8 | 22.8 | 68 | |
| 5 | 333 | 339 | 511 | 353.8 | 506 | 348.8 | 401 | 389 | 6 | 20.8 | 15.8 | 56 | |
| 6 | 332 | 342 | 487 | 329.8 | 504 | 346.8 | 400 | 388 | 10 | -2.2 | 14.8 | 56 | |
| 7 | 334 | 338 | 463 | 305.8 | 496 | 338.8 | 396 | 384 | 4 | -28.2 | 4.8 | 50 | |
| 8 | 333 | 366 | 494 | 336.8 | 494 | 336.8 | 365 | 353 | 33 | 3.8 | 3.8 | 20 | |
| 9 | 328 | 350 | 494 | 336.8 | 495 | 337.8 | 403 | 391 | 22 | 8.8 | 9.8 | 63 | |
| 1 site 8 position 4 | 326 | 334 | 497 | 339.8 | 510 | 352.8 | 379 | 367 | 8 | 13.8 | 26.8 | 41 | |
| 2 | 330 | 338 | 485 | 327.8 | 531 | 373.8 | 383 | 371 | 8 | -2.2 | 43.8 | 41 | |
| 3 | 340 | 345 | 492 | 334.8 | 502 | 344.8 | 395 | 383 | 5 | -5.2 | 4.8 | 43 | |
| 4 | 327 | 326 | 493 | 335.8 | 501 | 343.8 | 374 | 362 | -1 | 8.8 | 16.8 | 35 | |
| 5 | 330 | 327 | 491 | 333.8 | 507 | 349.8 | 399 | 387 | -3 | 3.8 | 19.8 | 57 | |
| 6 | 338 | 343 | 492 | 334.8 | 510 | 352.8 | 390 | 378 | 5 | -3.2 | 14.8 | 40 | |
| 7 | 328 | 330 | 496 | 338.8 | 510 | 352.8 | 375 | 363 | 2 | 10.8 | 24.8 | 35 | |
| 8 | 316 | 329 | 496 | 338.8 | 508 | 350.8 | 390 | 378 | 13 | 22.8 | 34.8 | 62 | |
| 9 | 326 | 343 | 494 | 336.8 | 504 | 346.8 | 392 | 380 | 17 | 10.8 | 20.8 | 54 | |

Table E11. Site BL9 raw data.

| | 2/14/03 | 4/20/04 | 3/1/05 | 3/1/2005corr | 6/3/08 | 6/3/2008corr | 10/2/18 | 10/2/18corr | 2004diff | 2005diff | 2008diff | 2018diff | 2018Accretion |
|---------------------|---------|---------|--------|--------------|--------|--------------|---------|-------------|----------|----------|----------|----------|---------------|
| 1 site 9 position n | 330 | 291 | 482 | 325 | 495 | 338 | 409 | 397 | -39 | -5 | 8 | 67 | 160 |
| 2 | 329 | 283 | 480 | 323 | 499 | 342 | 398 | 386 | -46 | -6 | 13 | 57 | 154 |
| 3 | 328 | 296 | 486 | 329 | 498 | 341 | 400 | 388 | -32 | 1 | 13 | 60 | 140 |
| 4 | 327 | 317 | 493 | 336 | 493 | 336 | 411 | 399 | -10 | 9 | 9 | 72 | 150 |
| 5 | 321 | 335 | 492 | 335 | 506 | 349 | 390 | 378 | 14 | 14 | 28 | 57 | 133 |
| 6 | 318 | 279 | 485 | 328 | 500 | 343 | 401 | 389 | -39 | 10 | 25 | 71 | |
| 7 | 325 | 324 | 497 | 340 | 492 | 335 | 360 | 348 | -1 | 15 | 10 | 23 | |
| 8 | 322 | 319 | 485 | 328 | 489 | 332 | 412 | 400 | -3 | 6 | 10 | 78 | |
| 9 | 317 | 319 | 500 | 343 | 495 | 338 | 404 | 392 | 2 | 26 | 21 | 75 | |
| 1 site 9 position e | 306 | 259 | 482 | 325 | 493 | 336 | 403 | 391 | -47 | 19 | 30 | 85 | |
| 2 | 313 | 272 | 483 | 326 | 498 | 341 | 391 | 379 | -41 | 13 | 28 | 66 | |
| 3 | 314 | 305 | 482 | 325 | 486 | 329 | 382 | 370 | -9 | 11 | 15 | 56 | |
| 4 | 314 | 320 | 481 | 324 | 490 | 333 | 398 | 386 | 6 | 10 | 19 | 72 | |
| 5 | 307 | 291 | 485 | 328 | 485 | 328 | 395 | 383 | -16 | 21 | 21 | 76 | |
| 6 | 312 | 304 | 490 | 333 | 496 | 339 | 403 | 391 | -8 | 21 | 27 | 79 | |
| 7 | 313 | 328 | 475 | 318 | 487 | 330 | 400 | 388 | 15 | 5 | 17 | 75 | |
| 8 | 306 | 307 | 485 | 328 | 487 | 330 | 390 | 378 | 1 | 22 | 24 | 72 | |
| 9 | 308 | 314 | 478 | 321 | 481 | 324 | 403 | 391 | 6 | 13 | 16 | 83 | |
| 1 site 9 position s | 307 | 306 | 490 | 333 | 488 | 331 | 405 | 393 | -1 | 26 | 24 | 86 | |
| 2 | 311 | 295 | 475 | 318 | 490 | 333 | 402 | 390 | -16 | 7 | 22 | 79 | |
| 3 | 318 | 270 | 482 | 325 | 491 | 334 | 373 | 361 | -48 | 7 | 16 | 43 | |
| 4 | 307 | 317 | 465 | 308 | 499 | 342 | 410 | 398 | 10 | 1 | 35 | 91 | |
| 5 | 307 | 316 | 476 | 319 | 495 | 338 | 401 | 389 | 9 | 12 | 31 | 82 | |
| 6 | 310 | 312 | 477 | 320 | 489 | 332 | 394 | 382 | 2 | 10 | 22 | 72 | |
| 7 | 313 | 308 | 486 | 329 | 500 | 343 | 393 | 381 | -5 | 16 | 30 | 68 | |
| 8 | 311 | 316 | 462 | 305 | 493 | 336 | 401 | 389 | 5 | -6 | 25 | 78 | |
| 9 | 305 | 319 | 465 | 308 | 499 | 342 | 391 | 379 | 14 | 3 | 37 | 74 | |
| 1 site 9 position w | 315 | 262 | 454 | 297 | 490 | 333 | 416 | 404 | -53 | -18 | 18 | 89 | |
| 2 | 317 | 315 | 480 | 323 | 492 | 335 | 383 | 371 | -2 | 6 | 18 | 54 | |
| 3 | 310 | 261 | 479 | 322 | 496 | 339 | 397 | 385 | -49 | 12 | 29 | 75 | |
| 4 | 315 | 319 | 472 | 315 | 515 | 358 | 428 | 416 | 4 | 0 | 43 | 101 | |
| 5 | 323 | 306 | 426 | 269 | 500 | 343 | 406 | 394 | -17 | -54 | 20 | 71 | |
| 6 | 332 | 313 | 457 | 300 | 500 | 343 | 407 | 395 | -19 | -32 | 11 | 63 | |
| 7 | 325 | 318 | 472 | 315 | 507 | 350 | 394 | 382 | -7 | -10 | 25 | 57 | |
| 8 | 317 | 309 | 475 | 318 | 494 | 337 | 396 | 384 | -8 | 1 | 20 | 67 | |
| 9 | 314 | 343 | 477 | 320 | 483 | 326 | 387 | 375 | 29 | 6 | 12 | 61 | |

Table E12. Site BL11 raw data.

| | 2/12/03 | 4/20/04 | 3/2/05 | 3/2/2005corr | 6/4/08 | 6/4/2008corr | 11/19/18 | 11/19/18corr | 2004 difff | 2005 diff | 2008diff | 2018dif | Accretion |
|----------------------|---------|---------|--------|--------------|--------|--------------|----------|--------------|------------|-----------|----------|---------|-----------|
| 1 site 11 position 1 | 321 | 282 | 468 | 310.8 | 495 | 337.8 | 365 | 353 | -39 | -10.2 | 16.8 | 32 | none |
| 2 | 315 | 294 | 471 | 313.8 | 499 | 341.8 | 366 | 354 | -21 | -1.2 | 26.8 | 39 | |
| 3 | 312 | 291 | 465 | 307.8 | 487 | 329.8 | 366 | 354 | -21 | -4.2 | 17.8 | 42 | |
| 4 | 316 | 228 | 480 | 322.8 | 503 | 345.8 | 365 | 353 | -88 | 6.8 | 29.8 | 37 | |
| 5 | 314 | 310 | 474 | 316.8 | 500 | 342.8 | 361 | 349 | -4 | 2.8 | 28.8 | 35 | |
| 6 | 315 | 304 | 475 | 317.8 | 502 | 344.8 | 354 | 342 | -11 | 2.8 | 29.8 | 27 | |
| 7 | 316 | 279 | 487 | 329.8 | 500 | 342.8 | 363 | 351 | -37 | 13.8 | 26.8 | 35 | |
| 8 | 304 | 307 | 485 | 327.8 | 506 | 348.8 | 368 | 356 | 3 | 23.8 | 44.8 | 52 | |
| 9 | 292 | 312 | 480 | 322.8 | 505 | 347.8 | 361 | 349 | 20 | 30.8 | 55.8 | 57 | |
| 1 site 11 position 2 | 324 | 312 | 475 | 317.8 | 496 | 338.8 | 367 | 355 | -12 | -6.2 | 14.8 | 31 | |
| 2 | 320 | 277 | 483 | 325.8 | 493 | 335.8 | 373 | 361 | -43 | 5.8 | 15.8 | 41 | |
| 3 | 326 | 285 | 476 | 318.8 | 488 | 330.8 | 375 | 363 | -41 | -7.2 | 4.8 | 37 | |
| 4 | 320 | 306 | 477 | 319.8 | 501 | 343.8 | 377 | 365 | -14 | -0.2 | 23.8 | 45 | |
| 5 | 313 | 294 | 475 | 317.8 | 500 | 342.8 | 369 | 357 | -19 | 4.8 | 29.8 | 44 | |
| 6 | 320 | 289 | 467 | 309.8 | 495 | 337.8 | 369 | 357 | -31 | -10.2 | 17.8 | 37 | |
| 7 | 329 | 297 | 482 | 324.8 | 502 | 344.8 | 380 | 368 | -32 | -4.2 | 15.8 | 39 | |
| 8 | 308 | 318 | 481 | 323.8 | 511 | 353.8 | 380 | 368 | 10 | 15.8 | 45.8 | 60 | |
| 9 | 310 | 303 | 474 | 316.8 | 502 | 344.8 | 377 | 365 | -7 | 6.8 | 34.8 | 55 | |
| 1 site 11 position 3 | 330 | 291 | 483 | 325.8 | 516 | 358.8 | 361 | 349 | -39 | -4.2 | 28.8 | 19 | |
| 2 | 324 | 298 | 485 | 327.8 | 514 | 356.8 | 364 | 352 | -26 | 3.8 | 32.8 | 28 | |
| 3 | 335 | 308 | 482 | 324.8 | 499 | 341.8 | 370 | 358 | -27 | -10.2 | 6.8 | 23 | |
| 4 | 323 | 275 | 488 | 330.8 | 502 | 344.8 | 358 | 346 | -48 | 7.8 | 21.8 | 23 | |
| 5 | 318 | 304 | 477 | 319.8 | 508 | 350.8 | 360 | 348 | -14 | 1.8 | 32.8 | 30 | |
| 6 | 319 | 307 | 483 | 325.8 | 506 | 348.8 | 362 | 350 | -12 | 6.8 | 29.8 | 31 | |
| 7 | 320 | 286 | 488 | 330.8 | 510 | 352.8 | 361 | 349 | -34 | 10.8 | 32.8 | 29 | |
| 8 | 311 | 309 | 480 | 322.8 | 497 | 339.8 | 361 | 349 | -2 | 11.8 | 28.8 | 38 | |
| 9 | 312 | 310 | 483 | 325.8 | 500 | 342.8 | 354 | 342 | -2 | 13.8 | 30.8 | 30 | |
| 1 site 11 position 4 | 310 | 316 | 487 | 329.8 | 515 | 357.8 | 390 | 378 | 6 | 19.8 | 47.8 | 68 | |
| 2 | 315 | 309 | 489 | 331.8 | 510 | 352.8 | 390 | 378 | -6 | 16.8 | 37.8 | 63 | |
| 3 | 320 | 307 | 499 | 341.8 | 525 | 367.8 | 391 | 379 | -13 | 21.8 | 47.8 | 59 | |
| 4 | 307 | 344 | 491 | 333.8 | 501 | 343.8 | 373 | 361 | 37 | 26.8 | 36.8 | 54 | |
| 5 | 311 | 313 | 490 | 332.8 | 509 | 351.8 | 396 | 384 | 2 | 21.8 | 40.8 | 73 | |
| 6 | 325 | 316 | 488 | 330.8 | 509 | 351.8 | 396 | 384 | -9 | 5.8 | 26.8 | 59 | |
| 7 | 315 | 306 | 495 | 337.8 | 518 | 360.8 | 380 | 368 | -9 | 22.8 | 45.8 | 53 | |
| 8 | 319 | 317 | 491 | 333.8 | 515 | 357.8 | 384 | 372 | -2 | 14.8 | 38.8 | 53 | |
| 9 | 323 | 293 | 480 | 322.8 | 503 | 345.8 | 399 | 387 | -30 | -0.2 | 22.8 | 64 | |

Table E13. Site BL12 raw data.

| | 2/12/03 | 4/20/04 | 3/1/05 | 3/2/2005corr | 6/3/08 | 6/3/2008corr | 11/19/18 | 11/19/18corr | 2004 diff | 2005 diff | 2008diff | 2018dif | Accretion |
|----------------------|---------|---------|--------|--------------|--------|--------------|----------|--------------|-----------|-----------|----------|---------|-----------|
| 1 site 12 position 1 | 313 | 324 | 480 | 322.8 | 479 | 321.8 | 360 | 348 | 11 | 9.8 | 8.8 | 35 | 80 |
| 2 | 298 | 305 | 492 | 334.8 | 484 | 326.8 | 364 | 352 | 7 | 36.8 | 28.8 | 54 | 94 |
| 3 | 294 | 301 | 483 | 325.8 | 469 | 311.8 | 367 | 355 | 7 | 31.8 | 17.8 | 61 | 95 |
| 4 | 310 | 318 | 489 | 331.8 | 473 | 315.8 | 357 | 345 | 8 | 21.8 | 5.8 | 35 | 79 |
| 5 | 302 | 304 | 484 | 326.8 | 480 | 322.8 | 361 | 349 | 2 | 24.8 | 20.8 | 47 | 100 |
| 6 | 295 | 331 | 504 | 346.8 | 477 | 319.8 | 364 | 352 | 36 | 51.8 | 24.8 | 57 | |
| 7 | 309 | 318 | 582 | 424.8 | 480 | 322.8 | 349 | 337 | 9 | 115.8 | 13.8 | 28 | |
| 8 | 307 | 316 | 580 | 422.8 | 480 | 322.8 | 371 | 359 | 9 | 115.8 | 15.8 | 52 | |
| 9 | 311 | 307 | 501 | 343.8 | 472 | 314.8 | 369 | 357 | -4 | 32.8 | 3.8 | 46 | |
| 1 site 12 position 2 | 308 | 304 | 470 | 312.8 | 513 | 355.8 | 368 | 356 | -4 | 4.8 | 47.8 | 48 | |
| 2 | 300 | 304 | 469 | 311.8 | 495 | 337.8 | 361 | 349 | 4 | 11.8 | 37.8 | 49 | |
| 3 | 299 | 300 | 476 | 318.8 | 487 | 329.8 | 367 | 355 | 1 | 19.8 | 30.8 | 56 | |
| 4 | 310 | 302 | 475 | 317.8 | 484 | 326.8 | 375 | 363 | -8 | 7.8 | 16.8 | 53 | |
| 5 | 300 | 296 | 471 | 313.8 | 484 | 326.8 | 369 | 357 | -4 | 13.8 | 26.8 | 57 | |
| 6 | 304 | 301 | 472 | 314.8 | 494 | 336.8 | 372 | 360 | -3 | 10.8 | 32.8 | 56 | |
| 7 | 297 | 310 | 479 | 321.8 | 490 | 332.8 | 368 | 356 | 13 | 24.8 | 35.8 | 59 | |
| 8 | 303 | 318 | 476 | 318.8 | 490 | 332.8 | 361 | 349 | 15 | 15.8 | 29.8 | 46 | |
| 9 | 311 | 314 | 480 | 322.8 | 493 | 335.8 | 367 | 355 | 3 | 11.8 | 24.8 | 44 | |
| 1 site 12 position 3 | 285 | 288 | 463 | 305.8 | 496 | 338.8 | 372 | 360 | 3 | 20.8 | 53.8 | 75 | |
| 2 | 288 | 285 | 452 | 294.8 | 498 | 340.8 | 372 | 360 | -3 | 6.8 | 52.8 | 72 | |
| 3 | 293 | 302 | 464 | 306.8 | 495 | 337.8 | 371 | 359 | 9 | 13.8 | 44.8 | 66 | |
| 4 | 281 | 293 | 465 | 307.8 | 495 | 337.8 | 375 | 363 | 12 | 26.8 | 56.8 | 82 | |
| 5 | 286 | 286 | 461 | 303.8 | 505 | 347.8 | 377 | 365 | 0 | 17.8 | 61.8 | 79 | |
| 6 | 286 | 286 | 454 | 296.8 | 496 | 338.8 | 372 | 360 | 0 | 10.8 | 52.8 | 74 | |
| 7 | 289 | 297 | 474 | 316.8 | 498 | 340.8 | 377 | 365 | 8 | 27.8 | 51.8 | 76 | |
| 8 | 282 | 283 | 465 | 307.8 | 490 | 332.8 | 380 | 368 | 1 | 25.8 | 50.8 | 86 | |
| 9 | 279 | 279 | 460 | 302.8 | 496 | 338.8 | 376 | 364 | 0 | 23.8 | 59.8 | 85 | |
| 1 site 12 position 4 | 300 | 318 | 465 | 307.8 | 488 | 330.8 | 369 | 357 | 18 | 7.8 | 30.8 | 57 | |
| 2 | 291 | 297 | 487 | 329.8 | 486 | 328.8 | 369 | 357 | 6 | 38.8 | 37.8 | 66 | |
| 3 | 292 | 299 | 491 | 333.8 | 480 | 322.8 | 372 | 360 | 7 | 41.8 | 30.8 | 68 | |
| 4 | 312 | 319 | 468 | 310.8 | 491 | 333.8 | 365 | 353 | 7 | -1.2 | 21.8 | 41 | |
| 5 | 286 | 305 | 479 | 321.8 | 491 | 333.8 | 370 | 358 | 19 | 35.8 | 47.8 | 72 | |
| 6 | 292 | 301 | 486 | 328.8 | 485 | 327.8 | 364 | 352 | 9 | 36.8 | 35.8 | 60 | |
| 7 | 311 | 309 | 480 | 322.8 | 484 | 326.8 | 368 | 356 | -2 | 11.8 | 15.8 | 45 | |
| 8 | 291 | 297 | 490 | 332.8 | 491 | 333.8 | 371 | 359 | 6 | 41.8 | 42.8 | 68 | |
| 9 | 294 | 296 | 483 | 325.8 | 481 | 323.8 | 379 | 367 | 2 | 31.8 | 29.8 | 73 | |

Table E14. Site BL14 raw data.

| | 2/12/03 | 4/20/04 | 3/1/05 | 3/1/2005corr | 6/4/08 | 6/4/2008corr | 11/19/18 | 11/19/18corr | 2004 diff | 2005 diff | 2008diff | 2018dif | Accretion |
|----------------------|---------|---------|--------|--------------|--------|--------------|----------|--------------|-----------|-----------|----------|---------|-----------|
| 1 site 14 position 1 | 326 | 310 | 480 | 322.8 | 520 | 362.8 | 408 | 396 | -16 | -3.2 | 36.8 | 70 | 85 |
| 2 | 324 | 321 | 510 | 352.8 | 502 | 344.8 | 399 | 387 | -3 | 28.8 | 20.8 | 63 | 85 |
| 3 | 312 | 330 | 522 | 364.8 | 528 | 370.8 | 389 | 377 | 18 | 52.8 | 58.8 | 65 | 85 |
| 4 | 323 | 311 | 485 | 327.8 | 488 | 330.8 | 398 | 386 | -12 | 4.8 | 7.8 | 63 | |
| 5 | 315 | 318 | 514 | 356.8 | 505 | 347.8 | 395 | 383 | 3 | 41.8 | 32.8 | 68 | |
| 6 | 309 | 305 | 523 | 365.8 | 503 | 345.8 | 382 | 370 | -4 | 56.8 | 36.8 | 61 | |
| 7 | 341 | 325 | 531 | 373.8 | 516 | 358.8 | 383 | 371 | -16 | 32.8 | 17.8 | 30 | |
| 8 | 345 | 316 | 495 | 337.8 | 500 | 342.8 | 382 | 370 | -29 | -7.2 | -2.2 | 25 | |
| 9 | 316 | 300 | 495 | 337.8 | 494 | 336.8 | 375 | 363 | -16 | 21.8 | 20.8 | 47 | |
| 1 site 14 position 2 | 292 | 300 | 486 | 328.8 | 514 | 356.8 | 391 | 379 | 8 | 36.8 | 64.8 | 87 | |
| 2 | 304 | 317 | 490 | 332.8 | 477 | 319.8 | 409 | 397 | 13 | 28.8 | 15.8 | 93 | |
| 3 | 306 | 336 | 530 | 372.8 | 457 | 299.8 | 384 | 372 | 30 | 66.8 | -6.2 | 66 | |
| 4 | 307 | 333 | 492 | 334.8 | 460 | 302.8 | 381 | 369 | 26 | 27.8 | -4.2 | 62 | |
| 5 | 308 | 325 | 503 | 345.8 | 446 | 288.8 | 390 | 378 | 17 | 37.8 | -19.2 | 70 | |
| 6 | 309 | 320 | 487 | 329.8 | 497 | 339.8 | 366 | 354 | 11 | 20.8 | 30.8 | 45 | |
| 7 | 327 | 328 | 492 | 334.8 | 514 | 356.8 | 396 | 384 | 1 | 7.8 | 29.8 | 57 | |
| 8 | 314 | 321 | 500 | 342.8 | 502 | 344.8 | 392 | 380 | 7 | 28.8 | 30.8 | 66 | |
| 9 | 310 | 316 | 488 | 330.8 | 483 | 325.8 | 380 | 368 | 6 | 20.8 | 15.8 | 58 | |
| 1 site 14 position 3 | 290 | 316 | 485 | 327.8 | 465 | 307.8 | 387 | 375 | 26 | 37.8 | 17.8 | 85 | |
| 2 | 299 | 305 | 497 | 339.8 | 467 | 309.8 | 373 | 361 | 6 | 40.8 | 10.8 | 62 | |
| 3 | 295 | 297 | 484 | 326.8 | 471 | 313.8 | 400 | 388 | 2 | 31.8 | 18.8 | 93 | |
| 4 | 303 | 313 | 463 | 305.8 | 475 | 317.8 | 392 | 380 | 10 | 2.8 | 14.8 | 77 | |
| 5 | 299 | 301 | 455 | 297.8 | 477 | 319.8 | 389 | 377 | 2 | -1.2 | 20.8 | 78 | |
| 6 | 295 | 296 | 470 | 312.8 | 462 | 304.8 | 392 | 380 | 1 | 17.8 | 9.8 | 85 | |
| 7 | 296 | 307 | 469 | 311.8 | 469 | 311.8 | 403 | 391 | 11 | 15.8 | 15.8 | 95 | |
| 8 | 302 | 322 | 474 | 316.8 | 473 | 315.8 | 390 | 378 | 20 | 14.8 | 13.8 | 76 | |
| 9 | 299 | 303 | 466 | 308.8 | 466 | 308.8 | 372 | 360 | 4 | 9.8 | 9.8 | 61 | |
| 1 site 15 position 4 | 309 | 330 | 505 | 347.8 | 496 | 338.8 | 380 | 368 | 21 | 38.8 | 29.8 | 59 | |
| 2 | 343 | 328 | 504 | 346.8 | 475 | 317.8 | 371 | 359 | -15 | 3.8 | -25.2 | 16 | |
| 3 | 302 | 318 | 521 | 363.8 | 500 | 342.8 | 372 | 360 | 16 | 61.8 | 40.8 | 58 | |
| 4 | 352 | 330 | 510 | 352.8 | 520 | 362.8 | 389 | 377 | -22 | 0.8 | 10.8 | 25 | |
| 5 | 318 | 341 | 501 | 343.8 | 481 | 323.8 | 384 | 372 | 23 | 25.8 | 5.8 | 54 | |
| 6 | 312 | 339 | 502 | 344.8 | 497 | 339.8 | 383 | 371 | 27 | 32.8 | 27.8 | 59 | |
| 7 | 326 | 343 | 504 | 346.8 | 516 | 358.8 | 400 | 388 | 17 | 20.8 | 32.8 | 62 | |
| 8 | 349 | 342 | 498 | 340.8 | 508 | 350.8 | 377 | 365 | -7 | -8.2 | 1.8 | 16 | |
| 9 | 327 | 329 | 467 | 309.8 | 514 | 356.8 | 359 | 347 | 2 | -17.2 | 29.8 | 20 | |

Appendix F: CRMS Data

CRMS4551

The CRMS4551 site is located approximately 1.9 miles north of the intersection of Bayou La Loutre and the Mississippi River Gulf-Outlet Canal (MRGO), north of the rock berm blocking MRGO (Chapter 2: Figure 6). Wetland surface elevation at this site increased by 0.82 cm/y (Figure F1). Accretion taken over five time periods ranged from 0.78-2.03 cm/y, and averaged 1.36 ± 0.20 cm/y (Table F1).

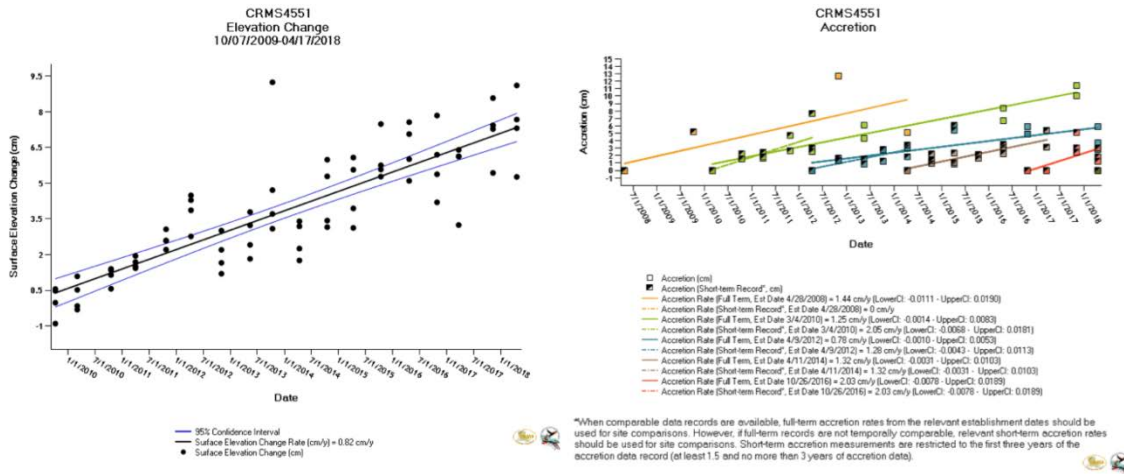


Figure F1. Surface elevation change data (left) and accretion data (right) for CRMS4551.

Table F1. Summary table of CRMS data from sites in the BMC.

| site | Accretion Est.2008 (cm/y) | Accretion Est.2010 (cm/y) | Accretion Est.2012 (cm/y) | Accretion Est.2014 (cm/y) | Accretion Est.2016 (cm/y) | Mean Accretion (cm/y) | Elevation (cm/y) | Subsidence (cm/y) |
|----------|---------------------------|---------------------------|---------------------------|---------------------------|---------------------------|-----------------------|------------------|-------------------|
| CRMS4551 | 1.44 | 1.25 | 0.78 | 1.32 | 2.03 | 1.36 | 0.82 | 0.54 |
| CRMS4557 | 1.61 | 1.55 | 1.17 | 2.38 | 1.79 | 1.70 | 1.03 | 0.67 |
| CRMS4572 | 0.86 | 0.69 | 0.54 | 0.79 | 2.05 | 0.99 | 0.56 | 0.43 |
| CRMS4596 | 1.08 | 0.90 | 1.66 | 1.70 | 2.06 | 1.48 | 0.41 | 1.07 |
| CRMS0108 | 0.61 | 0.92 | 1.37 | 0.88 | 1.94 | 1.14 | 0.68 | 0.53 |
| CRMS1024 | 1.66 | 0.96 | 0.57 | 1.20 | 1.24 | 1.13 | 0.84 | 0.29 |

CRMS4557

CRMS4557 is located approximately 1.7 miles east-southeast of the point of intersection of Bayou La Loutre and MRGO, south of the rock berm blocking MRGO (Figure 6). Surface elevation change at the site was 1.03 cm/y (Figure F2). Accretion, measured over five intervals, ranged from 1.17 to 2.38 cm/y, with a mean of 1.70 ± 0.20 cm/y (Table F1).

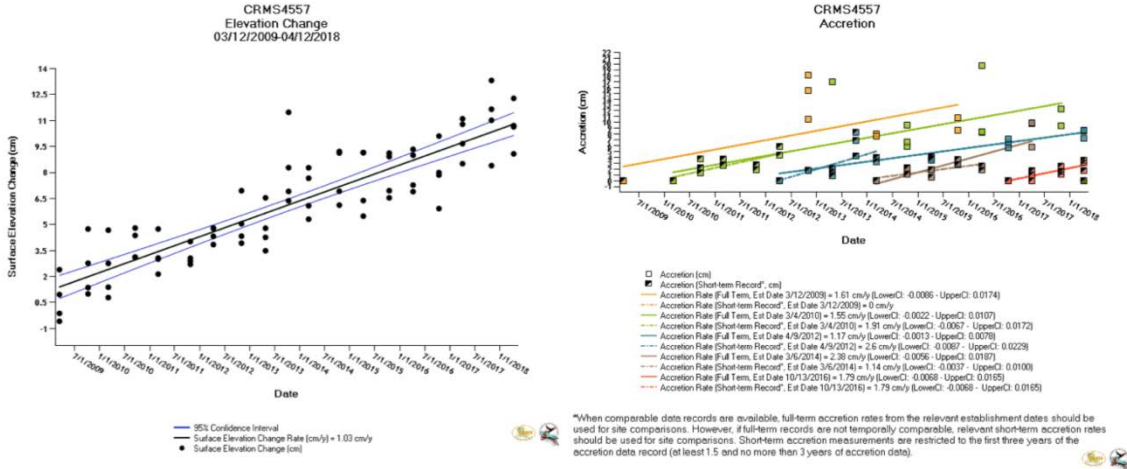


Figure F2. Surface elevation change data (left) and accretion data (right) for CRMS4557.

CRMS4572

CRMS4572 is one of two sites located in the northern BMC site (Figure 6). It is located approximately 1.0 miles northeast of the point of entry of Bayou La Fee into Lake Borgne. Marsh surface elevation increased by 0.56 cm/y since measurements began in 2009, and accretion ranged from 0.54 cm/y to 2.05 cm/y during the time intervals, with a mean of 0.99 ± 0.27 cm/y (Figure F3; Table F1).

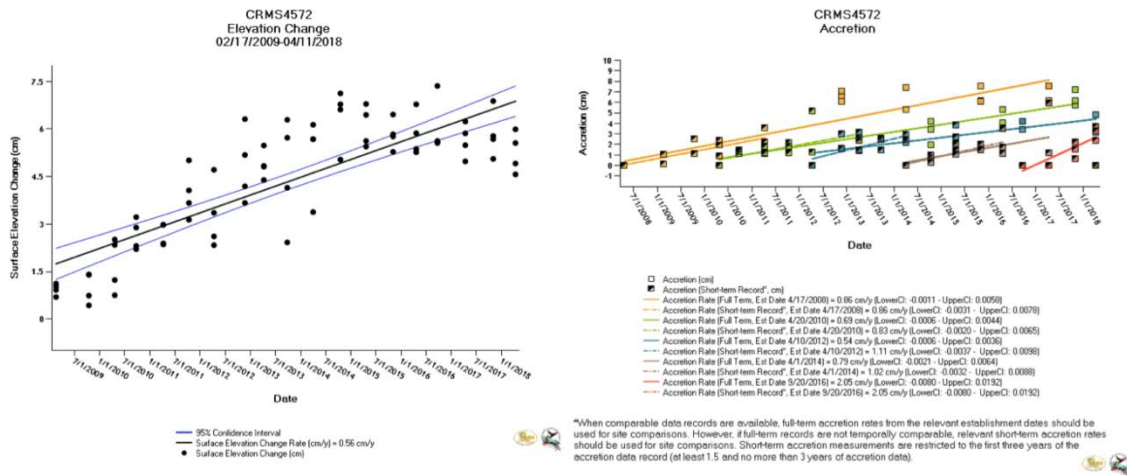


Figure F3. Surface elevation change data (left) and accretion data (right) for CRMS4572.

CRMS4596

CRMS4596 is the other of two sites located in the northern BMC site (Figure 6). It is located approximately 0.5 miles southeast of the point of entry of the Mosquito Inlet into Mississippi Sound. The elevation of the wetland surface increased at a rate of 0.41 cm/y

and accretion ranged from 0.90 to 2.06 cm/y, with an overall mean of 1.48 ± 0.21 cm/y (Figure F4; Table F1).

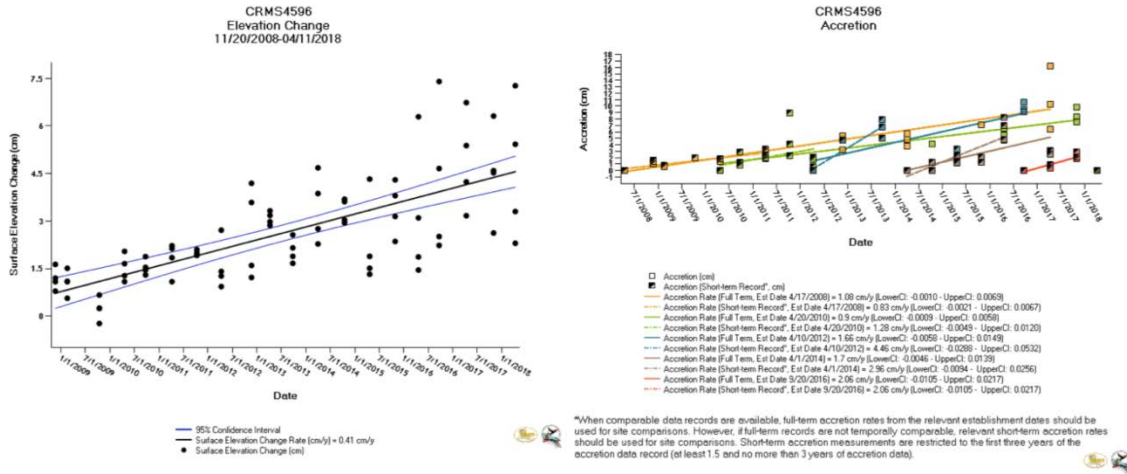


Figure F4. Surface elevation change data (left) and accretion data (right) for CRMS4596.

CRMS0108

Site CRMS0108 is located in the eastern BMC approximately 0.8 miles southwest of the entrance of Redfish Bayou into Bay Boudreau (Figure 6). Accretion over the five time intervals ranged from 0.61 to 1.94 cm/y, and an overall mean of 1.14 ± 0.23 cm/y (Figure F5). Surface elevation change at the site was 0.68 cm/y (Table F1).

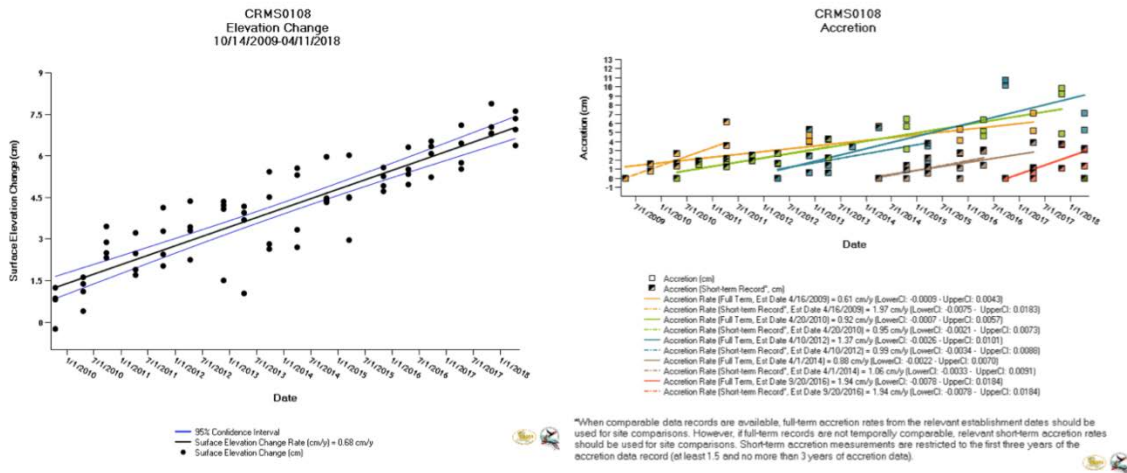


Figure F5. Surface elevation change data (left) and accretion data (right) for CRMS0108.

CRMS1024

The CRMS1024 site is located in the southeastern BMC approximately 4.6 miles northeast of the intersection of Bayou Petre and Bayou La Loutre (Figure 5). Accretion ranged from 0.56 to 1.66 cm/y over five measurement periods, with a mean of 1.13 ± 0.18 cm/y, and surface elevation increase of 0.84 cm/y (Figure F6; Table F1).

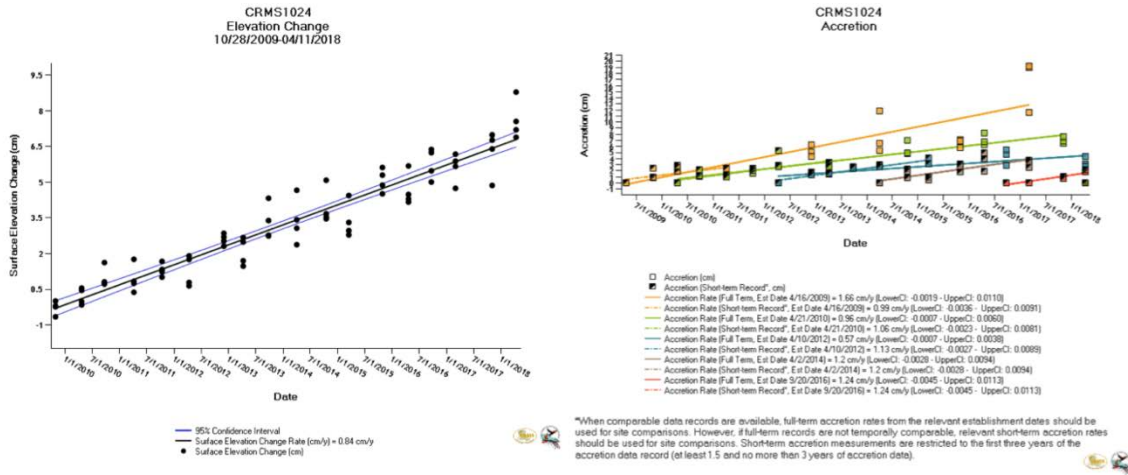


Figure F6. Surface elevation change data (left) and accretion data (right) for CRMS1024.

Appendix G: “*Status of Rangia Clams in Lakes Borgne after Closure of the Mississippi River Gulf Outlet,*” M. A. Poirrier 2019



Poirrier 2019 Status
of Rangia Clams in L

Appendix H: Drone video of Biloxi Marsh along the Lake Borgne Shoreline 11-23-2016

<https://www.youtube.com/watch?v=JzJvUpJsxOk&feature=youtu.be>

Appendix I: “*Leveraging Natural Resilience to ensure Long-Term Sustainability of the Biloxi Marsh Complex Surge Barrier: An Integrated Project,*” Day et al., 2019

<http://www.biloximarshlandscorp.com/bmlc2/wp-content/uploads/2017/05/BMC-2023-New-Project-Proposal-FINAL-Submitted.pdf>

Appendix J: “*MRGO Ecosystem Restoration Fact Sheet*”: USACE 2013



MRGO Ecosystem
Restoration Plan Fac

Appendix K: “*Three Mile Pass Marsh Creation and Hydrologic Restoration,*” Lake Pontchartrain Basin Foundation CMP 2023 Project Nomination



LPBF CMP 2023 proj
nomination Three M